Preparation of Cellulose Based Graft Copolymer; Characterization and Evaluation

A dissertation submitted in partial

fulfillment of the requirement for the degree of

DOCTOR OF PHILOSOPHY

(Pharmaceutics)

by

Ayesha Rashid

Pharm.D., M.Phil.

Department of Pharmacy,
Faculty of Pharmacy and Alternative Medicine,
The Islamia University of Bahawalpur,
Pakistan

2012-2015

IN THE NAME OF ALLAH THE MOST GRACIOUS THE MOST MERCIFUL

DEDICATION

Dedicated to,

My Dearest Mother
Mrs. Zubaida Rashid
For her endless support, appreciation and encouragement

My Ever Respected Teacher
Prof. Dr. Mahmood Ahmad
For his valuable guidance and encouragement,

My Dearest Nephew,
Ahmed Abdullah
For his love, care and affiliation,

My Dearest Father
Ch. Muhammad Rashid
For his love, care and confidence

My Husband
Muhammad Aamer Mushtaq
For his cooperation, care, confidence and encouragement

My Sweet Brothers and Younger Sister
For their love and Moral Support

DECLARATION

I, Ayesha Rashid, Ph.D Scholar of Department of Pharmacy, The Islamia University of Bahawalpur, hereby declare that the research work entitled **"Preparation of cellulose based graft copolymer; characterization and evaluation"** is done by me. I also certify that nothing has been incorporated in this research work without acknowledgement and that to the best of my knowledge and belief it does not contain any material previously published or written by any other person or any material previously submitted for a degree in any university where due reference is not made in the text.

Ayesha Rashid

CERTIFICATE

It is hereby certified that this thesis entitled **"Preparation of cellulose based graft copolymer; characterization and evaluation"** is based upon the results of experiments carried out by **Ms. Ayesha Rashid** under my supervision. No portion of this work has previously been presented for higher degree in this university or any other institute of learning and to the best of the knowledge, no material has been used in this thesis which is not her own work except where due acknowledgement has been made. She has fulfilled all the requirements and is qualified to submit this thesis for the Degree of Doctor of Philosophy in Pharmaceutics.

Prof. Dr. Mahmood Ahmad
Supervisor,
Dean, Faculty of Pharmacy and Alternative Medicines,
The Islamia University of Bahawalpur

Ph.D. Dissertation (Pharmaceutics) Open Defense Viva Voce Examination of **Ms. Ayesha Rashid** held on 19th August, 2015

Candidate

Supervisor/Internal Examiner
(Prof. Dr. Mahmood Ahmad)

External Examiner I
(Prof. Dr. Muhammad Jamshaid)

External Examiner II
(Prof. Dr. Nazar Muhammad Ranjha)

Chairman
Department of Pharmacy

Dean
Faculty of Pharmacy & Alternative Medicine

CERTIFICATE

It is hereby certified that this thesis entitled **"Preparation of cellulose based graft copolymer; characterization and evaluation"** is based upon the results of experiments carried out by **Ms. Ayesha Rashid** under my supervision. No portion of this work has previously been presented for higher degree in this university or any other institute of learning and to the best of the knowledge, no material has been used in this thesis which is not her own work except where due acknowledgement has been made. She has fulfilled all the requirements and is qualified to submit this thesis for the Degree of Doctor of Philosophy in Pharmaceutics.

Prof. Dr. Mahmood Ahmad
Supervisor,
Dean, Faculty of Pharmacy and Alternative Medicines,
The Islamia University of Bahawalpur

Acknowledgements

It is the deepest sense of gratitude to the **Almighty ALLAH** that I am bestowed upon the initiative and energy to learn by unwilling the nature. It has been great favour of Allah that I am granted the good fortune to complete the project with the blessing and the help of the noble and learned personalities.

All respects, blessings and love to the last **Holy Prophet MUHAMMAD**, (Sal-Allaho-alaihe-wa-aalehee-wasallam), who enabled me to recognize Creator and His creations and changed me from man to Muslim by teaching, "Seek knowledge from cradle to grave."

My profound gratitude and sincere thanks to my supervisor Prof. Dr. Mahmood Ahmad are many fold. I greatly acknowledge his help, kind and sagacious supervision, benevolent guidance, endless love and continuous encouragement throughout my study and research.

I would like to extend my deep felt appreciation and thanks to Dr. Naveed Akhtar, Chairman Department of Pharmacy.

I will record my sincere thanks and appreciation for my seniors, particularly Assistant Professor Dr. Muhammad Usman Minhas, and Assistant Professor Dr. Imran Masood, Assistant Professor Dr. Raees Muhammad Akhter and Assistant Professoir Dr. Muhammad Zubair Malik for their valuable guidance and support.

I would like to expresses deep sense of appreciation to my friend Ume Ruqia Tulain as she always encouraged me and provided every kind of support during my studies. I would like to expresses deep sense of love, affiliation and care to my nephew Ahmad Abdullah as he provided me with very sweet and supportive homely environment throughout my Ph.D. His innocent mischiefs kept me too far from study related depressions and tensions.

It would like to acknowledge cooperation and support of my class fellows Mrs. Ayesha Yaqoob, Mr. Furqan Muhammad Iqbal, Mr. Muhamad Sohail and Mr. Ikrima Khalid.

Also I would like to acknowledge Hafiz Muhammad Saleem, peon Dean Office, Mukhtar Ahmad, Lab attendant, M.Phil/Ph.D Research Lab. 25 and Muhammad Shafeeq, store in charge for their services and cooperation during whole of my research work.

I express my heartfelt gratitude to my father, mother, husband and all other family members. Their unlimited love and affection served me a beacon of light. It is through their benevolent help and wholehearted prayers that enabled me to complete my studies. I am also indebted to all those people who prayed for my success.

Ayesha Rashid

ABBREVIATIONS

HEMA	2-Hydroxyethyl methacrylate
AA	Acrylic acid
HPMC	Hydroxy propyle methy cellulose
CMC	Sodium carboxy methyl cellulose
MAA	Methacrylic acid
AMPS	2-Acrylamido-2-methylpropane sulfonic acid
MBA	N,N/ methylene-bis-acrylamide
KPS	Potassium persulphate
FTIR	Fourier transform infrared spectroscopy
XRD	X-ray diffraction
SEM	Scanning electron microscopy
TGA	Thermal gravimetric analysis
DSC	Differential scanning calorimetry
Hrs	Hours
Min	Minute
KH_2PO_4	Potassium dihydrogen phosphate
NaOH	Sodium hydroxide
UV	Ultraviolet
Rpm	Revolutions per minute
GFR	Glomerular filtration rate
cGMP	Cyclic guanosine monophosphate
PKG	Protein kinase G
%P	Percent porosity
$\%g_c$	Percent gel content
%ES	Percent equilibrium swelling
ATR	Attenuated total reflectance
$AUC_{0-\infty}$	Area Under the Curve from zero to infinity
$AUMC_{0-\infty}$	Area Under the Moment Curve from zero to infinity
C_{max}	Maximum Plasma Concentration

Conc	Concentration
HPLC	High Performance Liquid Chromatography
GIT	Gastro-intestinal Tract
MRT	Mean Residence Time
T_{max}	Time for Maximum Plasma Concentration
Cl_T	Total Body Clearance
V_d	Volume of Distribution.

CONTENTS

PART-I

PART-II

CHAPTER: 1. INTRODUCTION

CHAPTER: 2. LITERATURE REVIEW

CHAPTER: 3. MATERIALS AND METHODS

CHAPTER: 4. RESULTS

CHAPTER: 5. DISCUSSION

CHAPTER: 6. CONCLUSION

CHAPTER: 7. Future Suggestions/Recommendations

CHAPTER: 8. REFERENCES

List of Tables

List of Figures

Abstract

Background

Present study deals with development of an oral controlled release system to deliver anti-angina drug “nicorandil” at predetermined and reproducible rate over a desired period of time. To achieve these goal different crosslink polymeric networks were formulated and their competence of delivering drug at predefined rate over desired period was evaluated.

Objective

The basic purpose of study was to formulate and evaluate such oral drug delivery system for anti-angina drug “nicorandil” which can deliver drug at desired sustained rate. As nicorandil has shorter elimination half-life of 1 hour so that frequent daily dosing can be replaced with once sustained dose.

Experimental design and methods

Free radical solution polymerization technique was used to prepared pH sensitive crosslink polymeric networks using different polymer, monomer and crosslinker concentrations. Four different combinations i.e. HEMA-co-AA, HPMC-co-AA, HPMC-co-AA-co-HEMA and CMC-co-MAA-co-AMPS hydrogels were developed and their responsiveness to buffer solutions of different pH i.e. pH 1.2, pH5.8 and pH 7.4 was evaluated. Crosslinking structure of all formulations were confirmed by FTIR, XRD and SEM. For thermal stability formulations were also subjected to TGA and DSC studies. In-vitro drug release studies of all formulations were conducted moreover in-vivo evaluation of the best formulations was also performed.

Results

HEMA-co-AA hydrogels were prepared by using MBA as crosslinker. HEMA-co-AA hydrogels showed pH responsiveness as they showed maximum swelling at pH 7.4 as compared to pH 1.2. This property was used as a key factor to design sustained release

drug delivery system that deliver drug in gastrointestinal tract in response of different pH environment. Among combination HEMA-co-AA hydrogels F1 was found to be the best as it showed maximum cumulative drug release i.e. 92.878% at pH 7.4. Desired release profile was noticed to be greatly affected by varying concentrations of polymer, monomer or crosslinker.

HPMC-co-AA hydrogels had good pH sensitivity as these showed better and maximum swelling at pH 7.4 and minimum swelling at pH 1.2. Among this combination F1 depicted better desired properties regarding pH sensitivity, greater swelling ratio and desired sustained drug release profile etc. Swelling ratio, gel fraction and cumulative percent drug release was noted to be decreased with increasing crosslinker concentration i.e. MBA while these parameters were noted to be increased with increasing AA and HPMC concentrations. Desired sustained release profile could be attained by adjusting polymer, monomer and crosslinker ratio.

HPMC-co-AA-co-HEMA hydrogels were developed by free radical polymerization technique using MBA as crosslinker. Formulations were subjected to swelling (at pH 1.2, pH 5.8 and pH 7.4) and in-vitro drug release studies (at pH 1.2 and pH 7.4). Swelling and percent drug release was noted to be decreased with increasing MBA and HEMA concentration while it was noted to be increased with increasing AA and HPMC concentrations. More over swelling ratio and percent drug release was also increased gradually with increasing pH from acidic to alkaline i.e. pH 1.2 to pH 7.4. All formulations were noted to be stable and intact during swelling and in-vitro drug release studies. Among this combination F24 was found to be the best as it gave best results for swelling and cumulative percent drug release i.e. 82.820%. It also showed better pharmacokinetic profile as well.

Developed CMC-co-MAA-co-AMPS showed less pH sensitivity as compared to all other three combinations as difference in swelling ratio and cumulative percent drug release at acidic and alkaline pH was negligible. Formulations were noted to be unstable and broken during swelling and in-vitro drug release studies.

HEMA-co-AA (F1), HPMC-co-AA (F12) and HPMC-co-AA-co-HEMA (F24) hydrogels were selected for in-vivo evaluation using animal model rabbits as these showed better in-vitro sustained drug release profile. After oral administration of these formulations C_{max} was noted to be 60.608 ± 2.816 ng/mL, 108.388 ± 2.338 ng/mL and 92.322 ± 3.667 ng/mL respectively. MRT was noted to be 12.790 ± 0.310 hrs, 13.1786 ± 0.468 hrs and 13.600 ± 0.245 hrs for HEMA-co-AA (F1), HPMC-co-AA (F12) and HPMC-co-AA-co-HEMA (F24) hydrogels. On behalf of these in-vivo findings it can be concluded that these crosslink polymeric networks can be used as good sustain release drug delivery system.

Conclusion

From results of present study it could be concluded that among four different crosslink polymeric networks prepared, HPMC-co-AA (F12) hydrogel could be considered as superior as it gave better *in vitro/in vivo* release profile and thus proven suitable for desired sustained release effect at predetermined rate over prolong period of time. However these findings are preliminary and studies can proceed to further investigations.

Key Words: Hydrogel, Nicorandil, Polymeric networks, Crosslinker, Monomer, Swelling ratio, *In vitro and in vivo* evaluation

1.0. Introduction

Polymers have become marvelous icon of interest in many areas, such as the pharmaceutical industry, therapeutic innovation and others. Spreads in polymer science have open new gates to expansion of novel drug delivery systems (Veeran and Guru, 2011). Advances in polymers impart unique properties of interest to carrier system. Both natural and synthetic polymers are stand-in an auspicious tool for drug delivery, especially in oral administration therapeutic drugs having challenging issues like poor absorption or short half-life etc. (Chandel *et al.,* 2013). Because of unique properties like compatibility, degradation and nontoxic behavior of bio-composite polymers, these are becoming a tool of tremendous interest for controlled drug delivery. By suitable physical or chemical modification in polymers, properties of interest can be attained or enhanced (Sonia and Sharma, 2011).

Among polymers, natural ones are of enormous custom for manhood, as natural polymers offer attractive properties of interest and desired attributes (viz. low density, mechanical properties) **(**Ashish and Balbir, 2012**)**. On earth cellulose (a polydispersed, linear homopolymer composed of D-glucopyranose units, linked together by β-(1→4) glycosidic bonds) as natural polymer is the utmost plentiful renewable polymer (Gilberto *et al.,* 2010), offering enormous striking physical and chemical attributes like biodegradability, biocompatibility, stereo regularity, hydrophilicity, reactive hydroxyl groups and ability to form supra structures (Heinze and Liebert, 2001). Cellulose and cellulose derivatives have many uses in different areas such as fibers, films, coatings, laminates, optical films and sorption media, additives, building materials, pharmaceuticals, foodstuffs and cosmetics (Dieter *et al.,* 2005).

As far as water soluble polymers are concerned they dissolve, disperse or swell in water providing base to alter the physical properties of aqueous systems as gelation, thickening or emulsification/stabilization. These polymers are usually constituted from repeating units or blocks of units of hydrophilic groups those are substituted or attached the basic

backbone of structure. These hydrophilic groups could possess nonionic, anionic, cationic or amphoteric properties (Veeran and Guru, 2011).

In view of health related dysfunctions, reaching drug at site of action in appropriate concentration over a sufficiently prolong period of time is the main task. But the action of pharmaceutical agents is confined by enormous factors including degradation of agent, interaction with cells and inability to infiltrate tissues. These facts provide the basic to develop carrier systems of higher interest with desired profile as these systems act as right tool for time and distribution controlled drug delivery (Gemma *et al.,* 2012). For oral controlled release drug delivery systems hydrophilic gel forming polymeric systems are in extensive use to acquire an anticipated drug release profile, cost effectiveness and broad regulatory acceptance (Kamel *et al.,* 2008). Hydroxypropylmethylcellouse (HPMC) and sodium carboxymethylcellulose (CMC) are hydrophilic polymers attaining prominence in this regard as these approaches anticipated attributes of an ideal polymer. More over both hydrophilic and hydrophobic variants with different viscosity grades are also available making them more and more suitable candidate for desired release profile (Kajal *et al.,* 2011).

This polymeric area invites various modifications in properties of polymer viz. blending, grafting and curing to achieve targeted action. Among these graft copolymers have been extensively used to formulate a number of controlled release systems like hydrogels, microspheres or matrix tablets etc. 'Grafting' refers to a technique in which monomers are covalently bonded (modified) onto the polymer chain. Graft copolymerization mends the properties of polymers to stretch them a new anticipated property. These are gaining great attention in various areas like dyeing, printing, fiber strength, chemical resistance, water repellency, crease resistance and abrasion resistance etc. (Susheel *et al.,* 2011). On grafting, host polymer/monomer advances to looked-for properties. These grafted copolymeric systems are of inordinate status to mature into various stimuli-dependent controlled release systems such as pH sensitive hydrogels (Sabyasachi *et al.,* 2010).

Nicorandil, a nicotinamide derivative is an efficacious remedy in management of hypertension and angina pectoris. As a potassium channel opener it causes vasodilatation

of arterioles and large coronary arteries. Venous vasodilatation is attributed to its nitrate component. Chemically it has its place to organic nitrate groups. Nitrate moiety is considered responsible for its pharmacologic activities as it stimulates production of cyclic GMP in smooth muscle cells causing vasodilatation (Kukovetz and Holzmann, 1987). Opening of ATP sensitive K^+ channels attribute to dilatation of peripheral and coronary resistant arterioles. Moreover, it encompasses NO_2 group, responsible for dilation of systemic veins and epicardial coronary arteries (Markham *et al.*, 2000).

The study was planned to appraise graft polymeric carrier systems for sustained or controlled delivery of potassium channel opener "Nicorandil". With an elimination half-life of almost 1 hour it is a likely agent for development of controlled release formulations for treatment of hypertension and angina pectoris. Nicorandil is available in tablet form having dose 5 to 40 mg twice daily. To lessen frequency of administration and to improve patient compliance, once daily sustained release formulation of nicorandil is anticipated. With all these obvious truths Nicorandil is an appropriate applicant for development of controlled release dosage form. As study was proposed to account for the pharmaceutical features of nicorandil with superior emphasis on its suitable delivery system, cellulose based graft copolymeric system using different concentrations have been achieved with looked for controlled release of nicorandil.

Whole work flow chart has been given on the next page.

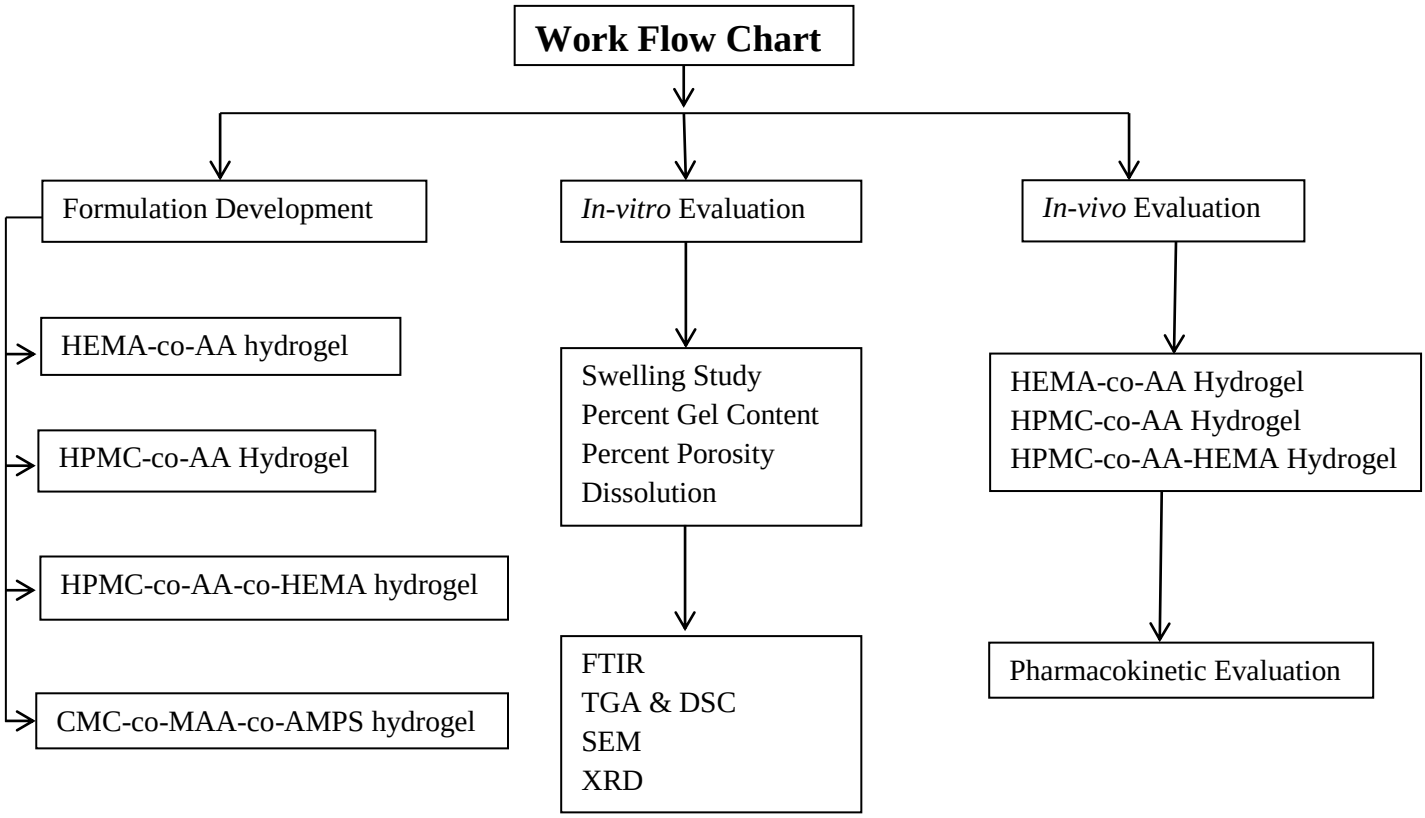
Work Flow Chart
Formulation Development
In-vitro Evaluation
In-vivo Evaluation
HEMA-co-AA hydrogel
HPMC-co-AA Hydrogel
HPMC-co-AA-co-HEMA hydrogel
CMC-co-MAA-co-AMPS hydrogel
Swelling Study
Percent Gel Content
Percent Porosity
Dissolution
FTIR
TGA & DSC
SEM
XRD
HEMA-co-AA Hydrogel
HPMC-co-AA Hydrogel
HPMC-co-AA-HEMA Hydrogel
Pharmacokinetic Evaluation

2.0 Literature Review

2.1 Introduction of polymers

Polymeric hydrogels have captured great attention of researchers in view of their biocompatibility (Jun *et al.*, 2003). Highly swelling hydrogels and polymers being three dimensional networks are capable of absorbing large amounts of water as compared to their dry weight. Depending upon the structure of final product and nature of components, hydrogels can absorb water ranging from 10 % to thousands of times of their dry weight (Mohammad, 2010). Modification of natural polymers by using various means like grafting of polymer has become of great importance. Copolymerization of natural polymers with variety of monomers is useful in achieving final formulation with desired and different physicochemical properties as that of individual components. Many natural polymers like chitin, cellulose, functionalized cellulose; hydroxypropyl methyl cellulose, methyl cellulose and other natural fibers are frequently studied for graft copolymer by using redox system as initiator.

2.2 Cellulose

Cellulose an organic compound having formula $(C_6H_{10}O_5)_n$ is actually a polysaccharide. Cellulose is composed of β (1→4) linked D-glucose repeated units linked together in linear fashion from hundreds to thousands (Updegraff, 1969). Being the most abundant organic polymer on earth (Klemm *et al.*, 2005) it is found as primary cell wall component of green plants, present in many forms of algae, accounts for 90% of cotton fibers, 40-50% of wood and 45% of dried hemp.

2.2.1 History

Cellulose first isolated from plant matter was discovered by a French chemist Anselme Payen. He also discovered its chemical formula (Payen, 1838). Celluloid was first thermoplastic polymer successfully produced from cellulose by Hyatt Manufacturing Company in 1870. Later on in 1890 and 1912 two derivatives rayon and cellophane was

produced, respectively (Kobayashi *et al.*, 1992). Structure of plant cell wall illustrating arrangement of cellulose and other poly saccharide is given in figure 2.1.

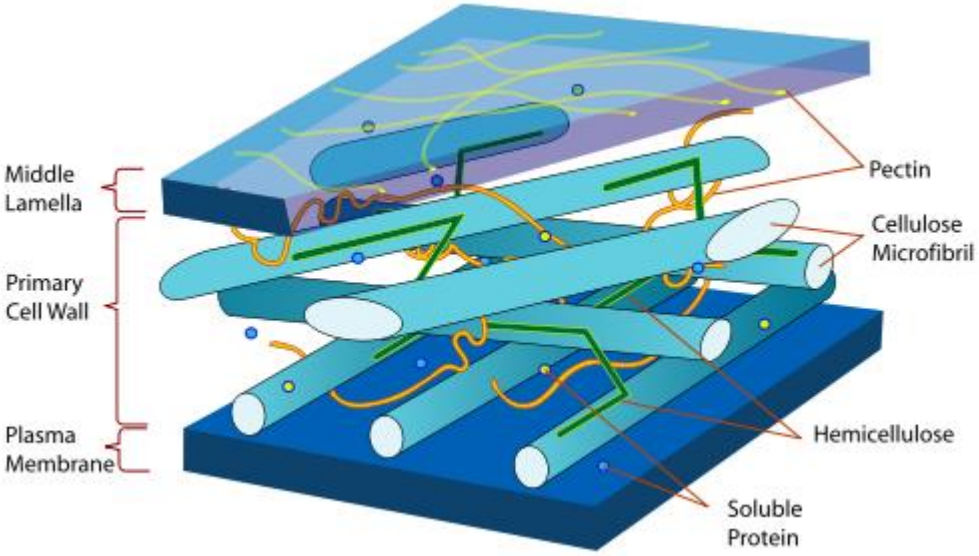

Figure 2.1. Arrangement of cellulose and other polysaccharide in plant cell wall (http://en.wikipedia.org/wiki/Cellulose)

2.2.2 Physicochemical properties

Cellulose is tasteless, odorless hydrophilic compound, insoluble in water and most of organic solvents. It is biodegradable in nature. With the help of acids at high temperature, chemically it can be converted into glucose units.

2.2.3 Structure

Structure of cellulose is given in figure 2.2.

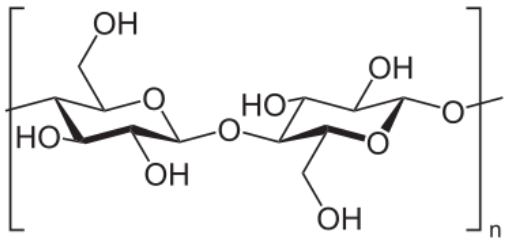

Figure 2.2. Structure of cellulose

http://en.wikipedia.org/wiki/Cellulose

Cellulose consisting of β (1→4) linked D-glucose units is a straight chain polymer. It has no coiling or branching, rather extended stiff rod-like conformation is found. Hydroxyl groups present on one chain shows hydrogen bonding with oxygen atoms present on same chain or other chain resulting in micro fibrils with high tensile strength. A temperature of 320°C and 25 MPa pressure is required for conversion of cellulose into amorphous state in water (Deguchi *et al.,* 2006).

On the bases of presence of hydrogen bonding between and within strands, various crystalline structures of cellulose are recognized. Natural cellulose is referred as cellulose I. It contains I_α and I_β strands. Bacterial cellulose is augmented in I_α while higher plants cellulose mainly contains I_β. Cellulose I can be converted into cellulose II. Similarly, cellulose III and cellulose IV are also reported at different conditions of temperature and pressure (Sherif, 2014).

Many properties of cellulose are attributed by various factors like chain length, degree of polymerization and number of glucose units etc. e.g. 300 and 1700 units are characteristics of wood pulp while cotton, plant fibers and bacterial cellulose have 800 to 10,000 units (Klemm *et al.,* 2005). Break down of cellulose into very small chain lengths results in structures referred cellodextrins. These are soluble in water and organic solvents as compared to long-chain cellulose.

Cellulose that is derived from plants is typically present in a mixture with pectin, lignin, hemicellulose and other substances. As far as bacterial cellulose is concerned it is quite pure, with greater water content and tensile strength attributed to longer chain lengths (Klemm *et al.,* 2005).

Cellulose contains crystalline and amorphous regions. Upon treating with strong acids, breakdown of amorphous region takes place resulting in nanocrystalline cellulose. Nanocrystalline cellulose is a novel material having looked-for attributes (Peng *et al.,* 2011).

2.2.4 Derivatives

Upon reaction with various reagents, hydroxyl groups (-OH) of cellulose reacts partially or fully and produce various derivatives having desired properties. For example many types of cellulose esters and cellulose ethers (-OR) are produced in this way.

Among ester derivatives cellulose acetate and cellulose triacetate are film forming derivatives with numerous uses. Nitrocellulose is regarded as early film forming substantial and used as an explosive.

Table 2.1. Ester derivatives

Cellulose ester	Example	Functional Group "R"
Organic esters	Cellulose triacetate	$-(C=O)CH_3$
	Cellulose acetate	H or $-(C=O)CH_3$
	Cellulose propionate	H or $-(C=O)CH_2CH_3$
	Cellulose acetate butyrate (CAB)	H or $-(C=O)CH_3$ or $-(C=O)CH_2CH_2CH_3$
	Cellulose acetate propionate (CAP)	H or $-(C=O)CH_3$ or $-(C=O)CH_2CH_3$
Inorganic esters	Cellulose sulfate	H or $-SO_3H$
	Nitrocellulose (cellulose nitrate)	H or $-NO_2$

Table 2.2. Ether derivatives

Cellulose ethers	Example	Functional Group "R" = H or
Alkyl	Ethyl cellulose	$-CH_2CH_3$
	Methylcellulose	$-CH_3$
	Ethyl methyl cellulose	$-CH_3$ or $-CH_2CH_3$
Hydroxyalkyl	Hydroxypropyl cellulose (HPC)	$-CH_2CH(OH)CH_3$
	Hydroxyethyl cellulose	$-CH_2CH_2OH$
	Hydroxyethyl methyl cellulose	$-CH_3$ or $-CH_2CH_2OH$
	Ethyl hydroxyethyl cellulose	$-CH_2CH_3$ or—CH_2CH_2OH
	Hydroxypropyl methyl cellulose (HPMC)	$-CH_3$ or $-CH_2CH(OH)CH_3$
Carboxyalkyl	Carboxymethyl cellulose (CMC)	$-CH_2COOH$

http://en.wikipedia.org/wiki/Cellulose

2.2.5 Applications

i. **Paper products:** Paper, card stock and paper board are mainly obtained from cellulose.

ii. **Fibers:** Cellulose is main constituent of linen and cotton textile industry. From it "rayon" can also be produced which is an important fiber for textile since start of 20th century.

iii. **Consumables:** A lot of uses of cellulose are found in pharmaceutical industry. In tablet manufacturing powdered cellulose (E460ii) and microcrystalline cellulose (E460i) are consumed as inactive fillers. Cellulose also has its role as thickener and stabilizer in processed food industry. Some cellulose powders are used to prevent caking inside package.

iv. **Science:** In research labs cellulose has many uses like stationary phase for (TLC) thin layer chromatography, filtration media either in combination with diatomaceous earth or alone, fillers, thickening agent and preservative etc.

v. **Building material:** Environment friendly building insulation obtained from recycling of paper is becoming popular. Cellulose materials which are alternative of plastics and resins and offer water and fire resistance are also becoming popular as these possess sufficient strength too.

vi. **Miscellaneous:** Thin transparent film cellophane can be made from cellulose. Nitrocellulose consumed as smokeless gunpowder, as base of photographic material celluloid, water soluble adhesives and binders come under some of its miscellaneous applications.

2.3 Graft Polymers

Graft copolymers are basically segmented copolymers residing linear back bone of one configuration and arbitrarily dispersed branches of other composite as represented in

figure 2.3. Grafted side chain though structurally different from main chain could be homopolymer/s or copolymer/s.

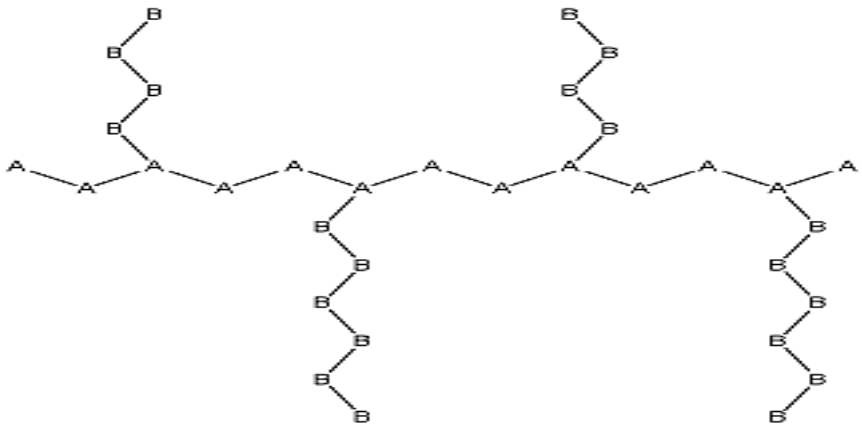

Figure 2.3. Graft copolymer
http://en.wikipedia.org/wiki/Graft_polymer

2.3.1 General properties

Being branched copolymer, graft copolymers are capable to form wormlike conformation and thus possessing confined and fit structures. Use of graft copolymers has its roots decade behinds. Various methods of preparation can be used to acquire various desired properties. They can be used in production of impact resistant materials, as compatibilizers or emulsifiers for stable blends or alloys and as thermoplastics elastomers (McNaught and Wilkinson, 1996). Grafting of copolymer generally results in more thermostable materials than that of their respective homopolymers (Jenkins *et al.*, 1996).

2.3.2 Methods of preparation

Three different methods have been reported for preparation of graft copolymers as depicted diagrammatically in figure 2.3 i.e.

a) Grafting onto
b) Grafting from
c) Grafting through

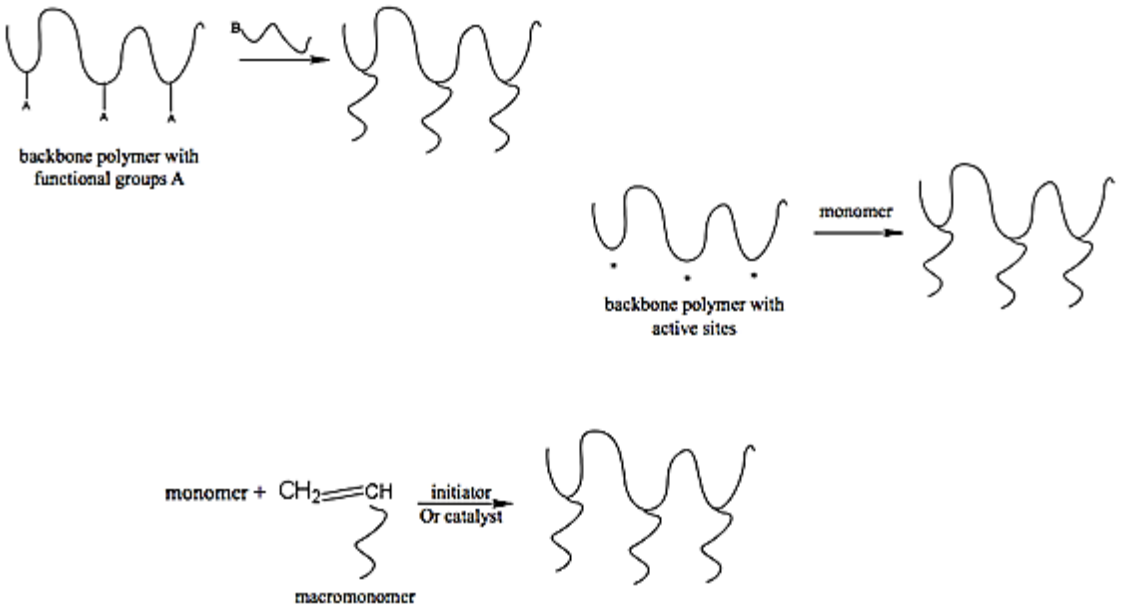

Figure 2.4. Grafting onto (top left), Grafting from (middle right), Grafting through (bottom left) and their generalized reaction scheme

2.3.2.1 Grafting onto

This method involves use of such backbone chain which bears functional groups "A". These functional groups have random distribution along chain. When functional groups present on main backbone and end groups of branches undergo coupling reaction graft polymer originates. These coupling reactions can be induced by chemical modification of backbone by various reaction mechanisms like atom-transfer radical-polymerization, free-radical polymerization, anionic polymerization and living polymerization. Grafting onto method usually use anionic polymerization technique. Without generation of reactive groups on polymer backbone this method could not be possible.

2.3.2.2 Grafting from

In this method macromolecular backbone is subjected to chemical modification to produce active sites which are capable of initiating functionality. These initiating sites can be incorporated in a post polymerization reaction or can previously be a portion of polymer backbone. Though number of branches along backbone can be controlled by

number of active sites along backbone but length of each chain may be different depending upon kinetic and steric hindrance effects. For grafting from synthesis of polymers various techniques like cationic grafting, anionic grafting, free radical polymerization and atom transfer radical-polymerization are employed.

2.3.2.3 Grafting through

To synthesize graft copolymer, monomer with lower molecular weight is copolymerized with macromonomer having an acrylate functionalized group using free radicals polymerization technique. Number of grafted chains is determined by aspects like ratio of monomer to macromonomer molar concentrations and copolymerization behavior. With change in concentrations of monomer to macro-monomer, random placement of branches occurs. Addition of these branches could be either heterogonous or homogenous depending upon reactivity ratio of terminal functional group to monomer (Koichi *et al.,* 1985). Though this method can utilizes any of known polymerization technique but living polymerization offers good control over the molecular weight and weight distribution.

2.3.3 Approaches of synthesis

For synthesis of graft copolymers, different approaches are there. These include;

a) Ring-opening metathesis polymerization (ROMP)
b) Atom transfer radical polymerization (ATRP)
c) Free radical living polymerization (FRLP)
d) Anionic and cationic polymerizations (ACP)

Some less common polymerization include;

a) Ring-opening olefin metathesis polymerization
b) Radiation-induced polymerization
c) Polycondensation reactions (Bellas and Rehahn, 2007).

2.3.4 Types of copolymers

As copolymers are composed of at least two different types of structural units, these can be classified on the basis of arrangement of these units (Jenkins *et al.*, 1996). Some important types are listed below:

a. **Alternating copolymers:** These have regular repeating alternative units e.g., A-B-A-B-A-B-A-B-A-B.

b. **Periodic copolymers:** In this type structural units are present in repeated sequence e.g., $(A\text{-}B\text{-}A\text{-}B\text{-}B\text{-}A\text{-}A\text{-}A\text{-}A\text{-}B\text{-}B\text{-}B)_n$

c. **Statistical copolymers:** In this type, structural units follow a statistical rule for sequence i.e., probability of presence of any type of monomer on a typical point of main chain is equal to mole fraction of that monomer. Thus units are randomly arranged and referred as truly random copolymer.

d. **Block copolymers**: These consist of two or more homopolymer units which are linked together by covalent bonds. There may be an intermediate non-repeating subunit, which is referred as a junction block. If block polymers have two distinct blocks then it is referred as di-block and if it possesses three then referred as tri-block copolymers.

On the bases of existence of or arrangement of branches, these can also be classified as;

a. **Linear copolymers**: It comprises of a single main chain.

b. **Terpolymer**: It comprises of three distinct monomers. (Origin, Latin word *"ter*" meaning thrice)

c. **Branched copolymers:** It comprises of a single main chain having one or more polymeric side chains. Other special types of branched copolymers include:

- Star copolymers
- Brush copolymers

- Comb copolymers

2.3.5 Applications of graft copolymers in pharmaceutical industry

Due to unique structure of graft copolymers as compared to copolymers, these have various applications in pharmaceutical industry.

Common applications include:

- Membranes for the separation of gases or liquids
- Polymeric emulsifiers
- Drug deliverers
- Thermoplastic elastomers
- Hydrogels
- Compatibilizers for polymer blend

2.4 Gel

Gel was first made by Thomas Graham, Scottish chemist in 19th-century. According to IUPAC definition of gel it is non-fluid colloidal network which enlarges throughout its entire volume by a fluid. Gel can be described as jelly like solid material which covers properties of soft and weak to hard and tough materials. Gels are considerably dilute crosslink system presenting no flow in steady state. It is crosslinking structure within gel that imparts hardness (Sing, 1985).

2.4.1 Types of gels

Following are some important types of gels

- Hydrogels
- Organogels
- Xerogels

2.4.2 Hydrogels

2.4.2.1 Introduction

Term hydrogel was first described in 1894. Hydrogels are hydrophilic polymeric chains network often found in colloidal gel where water acts as dispersion medium (Enas *et al.,* 2013). Over the years, researcher has used many days to define hydrogels. Most common definition of hydrogel is that it is water swollen polymeric crosslink network simply formed by reaction of one or more monomers. In other way it can be defined as polymeric network capable to swell and hold ample portion of water but importantly will not dissolve in water. Over past 50 years, hydrogels have gained considerable attention because of their wide range of applications (Brannon and Harland, 1991; Yuhui *et al.,* 2013). Hydrogels are highly absorbent in nature and can hold over 90% of water which possess degree of flexibility near to natural tissues (Peppas and Khare**,** 1993).

Water absorption ability of hydrogels can be attributed to hydrophilic functional groups present on polymeric backbone while their resistance to dissolution is attributed to crosslinking between polymeric network chains. Both naturally occurring and synthetic materials fit definition of hydrogels. During past two decades, synthetic hydrogels have replaced natural Hydrogels because of their various preferable quality attributes like longer service life, greater water absorption capacity and greater gel strength. Actually synthetic polymers possess well defined polymer network structures that can be modified to attain desired degradation and functional profile. Moreover, synthetic hydrogels are stable over sharp and strong variations of temperatures.

Now a days hydrogels fit definition of two or multi component systems containing three-dimensional polymer network and water which fills spaces present between macromolecules. On the basis of polymer properties and nature and density of network joints, hydrogels can retain various amounts of water. In swollen state this water absorption and retention capacity is greater as compared to non-swollen state. Water soluble polymers are preferable for synthesis of synthetic hydrogels. Hydrogels can contain chemical crosslink via covalent bonds, physically crosslinking via non-covalent interactions or may contain combination of both. Its water retaining capacity can be

attributed to capillaries action or osmotic and hydration forces created by polymer chain network (Roorda *et al.,* 1986).

Various "classical" chemical ways to synthesize hydrogels are there. One way involves one-step procedures i.e. polymerization with parallel crosslinking of multifunctional monomers. Other way involves multiple step procedures which involve synthesis of polymer molecules with reactive groups and then their subsequent crosslinking usually by suitable crosslinking agents. By synthetic hydro gels good controlled over desired properties like biodegradation, mechanical strength and response to chemical/biological stimuli can be attained (Sina *et al.,* 2007).

2.4.2.2 Classification

Hydrogels can be classified in different ways detailed below:

a) Classification based on source

Hydrogels can be classified on the bases of source of constituent polymer/monomer as;

- **Natural hydrogels**, consisting of natural polymers/monomer
- **Synthetic hydrogels**, containing synthetic polymer/monomer
- **Hybrid hydrogels**, having combination of both natural and synthetic polymer/monomer (Zhao *et al.,* 2013).

b) Classification according to polymeric composition

On the bases of polymeric composition, hydrogels can be classified as:

i. **Homopolymer hydrogels:** Polymeric network arisen from single species of monomer is referred as homopolymers. It is basic structural unit of any polymer network. Structure of crosslink network depends upon factors like nature of monomer and polymerization technique (Takashi *et al.,* 2007).

ii. **Copolymer hydrogel:** These consist of two or more different monomers having at least one hydrophilic component. These are arranged randomly or in blocks or alternating configuration along polymer backbone (Yang *et al.,* 2002).

iii. **Multipolymer Interpenetrating polymeric hydrogel (IPN):** These consist of two independent crosslink synthetic and/or natural polymer networks. In case of semi-IPN, one polymer is a crosslink and other is a noncrosslink (Maolin *et al.,* 2000).

c) Classification based on configuration

On the basis of physical or chemical composition, hydrogels can be classified as follows:

i. Amorphous (non-crystalline)
ii. Semi-crystalline (combination of amorphous and crystalline states)
iii. Crystalline

d) Classification based on type of crosslinking

On the bases of nature of crosslinking, hydrogels can be classified into two classes.

i. **Chemically crosslink hydrogels:** having permanent network junctions

ii. **Physical crosslink hydrogels:** having transient network junctions arising from either polymer chain entanglements or physical interactions.

e) Classification based on physical appearance

By virtue of technique of polymerization, hydrogels could appear as matrix, film or microsphere.

f) Classification according to network electrical charge

By virtue of presence or absence of electrical charge, hydrogels can be classified as;

i. Nonionic (neutral)
ii. Ionic (anionic or cationic)
iii. Amphoteric electrolyte (containing both acidic and basic groups)
iv. Zwitterionic (having both anionic and cationic groups in each structural repeating unit)

2.4.2.3 Hydrogel product sensitive to environmental conditions

Being three dimensional crosslink structure, hydrogels can swell or deswell in water reversibly and in swollen state can entrap large volume of water. Hydrogels can be designed in such a way that their responsiveness to change in external environment can be controlled by reversible swelling and deswelling. There is variety of physical and chemical stimuli in response to which hydrogels show dramatic volume transition. Among physical stimuli there is temperature, pressure, electric or magnetic field, light and sound. While solvent composition, pH, ionic strength and molecular species enlisted under chemical stimuli (Jinsub *et al.*, 2010). Response of hydrogels to various stimuli is represented in figure 2.5.

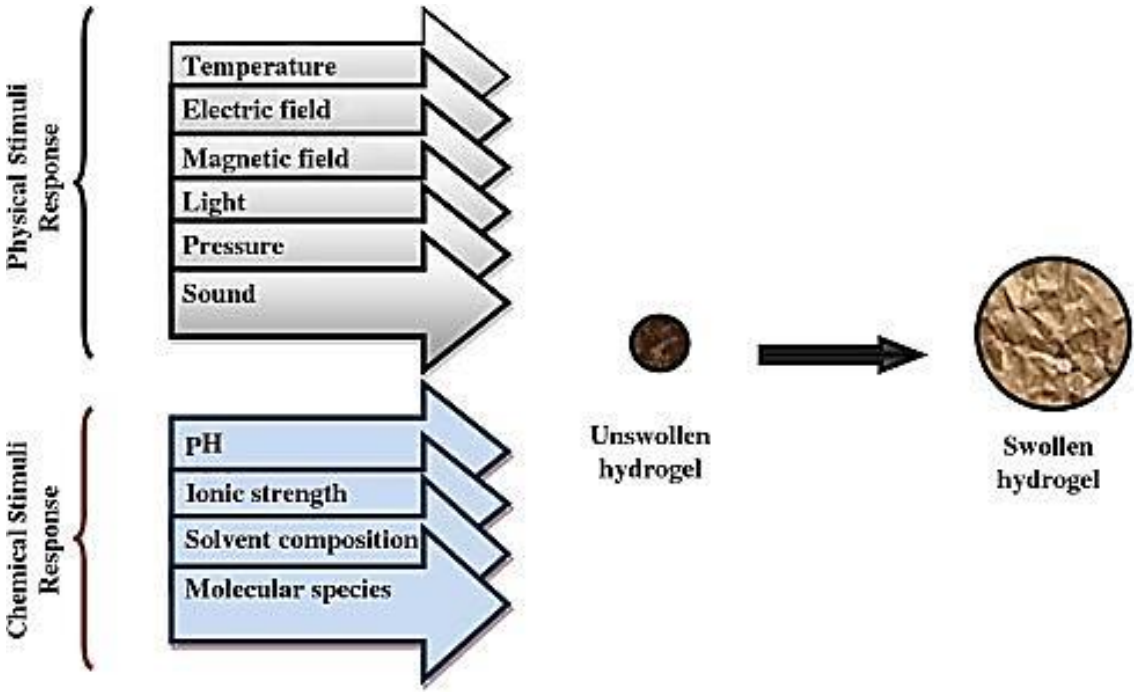

Figure 2.5. Response of hydrogel to various stimuli

Synthetic hydrogels have gained great attention in research field from last four decades and still is of great focus.

2.4.2.4 Uses of hydrogel products

First synthetic hydrogel was formulated by Wichterle and Lim in 1954 (Wichterle and Lim, 1960) after that hydrogel found their application in many field, like;

- Hygienic products (Singh *et al.,* 2010)
- Agriculture (Amulya, 2010)
- Drug delivery systems (Mehrdad *et al.,* 2009) and sealing (Singh *et al.,* 2010)
- Coal dewatering (Sun *et al.,* 2002)
- Artificial snow (Singh *et al.,* 2010)
- Food additives (Chen *et al.,* 1995).
- Pharmaceuticals (Kashyap *et al.,* 2005)
- Biomedical applications (Sachiko *et al.,* 2008; Dimitrios *et al.,* 2008)
- Tissue engineering and regenerative medicines (Ling *et al.,* 20011)
- Diagnostics (Van *et al.,* 2003)
- Wound dressing (Panprung *et al.,* 2011)
- Separation of biomolecules or cells (Feng *et al.,* 2010)
- Barrier materials to regulate biological adhesions (Debashish *et al.,* 2010)
- Biosensor (Peter *et al.,* 2009)

2.4.2.5 Techniques adopted in hydrogel preparation

Both natural and synthetic polymers can be used for preparation of hydrogels. Synthetic polymers are chemically stronger compared to natural polymers and possess greater mechanical strength but results in slow degradation (Tabata, 2009). So optimal designed should be preferred by using either natural or synthetic polymers with suitable functional groups (Shantha and Harding, 2002).

As hydrogel is a hydrophilic polymeric crosslink network, so any method that can create crosslink network can be employed to formulate hydrogel. Most commonly copolymerization/crosslinking free-radical polymerizations are used.

Various polymerization approaches listed as below:

1. Chemical reaction polymerization
2. Radiation polymerization
3. Physical interactions like entanglements and electrostatics

For the formation of gel, any polymerization techniques can be used including bulk, solution and suspension polymerization.

Generally, hydrogel preparation involves three integral components i.e. monomer, initiator, and crosslinker. Various types of diluents like water or other aqueous solutions are employed to have control over heat of polymerization and final hydrogels properties. Process impurities including non-reacted monomer, initiators, crosslinkers, and unwanted products needed to be washed. General representation of hydrogel preparation is shown in figures 2.6.

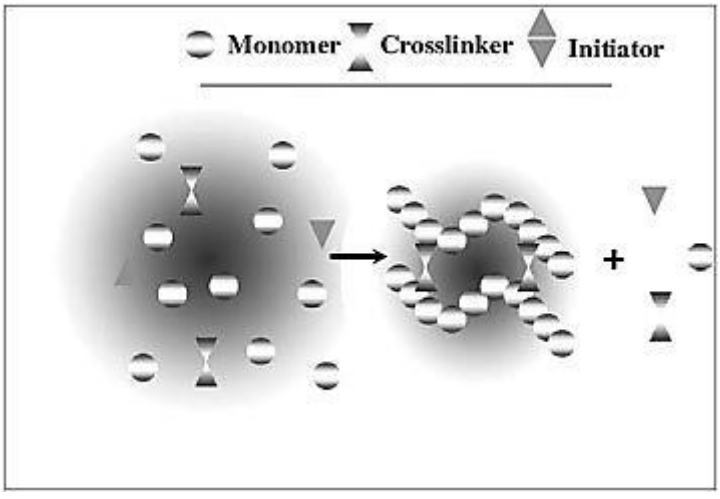

Figure 2.6. General method of hydrogel preparation

Acrylamide, acrylic acid and its salts based hydrogels were prepared by inverse-suspension polymerization (Raju and Raju, 2001). Solution polymerization of highly concentrated acrylic monomers solution was prepared (Takeda and Taniguchi, 1985). In 2000 Chen formulated acrylic acid sodium acrylate superabsorbent hydrogels via concentrated solution polymerization technique (Chen and Zhao, 2000).

Major polymerization methods have been stated below:

a) Bulk polymerization

One or more types of monomers can be employed for bulk hydrogel preparation. Wide variety of monomers is available to form a range of hydrogel with desired profile. For hydrogel preparation usually very small amounts of crosslinkers are needed. Polymerization can be initiated with ultraviolet radiation or chemical catalysts. Selection of appropriate initiator depends upon type of monomers and solvents being employed. Polymerized hydrogel can be prepared in the form of films, membranes, particles, rods and emulsions.

It is regarded as one of the simplest technique involving monomer and monomer soluble initiators. As concentration of monomer/s increases rate of polymerization increases while viscosity increases with conversion that generates heat. The problem can be overcome by continuing reaction at low conversion rates (Kiatkamjornwong *et al.*, 2007). As a result of bulk polymerization, homogenous glassy, transparent and hard hydrogels are produced which swell in water resulting in soft and flexible product.

b) Solution polymerization

In solution copolymerization/crosslinking reactions, the ionic or neutral monomers are mixed with multifunctional crosslinking agent. The polymerization is initiated thermally by UV-irradiation or by a redox initiator system. The presence of solvent serving as a heat sink is the major advantage of the solution polymerization over the bulk polymerization. The prepared hydrogels need to be washed with distilled water to remove the monomers, oligomers, crosslinking agent, the initiator, the soluble and extractable

polymer, and other impurities. Phase separation occurs and the heterogeneous hydrogel is formed when the amount of water during polymerization is more than the water content corresponding to the equilibrium swelling.

Typical solvents used for solution polymerization of hydrogels include water, ethanol, water–ethanol mixtures, and benzyl alcohol. The synthesized solvent may then be removed after formation of the gel by swelling hydrogels in water.

c) Suspension polymerization

It is an advantageous method as products are obtained in the form of powder or microspheres (beads) where no grinding is needed. In this method, dispersion of monomers and initiator in the hydrocarbon phase is formed as a homogenous mixture. In this technique particle size depends upon various factors like viscosity of monomer solution, rotor design, agitation speed and dispersant type (Tomonari *et al.*, 2006).

d) Grafting to a support

In this method free radicals are generated on the surface of stronger support, then chain of monomers are covalently attached on this surface. Thus, mechanical properties of hydrogel are improved. Various types of polymer supports are employed for the synthesis of hydrogel by this method (Talaat *et al.*, 2008; Tong and Zhang, 2005)

e) Polymerization by irradiation

High energy radiations e.g., gamma rays (Karadao *et al.*, 2001) and electron beams (Ajji *et al.*, 2008) could be useful as an initiator. This method could be employed for unsaturated compounds. Radicals are formed on polymer chain by irradiation of aqueous polymer solution. Moreover, hydroxyl radicals are formed by radiolysis of water molecules. These hydroxyl groups attack the polymer chains to form macro-radicals. These macro-radicals are covalently bonded on different chains resulting in the formation of crosslink structure.

2.4.2.6. Swelling behaviour of hydrogels

The most desirable characteristic of hydrogels is their ability to swell, when come in contact with a compatible solvent. In initial state, solvent molecules attack hydrogel surface and start penetrating in polymeric network resulting in surface rubbery phase. In such situation unsolvated glassy phase remains separated from rubbery state with a moving boundary. Rubbery phase continue expanding on regular bases thus solvent penetrates throughout polymeric network. Achilleos *et al.* (2000) has studied dynamic deformation of hydrogels during swelling. Against osmotic force an opposite force is acting referred as elasticity force, which balances network stretching and thus avoids deformation of polymeric network. At swelling equilibrium both elasticity and osmotic forces are in balance state so no further swelling occurs (Vervoort *et al.*, 2005).

When hydrogels are neutral in nature, Van der Waals repulsive forces between monomer are suppressed by applied pressure resulting in decreased gel volume. While considering polyelectrolyte hydrogels pressure of counter-ions will restrict applied pressure resulting in large solvent volume release (Vervoort *et al.*, 2005).

Swelling rate is also another important feature of hydrogel determined by various physicochemical properties of hydrogel like type of porous structure and extent of porosity. On the basis of porosity, hydrogels can be classified into following four classes which are given in table 2.3;

Table 2.3. Swelling behaviour of different types of hydrogels

Type	Swelling mechanism	Morphology	Swelling rate	Application
Micro-porous	Combination of diffusion and confection through water filled channels	Varying porosity having closed cell structure (100-1000 A˚)	Depends upon sample size, generally slow	Various biomedical applications and controlled release techniques
Macro-porous	Diffusion through water filled channels	Varying porosity having closed cell structure (0.1-1µm)	Depends upon sample size, generally fast	Used in baby diapers
Non-porous	Diffusion through free volumes	No pores	Depends upon sample size, generally very slow	Various applications ranging from contact lenses to artificial muscles
Super-porous	Capillary forces	Highly porous having inter connected open cell structure	Depends upon sample size, generally very fast	Drug delivery system spatially for delivery to GIT

(Fariba *et al.,* 2010)

In view of Lowman definition, non-porous gels have molecular sized pores. That's why non porous hydrogels are densely packed resulting in limited solute transport by diffusion process. So degree of hydration depends upon diffusion coefficient of solute in membrane to diffusion coefficient of solute in pure solvent.

Dry state hydrogel volume and hydrogel volume in equilibrium swollen state can be calculated by following equations i.e., equation 2.1 and 2.2 (Hickey and Peppas, 1997; Hamid and Oguz, 1996).

$$\mathrm{Vs} = \frac{m_{a,s} - m_{h,s}}{\rho_h} \qquad \text{(Equation…… 2.1)}$$

$$\mathrm{Vs} = \frac{m_a - m_h}{\rho_h} \qquad \text{(Equation…… 2.2)}$$

Where m_a denotes mass of initial dry polymer in air and m_h mass of dry polymer in n-heptane while $m_{a,s}$ is mass of swollen hydrogel in air in swelling equilibrium state, $m_{h,s}$ is mass of swollen hydrogel in n-heptane in swelling equilibrium state. Where "h" refers to density of n-heptane (0.688 g cm^{-3}).

2.4.2.7. Mechanism of release from hydrogels

Depending upon type of polymer, additives, drug, pore size and shape, method of preparation, experimental conditions and various other physic-chemical phenomena affect drug release kinetics.

Depending on the composition of hydrogel (type of polymer, type of drug and additives), geometry (size and shape), preparation technique and environmental conditions during drug release, one or more of the following physical and chemical phenomena affect the drug release kinetics (Siepmann and Siepmann, 2008; Siepmann and Gopferich, 2001):

1. Wetting of the drug delivery device
2. Degradation of drug/polymer
3. pH changes inside the hydrogel matrix
4. Creation of pores filled with water
5. Diffusion of drug inside the hydrogel matrix
6. Swelling of polymer
7. Osmotic effects

All above mentioned phenomena could not be considered simultaneously. Only prominent physical and chemical processes are taken into account by any mathematical model. Moreover these phenomena only consider drug transport in model system rather in living organism. While considering drug transport in living organism, various additional phenomena become important like enzymatic degradation, active and passive transport, protein binding, drug interactions with compounds in extra and intracellular space (Siepmann and Siepmann, 2008).

Regarding process engineering, release mechanism involves following phenomena:

i. Exterior diffusion
ii. Interior diffusion
iii. Desorption
iv. Chemical reactions

i. Exterior diffusion

Release mechanism collectively consists of exterior and interior diffusion processes. In exterior diffusion from surface of hydrogel drug molecules diffuse into bulk of solvent. In this process mass transfer can be described as below:

The rate of mass transfer can be described by the following expressions:

$$N_A = K_L(C^*_{AL} - C^{\delta}_{AL}) \qquad \text{(Equation ……..2.3)}$$

$$G_A = k_L A\left(C^*_{AL} - C^{\delta}_{AL}\right) \qquad \text{(Equation ……..2.4)}$$

Here:

NA	Drug flux
kL	Mass transfer coefficient
GA	Mass transfer rate
C^*_{AL}	Surface concentration of drug
A	Area of mass transfer
C^{δ}_{AL}	Bulk concentration of drug

ii. Interior diffusion

Generally release rate is controlled by interior diffusion.

In general, the rate of drug release is controlled by interior diffusion. Fick's law based theories describes two distinguish types of systems which are diagrammatically represented in figure 2.7 i.e.

a) Reservoir type devices

b) Monolithic type devices

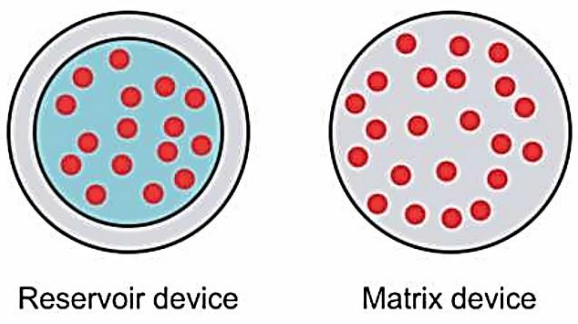

Figure 2.7. Reservoir and matrix type device

a) Reservoir type devices

In this type of system, pure drug, drug solution or suspension is enclosed by a polymer membrane (Arifin *et al.,* 2006; Bajpai *et al.,* 2008). In such systems diffusion of drug from membrane is derived by concentration gradient that is rate limiting step. Sink condition I achieved then drug is diffused into surrounding device. This drug diffusion can be elaborated by Fick's first law of diffusion.

where:

J	Drug flux
D	Diffusion coefficient
ϕ	Concentration in dimensions of amount of substance per unit volume
$\varkappa$	Length in "m"

$$J = -D \frac{\partial \emptyset}{\partial x} \qquad \text{(Equation……. 2.5)}$$

b) Matrix type devices

In matrix-type devices, drug release is followed by Fickian diffusion, which is related with concentration gradient, diffusion length and the degree of swelling (Siepmann and Siepmann, 2008).

iii. Simultaneous diffusion and desorption of drug

Drug molecules can be adsorbed either chemically or physically on the pore surface either physically or chemically (Berger *et al.,* 2004). In case of chemical adsorption, electronic density of adsorbate molecule is altered while in case of physical adsorption, adsorbate molecule show weak adherence secondary interactions like van der Waals forces.

iv. Chemical reactions

Various types of chemical reactions taking place during drug release can result in drug or polymer degradation resulting in various degradation products. When dissolution media diffuses with in hydrogel it can react chemically with these degradation products. This reaction can be slow, fast, reversible, irreversible, simple or complex resulting over all diffusion or release process.

2.4.2.8. Features of an ideal hydrogel

The functional characteristics of an ideal hydrogel are given below (Mohammad and Kourosh, 2008):

- Greatest absorption capacity in basic medium
- Desired absorption or release profile
- Less soluble content and monomer residues
- Economical
- Appealing stability upon storage and in swelling medium
- Biodegradability, no toxic residues
- Odorless

- Photo stability
- Re-wetting capability

2.4.2.9. Applications

Common uses of hydrogels are;

- In tissue engineering as scaffolds for tissue repair
- Hydrogel coated wells for cell culture (Amir *et al.,* 2014)
- Smart hydrogels for targeted delivery
- Sustain release drug delivery
- Used as biosensor
- Used in contact lenses
- EEG and ECG medical electrodes using hydrogels
- Rectal drug delivery and diagnosis

2.4.3. Organogels

Organogels are thermoplastic solid material which is non-crystalline and non-glassy consisting of liquid organic phase that is enclosed by a three dimensionally crosslink network. Liquid could be mineral oil, vegetable oil or organic solvent. Firmness or elastic properties of organogels are two important factors that control solubility and particle dimensions of structure. Organogels have various applications in different areas like pharmaceuticals (Kumar and Katare, 2005), cosmetics, art conservation (Carretti *et al.,* 2005) and food (Pernetti *et al.,* 2007).

2.4.4. Xerogels

A gel which is formed by drying with unhindered shrinkage is referred as xerogel. It possesses greater porosity (15–50%). When solvent is removed under various conditions, network does not shrink resulting in highly porous, low-density material referred as an aerogel.

2.5. Polymers and advanced drug delivery system

Initial use of polymers as stabilizers, solubilizes and mechanical supporter has now been replaced by various other functionalities of polymer e.g. specific need or problem solving ability of polymer in various advanced drug delivery systems. Regarding advanced drug delivery systems polymers can be classified on various bases are given in table number 2.4, 2.5, 2.6 and 2.7 as follows (Chandel and Rajkumari, 2013):

Table 2.4. On the basis of source

Natural	Synthetic	Semi synthetic
Alginate, Albumin, Dextran, Polyethylene glycol (PEG), Chitosan, Gelatin, Collagen, Cyclodextrin	Polyethylene, Polyglycolic acid, Polylactic acid, Polyhydroxy butyrate, Polypropylene, Poly acrylamide	Hydroxy propyl cellulose (HPC), Hydroxy propyl methyl cellulose (HPMC), Methyl cellulose (MC), Hydroxy ethyl cellulose, Sodium carboxymethyl cellulose (Na-CMC)

Table 2.5. On the basis of type of polymerization

Addition polymer	Condensation polymers
Poly ethylene glycol, Polyvinyl chloride, Polypropylene	Polyester, polyurethane

Table 2.6. On the basis of degradability

Biodegradable	Non-biodegradable
Polyglycolic acid, Polylactic acid, Polyanhydrides, Polycarpolactone	Polyether urethane, Polydimethyl siloxane, Ethyl cellulose

Table 2.7. On the basis of nature of water polymer interaction

Hydrophobic polymer	Hydrophilic polymer	Hydrogel material
Polydimethyl siloxane, Ethyl cellulose	Methyl cellulose, Hydroxypropyl methyl cellulose, Sod. Carboxymethyl cellulose, Sodium alginate, Xanthan gums, Guar gum, Pectin	Polyethylene oxide, Crosslink polyvinyl alcohol, Polyacrylamide

(Chandel and Rajkumari, 2013)

2.5.1. Hydroxy propyl methyl cellulose (HPMC)

HPMC chemically shown as $C_6H_7O_2(OH)_x(OCH_3)_y(OC_3H_7)_z$ where $x + y + z = 3$ (Sunil, 2011). Structure of HPMC is shown in figure 2.8.

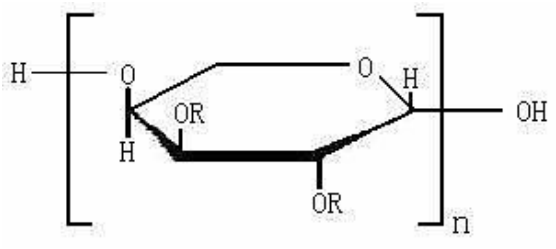

Figure 2.8. Structure of HPMC
Where n is number of glucose units in cellulose molecule

It is tasteless, odorless white to off white free flowing powder regarded as semisynthetic and hydrophilic polymer. It is produced by modification of alkali cellulose by treating it with 18% sodium hydroxide solution. It has many valuable applications e.g., used as basic material for sustained release formulations, as enteric coating film material and as matrix binders. As it has non-toxic, easy compression, appealing swelling profile and greater drug loading capacity, so it is an ideal candidate for oral drug delivery system when sustain release profile is needed (Croweley *et al.,* 2000).

On the basis of desired properties or application, degree of substitution of HPMC can be varied as added groups/molecules, impart various unique or desired properties. Ideal properties for its wide spread acceptance includes (Kajal *et al.,* 2011):

1. Wide range of solubility profile in GI fluids and in various aqueous solvent systems
2. Attractive stability profile in numerous conditions like light, heat or moisture etc.
3. Capacity to accommodate color and other additives
4. Biocompatibility, biodegradability and non-toxic profile
5. Easy availability and handling
6. Attribute for an ideal film coating material
7. Ideal candidate for controlled release drug delivery system (Kajal *et al.,* 2011)

In virtue of high swellability and thermal gelation properties, HPMC has gained attention as important carrier material for advance drug delivery systems (Kajal *et al.,* 2011).

2.5.2. Sodium carboxy methyl cellulose (Sod. CMC)

As name indicates it is a cellulose derivative in which carboxymethyl groups (-CH_2-COOH) are linked with the hydroxyl groups of glucopyranose. Chemically it is $[C_6H_7O_2(OH)_x(OCH_2COONa)_y]_n$ where n is degree of polymerization, x = 1.50 to 2.80, y = 0.2 to 1.50, (y = degree of substitution). Structure of CMC is shown in figure 2.9.

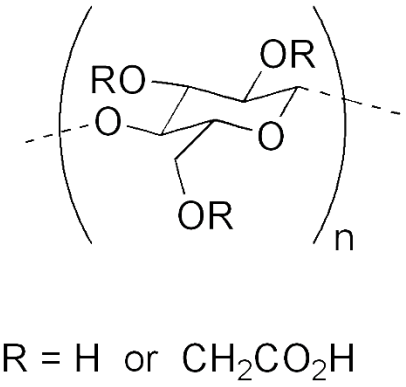

Figure 2.9. Structure of CMC

Physically it is odorless white or slightly yellowish hygroscopic granules, powder or fine fibers. It is classified as semisynthetic hydrophilic anionic polymer. It is produced from cellulose by treating with alkali and chloroacetic acid. Its polar groups impart solubility and chemically reactivity resulting in its increased functionality. Its functional properties are attributed to (Croweley *et al.,* 2002);

a) Hydroxyl groups taking part in reaction
b) Chain length of cellulose back bone
c) Degree of clustering of carboxymethyl groups

It has numerous reported applications like in food industry, various paper products, stabilizer, viscosity modifier, thickening agent, suspending agent lubricant in artificial tears. It also has wide spread acceptance as controlled/advanced drug delivery system. It is also employed to characterize enzyme activity (Croweley *et al.,* 2002).

2.5.3. Acrylic acid (AA)

Structure of acrylic acid is shown in figure 2.10.

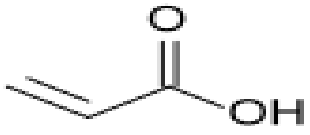

Figure 2.10. Structure of AA

Acrylic acid (prop-2-enoic acid) is an organic compound having formula CH_2=$CHCO_2H$. It is one of the simplest unsaturated carboxylic acid containing vinyl group linked with terminal carboxylic acid group. It is a colorless liquid with characteristic tart smell. As far as miscibility is concerned, it is miscible with chloroform, alcohols, water and ethers.

A byproduct of ethylene and gasoline production called propene which is used to produce acrylic acid. It undergoes typical carboxylic acid reactions. It formulates respective ester upon treating with an alcohol. Acrylic acid salts are referred as propenoates or acrylates which include methyl butyl ethyl acrylate and 2-ethylhexyl acrylate. Acrylic acid and esters have ability to combine with themselves or with other monomers to form homopolymers or copolymers.

Being severely irritating and corrosive in nature it can damage skin, respiratory tract and eyes. However, low exposure levels had no health hazard.

Due to presence of carboxylic acid groups, ionic repulsion is produced imparting pH sensitivity to material. That's why it can cause complexes with polybases (Ray *et al.,* 2008). All these characteristics make it ideal for advanced delivery systems (Dimitrov *et al.,* 2003).

Its pharmaceutical applications include drug delivery systems for nasal, gastrointestinal, buccal, ocular and transdermal use as it is a biocompatible material and have little

antigenic profile (Huang *et al.*, 2007). High tolerance profile of acrylic acid has been exhibited in living cells (Fournier *et al.*, 2003).

2.5.4. Hydroxyethylmethacrylate (HEMA)

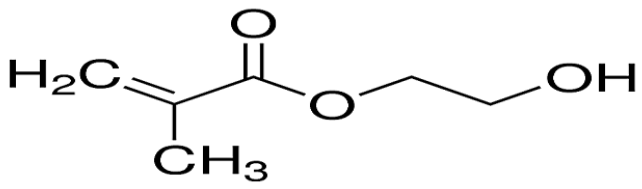

Figure 2.11. Structure of HEMA

Structure of HEMA is given in figure 2.11**.** 2-Hydroxyethylmethacrylate (HEMA) (molecular formula $C_6H_{10}O_3$ having molecular weight 130.14 g mol^{-1}) is a hydrophilic monomer but upon contact with water it swell because of molecule's hydrophilic pendant group. This monomer is employed to formulate polymer polyhydroxyethylmethacrylate. In combination with various other polymers or monomers it is used to synthesize new formulations with desired characteristic. On the basis of physicochemical properties it can absorb 10 to 600% water as compared to its dry weight. This property makes it first materials to be positively employed in the synthesis of flexible contact lenses.

It is a colorless liquid with pungent smell. Its acute toxicity profile is low (Oral LD50 > 4000 mg/kg; Dermal LD50 > 3000 mg/kg). It is somewhat irritating to skin and moderately irritating to eyes. It is hydrolyzed to methacrylic acid and ethylene glycol (Podkoecielna *et al.*, 2012).

2.5.5. Methacrylic acid (MAA)

Methacrylic acid (an organic compound) is a colorless viscous liquid having unpleasant smell. It has good solubility profile in warm water. It is miscible with lots of organic solvents. Structure of Methacrylic acid is shown in figure 2.12.

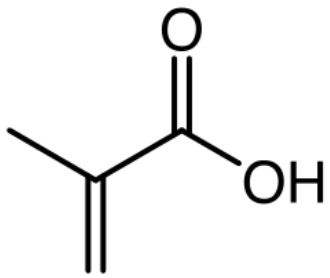

Figure 2.12. Structure of Methacrylic acid
Source: http://en.wikipedia.org/wiki/Methacrylic_acid

Various uses of MAA has been reported e.g. used in manufacturing of polymers such as Lucite and Plexiglas. Methacrylic acid was initially obtained as its ethyl ester by treating phosphorus pentachloride with oxyisobutyric ester. It can also be prepared by boiling citra- or meso-brompyrotartaric acids with alkalis. Methacrylic acid its self naturally obtained from oil of Roman chamomile in small amounts. MAA has distinctive properties as carriers for various types of drugs (Aaron and Nicholas, 2004; Ahmet *et al.*, 2002).

2.6 Angina

Transient myocardial ischemia can lead to chest pain that is termed as angina or angina pectoris. Various diseases like coronary artery disease, as atherosclerosis and aortic stenosis can lead to situation called angina. The root cause of angina involves vasospasm of coronary arteries. One of the reasons of coronary vasospasm includes enhanced Rho kinase activity. This increased level of Rho kinase activity inhibits myosin phosphatase activity resulting in enhanced calcium sensitivity and ultimately leading to hypercontraction (Kandabashi *et al.,* 2000). Rho-kinase also causes reduction in nitric oxide synthase resulting in decreased nitric oxide concentrations (Takemoto *et al.,* 2002). Angina can be really severe in some cases; even in start of 20th century this was acknowledged to be a forerunner of death. Current therapeutic regimens has somehow overcome problem. Morbidity rate was found 8% approximately in 62 years old age people with complaint of moderate to severe angina (William *et al.,* 2014).

2.6.1 Classification

Angina can be classified into different types as given below:

a) Stable angina
b) Unstable angina
c) Microvascular angina

2.6.1.1 Stable angina

It is typical kind of angina associated with myocardial ischemia also called as *effort angina*. Its characteristic presentations include chest discomfort and activity related symptoms (like walk, stairs climbing or running). Its symptoms are relieved or minimized by rest or taking sublingual nitroglycerin (Tobin, 2010). Other factors that aggravate symptoms include heavy meals, cold weather and emotional stress.

2.6.1.2 Unstable angina

It is referred as angina pectoris which changes or worsens with time. It is also called as "crescendo angina" which is a type of acute coronary syndrome.

One or more of following features can be depicted in unstable angina;

- ❖ It usually stays for 3-5 minutes occurring at rest or even with less exertion
- ❖ Within early 4-6 weeks it worsens with new onset
- ❖ It has a an outline in which symptoms get worsen, prolonged and frequent

Unpredictable attack of unstable angina at rest could be serious pointer of an imminent heart attack. Pathophysiology of atherosclerosis is a major difference between stable angina and unstable angina. In unstable angina coronary flow is decreased because of transient platelet aggregation, coronary artery spasms or coronary thrombosis which is basic pathophysiology of unstable angina (Hombach *et al.,* 1998). It involves development of atheroma which is covered by fibrous cap referred as atherosclerotic plaque. Rupture of this atherosclerotic plaque in unstable angina results in blood clots

causing narrowing of coronary vessel's lumen. This pathophysiology depicts how unstable angina is independent of activity.

2.6.1.3 Microvascular angina

This type of angina is recognized by chest pain, in view of normal epicardial coronary arteries upon angiography. It is also called as Syndrome X depicting that patient shows ischemic changes on exercise (ST depressions with stress) instead of normal coronary arteries. Since microvascular angina is not characterized by major arterial blockages, it is harder to recognize and diagnose. Basic reason of microvascular angina is not known but some aggravation factors include reduced blood flow as a result of spasm and resistance of blood vessels of heart. As microvascular angina is not caused by arterial blockages, it is difficult to identify and diagnose.

2.6.2 Signs and symptoms of angina pectoris

Typical symptoms include:

- Chest pain (moderate to severe)
- Chest discomfort (tightness, heaviness, burning, squeezing, pressure or choking sensation)
- Pain in inner left arm, upper central abdomen, neck, jaw, back or shoulders
- Breathlessness
- Rarely sweating
- Increased pulse rate and blood pressure
- Rarely autonomic symptoms, nausea and vomiting

2.6.3 Major risk factors for angina

Major risk factors include:

- Age ($\geq$ 55 for females, $\geq$ 45 years for males)
- Cigarette smoking
- Dyslipidemia

- Diabetes mellitus
- Family history (e.g., premature heart disease)
- High cholesterol
- High blood pressure
- Hypertension
- Obesity (Body mass index ≥ 30 kg/m2)
- Kidney disease (GFR<60 mL/min)
- Physical stillness
- Persistent psychosocial stress

(Chobanian *et al.,* 2003; Linden *et al.,* 1996; Sun *et al.,* 2002)

Avoiding these risk factor and life style modification can reduce chance of occurrence (Moyer, 2012).

2.6.4 Clinical Situations enhancing risk factors

- Medications
- Hypovolaemia
- Hypervolaemia
- Anemia
- Hyperthyroidism
- Tachyarrhythmia
- Bradyarrhythmia
- Valvular heart disease
- Hypertrophic cardiomyopathy

(Daly *et al.,* 1985; Daly *et al.,* 1983; Shinozaki *et al.,* 2008)

2.6.5 Treatment

Basic aim of treating angina pectoris is to relief symptoms and reduce advancement of disease and avoid future events like heart attacks and even death. Morbidity and mortality can significantly be reduced by using beta blockers (e.g. carvedilol, atenolol

and propranolol). For symptomatic treatment of angina pectoris short acting nitroglycerin has been employed since 1879. Moreover, isosorbide mononitrate, calcium channel blockers (e.g., nifedipine and amlodipine) and nicorandil are commonly recommended vasodilators for chronic stable angina (Sulfi and Timmis, 2006). Minimal dose of aspirin lessen chances of heart attack in patients having complaint of chronic stable angina and it takes position as part of standard treatment. However, because of greater risk of haemorrhagic stroke and gastrointestinal bleeding, are limiting factor of aspirin use and now it is not advised until risk of infarction is really high (Barnett *et al.,* 2010). Regular physical activity or exercise is good long term management for angina (Ades *et al.,* 1993).

2.7 Nicorandil

2.7.1 Introduction

Nicorandil (IUPA name; 2-(pyridine-3-carbonylamino)ethyl nitrate is a derivative of niacinamide. It is a vasodilator indicated for angina having dual properties of nitrate and K^+ATP channel agonist. Nitrate component of nicorandil dilates large coronary arteries in humans. When plasma concentrations of nicorandil are higher it causes reduction in coronary vascular resistance resulting in K^+ATP channel opening (Nakae *et al.,* 2002).

2.7.2 Physicochemical properties

Its molecular formula is $C_8H_9N_3O_4$ with molecular weight 211.174 g/mol, apparently it is white to off white crystalline powder. It is freely soluble in acetone, ethanol, methanol and acetonitrile, soluble in chloroform and ethyl acetate, sparingly soluble in water and slightly soluble in ether. Structure of nicorandil is illustrated in figure 2.13.

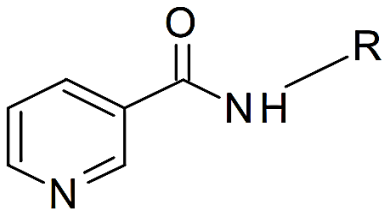

Figure 2.13. Structure of nicorandil

2.7.3 Mechanism of action

As nitrate; Nitrate component of nicorandil excites guanylate cyclase to raise formation of cyclic GMP (cGMP) which further stimulates protein kinase G (PKG) leading to phosphorylation and inhibition of GTPase RhoA and thus reduced Rho-kinase activity. This decreased Rho-kinase activity allows enhanced myosin phosphatase activity which ultimately reduces the calcium sensitivity of smooth muscles (Sauzeau *et al.,* 2006). Protein kinase G (PKG) promotes sarcolemma calcium pump to eradicate activating calcium (Vrolix *et al.,* 1988). PKG turns on K^+ channels to stimulate K^+ efflux and succeeding hyperpolarization hinders voltage-gated calcium channels (Nakae *et al.,* 2002). Ultimately easing of smooth muscle and coronary vasodilation ensues.

As K^+ATP channel opener: Nicorandil triggers K^+ATP channel leading to K^+ efflux which results into hyperpolarization of cells that results in inactivation of voltage gated calcium channels and diminishes free intracellular Ca^{2+} (Nakae *et al.,* 2002).

Vasodilator effect of nicorandil is primarily accredited to its nitrate property. It is also found that nicorandil is operative in situations where nitrates (like nitroglycerine) are not effective. Nicorandil triggers K^+ATP channels in mitochondria of myocardium that seems to relay cardio protective effects, though mechanism is not known till now (Liu *et al.,* 1998).

2.7.4 Clinical uses

It possesses a variety of advantageous hemodynamic effects and has proven to be operative in treating angina with appreciable efficacy. Moreover, it has beneficial effects

in unstable and variant angina. Treatment benefits also include prevention and/or reduction of complaint arising from angina pectoris (Knight *et al.,* 1995).

2.7.5 Side effects

Side effects according to British National Formulary include;

- Palpitations
- Flushing
- Weakness
- Perianal, illeal, peristomal and anal ulceration
- Vomiting
- Nasal congestion
- Toothache

2.7.6 Pharmacokinetics

Absorption of nicorandil from GIT is rapid and almost complete. It lacks first-pass effect as its metabolism by liver is not significant. Its reported bioavailability is 75-100%. When administered with food, absorption is delayed with little or no effect on C_{max}. However, plasma concentration and area under the curve (AUC) has linear relationship with administered dose (i.e., 5, 10, 20 or 40 mg). Steady state plasma concentration is achieved within 96-120 h after constant dosing of 20 mg twice daily which is attributed to its distribution and metabolism designs. Approximately reported average C_{max} is 300ng/mL reached within 30 min of administration. It has low plasma protein binding profile i.e. approximately 25%. Reported volume of administration (V_d) is 1.0 L/kg body weight approximately. It is metabolized extensively and majorly eliminated via kidney, only less than 2% is excreted via biliary route. Its elimination half-life is very short i.e. about 1 h and total body clearance is almost 1.15 L/min i.e., less than blood flow to liver (Frydman, 1992).

2.7.7 Dosage

Its recommended dose is 10-20 mg twice daily with maximum 30-40 mg twice daily.

2.7.8 Warnings and precaution

Patients with complaint of hypovolaemia (low volume of blood), heart disease, low blood pressure and during pregnancy it should be administered with precaution. It may result in dizziness so do not drive while on this medication.

3.0. Materials & methods

3.1. Instrumentation and chemicals

3.1.1. Instrumentation and apparatus

High Performance Liquid Chromatographic Pump[1], UV/Visible Spectrophotometer Detector[2], HPLC Modular[3], Sonicator[4], Centrifuge Machine[5], pH Meter[6], Ultrasonic Bath[7], Digital Weighing Balance[8], Membrane Filter[9], Magnetic Stirrer[10], B.P. Apparatus[11], Vacuum Pump[12], Distillation Plant[13], Ultra-low Freezer[14], Micropipettes[15], Filtration Assembly[16], Measuring Cylinder[17], Beakers[18] 50, 100, 250, 500 & 1000 mL, Measuring Flasks[19] 50, 100, 250, 500 & 1000 mL, Centrifuge Tubes[20], Sample Test Tubes[21], Disposable Syringes[22], Vortex Mixer[23], Incubator[24], Centrifuge[25], Fourier Transform Infrared Spectroscopy (FTIR)[26], Scanning Electron Microscopy (SEM)[27], Differential Scanning Calorimeter and Thermo Gravimetric Analyzer (DSC & TGA)[28], XRD[29], , Dissolution apparatus[30], Automated sample collector[31]

1-3. Agilent 1100 Series U.S.A.

4. Elma, Germany

5. Model 4000-China

6. WTW pH 300-Germany

7. Fisher Scientific FS 28 H-Germany

8. Percia XB 120A

9. Sartorius (0.45 μm filters)-Germany

10. Gallen Kamp-England

11. Model No 500-China

12. Rotary Vane Pump ILMVAC-Germany

13. WDA/4 R & M England

14. Sanyo-Japan

15. Softpet- Finland

16-21. Pyrex-France

22. BD-Pakistan

23. Seouline BioScirnce-Korea

24. Velp Scientifica-Italy
25. Hettich-Germany
26. Bruker, Tenser 27, Germany
27. Hitachi, S3400N, Quanat 300-500 µm
28. DuPont thermal analyzer with 2010 DSC194 module
29. Philips Analytical XRD Model: PW 3710, Holland
30. PTCF II Pharma Test-Germany
31. PT-DT7 Pharma Test- Germany

3.1.2. Chemicals

Acrylic Acid[1] (Anhydrous, 180-200ppm MEHQ as inhibitor, 99%), 2-Hydroxyethyl Methacrylate[2] (97%, 200-220 ppm monomethyl ether hydroquinone as inhibitor), Methanol[3] HPLC grade, Distilled water[4], Acetonitrile[5] HPLC grade, (Hydroxypropyl)methyl cellulose (80-120cP)[6], N,N Methylene-bis-acrylamide[7] (98%), Potassium persulphate[8] (99%), Potassium dihydrogen phosphate[9] (98-100%), Ethanol Absolute[9], Nicorandil[10], (99.8%), Heparin [16]

1. Sigma Aldrich-Netherlands
2. Sigma Aldrich-Germany
3. Merck-Germany.
4. The Islamia University of Bahawalpur.
5. Wilson Pharmaceuticals
6. Sigma Aldrich-USA
7. Fluka-Switzerland
8. AnalaR, BDH-England
9. Merck- Germany
10. Getz Pharma-Pakistan
16. Medicare Pharma-Malaysia

。

3.2. Methods

3.2.1. Formulation development

Synthesis of hydrogels

a) Preparation of HEMA-co-AA hydrogel

Method for preparing hydrogels was free radical polymerization. Acrylic acid (AA) solution was maintained on water bath at 70 °C with stirring at 300 rpm. Potassium persulphate (KPS) solution as an initiator was added drop wise in above solution and continue stirring at 300 rpm and 70 °C for 35 min. The mixture was cooled down to ambient temperature. Calculated amount of 2-hydroxyethyl methacrylate solution was added to mixture at room temperature and stirred at 300 rpm for 1-2 min. N,N Methylene-bis-acrylamide solution was also added to above mixture in drop wise manner at room temperature and whole mixture was stirred at room temperature for 2-3 minutes. Final volume was make up with water quantity sufficient up to 100 g. Final solution was poured into glass test tube and placed in water bath at 80 °C for 3 hrs. After completion of 3 hr reaction time formulated hydrogel was cut into small discs of 4 mm thickness with sharp scissors. These discs were first washed with distilled water and then placed in ethanol:water (50:50) solution for 24 hrs to dewater formulation. Discs were oven dried at 46 °C till drying equilibrium is reached. These discs were subjected to further *in vitro* and *invivo* studies. HEMA-co-AA hydrogels in different weight ratios were prepared as given in table 3.1.

b) Preparation of HPMC-co-AA hydrogel

HPMC-co-AA hydrogels were prepared by free radical polymerization. Hydroxypropyl methyl cellulose (HPMC) solution was maintained on water bath at 75 °C with stirring at 300 rpm. Potassium persulphate (KPS) solution as an initiator was added drop wise in above solution and continue stirring at 300 rpm and 75 °C for 35 min. The mixture was cooled down to room temperature. Calculated amount of acrylic acid was added to mixture at room temperature and stirred at 300 rpm for 1-2 min. N,N Methylene-bis-

acrylamide solution was also added to above mixture in drop wise manner at same time and whole mixture was stirred at room temperature for 2-3 minutes. Final volume was make up with water quantity sufficient up to 100 g. Final solution was poured into glass test tube and placed in water bath at 80 °C for 3 hrs. After completion of 3 hours reaction time formulated hydrogel was cut into small discs of 4 mm thickness with sharp scissors. These discs were first washed with distilled water and then placed in ethanol: water (50:50) solution for 24 hrs to dewater formulation. Discs were oven dried at 46 °C till drying equilibrium is reached. These discs were subjected to further *in-vitro* and *in-vivo* studies. HPMC-co-AA hydrogels in different weight ratios were prepared as given in table 3.2.

c) Preparation of HPMC-co-AA-co-HEMA hydrogel

HPMC-co-AA-co-HEMA hydrogels were prepared by free radical solution polymerization. Hydroxypropyl methyl cellulose (HPMC) solution was maintained on water bath at 75 °C with stirring at 300 rpm. Potassium persulphate (KPS) solution as an initiator was added drop wise in above solution and continue stirring at 300 rpm and 75 °C for 35 min. The mixture was cooled down to room temperature. Calculated amount of acrylic acid and 2-hydroxyethyl methacrylate solution was added to mixture at room temperature and stirred at 300 rpm for 1-2 min. N, N Methylene-bis-acrylamide solution was also added to above mixture in drop wise manner at room temperature and whole mixture was stirred at room temperature for 2-3 minutes. Final volume was make up with water quantity sufficient up to 100 g. Final solution was poured into glass test tube and placed in water bath at 80 °C for 3 hrs. After completion of 3 hours reaction time formulated hydrogel was cut into small discs of 4 mm thickness with sharp scissors. These discs were first washed with distilled water and then placed in ethanol: water (50:50) solution for 24 hrs to dewater formulation. Discs were oven dried at 46 °C till drying equilibrium is reached. These discs were subjected to further *in-vitro* and *in-vivo* studies. HPMC-co-AA-co-HEMA hydrogels in different weight ratios were prepared as given in table 3.3.

d) Preparation of CMC-co-MAA-co-AMPS hydrogel

CMC-co-MAA-co-AMPS hydrogels were prepared by free radical solution polymerization. Carboxy methyl cellulose (CMC) solution was maintained on water bath at 70 °C with stirring at 300 rpm. Potassium persulphate (KPS) solution as an initiator was added drop wise in above solution and continue stirring at 300 rpm and 70 °C for 35 min. The mixture was cooled down to room temperature. Calculated amount of methacrylic acid and 2-hydroxyethyl methacrylate solution was added to mixture at room temperature and stirred at 300 rpm for 1-2 min. N,N Methylene-bis-acrylamide solution as crosslinker was also added to above mixture in drop wise manner at room temperature and whole mixture was stirred at room temperature for 2-3 minutes. Final volume was make up with water quantity sufficient up to 100 g. Final solution was poured into glass test tube and placed in water bath at 80 °C for 3 hrs. After completion of 3 hours reaction time formulated hydrogel was cut into small discs of 4 mm thickness with sharp scissors. These discs were first washed with distilled water and then placed in ethanol: water (50:50) solution for 24 hrs to dewater formulation. Discs were oven dried at 46 °C till drying equilibrium is reached. These discs were subjected to further *in-vitro* and *in-vivo* studies. CMC-co-MAA-co-AMPS hydrogels in different weight ratios were prepared as given in table 3.4.

Where:

AA	Acrylic Acid
HEMA	2-Hydroxyethyl Methacrylate
KPS	Potassium persulphate
MBA	N,NMrthylene-bis-acrylamide
HPMC	(Hydroxypropyl)methyl cellulose
CMC	Carboxymethyl Cellulose
MAA	Methacrylic acid
AMPS	2-Acrylamido-2-methylpropane sulfonic acid

Table 3.1: Composition of HEMA-co-AA hydrogels/100g

Formulations	AA g (%w/w)	HEMA g (%w/w)	KPS g (%w/w)	MBA g (%w/w)
F1	16.5	**0.84**	0.015	0.015
F2	16.5	**1.68**	0.015	0.015
F3	16.5	**3.36**	0.015	0.015
F4	**10.5**	2.52	0.015	0.015
F5	**12.5**	2.52	0.015	0.015
F6	**14.5**	2.52	0.015	0.015
F7	14.5	2.52	0.015	**0.020**
F8	14.5	2.52	0.015	**0.025**
F9	14.5	2.52	0.015	**0.030**

Table 3.2: Composition of HPMC-co-AA hydrogels/100g

Formulations	AA g (%w/w)	HPMC g (%w/w)	KPS g (%w/w)	MBA g (%w/w)
F10	12.5	**0.6**	0.15	0.15
F11	12.5	**0.9**	0.15	0.15
F12	12.5	**1.2**	0.15	0.15
F13	**7.5**	0.3	0.15	0.15
F14	**10**	0.3	0.15	0.15
F15	**12.5**	0.3	0.15	0.15
F16	7.5	0.3	0.15	**0.20**
F17	7.5	0.3	0.15	**0.25**
F18	7.5	0.3	0.15	**0.30**

Table 3.3: Composition of HPMC-co-AA-co-HEMA hydrogels/100g

Formulations	AA g (%w/w)	HPMC g (%w/w)	HEMA g (%w/w)	KPS g (%w/w)	MBA g (%w/w)
F19	7.5	2.5	**0.5**	0.15	0.15
F20	7.5	2.5	**1**	0.15	0.15
F21	7.5	2.5	**1.5**	0.15	0.15
F22	**10**	2.5	0.5	0.15	0.15
F23	**12.5**	2.5	0.5	0.15	0.15
F24	**15**	2.5	0.5	0.15	0.15
F25	7.5	**5**	0.5	0.15	0.15
F26	7.5	**7.5**	0.5	0.15	0.15
F27	7.5	**10**	0.5	0.15	0.15
F28	7.5	2.5	0.5	0.15	**0.20**
F29	7.5	2.5	0.5	0.15	**0.25**
F30	7.5	2.5	0.5	0.15	**0.30**

Table 3.4: Composition of CMC-co-MAA-co-AMPS hydrogels/100g

Formulations	CMC g (%w/w)	AMPS g (%w/w)	MAA g (%w/w)	KPS g (%w/w)	MBA g (%w/w)
F31	0.5	3	**6**	0.040	0.040
F32	0.5	3	**7**	0.040	0.040
F33	0.5	3	**8**	0.040	0.040
F34	0.5	**4**	6	0.040	0.040
F35	0.5	**5**	6	0.040	0.040
F36	0.5	**6**	6	0.040	0.040
F37	**1.0**	4	6	0.040	0.040
F38	**1.5**	4	6	0.040	0.040
F39	**2.0**	4	6	0.040	0.040
F40	0.5	4	6	0.040	**0.045**
F41	0.5	4	6	0.040	**0.050**
F42	0.5	4	6	0.040	**0.055**

3.2.2. Preparation of buffer (British Pharmacopoeia Volume V) solutions of different pH for swelling studies

3.2.2.1. Buffer of pH 1.2

250 mL solution of 0.2 M sodium chloride (NaCl) was taken and mixed with 425 mL of 0.2 M hydrochloric acid (HCl). The final volume was made up to 1000 mL with distilled water.

3.2.2.2. Buffer of pH 5.8

250 mL solution of 0.2 M potassium dihydrogen phosphate (KH_2PO_4) was mixed with 18 mL of sodium hydroxide (NaOH) solution 0.2 M. The final solution was diluted up to 1000 mL with distilled water.

3.2.2.3. Buffer of pH 7.4

250 mL solution of 0.2 M potassium dihydrogen phosphate (KH_2PO_4) was mixed with 195.5 mL of sodium hydroxide (NaOH) solution 0.2 M. The final solution was diluted up to 1000 mL with distilled water.

3.2.3. Preparation of stock solutions and standard curve

Stock solution of nicorandil was prepared by dissolving 100 mg in 100 mL of phosphate buffer of pH 7.4. Further serial dilutions of 2, 4, 6, 8, 10, 15, 20, 25 and 30 µg/mL were made from this stock solution in phosphate buffer of pH 7.4. These serial dilutions were analyzed in triplicates by using UV visible spectrophotometer at 225 nm. Standard curve was constructed by absorbance verses concentration (Andrew *et al.,* 2004).

3.2.4. Swelling studies

Swelling studies of all formulations were performed at pH 1.2, 5.8 and 7.4 till swelling equilibrium, at prescheduled time points. For swelling study, weighed disc of formulation was soaked in 100 mL buffer of relevant pH. At specific time points, discs were blot dried and weighed at analytical weight balance.

Dynamic swelling and equilibrium swelling ratio of all formulations were determined by using following equation.

$$\mathbf{q} = W_h/W_d \qquad \textit{(Equation……3.1)}$$

Where "q" is dynamic swelling

W_h shows swollen gel's weight at time t

W_d shows initial weight of dried hydrogel disc (Peppas and Barr-Howell, 1987)

3.2.4.1 Equilibrium swelling measurements (%ES)

The swelling measurement was carried out until equilibrium weight of gel. Percent equilibrium swelling was carried out by following equation.

$$\%\,\boldsymbol{ES} = \frac{\boldsymbol{Meq-Mo}}{\boldsymbol{Meq}} \times \mathbf{100} \qquad \textit{(Equation ……3.2)}$$

M*eq* is mass of swollen gel at equilibrium

M*o* is mass of dried gel disc (Ranjha *et al.,* 2011)

3.2.4.2. Percent gel content ($\%g_c$)

Freshly prepared hydrogel discs (3-4 mm) were subjected to drying in a vacuum oven at 45^{o}C to a constant weight (W_o). Then this constant weight dried gel disc was processed through extraction with deionized water for 24hr. Non reacted polymer/monomer was washed away via this extraction. The disc was again dried in oven at 45^{o}C till constant weight (W_1). By using following formula % gel content was determined.

$$\textbf{\textit{Percent gel content}}\ (\%\boldsymbol{gc}) = \frac{\boldsymbol{W1}}{\boldsymbol{Wo}} \times \mathbf{100} \qquad \textit{(Equation……..3.3)}$$

Where W_1 is the weight of dry gel after extraction in distilled water and W_0 is the initial weight of dry gel (Dafader *et al.,* 2011).

3.2.4.3. Porosity measurement

Computing fraction of voids volume over total volume between 0 and 1 or in case of percent between 0 to 100 % is stated as porosity. Solvent replacement method was chosen to figure out porosity measurement. Dried weighed hydrogel disc (Md) was immersed in absolute ethanol for 24 hrs (till constant weight). After 24 hrs, hydrated hydrogel disc (Mh) was blot dried to remove excess surface ethanol and weighed on analytical weight balance. Percent porosity (%P) was computed by equation 3.4.

$$\textbf{\textit{Porosity}} = \frac{(\boldsymbol{Mh}-\boldsymbol{Md})}{\boldsymbol{\rho V}} \times \mathbf{100} \qquad \textit{(Equation……..3.4)}$$

Where ρ refers to density of absolute ethanol and V is hydrogel volume (Samiullah and Nazar, 2014).

3.2.5. Drug loading

Drug loading was done by absorption method. 1% solution of drug in phosphate buffer of pH 7.4 was prepared. One disc of each formulation was allowed to swell and reach to swelling equilibrium in 100 mL of 1% drug solution. After swelling, equilibrium was achieved, discs were removed from solution and washed out with distilled water to remove surplus surface drug. Then allowed to air dry at room temperature first and then in oven at 40 °C till drying

equilibrium (Sudhair *et al.,* 2013). Drug loading in discs was determined by following formula, given in equation number 3.5.

$$\textbf{Total drug loaded} = \frac{\mathbf{WL - Wu}}{\mathbf{Wu}} \times \mathbf{100} \qquad \textit{(Equation……..3.5)}$$

Where W_L is weight of dried drug loaded disc and W_u is weight of dried unloaded disc (Liu *et al.,* 2004).

3.2.6. Characterization

3.2.6.1. Fourier Transform Infra Red (FTIR) Spectroscopy

All formulated combinations along with polymers, monomers and drug were subjected to Fourier transform infrared analyzer (Bruker, Tensor 27, Germany) at 25ºC.

3.2.6.2. X-Ray Diffraction (XRD)

To check crystallinity of blank formulations, one optimum formulation from each combinations of hydrogels was subjected to X-ray diffractometer (Bruker D8 Discover, Germany) with Ni-filtered CuK alpha radiation source having tube voltage of 35 KV, current of 35 mA and scanning rate of 5° min^{-1}, over a range of 8°-60° diffraction angle (2θ) range (Osiris and Manal, 2012).

3.2.6.3. Thermal Gravimetric Analysis and Differential Scanning Calorimetry (TGA & DSC)

All combination of hydrogel formulations were subjected to thermal analysis and differential scanning calorimetry by sealing prior to test and putting them in aluminum pans. Measurements were achieved at a rate of 10 °C per minute, under nitrogen flow of 25 mL per minute, at temperature range of 20 °C to 900 °C. The standard uncertainty of sample mass measurement was ± 1%. Equipment calibration was accomplished with calcium oxalate supplied with instrument (Osiris and Manal, 2012).

3.2.6.4. Scanning Electron Microscopy (SEM)

Surface morphology of all combinations of hydrogel formulations was determined by scanning electron microscope (Hitachi, S3400N). Samples were coated with gold by Hummer Sputter Coater (Richard *et al.*, 2000).

3.2.6. *In vitro* drug release evaluation

In vitro drug release of hydrogel discs loaded with nicorandil was evaluated according to specifications of United States Pharmacopeia by using USP apparatus II. 900 mL of required dissolution medium i.e. 0.1 M HCl pH 1.2 and phosphate buffer pH 7.4 were used. Stirring of media was maintained at 50 rmp at 37 °C ± 0.5 °C. 5 mL of aliquot was drawn at intervals of 0, 0.5, 1, 1.5, 2, 4, 6, 8, 10, 12 and 24 hour with an automated sample collector after filtering through sintered filters (10 µm). At each interval, fresh 5 mL medium was added to preserve volume. Collected samples were diluted up to 50 mL with respective buffer and analyzed at 225 nm using a UV-spectrophotometer. The *in vitro* cumulative drug release study was conducted in triplicate (Fatemeh *et al.*, 2004).

Different kinetic models are pragmatic to appraise release kinetics, given as under in equations 3.6 to 3.10;

Zero order kinetic model	$D_t=D_o+K_ot$	*(Equation……..3.6)*
First order kinetics model	$\ln D_t=\ln D_o+K_1t$	*(Equation……..3.7)*
Higuchi kinetic model	$D_t=D_o + K_Ht^{½}$	*(Equation……..3.8)*
Hixson Crowell kinetic model	$D_t^3-D_o^3=K_{HC}t$	*(Equation……..3.9)*
Korsmeyer – Peppas kinetic model	$D_t/D\alpha=K_kt^n$	*(Equation……..3.10)*

D_t refers to cumulative amount of drug is released by the formulation at time t and D_o refers to initial drug amount in formulation. K_o, K_1, K_H, K_{HC} and K_k are rate constants for zero order, first order, and Higuchi, Hixson-Crowell and Korsmeyer-Peppas models, respectively.

D_t/D_α refers to drug fraction release at any time point t and "n" denotes release exponent. Value of n was computed from slope of Korsmeyer-Peppas plot.

3.2.7. *In vivo* studies

3.2.7.1 Animals

Twelve healthy male rabbits were enrolled in study weighing 2 ± 0.5 kg in agreement with standard protocols by "the Pharmacy Research Ethics Committee" of Faculty of Pharmacy and Alternative medicine (approval certificate number 105-2014/PREC), The Islamia University of Bahawalpur, Punjab, Pakistan. All animal handling was in good agreement with the animal scientific procedure Act, 1986 (Muhammad *et al.,* 2014). Weights of animals are given in table 3.5.

Table 3.5. Weight of rabbits (Kifayat and Gul, 2012)

Sr. No.	Animal	Weight
1	A	2.3
2	B	2.1
3	C	2.2
4	D	2.2
5	E	2.3
6	F	2.1
7	G	2.4
8	H	2.5
9	I	2.5
10	J	2.4
11	K	2.3
12	L	2.3

3.2.7.2. Experimental design

Single dose study was conducted on animal model (rabbits). Each animal received single dose (6.5 mg/kg) orally with the help of a 3 mL syringe having smoothly cut barrel at needle end in view of avoiding damage to oral mucosa of rabbit. Dose was given to rabbits shifting them to placement restraints (wooden catcher) at time of administration. During intervals, rabbits were resting in their respective cages having free access to water and feed. After ratifying swallowing of formulation, 10 mL of tape water was given to rabbit by a 10 mL syringe with oral tube (Muhammad *et al.,* 2014).

3.2.7.3. Sample collection

2 mL blood sample was withdrawn from jugular vein of rabbit by 3 mL syringe. Samples were collected into heparinized centrifuge tubes at zero time before dosing and at intervals of 0.5, 1, 2, 3, 4, 6, 8, 10, 12 and 24 hours after dosing. Collected blood samples were centrifuged at 5000 rpm for 10 minutes. Separated plasma samples were frozen at -70° C in ultra-low freezer (Sanyo-Japan, maximum -86° C) until assay (Kifayat and Gul, 2012). Steadiness of plasma samples were appraised at -70° C for two months and at room temperature for 24 h with potency (>95%).

3.2.7.4. Preparation of the mobile phase

Mobile phase of Water and acetonitrile (750: 250 v/v) was transported at flow rate of 1 mL/min at ambient temperature. Injection volume was 20 µL. Detection was achieved at 256 nm.

3.2.7.5 Method for sample analysis

a) Preparation of stock solutions

The stock solution was prepared by dissolving 100 mg of nicorandil in 100 mL of mobile phase. Stock solutions of nicorandil were prepared in triplicate. Additional dilutions were made from this stock solution in mobile phase. Dilutions in range of 31.25 ng/mL to 500 ng/mL were prepared.

b) Preparation of standard curve

Standard curve was raised to embrace projected ranges of plasma concentrations. By spiking different drug concentrations in 0.5 mL plasma standard curve was constructed covering points equivalent to 31.25 ng/mL to 500 ng/mL. 20 µl were injected into loop and spectra were taken of each concentration. Peak areas were figured out for each concentration.

c) Preparation of the sample (Extraction)

0.5 mL of plasma aliquot was taken into glass centrifuge tube with teflon lined cap. 0.2 mL of 0.1M sodium hydroxide was added to plasma sample followed by addition of 2 mL of chloroform as organic solvent. Mixture was vortexed for 5 min followed by centrifugation at 50000 rpm for 10 min. Organic layer was separated into another glass tube with teflon lined cap. Remaining aqueous portion was again extracted with 2 mL of chloroform. Organic layer evaporated to dryness under nitrogen gas stream. Residues were reconstituted with 0.2 mL of mobile phase just before injection (Hassan *et al.*, 2003).

d) High Performance Liquid Chromatographic Conditions

An HPLC system of Agilent consisted of a pump, a column (BDS hypersil C_8 4.6 mm x 250 mm) and UV visible detector used to examine prepared plasma samples. The UV detection of nicorandil was set at 256 nm. Mobile phase consisting of water and acetonitrile (750: 250 v/v) was transported at flow rate of 1 mL/min at ambient temperature. HPLC conditions are given in table 3.6.

Table.3.6. HPLC conditions

Flow rate	HPLC Pump	HPLC Detector	HPLC Column	λ_{max}
1.00 mL/min	Agilent	Agilent	BDS Hypersil C_8	256 nm

e) Pharmacokinetic analysis

Pharmacokinetic parameters were evaluated by non-compartmental pharmacokinetic approach. Maximum concentration (C_{max}), time to reach peak plasma concentrations (T_{max}) and other bioparameters ($AUC_{0-\infty}$, $AUMC_{0-\infty}$, $t_{1/2}$, Ke and MRT were analyzed by using pharmacokinetic software, Kinetica version 4.1.1.

3.2.8. Statistical analysis

Software Kinetica version 4.1.1 was used for evaluation of pharmacokinetic parameters and Microsoft Excel 2010 was engaged for estimation of bio parameters of nicorandil. One way ANOVA was used to compare major pharmacokinetic parameters e.g. C_{max}, T_{max} and AUC.

4.0 Results

4.1 Swelling ratios at pH 1.2, pH 5.8 and pH 7.4

Dynamic swelling of formulated hydrogels was determined at different time intervals over a period of 72 hrs (till swelling equilibrium reached) in buffer solution of different pH. These swelling ratios are given in tables 4.1 to 4.14 and represented diagrammatically in figures 4.1 to 4.14.

Formulations (F1 to F3) having different concentrations of HEMA exhibited excellent swelling ratio F1 (1 to 3.498), F2 (1 to 3.190) and F3 (1 to 3.013) at pH 1.2; F1 (1 to 10.810), F2 (1 to 9.635) and F3 (1 to 9.163) at pH 5.8; F1 (1 to 16.358), F2 (1 to 14.824) and F3 (1 to 13.696) at pH 7.4 as shown in table 4.1.

Table 4.1. Comparative swelling ratios of HEMA-co-AA hydrogels using different concentrations of HEMA (n=3)

Time (hrs)	Swelling ratio (q) at pH 1.2			Swelling ratio (q) at pH 5.8			Swelling ratio (q) at pH 7.4		
	F1	F2	F3	F1	F2	F3	F1	F2	F3
0.0	1±0	1±0	1±0	1±0	1±0	1±0	1±0	1±0	1±0
0.16	1.33±0.23	1.17±0.19	1.15±0.22	1.26±0.22	1.23±0.21	1.17±0.2	1.38±0.21	1.28±0.23	1.26±0.24
0.33	1.50±0.21	1.25±0.22	1.23±0.24	1.42±0.23	1.33±0.24	1.24±0.22	1.61±0.32	1.47±0.33	1.41±0.28
0.5	1.59±0.29	1.31±0.28	1.31±0.27	1.49±0.34	1.40±0.33	1.32±0.31	1.78±0.33	1.62±0.35	1.58±0.31
1.0	1.83±0.43	1.44±0.29	1.43±0.31	1.73±0.38	1.63±0.34	1.45±0.35	2.22±0.67	1.96±0.61	1.89±0.42
2.0	2.18±0.32	1.66±0.31	1.65±0.32	2.15±0.41	2.02±0.38	1.75±0.39	3.01±0.77	2.62±0.73	2.48±0.47
3.0	2.46±0.22	1.85±0.3	1.85±0.27	2.47±0.43	2.35±0.42	1.96±0.41	3.59±0.79	3.10±0.77	2.96±0.54
4.0	2.49±0.32	1.94±0.28	1.91±0.3	2.81±0.45	2.68±0.46	2.21±0.44	4.21±0.79	3.58±0.75	3.43±0.66
5.0	2.61±0.33	2.02±0.32	2.00±0.31	3.20±0.54	3.01±0.53	2.47±0.51	4.74±0.57	4.16±0.67	3.92±0.68
6.0	2.73±0.35	2.10±0.31	2.09±0.33	3.63±0.68	3.36±0.63	2.72±0.62	5.21±0.35	4.47±0.75	4.32±0.71
8.0	2.85±0.35	2.20±0.32	2.18±0.34	4.03±0.77	3.76±0.74	3.08±0.73	5.70±0.87	5.03±0.77	5.00±0.75
10.0	2.96±0.36	2.34±0.33	2.29±0.31	4.44±0.79	4.25±0.75	3.46±0.77	6.61±0.83	5.88±0.79	5.59±0.79
12.0	3.16±0.34	2.51±0.33	2.47±0.33	4.88±0.81	4.68±0.81	3.88±0.8	7.20±0.65	6.32±0.71	6.08±0.81
24.0	3.41±0.34	2.85±0.34	2.73±0.33	6.81±0.83	6.22±0.82	5.51±0.83	10.53±0.74	9.40±0.75	8.93±0.83
48.0	3.50±0.35	3.14±0.33	2.95±0.34	9.14±0.86	8.15±0.84	7.39±0.85	13.88±0.79	12.65±0.78	11.77±0.84
72.0	3.50±0.35	3.19±0.35	3.01±0.34	10.81±0.88	9.64±0.89	9.16±0.87	16.36±0.85	14.82±0.81	13.70±0.85

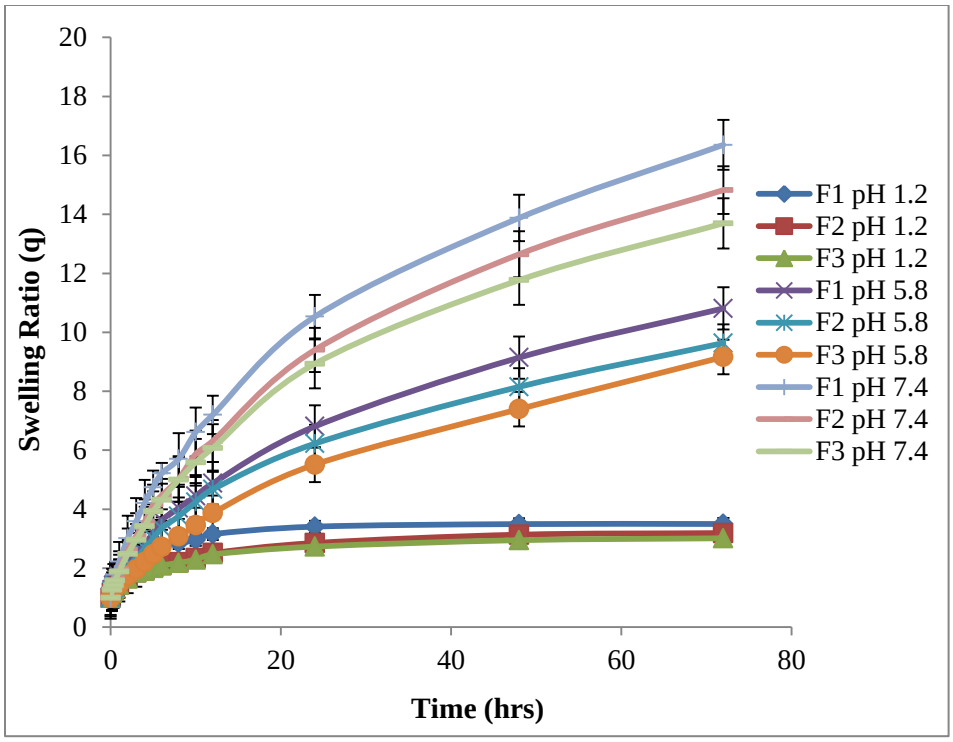

Figure 4.1. Comparative swelling ratios of HEMA-co-AA hydrogels using different concentrations of HEMA

Formulations (F4 to F6) having varying compositions of AA showed good swelling ratio F4 (1 to 2.932), F5 (1 to 3.115) and F6 (1 to 3.173) at pH 1.2; F4 (1 to 9.397), F5 (1 to 10.188) and F6 (1 to 10.508) at pH 5.8; F4 (1 to 15.013), F5 (1 to 16.005) and F6 (1 to 16.420) at pH 7.4 as shown in table 4.2.

Table 4.2. Comparative swelling ratios of HEMA-co-AA hydrogels using different concentrations of AA (n=3)

Time (hrs)	Swelling ratio (q) at pH 1.2			Swelling ratio (q) at pH 5.8			Swelling ratio (q) at pH 7.4		
	F4	F5	F6	F4	F5	F6	F4	F5	F6
0.0	1±0	1±0	1±0	1±0	1±0	1±0	1±0	1±0	1±0
0.16	1.19±0.23	1.18±0.19	1.17±0.22	1.20±0.22	1.19±0.21	1.18±0.2	1.24±0.21	1.25±0.23	1.28±0.24
0.33	1.27±0.21	1.31±0.24	1.26±0.24	1.31±0.33	1.29±0.24	1.28±0.22	1.47±0.32	1.43±0.33	1.51±0.33
0.5	1.36±0.29	1.42±0.27	1.33±0.27	1.42±0.34	1.36±0.33	1.39±0.31	1.60±0.33	1.58±0.35	1.96±0.67
1.0	1.45±0.43	1.50±0.31	1.44±0.31	1.58±0.38	1.54±0.34	1.53±0.35	1.95±0.67	1.91±0.61	2.08±0.77
2.0	1.70±0.32	1.66±0.31	1.68±0.32	1.98±0.42	1.89±0.38	1.94±0.39	2.55±0.67	2.50±0.73	2.86±0.79
3.0	1.90±0.22	1.91±0.3	1.87±0.27	2.28±0.43	2.16±0.42	2.23±0.41	2.99±0.77	2.96±0.77	3.51±0.79
4.0	1.96±0.32	1.99±0.28	1.96±0.3	2.59±0.45	2.41±0.46	2.54±0.44	3.50±0.79	3.78±0.75	4.06±0.66
5.0	2.03±0.33	2.07±0.32	2.05±0.29	2.86±0.54	2.70±0.53	2.87±0.51	3.99±0.79	3.88±0.67	4.73±0.68
6.0	2.15±0.35	2.21±0.31	2.15±0.31	3.19±0.51	2.99±0.54	3.20±0.74	4.40±0.35	4.55±0.75	5.23±0.71
8.0	2.25±0.31	2.30±0.27	2.26±0.31	3.70±0.62	3.43±0.51	3.66±0.75	4.91±0.87	5.02±0.77	6.74±0.75
10.0	2.33±0.33	2.51±0.31	2.41±0.27	4.06±0.73	3.89±0.62	4.11±0.81	5.74±0.83	5.56±0.71	7.75±0.35
12.0	2.55±0.34	2.64±0.32	2.58±0.31	4.48±0.77	4.35±0.73	4.64±0.8	6.30±0.65	6.10±0.75	8.67±0.87
24.0	2.80±0.31	2.93±0.34	2.90±0.34	6.31±0.83	5.84±0.82	6.54±0.83	9.24±0.74	10.78±0.79	12.95±0.83
48.0	2.90±0.33	3.11±0.33	3.13±0.34	7.98±0.86	7.95±0.84	8.99±0.86	12.57±0.79	14.85±0.81	15.64±0.65
72.0	2.93±0.35	3.12±0.35	3.17±0.34	9.40±0.88	10.19±0.89	10.51±0.88	15.01±0.85	16.01±0.81	16.42±0.74

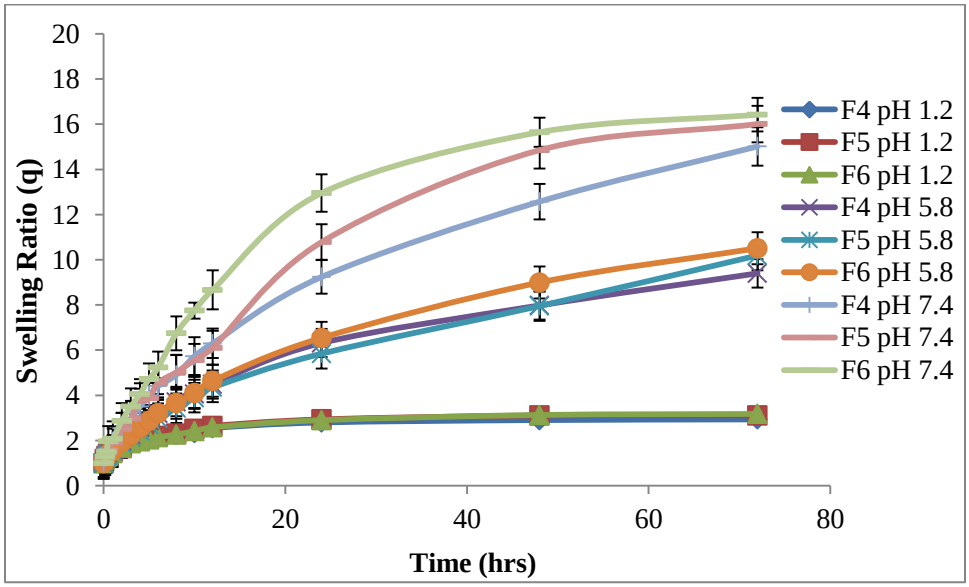

Figure 4.2. Comparative swelling ratios of HEMA-co-AA hydrogels using different concentrations of AA

Formulations (F7 to F9) with changing concentration of crosslinker MBA exhibited less swelling ratio F7 (1 to 2.917), F8 (1 to 2.805) and F9 (1 to 2.528) at pH 1.2; F7 (1 to 9.904), F8 (1 to 8.986) and F9 (1 to 6.193) at pH 5.8; F7 (1 to 10.104), F8 (1 to 15.066) and F9 (1 to 13.775) at pH 7.4 as shown in table 4.3.

Table 4.3. Comparative swelling ratios of HEMA-co-AA hydrogels using different concentrations of MBA (n=3)

Time (hrs)	Swelling ratio (q) at pH 1.2			Swelling ratio (q) at pH 5.8			Swelling ratio (q) at pH 7.4		
	F7	F8	F9	F7	F8	F9	F7	F8	F9
0.0	1±0	1±0	1±0	1±0	1±0	1±0	1±0	1±0	1±0
0.16	1.14±0.19	1.09±0.23	1.01±0.22	1.18±0.21	1.22±0.22	1.19±0.21	1.28±0.23	1.43±0.24	1.06±0.21
0.33	1.22±0.22	1.14±0.29	1.05±0.24	1.28±0.24	1.34±0.23	1.39±0.24	1.51±0.32	1.76±0.28	1.41±0.32
0.5	1.31±0.32	1.25±0.31	1.1±0.19	1.42±0.33	1.48±0.34	1.41±0.33	1.96±0.33	2.02±0.31	1.53±0.33
1.0	1.45±0.27	1.46±0.3	1.28±0.22	1.54±0.34	1.67±0.38	1.6±0.45	2.08±0.61	2.58±0.42	1.73±0.77
2.0	1.61±0.3	1.56±0.28	1.42±0.32	1.98±0.38	1.7±0.41	1.75±4.21	2.86±0.73	3.63±0.47	1.91±0.77
3.0	1.83±0.31	1.76±0.32	1.5±0.33	2.28±0.42	1.86±0.43	1.89±4.76	3.51±0.77	4.44±0.77	2.12±0.75
4.0	1.94±0.33	1.97±0.31	1.75±0.35	0.43±0.46	1.93±0.45	1.97±6.73	4.06±0.75	5.04±0.75	2.89±0.67
5.0	1.99±0.32	2.04±0.33	1.86±0.35	0.45±0.53	2.56±4.21	2.36±0.53	4.73±0.67	5.73±0.67	3.36±0.77
6.0	2.09±0.31	2.13±0.35	1.94±0.36	0.54±0.63	2.78±4.76	2.43±0.63	5.23±0.75	6.56±0.87	3.77±0.35
8.0	2.19±0.32	2.17±0.35	1.99±0.34	0.68±0.74	3.38±6.73	3.05±0.74	6.74±0.77	7.26±0.83	4.3±0.87
10.0	2.28±0.35	2.26±0.36	2.11±0.34	4.21±0.75	3.97±0.74	3.29±0.75	7.75±0.79	8.32±0.65	5.02±0.83
12.0	2.5±0.36	2.55±0.34	2.33±0.33	4.76±0.81	4.13±0.75	3.39±0.81	8.67±0.71	9.11±0.74	5.58±0.65
24.0	2.73±0.34	2.76±0.34	2.39±0.33	6.73±0.82	5.45±0.81	4.45±0.82	12.95±0.75	12.58±0.79	9.15±0.74
48.0	2.9±0.34	2.78±0.35	2.5±0.34	9.22±0.84	7.34±0.82	5.43±0.84	15.64±0.78	14.77±0.84	12.74±0.79
72.0	2.92±0.35	2.81±0.35	2.53±0.34	9.9±0.89	8.99±0.88	6.19±0.89	10.1±0.81	15.07±0.85	13.78±0.85

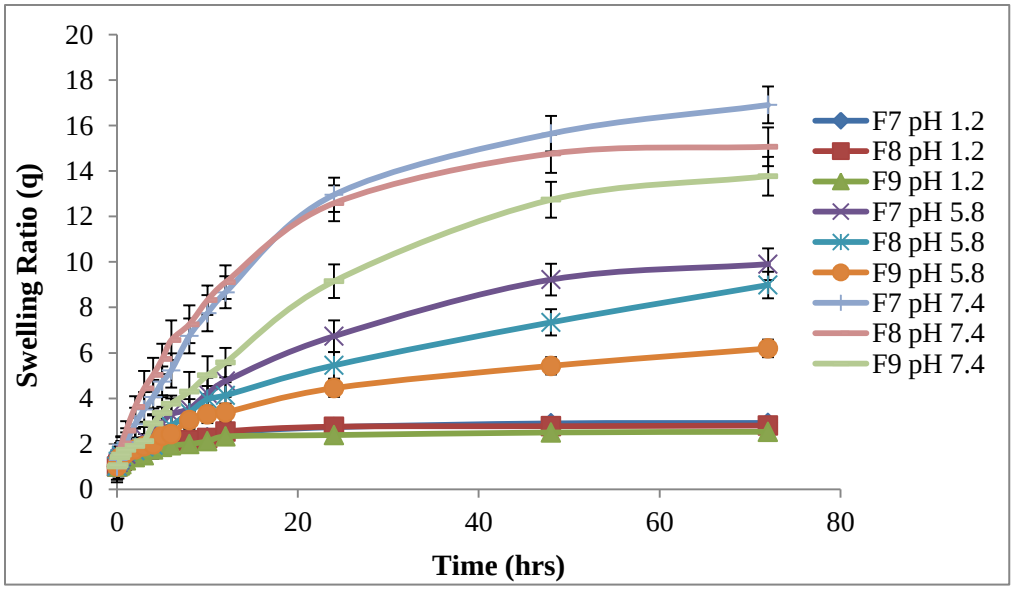

Figure 4.3. Comparative swelling ratios of HEMA-co-AA hydrogels using different concentrations of MBA

Formulations (F10 to F12) with varying compositions of HPMC were subjected to swelling at various pH and exhibited excellent swelling ratio F10 (1 to 5.412), F11 (1 to 5.878) and F12 (1 to 6.245) at pH 1.2; F10 (1 to 22.974), F11 (1 to 27.902) and F12 (1 to 31.327) at pH 5.8; F10 (1 to 51.033), F11 (1 to 55.027) and F12 (1 to 69.647) at pH 7.4 as shown in table 4.2.

Table 4.4. Comparative swelling ratios of HPMC-co-AA hydrogels using different concentrations of HPMC (n=3)

Time (hrs)	Swelling ratio (q) at pH 1.2			Swelling ratio (q) at pH 5.8			Swelling ratio (q) at pH 7.4		
	F10	F11	F12	F10	F11	F12	F10	F11	F12
0.0	1±0	1±0	1±0	1±0	1±0	1±0	1±0	1±0	1±0
0.16	1.09±0.23	1.27±0.19	1.37±0.22	1.23±0.24	1.23±0.21	1.32±0.2	1.31±0.21	1.37±0.23	1.86±1.17
0.33	1.19±0.21	1.43±0.22	1.55±0.24	1.42±0.33	1.56±0.24	1.73±0.22	1.6±0.32	1.78±1.17	2.23±1.44
0.5	1.27±0.29	1.54±0.32	1.66±0.33	1.62±0.34	1.74±0.33	1.88±0.31	1.81±1.17	2.08±1.44	2.71±2.13
1.0	1.4±0.43	1.6±0.33	1.75±0.51	1.81±0.68	1.9±0.63	2.25±0.62	2.06±1.26	2.62±2.13	3.27±2.23
2.0	1.46±0.32	2.08±0.35	2.3±0.62	1.88±0.77	2.88±0.74	3.5±0.73	2.33±1.44	4.84±2.23	5.95±2.48
3.0	1.52±0.22	2.27±0.35	2.49±0.73	2.18±0.79	3.2±0.75	3.63±0.77	3.68±2.13	5.68±2.29	6.95±2.5
4.0	1.99±0.32	2.45±0.36	2.63±0.77	2.75±0.81	3.65±0.81	4.61±0.8	5.21±2.19	6.7±2.37	8.11±2.31
5.0	2.14±0.33	2.62±0.54	2.89±0.65	3.44±0.83	3.92±0.82	5.22±0.83	5.83±2.23	8.16±2.48	9.79±2.41
6.0	2.27±0.35	2.88±0.68	3.13±0.74	3.73±0.86	4.4±0.84	6.65±0.85	7.03±2.31	9.57±2.5	11.29±2.38
8.0	2.46±0.35	3.1±0.77	3.33±0.79	3.94±0.88	5.41±0.89	8.11±0.87	8.17±2.5	9.8±2.38	12.56±2.56
10.0	2.63±0.36	3.25±0.79	3.46±0.85	4.96±0.79	7.13±0.75	9.2±0.77	9.83±2.41	10.89±2.56	14.54±3.33
12.0	2.82±0.34	3.59±0.68	3.59±0.77	7.35±0.85	8.79±0.81	10.45±0.8	10.92±2.56	14.24±3.33	18.19±3.34
24.0	3.77±0.34	4.45±0.81	4.9±0.8	9.89±0.92	11.66±0.8	12.55±1.1	18.14±2.33	23.64±3.34	27.63±3.46
48.0	4.61±0.35	5.27±0.82	5.34±0.83	13.42±1.0	18.15±1.2	20.91±1.3	30.46±2.54	36.79±3.46	43.2±3.57
72.0	5.41±0.35	5.88±0.84	6.25±0.85	22.97±1.4	27.9±1.3	31.33±1.5	51.03±2.85	55.03±3.57	69.65±3.62

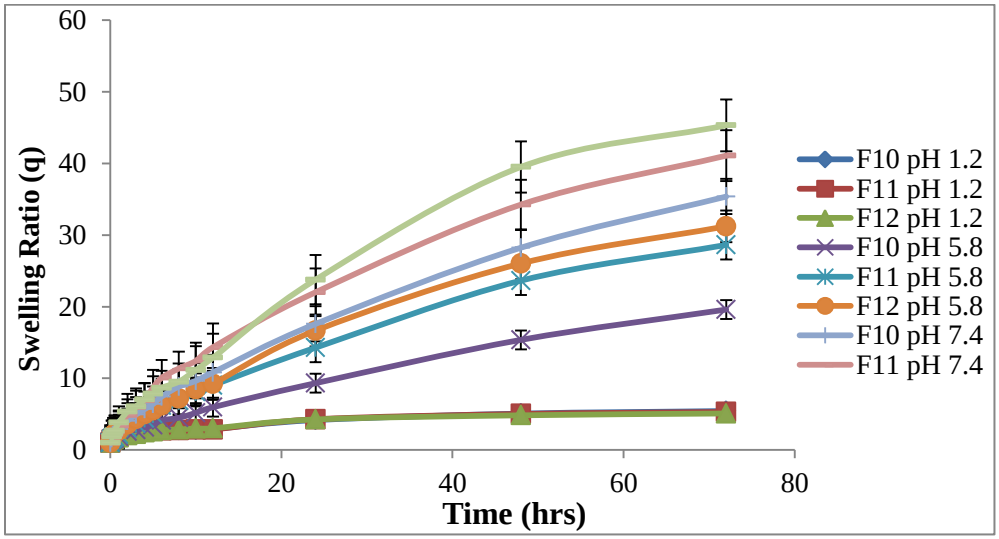

Figure 4.4. Comparative swelling ratios of HPMC-co-AA hydrogels using different concentrations of HPMC

Formulations (F13 to F15) with changing concentration of monomer AA exhibited swelling ratio F13 (1 to 6.395), F14 (1 to 6.457) and F15 (1 to 6.719) at pH 1.2; F13 (1 to 17.640), F14 (1 to 19.927) and F15 (1 to 25.963) at pH 5.8; F13 (1 to 37.716), F14 (1 to 40.668) and F15 (1 to 47.380) at pH 7.4 as shown in table 4.5.

Table 4.5. Comparative swelling ratios of HPMC-co-AA hydrogels using different concentrations of AA (n=3)

Time (hrs)	Swelling ratio (q) at pH 1.2			Swelling ratio (q) at pH 5.8			Swelling ratio (q) at pH 7.4		
	F13	F14	F15	F13	F14	F15	F13	F14	F15
0	1±0	1±0	1±0	1±0	1±0	1±0	1±0	1±0	1±0
0.16	1.4±0.23	1.31±0.19	1.5±0.22	1.07±0.24	1.02±0.21	1.48±0.2	1.08±0.21	1.08±0.23	1.75±1.17
0.33	1.57±0.22	1.56±0.22	1.61±0.24	1.13±0.33	1.04±0.31	1.66±0.22	1.13±0.32	1.09±1.17	2.18±1.44
0.5	1.68±0.32	1.65±0.32	1.71±0.32	1.2±0.34	1.17±0.62	1.82±0.31	1.23±1.17	1.31±1.44	2.46±1.17
1	1.74±0.43	1.72±0.33	1.93±0.33	1.32±0.68	1.3±0.73	2.18±0.62	1.44±1.26	1.61±2.13	3.21±1.44
2	2.28±0.32	2.24±0.35	2.24±0.35	1.57±0.77	2.07±0.77	2.89±0.73	2.51±1.44	2.83±2.23	4.58±2.13
3	2.42±0.22	2.42±0.35	2.5±0.35	2.18±0.79	2.8±0.75	3.53±0.77	3.19±2.13	3.41±2.29	5.56±2.5
4	2.66±0.32	2.64±0.36	2.68±0.68	2.52±0.81	3.09±0.81	4.12±0.75	3.69±2.19	4.07±2.37	6.41±2.31
5	2.82±0.33	2.82±0.54	2.78±0.77	2.9±0.83	3.84±0.82	4.6±0.81	4.1±2.23	4.92±2.13	7.13±2.41
6	2.92±0.35	2.98±0.85	2.88±0.74	3.5±0.86	4.68±0.84	5.38±0.82	5.2±2.31	5.85±2.23	7.84±2.38
8	3.16±0.35	3.06±0.77	3.09±0.79	4.2±0.88	5.55±0.89	6.33±0.84	5.8±2.5	6.85±2.48	9.13±2.46
10	3.31±0.36	3.14±0.8	3.38±0.85	4.74±0.79	6.51±0.75	7.36±0.77	6.55±2.41	7.84±2.5	10.48±2.33
12	3.36±0.34	3.25±0.83	3.5±0.77	6.03±0.85	7.47±0.8	8.39±0.83	9.19±0.81	9.61±2.33	12.71±2.34
24	4.87±0.34	4.91±0.81	4.74±0.8	9.54±0.92	11.01±1.1	13.47±1.1	13.69±0.8	14.76±2.34	21.79±2.46
48	5.97±0.35	4.99±0.82	6.07±0.83	14.25±1.01	18.24±1.3	21.23±1.4	19.32±1.1	23.8±2.46	36.9±2.57
72	6.4±0.35	6.46±0.84	6.72±0.85	17.64±1.44	19.93±1.5	25.96±1.4	37.72±1.4	40.67±2.57	47.38±2.62

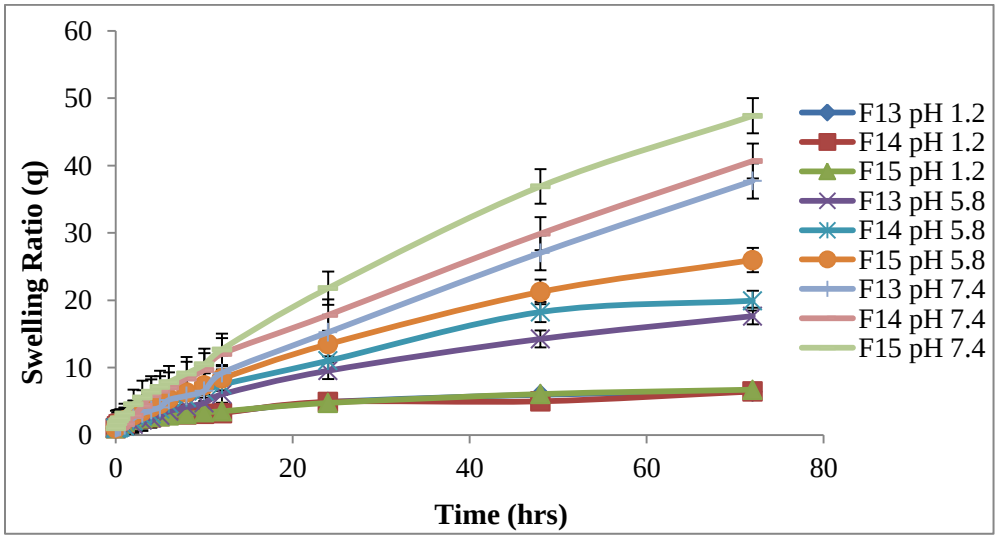

Figure 4.5. Comparative swelling ratios of HPMC-co-AA hydrogels using different concentrations of AA

Formulations (F16 to F18) with varying compositions of crosslinker showed less swelling ratio F16 (1 to 5.434), F17 (1 to 5.303) and F18 (1 to 5.091) at pH 1.2; F16 (1 to 19.606), F17 (1 to 16.741) and F18 (1 to 14.631) at pH 5.8; F16 (1 to 35.379), F17 (1 to 31.230) and F18 (1 to 28.633) at pH 7.4 as shown in table 4.6.

Table 4.6. Comparative swelling ratios of HPMC-co-AA hydrogels using different concentrations of MBA (n=3)

Time (hrs)	Swelling ratio (q) at pH 1.2			Swelling ratio (q) at pH 5.8			Swelling ratio (q) at pH 7.4		
	F16	F17	F18	F16	F17	F18	F16	F17	F18
0.0	1±0	1±0	1±0	1±0	1±0	1±0	1±0	1±0	1±0
0.16	1.45±0.23	1.43±0.19	1.37±0.22	1.36±0.24	1.31±0.21	1.3±0.2	1.66±0.21	1.84±0.23	1.45±1.17
0.33	1.55±0.22	1.53±0.22	1.47±0.24	1.52±0.33	1.43±0.31	1.41±0.22	2.02±0.32	2.07±1.17	1.65±1.44
0.5	1.63±0.32	1.62±0.32	1.55±0.32	1.6±0.34	1.52±0.62	1.48±0.31	2.3±1.44	2.25±1.44	1.8±1.17
1.0	1.8±0.43	1.82±0.22	1.73±0.33	1.88±0.68	1.74±0.73	1.62±0.62	2.93±2.13	2.73±2.13	2.19±1.44
2.0	2.1±0.32	2.16±0.32	2.05±0.35	2.6±0.77	2.32±0.31	2.16±0.73	4.07±2.5	3.57±2.23	3.02±2.13
3.0	2.3±0.22	2.38±0.33	2.24±0.35	2.81±0.79	2.65±0.62	2.45±0.77	4.93±2.31	4.34±2.29	3.72±2.5
4.0	2.46±0.32	2.58±0.36	2.45±0.68	3.16±0.81	2.96±0.73	2.71±0.75	5.7±2.41	4.99±2.31	4.39±2.31
5.0	2.55±0.33	2.65±0.54	2.57±0.77	3.49±0.83	3.23±0.77	3.11±0.81	6.42±2.38	5.55±2.5	5.03±2.41
6.0	2.68±0.35	2.72±0.85	2.75±0.74	4.13±0.86	3.92±0.84	3.64±0.81	7.46±2.31	6.2±2.41	6.22±2.38
8.0	2.77±0.35	2.77±0.77	2.87±0.79	4.49±0.88	4.28±0.89	3.73±0.83	8.84±2.5	7.17±2.48	6.87±2.33
10.0	2.81±0.77	2.84±0.8	2.99±0.85	5.19±0.89	4.96±0.75	4.82±0.86	9.65±2.41	8.5±2.5	8.1±2.34
12.0	2.92±0.8	2.85±0.83	3.02±0.77	5.97±0.75	5.52±0.8	5.13±0.83	10.82±2.34	9.25±2.33	9.03±2.46
24.0	4.18±0.83	4.29±0.81	4.26±0.8	9.33±0.8	9.11±1.1	8.16±1.19	17.6±2.46	16.68±2.34	14.28±2.59
48.0	5.07±0.81	5.02±0.82	4.84±0.83	15.37±1.2	14.52±1.3	13.11±1.3	28.24±1.26	26.03±2.36	23.64±2.55
72.0	5.43±0.81	5.3±0.84	5.09±0.85	19.61±1.3	16.74±1.4	14.63±1.3	35.38±1.39	31.23±2.47	28.63±2.65

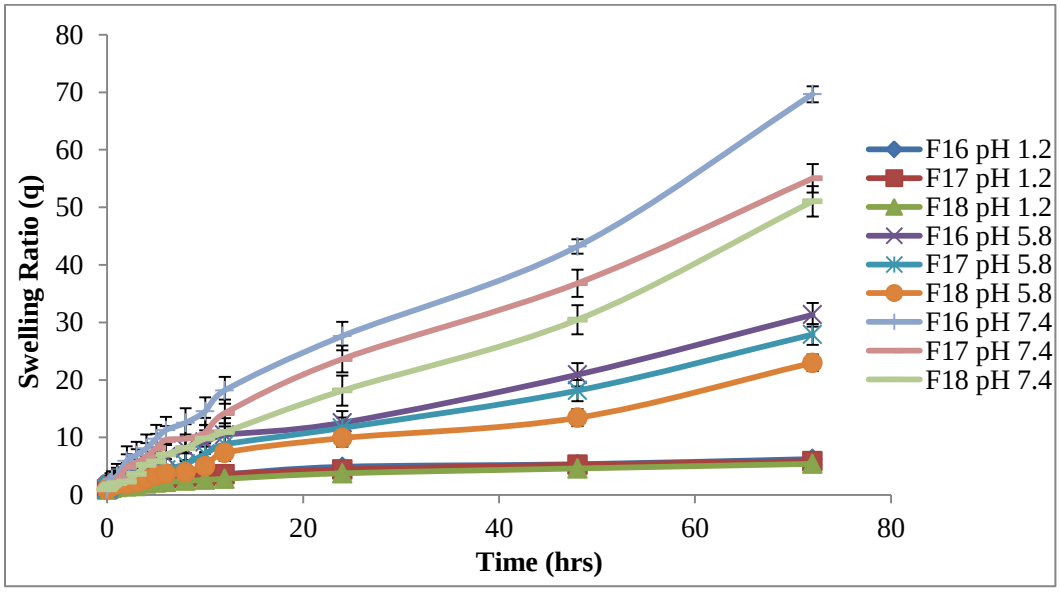

Figure 4.6. Comparative swelling ratios of HPMC-co-AA hydrogels using different concentrations of MBA

Formulations (F19 to F21) having varying compositions of HEMA showed swelling ratio ranging F19 (1 to 5.416), F20 (1 to 4.374) and F21 (1 to 3.368) at pH 1.2; F19 (1 to 25.284), F20 (1 to 23.104) and F21 (1 to 21.970) at pH 5.8; F19 (1 to 50.796), F20 (1 to 46.482) and F21 (1 to 39.365) at pH 7.4 as shown in table 4.7.

Table 4.7. Comparative swelling ratios of HPMC-co-AA-co-HEMA hydrogels using different concentrations of HEMA (n=3)

Time (hrs)	Swelling ratio (q) at pH 1.2			Swelling ratio (q) at pH 5.8			Swelling ratio (q) at pH 7.4		
	F19	F20	F21	F19	F20	F21	F19	F20	F21
0.0	1±0	1±0	1±0	1±0	1±0	1±0	1±0	1±0	1±0
0.16	1.1±0.23	1.08±0.19	1.13±0.22	1.4±0.24	1.34±0.21	1.23±0.2	1.21±0.21	1.04±0.23	1.02±0.34
0.33	1.53±0.22	1.18±0.22	1.21±0.24	1.79±0.33	1.58±0.31	1.46±0.22	1.77±0.32	1.25±0.22	1.2±0.68
0.5	1.68±0.32	1.45±0.32	1.33±0.32	2.06±0.34	1.77±0.62	1.66±0.31	2.01±1.17	1.51±0.31	1.5±0.77
1.0	1.96±0.43	1.67±0.33	1.48±0.33	2.24±0.68	2.07±0.73	1.81±0.62	2.54±1.26	1.8±0.62	1.79±0.79
2.0	2.21±0.32	1.86±0.35	1.65±0.35	2.72±0.77	2.48±0.77	1.98±0.73	3.99±1.44	2.71±0.73	2.34±0.81
3.0	2.55±0.22	2.15±0.35	1.76±0.35	3.39±0.79	3.07±0.75	2.29±0.77	5.47±2.13	3.34±0.77	3.01±0.83
4.0	2.83±0.32	2.29±0.36	1.87±0.68	3.64±0.81	3.37±0.73	2.63±0.75	6.78±2.19	4.38±0.75	3.9±0.8
5.0	3.05±0.33	2.49±0.54	2.01±0.77	4.04±0.83	3.49±0.77	3.05±0.81	7.5±2.23	4.76±0.75	4.98±0.83
6.0	3.3±0.35	2.81±0.85	2.09±0.77	4.33±0.86	3.8±0.75	3.44±0.82	11.23±2.3	5.98±0.89	5.35±0.85
8.0	3.52±0.35	3.01±0.77	2.23±0.68	5.29±0.88	4.07±0.89	3.64±0.84	14.43±2.5	8.75±0.75	6.6±0.75
10.0	3.8±0.36	3.28±0.68	2.4±0.65	6.02±0.79	4.99±0.75	4±0.77	17.39±2.4	11.22±0.8	10.64±0.8
12.0	4.05±0.34	3.42±0.77	2.61±0.77	7.47±0.85	5.54±0.8	4.31±0.89	19.93±0.8	14.36±1.1	11.63±1.1
24.0	4.34±0.34	3.67±0.74	2.84±0.8	11.59±0.9	9.14±1.17	7.35±0.75	27.85±0.8	22.79±1.3	18.88±1.3
48.0	4.6±0.35	3.91±0.79	2.96±0.73	17.12±1.0	14.68±1.3	13.16±0.8	39.8±1.17	36.59±1.4	30.62±1.5
72.0	5.42±0.35	4.37±0.75	3.37±0.75	25.28±1.4	23.1±1.32	21.97±1.1	50.8±1.44	46.48±1.5	39.37±1.6

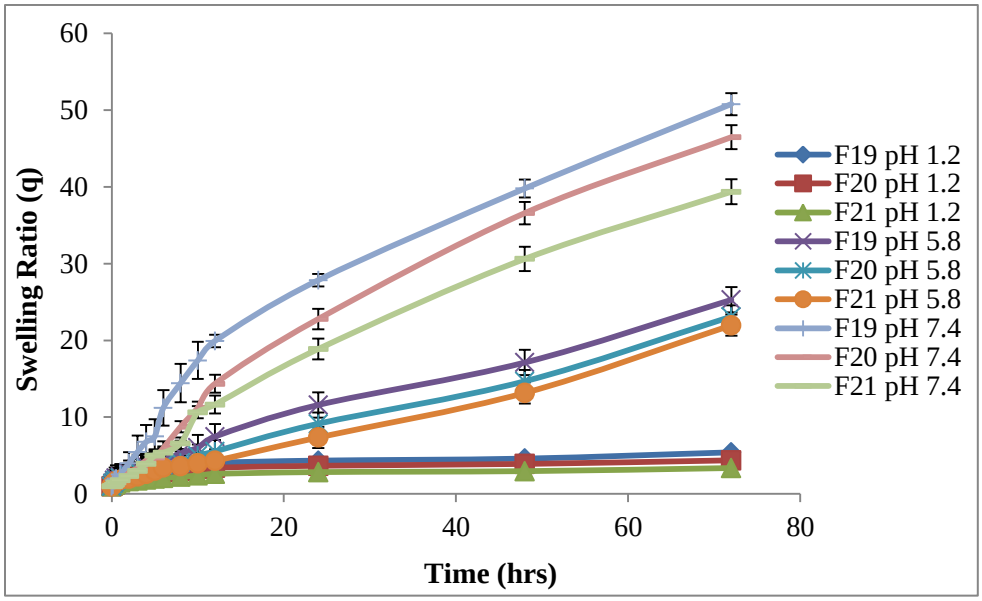

Figure 4.7. Comparative swelling ratios of HPMC-co-AA-co-HEMA hydrogels using different concentrations of HEMA

Formulations (F22 to F23) with increasing concentration of AA showed increasing trend in swelling ratio as F22 (1 to 5.00), F23 (1 to 5.280) and F24 (1 to 5.784) at pH 1.2; F22 (1 to 26.849), F23 (1 to 31.258) and F24 (1 to 36.369) at pH 5.8; F22 (1 to 47.436), F23 (1 to 56.431) and F24 (1 to 62.270) at pH 7.4 has shown in table 4.8.

Table 4.8. Comparative swelling ratios of HPMC-co-AA-co-HEMA hydrogels using different concentrations of AA (n=3)

Time (hrs)	Swelling ratio (q) at pH 1.2			Swelling ratio (q) at pH 5.8			Swelling ratio (q) at pH 7.4		
	F22	F23	F24	F22	F23	F24	F22	F23	F24
0.0	1±0	1±0	1±0	1±0	1±0	1±0	1±0	1±0	1±0
0.16	1.04±0.23	1.28±0.19	1.24±0.22	1.23±0.24	2.04±0.21	2.43±0.2	1.56±0.21	1.93±0.23	1.64±0.86
0.33	1.1±0.22	1.49±0.22	1.39±0.32	1.26±0.33	2.3±0.31	2.94±0.22	1.85±0.32	2.3±0.83	2.87±0.83
0.5	1.16±0.32	1.61±0.32	1.5±0.43	1.46±0.34	2.57±0.62	4.01±0.34	2.18±0.86	2.67±0.86	3.32±0.88
1.0	1.27±0.43	1.53±0.22	1.62±0.32	1.57±0.68	2.9±0.73	4.64±0.68	2.33±0.83	4.11±0.88	3.85±1.38
2.0	1.48±0.32	1.9±0.32	1.98±0.35	2.02±0.77	3.42±0.31	5.89±0.77	4.28±0.86	5.51±1.38	7.61±1.17
3.0	1.54±0.22	2.01±0.33	2.09±0.35	3.07±0.79	4.17±0.62	6.71±0.77	4.89±0.88	7.2±1.44	10.13±1.24
4.0	1.59±0.32	2.16±0.36	2.26±0.68	3.56±0.81	5.18±0.73	7.05±0.75	5.73±1.38	8.54±1.17	11.27±1.31
5.0	1.66±0.33	2.26±0.35	2.37±0.77	4.24±0.83	5.83±0.77	7.76±0.81	7.25±1.17	10.71±1.44	12.3±1.41
6.0	1.87±0.35	2.33±0.68	2.6±0.74	5.6±0.86	6.13±0.84	8.28±0.81	8.01±1.24	11.47±1.41	13.83±1.38
8.0	2.01±0.35	2.42±0.77	2.53±0.79	5.8±0.88	7.09±0.89	9.43±0.83	10.48±1.42	14.08±1.48	17.56±1.33
10.0	2.28±0.35	2.58±0.74	2.63±0.85	6.98±0.8	8.15±0.7	11.27±0.86	12.89±1.41	16.57±0.8	19.54±1.34
12.0	2.48±0.68	2.69±0.79	2.88±0.77	7.98±0.7	9.71±0.8	12.49±0.83	14.25±1.34	18.37±1.17	21.61±1.46
24.0	3.23±0.77	3.52±0.81	3.76±0.8	12.52±0.8	14.68±1.1	18.43±0.86	22.37±1.46	26.15±1.24	30.52±1.59
48.0	3.99±0.74	4.21±0.82	4.48±0.83	20.58±1.1	24.03±1.2	27.94±0.88	34.25±1.26	38.81±1.42	44.28±2.15
72.0	5±0.79	5.28±0.84	5.78±0.85	26.85±1.3	31.26±1.4	36.37±1.38	47.44±1.39	56.43±2.17	62.27±2.25

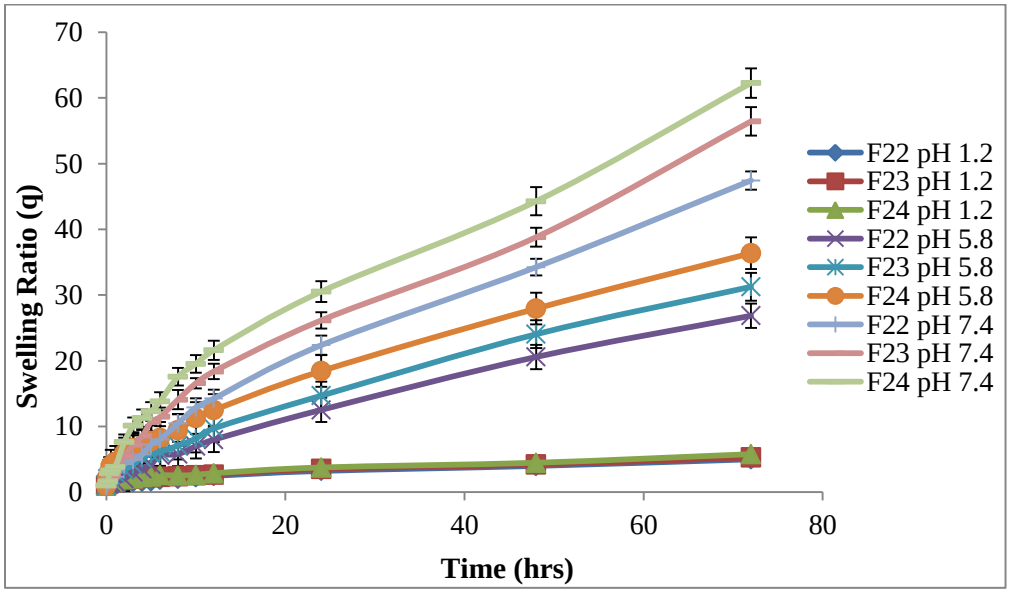

Figure 4.8. Comparative swelling ratios of HPMC-co-AA-co-HEMA hydrogels using different concentrations of AA

Formulations (F25 to F27) with different concentrations of HPMC showed swelling ratio ranging F25 (1 to 4.127), F26 (1 to 4.294) and F27 (1 to 4.500) at pH 1.2; F25 (1 to 23.500), F26 (1 to 25.826) and F27 (1 to 29.075) at pH 5.8; F25 (1 to 42.618), F26 (1 to 45.604) and F27 (1 to 49.011) at pH 7.4 as shown in table 4.9.

Table 4.9. Comparative swelling ratios of HPMC-co-AA-co-HEMA hydrogels using different concentrations of HPMC (n=3)

Time (hrs)	Swelling ratio (q) at pH 1.2			Swelling ratio (q) at pH 5.8			Swelling ratio (q) at pH 7.4		
	F25	F26	F27	F25	F26	F27	F25	F26	F27
0	1±0	1±0	1±0	1±0	1±0	1±0	1±0	1±0	1±0
0.16	1.29±0.23	1.33±0.22	1.43±0.22	1.66±0.24	1.53±0.21	1.78±0.2	1.45±0.23	1.58±0.23	1.98±0.34
0.33	1.43±0.22	1.46±0.32	1.63±0.24	1.74±0.33	1.88±0.31	2.25±0.22	1.75±0.22	1.92±0.22	2.21±0.68
0.5	1.51±0.32	1.56±0.43	1.74±0.32	1.88±0.34	2.16±0.62	2.62±0.31	2.09±0.31	2.2±0.31	2.51±0.77
1	1.56±0.43	1.65±0.32	1.87±0.33	2.06±0.68	2.47±0.73	3.03±0.62	2.52±0.62	2.72±0.62	3.09±0.79
2	2.01±0.32	2.09±0.35	2.2±0.35	2.63±0.77	3.03±0.31	3.67±0.73	4.33±0.73	4.8±0.73	5.18±0.81
3	2.12±0.22	2.25±0.35	2.36±0.35	2.87±0.79	3.9±0.62	4.52±0.62	5.05±0.77	5.6±0.77	7.1±0.83
4	2.31±0.32	2.35±0.68	2.45±0.68	3.51±0.81	4.68±0.73	5.9±0.73	5.92±0.75	6.5±0.75	8.03±0.8
5	2.43±0.33	2.54±0.77	2.59±0.77	4.76±0.83	5.88±0.77	7.25±0.75	7.7±0.75	8.57±0.75	9.73±0.83
6	2.57±0.35	2.59±0.74	2.77±0.74	5.92±0.86	7.17±0.84	8.7±0.75	8.38±0.89	9.28±0.83	11.07±0.85
8	2.75±0.35	2.69±0.83	2.98±0.79	6.48±0.88	8.55±0.89	10.26±0.8	9.28±0.75	10.95±0.8	13.55±0.75
10	2.91±0.77	2.86±0.86	3.12±0.85	7.41±0.89	9.26±0.75	11.06±1.17	10.59±0.8	13.11±0.8	15.53±0.8
12	3.05±0.8	3.15±0.88	3.26±0.77	8.62±0.75	10.29±0.8	12.21±0.83	11.92±1.1	14.9±0.8	16.93±1.17
24	3.56±0.83	3.75±0.8	3.93±0.8	13.02±0.8	15.26±1.1	17.81±1.19	18.56±1.3	21.45±1.3	24.67±1.34
48	4.02±0.81	4.12±0.83	4.26±0.83	19.22±1.1	21.93±1.2	24.69±1.33	29.88±1.4	33.5±1.46	36.67±1.57
72	4.13±0.81	4.29±0.85	4.5±0.85	23.5±1.34	25.83±1.4	29.08±1.38	42.62±1.5	45.6±1.57	49.01±1.62

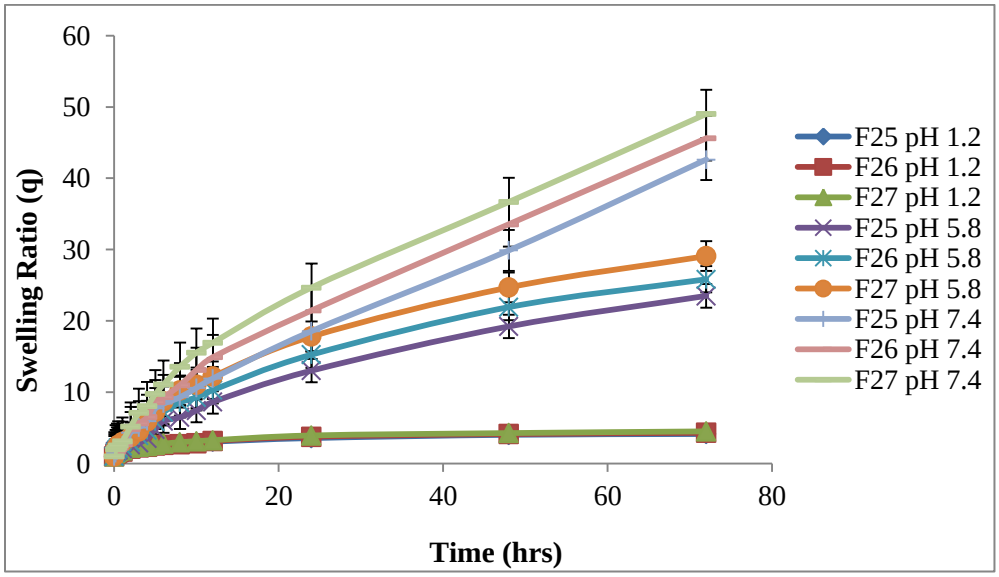

Figure 4.9. Comparative swelling ratios of HPMC-co-AA-co-HEMA hydrogels using different concentrations of HPMC

Formulations (F28 to F30) having varying composition of MBA showed swelling ratio ranging F28 (1 to 2.896), F29 (1 to 2.663) and F30 (1 to 2.322) at pH 1.2; F28 (1 to 16.690), F29 (1 to 14.972) and F30 (1 to 12.582) at pH 5.8; F28 (1 to 30.398), F29 (1 to 26.659) and F30 (1 to 21.592) at pH 7.4 as shown in table 4.10.

Table 4.10. Comparative swelling ratios of HPMC-co-AA-co-HEMA hydrogels using different concentrations of MBA (n=3)

Time (hrs)	Swelling ratio (q) at pH 1.2			Swelling ratio (q) at pH 5.8			Swelling ratio (q) at pH 7.4		
	F28	F29	F30	F28	F29	F30	F28	F29	F30
0	1±0	1±0	1±0	1±0	1±0	1±0	1±0	1±0	1±0
0.16	0.91±0.19	0.85±0.23	0.72±0.22	0.99±0.21	1.06±0.22	0.77±0.21	1.04±0.23	0.92±0.24	0.87±0.21
0.33	1±0.22	0.96±0.29	0.79±0.24	1.22±0.24	1.11±0.23	0.97±0.24	1.25±0.32	1.12±0.28	0.97±0.32
0.5	1.06±0.32	1.03±0.31	0.84±0.19	1.39±0.33	1.2±0.34	1.13±0.33	1.49±0.33	1.29±0.31	1.11±0.33
1	1.1±0.27	1.11±0.3	0.89±0.22	1.6±0.34	1.32±0.42	1.31±0.45	1.8±0.61	1.59±0.42	1.36±0.61
2	1.41±0.3	1.3±0.28	1.13±0.32	1.96±0.38	1.67±0.46	1.58±0.21	3.09±0.73	2.81±0.47	2.28±0.73
3	1.49±0.31	1.4±0.32	1.22±0.33	2.52±0.42	1.83±0.53	1.95±0.76	3.6±0.77	3.28±0.77	3.13±0.77
4	1.62±0.33	1.45±0.31	1.27±0.35	3.03±0.46	2.23±0.45	2.54±0.73	4.22±0.75	3.8±0.75	3.54±0.67
5	1.71±0.32	1.53±0.32	1.37±0.35	3.8±0.53	3.03±0.21	3.13±0.53	5.5±0.67	5.01±0.67	4.28±0.77
6	1.8±0.31	1.64±0.35	1.4±0.36	4.64±0.63	3.77±0.76	3.75±0.63	5.98±0.75	5.43±0.87	4.88±0.35
8	1.93±0.32	1.77±0.36	1.45±0.34	5.53±0.74	4.13±0.73	4.42±0.74	6.62±0.67	6.4±0.83	5.97±0.87
10	2.05±0.35	1.85±0.36	1.54±0.34	5.99±0.75	4.72±0.74	4.76±0.75	7.56±0.77	7.66±0.65	6.84±0.83
12	2.14±0.36	1.93±0.34	1.7±0.33	6.65±0.81	5.49±0.75	5.26±0.81	8.5±0.71	8.71±0.74	7.46±0.65
24	2.5±0.34	2.32±0.34	2.03±0.33	9.86±0.82	8.29±0.81	7.67±0.82	13.24±0.7	12.54±0.79	10.87±0.74
48	2.82±0.34	2.52±0.35	2.23±0.34	14.17±0.8	12.24±0.8	10.64±0.8	21.31±0.7	19.61±0.84	16.16±0.79
72	2.9±0.35	2.66±0.35	2.32±0.34	16.69±0.8	14.97±0.8	12.53±0.8	30.4±0.81	26.66±0.85	21.59±0.85

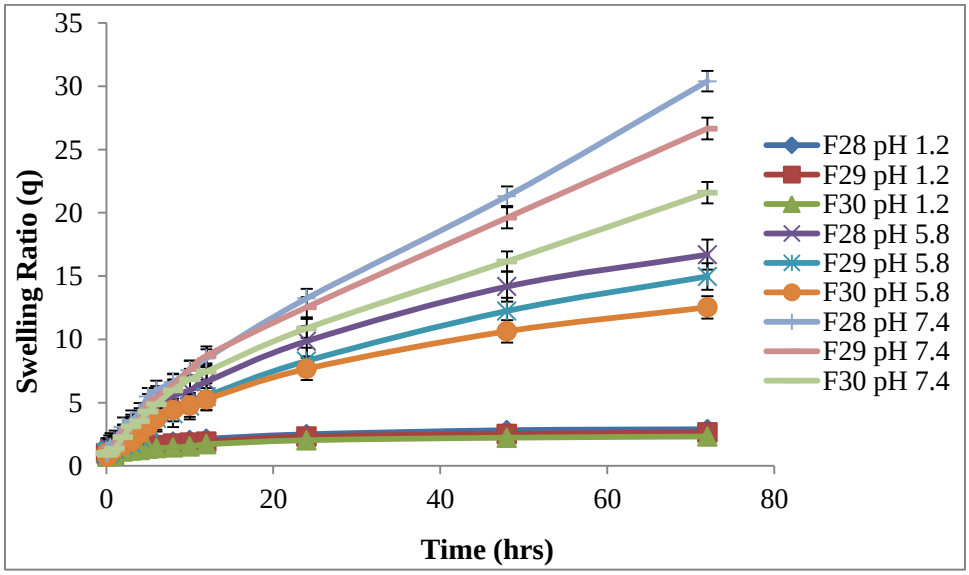

Figure 4.10. Comparative swelling ratios of HPMC-co-AA-co-HEMA hydrogels using different concentrations of MBA

Formulations (F31 to F33) having different concentrations of MAA showed swelling ratio ranging F31 (1 to 58.692), F32 (1 to 57.404) and F33 (1 to 56.754) at pH 1.2; F31 (1 to 59.545), F32 (1 to 59.791) and F33 (1 to 59.003) at pH 5.8; F31 (1 to 69.052), F32 (1 to 65.532) and F33 (1 to 62.716) at pH 7.4 as shown in table 4.11.

Table 4.11. Comparative swelling ratios of CMC-co-MAA-co-AMPS hydrogels using different concentrations of MAA (n=3)

Time (hrs)	Swelling ratio (q) at pH 1.2			Swelling ratio (q) at pH 5.8			Swelling ratio (q) at pH 7.4		
	F31	F32	F33	F31	F32	F33	F31	F32	F33
0.0	1±0	1±0	1±0	1±0	1±0	1±0	1±0	1±0	1±0
0.16	6.29±0.21	5.86±0.23	5.71±1.17	62.21±0.2	6.08±0.23	6.46±1.17	7.45±0.2	6.66±0.2	6.87±1.1
0.33	9.31±0.32	8.5±1.17	8.24±1.44	6.65±0.32	8.92±1.17	9.86±1.44	11.2±0.3	9.77±1.1	10.5±1.4
0.5	16.53±1.17	16.09±1.44	15.42±1.17	10.02±1.4	16.42±1.4	16.34±1.1	19.1±1.1	17.9±1.4	17.4±2.1
1.0	21.59±1.26	21.08±2.13	20.03±1.44	17.05±2.1	21.45±2.1	21.35±1.4	24.7±1.3	23.5±2.1	22.7±2.2
2.0	31.52±1.44	30.67±2.23	29.35±2.13	22.07±2.5	31.31±2.2	31.15±2.1	35.9±1.4	34.3±2.2	33.1±2.4
3.0	34.34±2.13	33.29±2.29	31.29±2.5	32.1±2.31	34.11±2.2	32.79±2.5	39.3±2.1	37.3±2.2	34.9±2.5
4.0	43.15±2.19	41.95±2.37	40.5±2.31	35.06±2.4	42.86±2.3	42.65±2.3	49.1±2.1	46.9±2.3	45.3±2.3
5.0	48.72±2.23	47.84±2.13	45.68±2.41	43.8±2.38	49.47±2.5	47.58±2.4	55.9±2.2	54.2±2.4	50.6±2.4
6.0	54.21±2.31	53.21±2.23	50.99±2.38	49.96±2.3	54.4±2.41	52.48±2.3	61.5±2.3	59.6±2.5	55.8±2.4
8.0	56.45±2.5	55.36±2.48	53.11±2.46	54.98±2.5	56.07±2.4	54.27±2.3	63.5±2.5	61.5±2.3	57.7±2.6
10.0	56.75±2.41	55.66±2.5	55.03±2.33	56.73±2.4	58.03±2.5	57.41±2.3	66.7±2.4	63.6±2.5	61.1±3.3
12.0	58.69±0.81	57.4±2.33	56.75±2.34	59.55±2.3	59.79±2.3	59±2.46	69.1±2.5	65.5±3.3	62.7±3.3

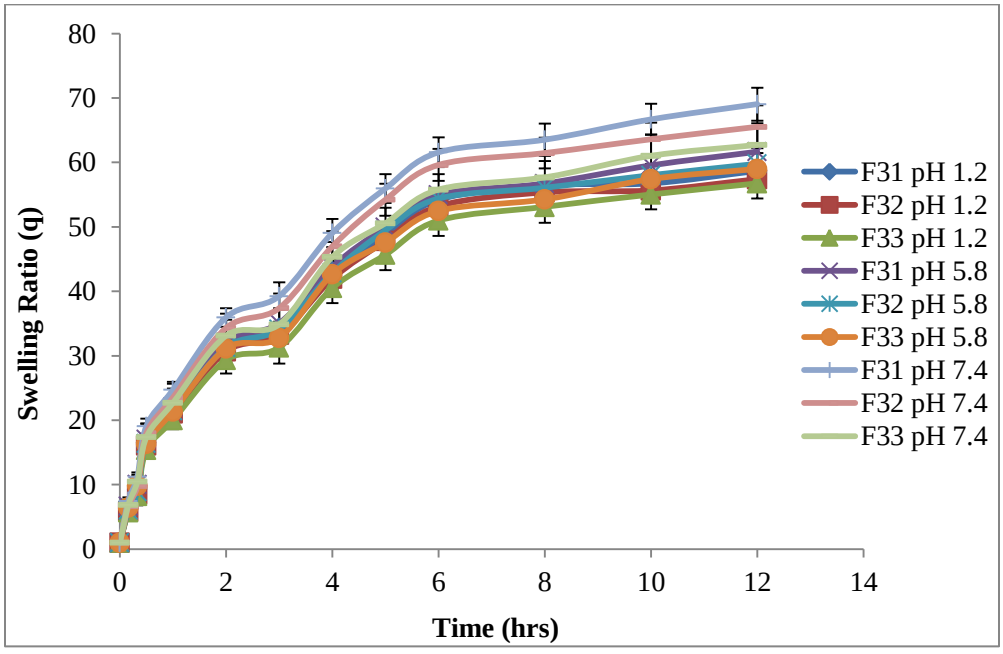

Figure 4.11. Comparative swelling ratios of CMC-co-MAA-co-AMPS hydrogels using different concentrations of MAA

Formulations from F34 to F36 with increasing concentration of AMPS showed increasing trend in swelling ratio as F34 (1 to 65.963), F35 (1 to 69.005) and F36 (1 to 75.030) at pH 1.2; F34 (1 to 66.184), F35 (1 to 70.075) and F36 (1 to 76.050) at pH 5.8; F34 (1 to 66.638), F35 (1 to 70.562) and F36 (1 to 76.476) at pH 7.4 has shown in table 4.12.

Table 4.12. Comparative swelling ratios of CMC-co-MAA-co-AMPS hydrogels using different concentrations of AMPS (n=3)

Time (hrs)	Swelling ratio (q) at pH 1.2			Swelling ratio (q) at pH 5.8			Swelling ratio (q) at pH 7.4		
	F34	F35	F36	F34	F35	F36	F34	F35	F36
0.0	1±0	1±0	1±0	1±0	1±0	1±0	1±0	1±0	1±0
0.16	14.61±0.21	16.6±0.23	18.31±0.3	14.59±0.2	16.86±0.2	18.55±1.1	14.1±0.2	16.9±0.2	18.6±1.1
0.33	20.96±0.32	23.08±1.1	25.49±1.4	21.17±0.3	23.44±0.2	25.96±1.4	21.3±0.3	23.6±0.2	26.1±1.4
0.5	33.16±0.32	35.54±1.4	40.24±1.1	33.81±1.4	36.09±0.3	40.8±1.17	34.1±1.1	36.3±0.3	41.1±2.1
1.0	44.89±1.44	47.5±1.44	53.17±1.4	45.48±2.1	48.24±0.3	53.8±1.44	45.7±1.2	48.5±1.1	54.1±2.3
2.0	61.47±1.17	64.42±1.1	71.45±2.1	62.22±2.5	65.42±1.4	72.34±2.1	62.6±1.4	65.8±1.2	72.7±2.4
3.0	65.96±1.44	69±1.44	74.93±2.5	66.16±2.3	70.07±1.1	75.95±2.5	66.6±2.1	70.5±1.4	76.3±2.5
4.0	65.96±1.13	69±2.13	74.94±2.3	66.17±2.4	70.07±1.4	75.96±2.3	66.6±2.1	70.5±2.1	76.4±2.5
5.0	65.96±1.23	69±2.13	74.96±2.4	66.12±2.3	70.07±2.5	75.98±2.4	66.5±2.2	70.5±2.4	76.4±2.4
6.0	65.96±1.31	69±2.23	74.98±2.3	66.15±2.3	70.07±2.4	76±2.38	66.6±2.3	70.5±2.5	76.4±2.3
8.0	65.96±1.5	69±2.48	75.02±2.4	66.17±2.3	70.07±2.4	76.04±2.3	66.6±2.4	70.5±2.3	76.4±2.5
10.0	65.96±1.41	69±2.5	75.01±2.3	66.18±2.4	70.07±2.5	76.04±2.3	66.6±2.5	70.5±2.4	76.4±3.1
12.0	65.96±1.81	69.01±2.3	75.03±2.3	66.18±2.3	70.08±2.3	76.05±2.4	66.6±2.5	70.5±2.5	76.5±3.2

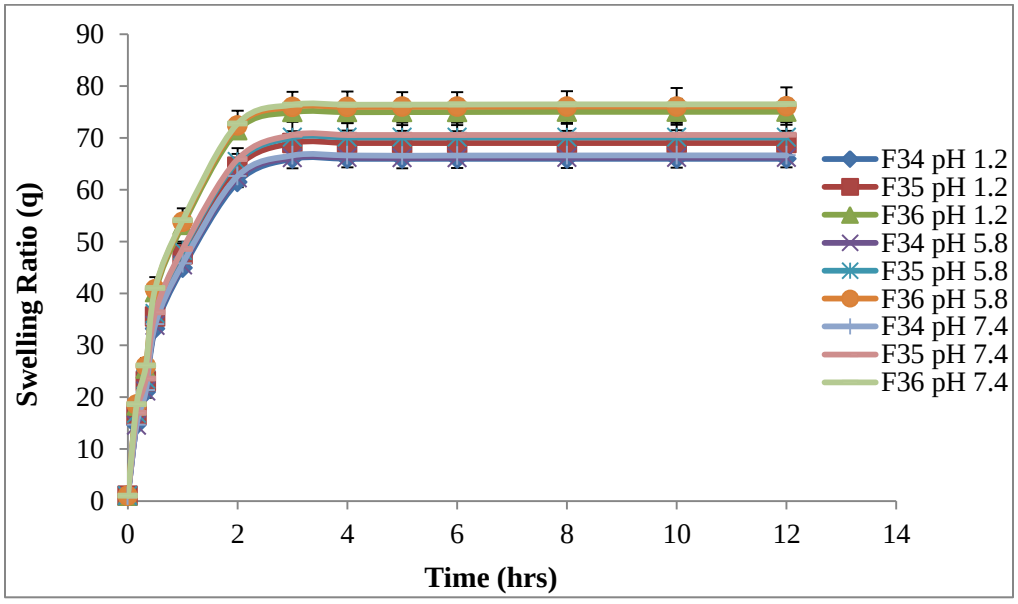

Figure 4.12. Comparative swelling ratios of CMC-co-MAA-co-AMPS hydrogels using different concentrations of AMPS

Formulations from F37 to F39 with increasing concentration of CMC exhibited drift in swelling ratio as F37 (1 to 66.626), F38 (1 to 67.627) and F39 (1 to 68.856) at pH 1.2; F37 (1 to 68.241), F38 (1 to 69.694) and F39 (1 to 70.425) at pH 5.8; F37 (1 to 71.111), F38 (1 to 73.524) and F39 (1 to 75.309) at pH 7.4 has shown in table 4.13.

Table 4.13. Comparative swelling ratios of CMC-co-MAA-co-AMPS hydrogels using different concentrations of CMC (n=3)

Time (hrs)	Swelling ratio (q) at pH 1.2			Swelling ratio (q) at pH 5.8			Swelling ratio (q) at pH 7.4		
	F37	F38	F39	F37	F38	F39	F37	F38	F39
0.0	1±0	1±0	1±0	1±0	1±0	1±0	1±0	1±0	1±0
0.16	14.69±0.2	14.6±0.2	15.5±1.1	17.39±0.2	16.98±0.2	17.07±1.1	15.7±0.2	16.8±0.2	17.81±1.1
0.33	21.3±0.32	21.3±1.1	22.23±1.4	24.04±0.3	23.6±1.17	24.13±1.4	22.3±0.3	23.7±0.2	24.85±1.4
0.5	34.03±1.1	34.4±1.4	34.86±1.1	36.94±1.1	36.34±1.4	37.28±2.1	35.4±1.4	36.95±0.3	39.13±1.1
1.0	45.77±1.1	45.8±2.1	47.42±1.4	48.77±1.2	48.57±2.1	50.13±2.2	47.1±2.1	49.12±0.3	51.98±1.4
2.0	62.63±1.4	62.3±2.2	63.23±2.1	65.95±1.4	65.87±2.2	66.79±2.4	63.5±2.5	65.5±1.44	68.65±2.1
3.0	66.59±2.1	67.6±2.3	67.81±2.5	66.68±2.1	69.69±2.2	70.5±2.5	68.7±2.3	71.79±1.1	72.35±2.5
4.0	66.6±2.23	67.6±2.3	68.15±2.3	68.15±2.1	69.69±2.3	70.38±2.3	71.1±2.4	73.52±1.4	74.29±2.3
5.0	66.54±2.2	67.6±2.1	68.15±2.4	68.17±2.2	69.69±2.4	70.42±2.4	71.1±2.3	73.52±2.5	74.87±2.4
6.0	66.59±2.3	67.6±2.2	68.17±2.4	68.19±2.3	69.69±2.5	70.42±2.3	71.1±2.3	73.52±2.4	75.26±2.3
8.0	66.61±2.5	67.6±2.4	68.85±2.5	68.23±2.5	69.69±2.3	70.47±2.5	71.1±2.3	73.52±2.4	75.3±2.33
10.0	66.63±2.4	67.6±2.5	68.85±2.3	68.23±2.4	69.69±2.5	70.47±3.3	71.1±2.4	73.52±2.5	75.29±2.3
12.0	66.63±0.8	67.6±2.3	68.86±2.3	68.24±2.5	69.69±3.3	70.43±3.3	71.1±2.4	73.52±2.3	75.31±2.4

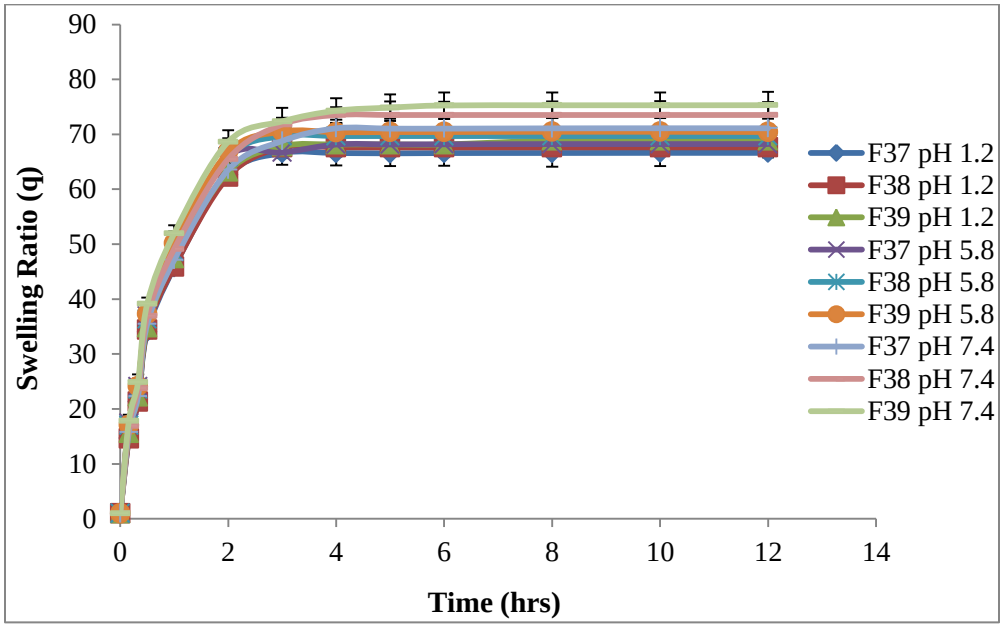

Figure 4.13. Comparative swelling ratios of CMC-co-MAA-co-AMPS hydrogels using different concentrations of CMC

Formulations (F40 to F42) having varying concentrations of MBA showed swelling ratio ranging F40 (1 to 51.427), F41 (1 to 49.171) and F42 (1 to 52.899) at pH 1.2; F40 (1 to 56.680), F41 (1 to 54.617) and F42 (1 to 52.901) at pH 5.8; F40 (1 to 66.829), F41 (1 to 64.300) and F42 (1 to 57.864) at pH 7.4 as shown in table 4.14.

Table 4.14. Comparative swelling ratios of CMC-co-MAA-co-AMPS hydrogels using different concentrations of MBA (n=3)

Time (hrs)	Swelling ratio (q) at pH 1.2			Swelling ratio (q) at pH 5.8			Swelling ratio (q) at pH 7.4		
	F40	F41	F42	F40	F41	F42	F40	F41	F42
0.0	1.00	1.00	1.00	1.00	1.00	1.00	1.00	1.00	1.00
10 min	12.91	11.27	11.44	13.77	11.49	11.44	14.27	13.77	11.82
20 min	18.87	18.57	17.44	20.12	18.01	17.44	20.96	20.12	19.47
0.5	29.69	29.00	28.35	31.67	27.65	28.35	32.83	31.67	30.41
1.0	40.53	37.74	37.70	43.23	37.46	37.70	44.72	43.23	40.55
2.0	56.07	45.88	45.51	55.07	48.77	50.38	60.97	59.80	55.26
3.0	51.43	47.43	46.60	56.68	54.61	51.32	64.79	64.29	57.86
4.0	51.43	48.98	47.27	56.68	54.61	52.89	65.13	64.29	57.86
5.0	51.43	49.17	47.27	56.68	54.61	52.90	66.79	64.30	57.86
6.0	51.43	49.17	47.27	56.68	54.61	52.90	66.83	64.30	57.86
8.0	51.43	49.17	47.27	56.68	54.61	52.90	66.83	64.30	57.86
10.0	51.43	49.17	47.27	56.68	54.62	52.90	66.83	64.30	57.86
12.0	51.43	49.17	47.27	56.68	54.62	52.90	66.83	64.30	57.86

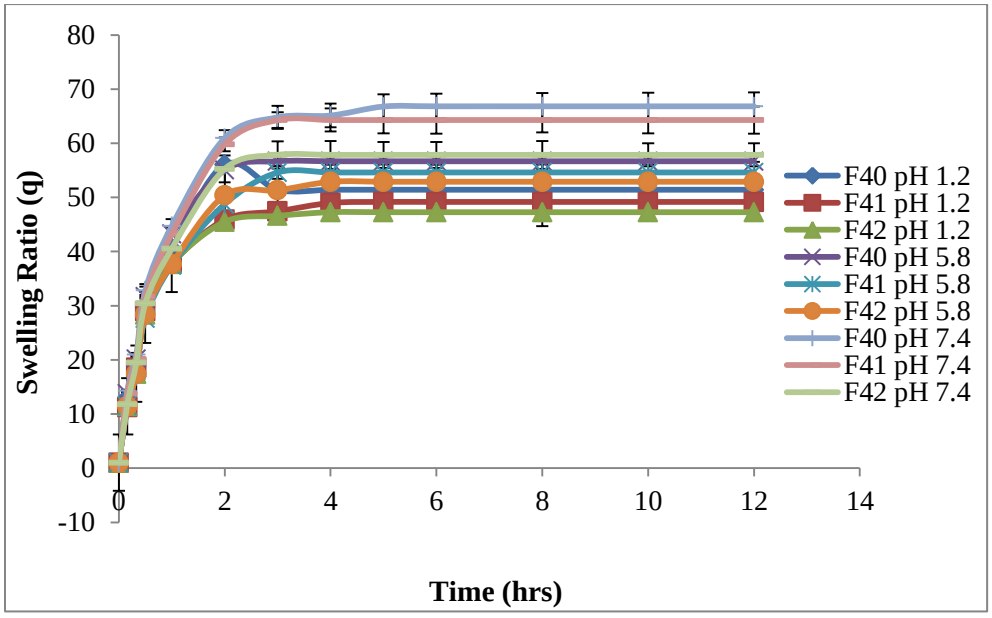

Figure 4.14. Comparative swelling ratios of CMC-co-MAA-co-AMPS hydrogels using different concentrations of MBA

4.2. Percent equilibrium swelling (%ES)

The swelling measurement was carried out until equilibrium weight of gel was obtained (i.e. 72 hrs) and then percent equilibrium swelling was carried out. Percent equilibrium swelling (%ES) covering different concentrations of all components at pH 1.2, 5.8 and 7.4 is given in tables 4.15 to 4.21 and represented graphically in figures 4.15 to 4.21.

With increasing concentration of HEMA from 0.8 g to 2.5 g (%w/w) percent equilibrium swelling was noted to be decreased 93.886 % to 92.699 % at pH 7.4, 90.749 % to 89.087 % at pH 5.8 and 71.416 % to 66.818 % at pH 1.2 as given in table 4.15.

Table 4.15. Percent equilibrium swelling (%ES) at different pH containing different %w/w ratio of HEMA from HEMA-co-AA hydrogels

% w/w of HEMA	% Equilibrium Swelling (%ES)		
	pH 1.2	pH 5.8	pH 7.4
0.8	71.416	90.749	93.886
1.6	68.661	89.621	93.254
2.5	66.818	89.087	92.699

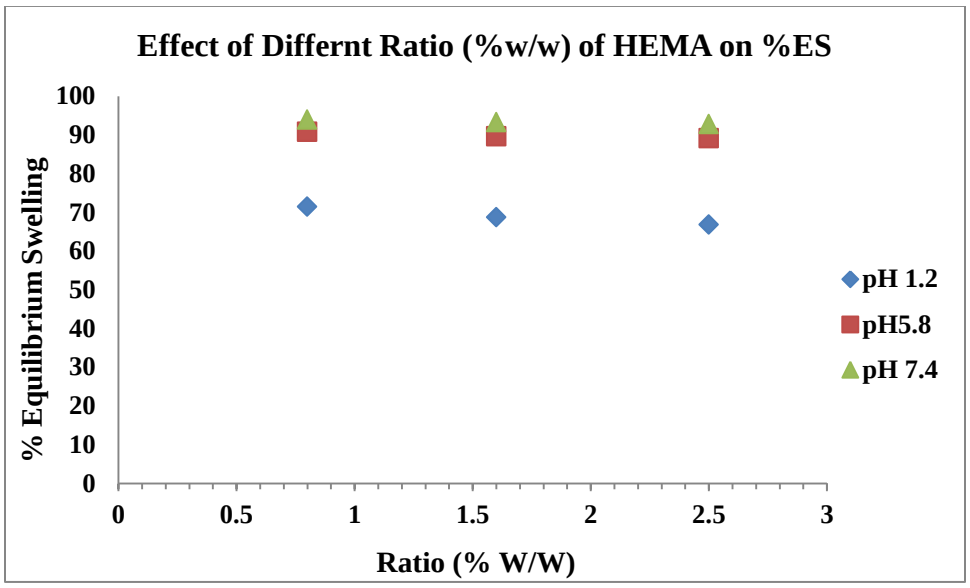

Figure 4.15. Percent equilibrium swelling (%ES) at different pH containing different %w/w ratio of HEMA from HEMA-co-AA hydrogels

Percent equilibrium swelling has direct relation with increasing concentration of AA from 10.5 g to 14.5 g (%w/w) as percent equilibrium swelling was noted to be increased from 93.339 % to 93.909 % at pH 7.4, 89.359 % to 90.483 % at pH 5.8 and 65.897 % to 68.491 % at pH 1.2 as given in table 4.16.

Table 4.16. Percent equilibrium swelling (%ES) at different pH containing different %w/w ratio of AA from HEMA-co-AA hydrogels

% w/w of AA	% Equilibrium Swelling (%ES)		
	pH 1.2	pH 5.8	pH 7.4
10.5	65.897	89.359	93.339
12.5	67.904	90.184	93.752
14.5	68.491	90.483	93.909

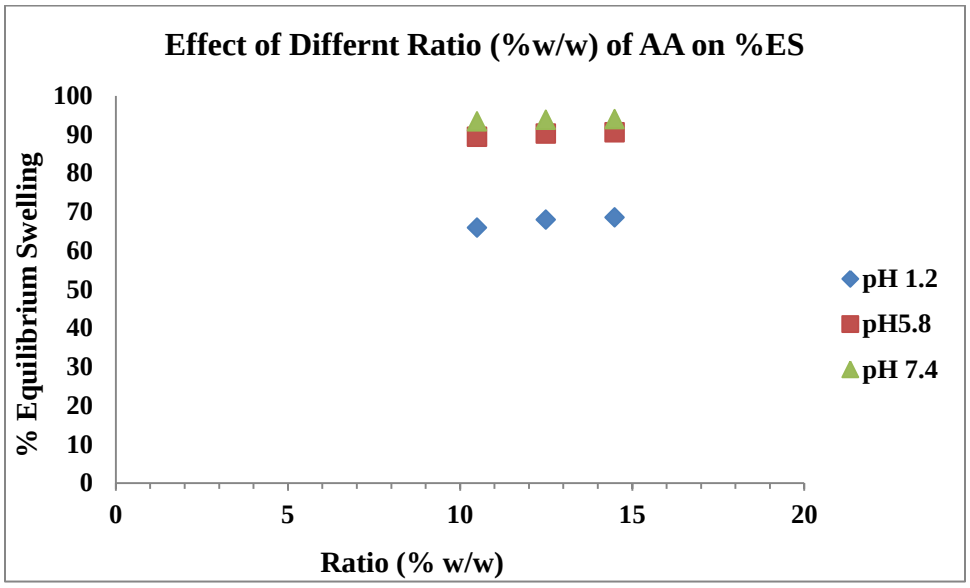

Figure 4.16. Percent equilibrium swelling (%ES) of HEMA-co-AA hydrogels at different pH containing different %w/w ratio of AA

Influence of increasing concentration of MBA on percent equilibrium swelling was noted. As %w/w ratio of MBA was increased from 0.020 g to 0.030 g, percent equilibrium swelling was noted to be decreased from 94.084 % to 92.740 % at pH 7.4, 89.903 % to 83.853 % at pH 5.8 and 65.728 % to 60.451 % at pH 1.2 as given in table 4.17.

Table 4.17. Percent equilibrium swelling (%ES) at different pH containing different %w/w ratio of MBA from HEMA-co-AA hydrogels

% w/w of MBA	% Equilibrium Swelling (%ES)		
	pH 1.2	pH 5.8	pH 7.4
0.020	65.728	89.903	94.084
0.025	64.349	88.872	93.362
0.030	60.451	83.853	92.740

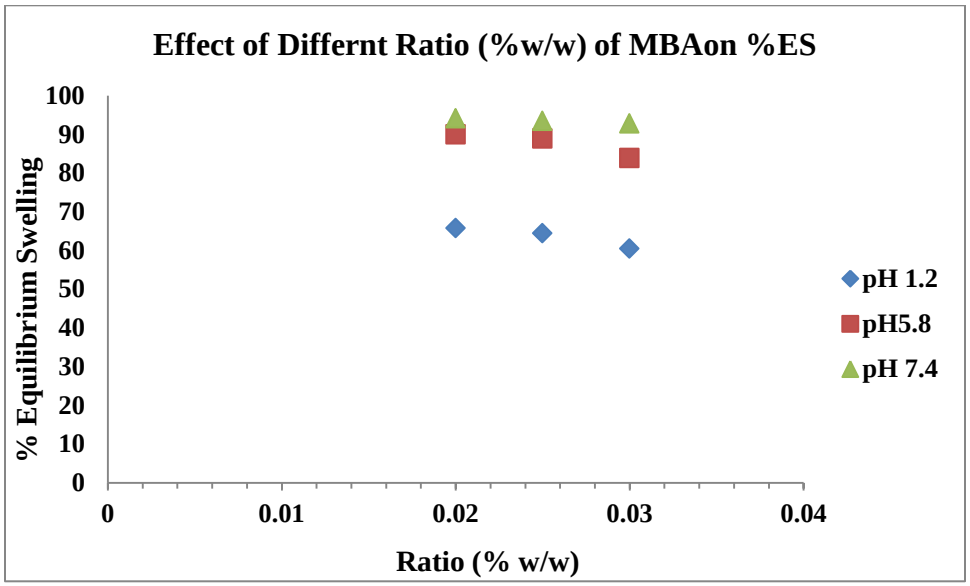

Figure 4.17. Percent equilibrium swelling (%ES) at different pH containing different %w/w ratio of MBA from HEMA-co-AA hydrogels

With increasing concentration of HPMC from 0.6 g to 1.2 g (%w/w) percent equilibrium swelling was noted to be increased from 97.173 % to 97.793 % at pH 7.4, 94.899 % to 96.797 % at pH 5.8 and 81.598 % to 80.359 % at pH 1.2 as given in table 4.18.

Table 4.18. Percent equilibrium swelling (%ES) at different pH containing different %w/w ratio of HPMC from HPMC-co-AA hydrogels

% w/w of HPMC	% Equilibrium Swelling (%ES)		
	pH 1.2	pH 5.8	pH 7.4
0.6	81.598	94.899	97.173
0.9	81.142	96.507	97.566
1.2	80.359	96.797	97.793

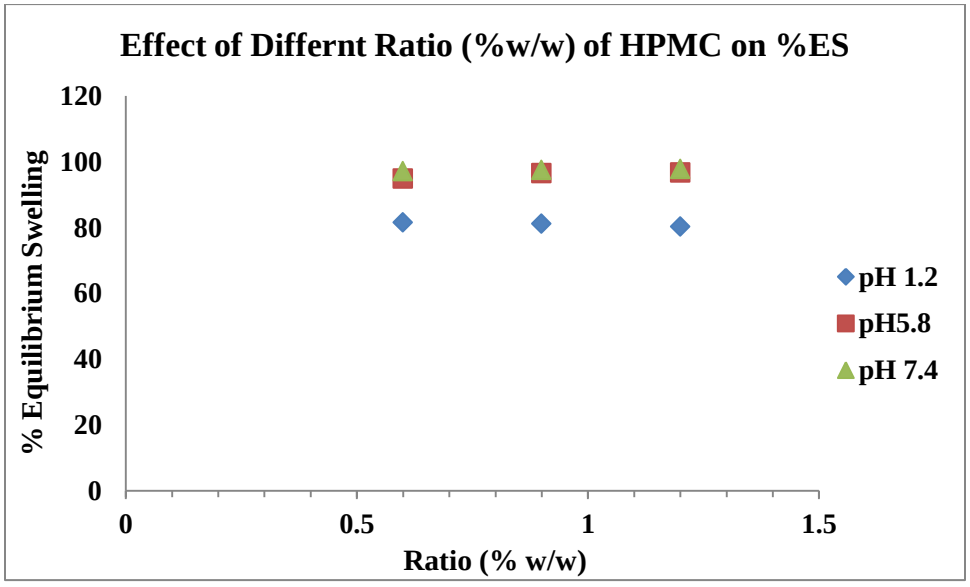

Figure 4.18. Percent equilibrium swelling (%ES) at different pH containing different %w/w ratio of HPMC from HPMC-co-AA hydrogels

Percent equilibrium swelling has relation with increasing concentration of MAA from 6 g to 8 g (%w/w) as percent equilibrium swelling was noted to be decreased from 98.564 % to 98.454 % at pH 7.4, 98.392 % to 98.356 % at pH 5.8 and 98.330 % to 98.259 % at pH 1.2 as given in table 4.19.

Table 4.19. Percent equilibrium swelling (%ES) at different pH containing different %w/w ratio of MAA from CMC-co-MAA-co-AMPS hydrogels

% w/w of MAA	% Equilibrium Swelling (%ES)		
	pH 1.2	pH 5.8	pH 7.4
6	98.330	98.392	98.564
7	98.278	98.364	98.508
8	98.259	98.356	98.454

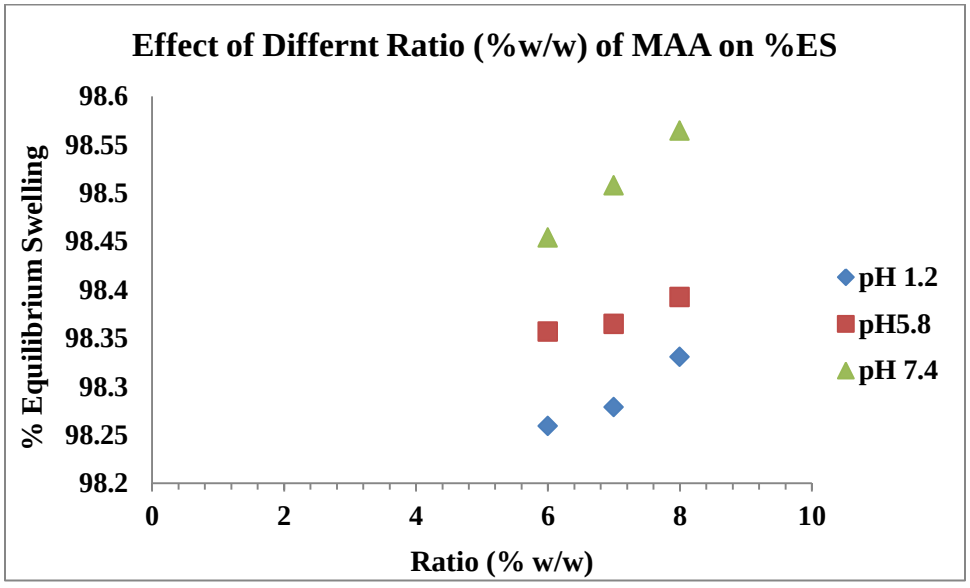

Figure 4.19. Percent equilibrium swelling (%ES) at different pH containing different %w/w ratio of MAA from CMC-co-MAA-co-AMPS hydrogels

Influence of increasing concentration of AMPS on percent equilibrium swelling was noted. As %w/w ratio of AMPS was increased from 4 g to 6 g, percent equilibrium swelling was noted to be increased from 98.499 % to 98.692 % at pH 7.4, 98.489 % to 98.685 % at pH 5.8 and 98.484 % to 98.667 % at pH 1.2 as given in table 4.20.

Table 4.20. Percent equilibrium swelling (%ES) at different pH containing different %w/w ratio of AMPS from CMC-co-MAA-co-AMPS hydrogels

% w/w of AMPS	% Equilibrium Swelling (%ES)		
	pH 1.2	pH 5.8	pH 7.4
4	98.484	98.489	98.499
5	98.550	98.573	98.582
6	98.667	98.685	98.692

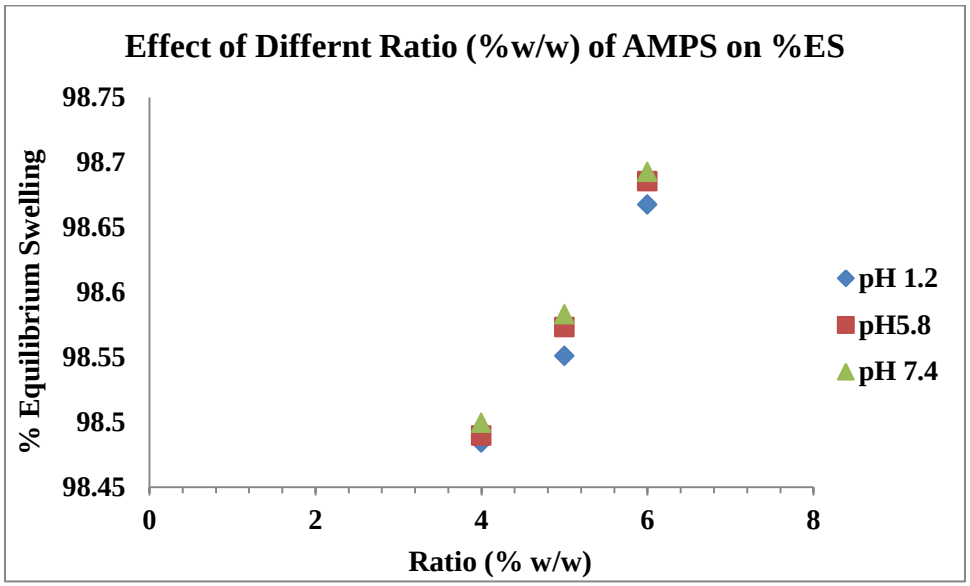

Figure 4.20. Percent equilibrium swelling (%ES) at different pH containing different %w/w ratio of AMPS from CMC-co-MAA-co-AMPS hydrogels

Effect of increasing concentration of CMC on percent equilibrium swelling was observed. It was noted that as %w/w ratio of CMC was increase from 1 g to 2 g percent equilibrium swelling was increased from 98.594 % to 98.672 % at pH 7.4, 98.534 % to 98.580 % at pH 5.8 and 98.499 % to 98.547 % at pH 1.2 as given in table 4.21.

Table 4.21. Percent equilibrium swelling (%ES) at different pH containing different %w/w ratio of CMC from CMC-co-MAA-co-AMPS hydrogels

% w/w of CMC	% Equilibrium Swelling (%ES)		
	pH 1.2	pH 5.8	pH 7.4
1	98.499	98.534	98.594
1.5	98.521	98.565	98.639
2	98.547	98.580	98.672

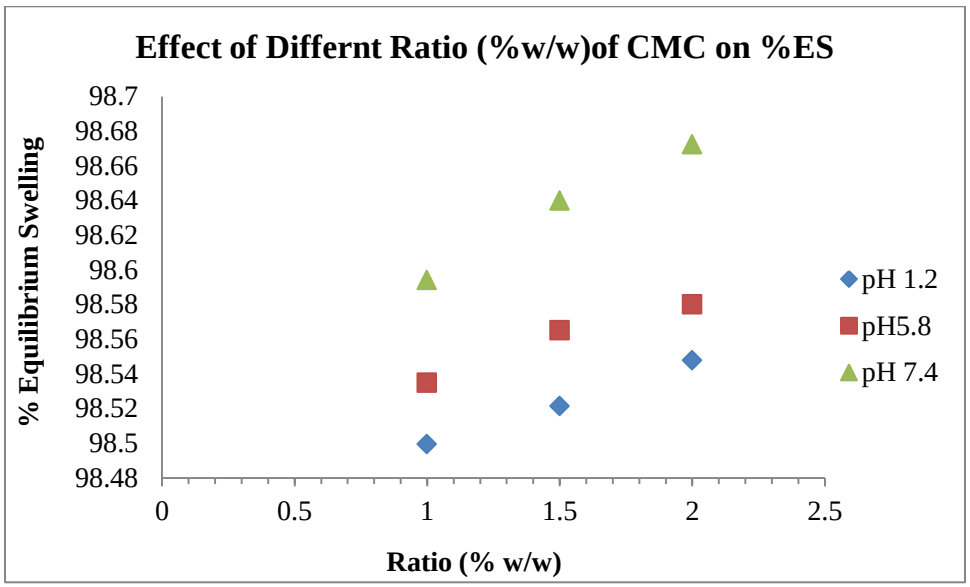

Figure 4.21. Percent equilibrium swelling (%ES) at different pH containing different %w/w ratio of CMC from CMC-co-MAA-co-AMPS hydrogels

4.3. Determination of percent gel content (%g_c), %porosity (%P) measurement and drug loading

Percent gel content (%g_c), percent porosity (%P) and drug loading measurements of all formulations casing different concentrations of components computed thereby evaluating effects of varying concentrations of all components on these parameters were noted and results are given in tables 4.22 to 4.25 and in figures 4.22 to 4.29.

Effect of varying concentrations of HEMA, AA and MBA on percent gel content (%g_c), percent porosity (%P) and drug loading was determined as in formulations F1 to F9. Formulations (F1 to F3) having variable quantities of HEMA exhibited % gel fraction ranging from 83.758 % to 93.269 %, % porosity from 14.425 % to 11.744 % and drug loading from 58.501 mg to 45.037 mg indicating that with increasing concentration of HEMA percent gel content (%g_c) was increased while percent porosity (%P) and drug loading was noted to be decreased. Moreover increasing concentration of AA (10.5 g to 14.5 g) also has direct influence on percent gel content (%g_c), percent porosity (%P) and drug loading as these were noted to be increased from 80.577 % to 85.536 %, 8.974 to 11.151 % and 29.465 mg to 35.055 mg respectively as in formulation F4 to F6. Increasing concentration of MBA (F7 to F9) resulted in increased percent gel content (81.382 % to 87.988), decreased percent porosity (8.926 % to 5.377 %) and decrease drug loading (25.465 mg to 20.130 mg).

Table 4.22. Percent gel content (%g_C), percent porosity (%P) measurement and drug loading of HEMA-co-AA hydrogels containing different %w/w of components

Formulation Code	Varying Component	%w/w Ratio (g)	% g_c	% P	Drug loading (mg/0.45g disc)
F1	HEMA	0.84	83.758	14.425	58.501
F2		1.68	86.885	12.845	53.811
F3		3.36	93.269	11.744	45.037
F4	AA	10.5	80.577	8.974	29.465
F5		12.5	82.741	9.321	32.608
F6		14.5	85.536	11.151	35.055
F7	MBA	0.02	81.382	8.926	25.465
F8		0.025	84.764	6.078	22.265
F9		0.03	87.988	5.377	20.130

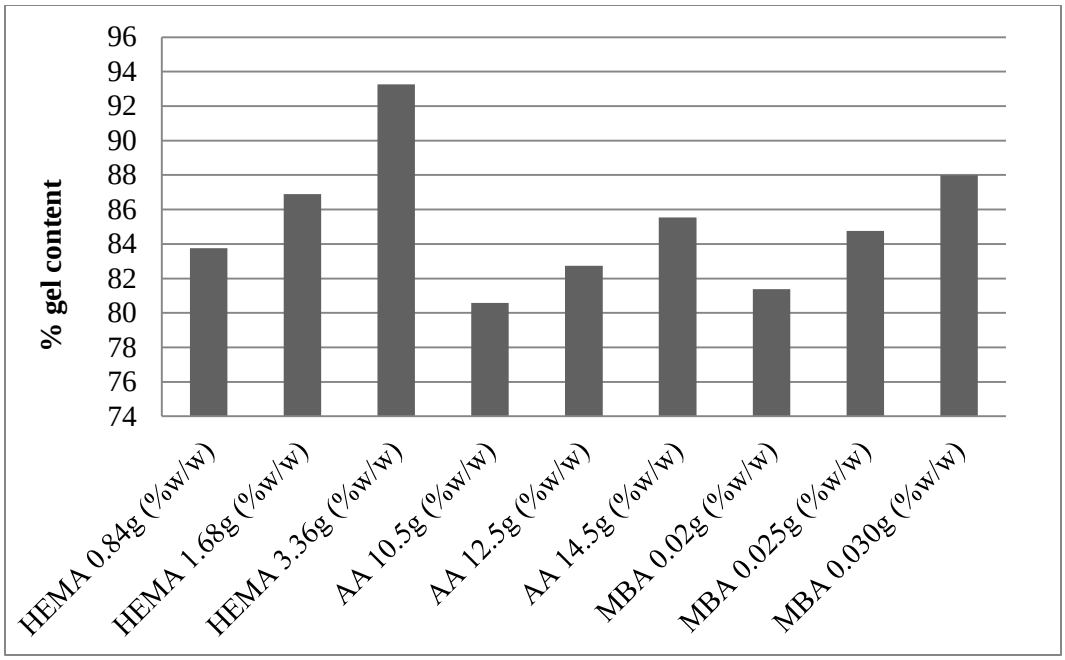

Figure 4.22. Percent gel content ($\%g_C$) of HEMA-co-AA hydrogels containing different %w/w of components

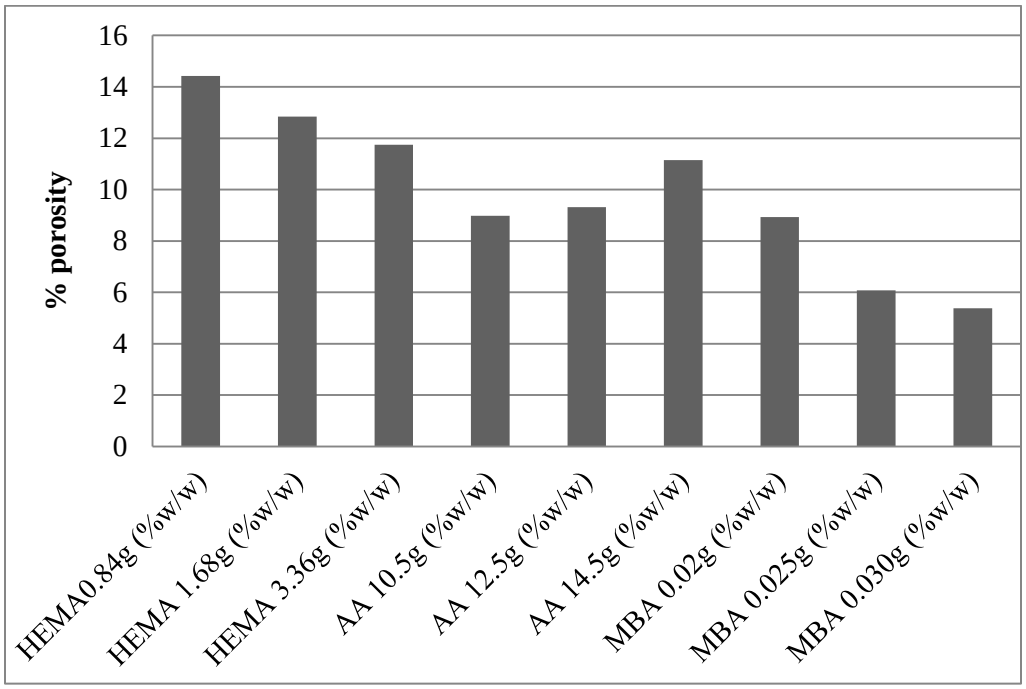

Figure 4.23. Percent porosity (% P) of HEMA-co-AA hydrogels containing different %w/w of components

Effect of changing concentrations of HPMC, AA and MBA on percent gel content (%g_c), percent porosity (%P) and drug loading was noted as in formulations F10 to F18. Formulations (F10 to F12) with changing concentration of HPMC showed % gel fraction ranging from 85.614 % to 93.990 %, % porosity from 27.037 % to 33.157 % and drug loading from 84.101 mg to 93.077 mg indicating that with increasing concentration of HPMC percent gel content (%g_c), percent porosity (%P) and drug loading was increased. Similarly increasing concentration of AA (12.5 g to 7.5 g) also has direct influence on percent gel content (%g_c), percent porosity (%P) and drug loading as these were noted to be increased from 86.352 % to 80.468 %, 32.771 to 29.670 % and 81.632 mg to 73.166 mg respectively as in case of formulation F13 to F15. Increasing concentration of MBA (F16 to F18) resulted in increased percent gel content (82.180 % to 88.268), decreased percent porosity (61.325 % to 39.831 %) and decrease drug loading (61.325 mg to 39.831 mg).

Table 4.23. Percent gel content (%g_C), percent porosity (%P) measurement and drug loading of HPMC-co-AA hydrogels containing different %w/w of components

Formulation Code	**Varying Component**	**%w/w Ratio (g)**	**% g_c**	**% P**	**Drug loading (mg/0.46g disc)**
F10	HPMC	0.6	85.614	27.037	84.101
F11		0.9	90.866	30.698	88.211
F12		1.2	93.990	33.157	93.077
F13	AA	12.5	86.352	32.771	81.632
F14		10	83.291	32.607	78.228
F15		7.5	80.468	29.670	73.166
F16	MBA	0.2	82.180	28.708	61.325
F17		0.25	84.764	24.506	52.445
F18		0.3	88.268	21.860	39.831

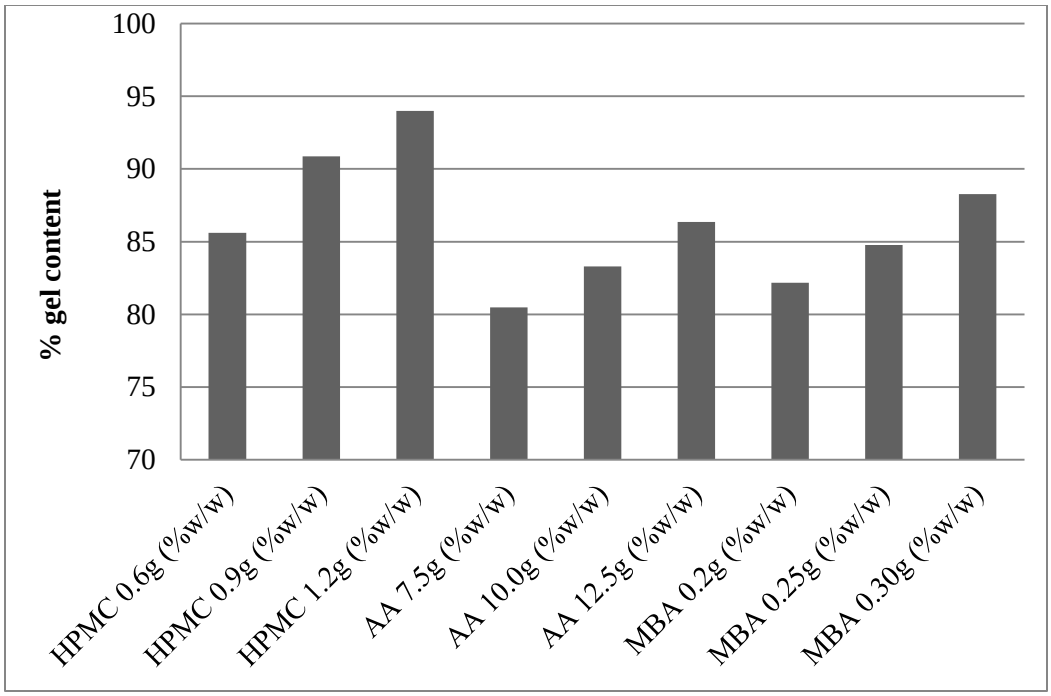

Figure 4.24. Percent gel content (%g_C) of HPMC-co-AA hydrogels containing different %w/w of components

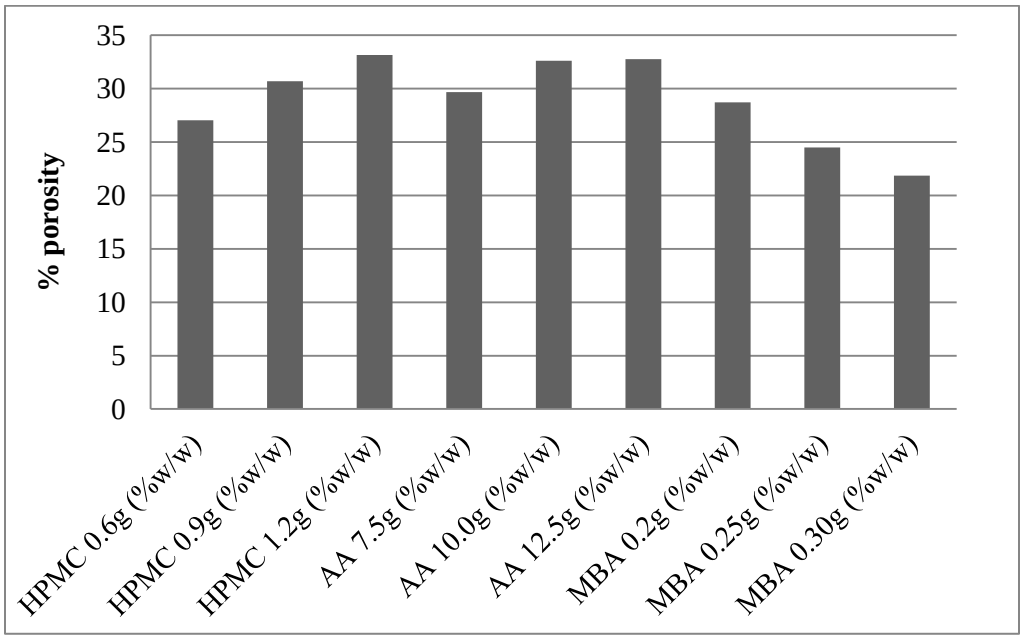

Figure 4.25. Percent porosity (% P) of HPMC-co-AA hydrogels containing different %w/w of components

Effect of changing concentrations of HEMA, AA, HPMC and MBA on percent gel content (%g_c), percent porosity (%P) and drug loading was noted as in formulations F19 to F30. Formulations (F19 to F21) with increasing concentration of HEMA exhibited % gel fraction ranging from 82.844 % to 90.569 %, % porosity from 19.567 % to 16.473 % and drug loading from 47.862 mg to 38.623 mg indicating that with increasing concentration of HEMA percent gel content (%g_c) was increased while percent porosity (%P) and drug loading was decreased. Similarly increasing concentration of AA (10 g to 15 g) also has direct influence on percent gel content (%g_c), percent porosity (%P) and drug loading as these were noted to be increased from 86.352 % to 93.489 %, 25.394 to 38.934 % and 69.832 mg to 79.271 mg respectively as in case of formulation F22 to F24. Increasing concentration of HPMC (F25 to F27) also resulted in increase in percent gel content (%g_c), percent porosity (%P) and drug loading (84.840 to 93.854, 20.205 to 25.383 and 58.521 mg to 67.261 mg respectively). Increasing concentration of MBA (F28 to F30) resulted in increased percent gel content (85.372% to 94.413), decreased percent porosity (16.961% to 12.911%) and decrease drug loading (35.831 mg to 24.862 mg).

Table 4.24. Percent gel content (%g_C), percent porosity (%P) measurement and drug loading of HPMC-co-AA-co-HEMA hydrogels containing different %w/w of components

Formulation Code	Varying Component	%w/w Ratio (g)	% g_c	% P	Drug loading (mg/0.46g disc)
F19	HEMA	0.5	82.844	19.567	47.862
F20		1	86.529	17.278	42.331
F21		1.5	90.596	16.473	38.623
F22	AA	10	86.352	25.394	69.832
F23		12.5	88.354	31.164	74.115
F24		15	93.489	38.934	79.271
F25	HPMC	5	84.840	20.205	58.521
F26		7.5	88.642	23.793	63.142
F27		10	93.854	25.383	67.261
F28	MBA	0.2	85.372	16.961	35.831
F29		0.25	89.196	14.174	30.613
F30		0.3	94.413	12.911	24.862

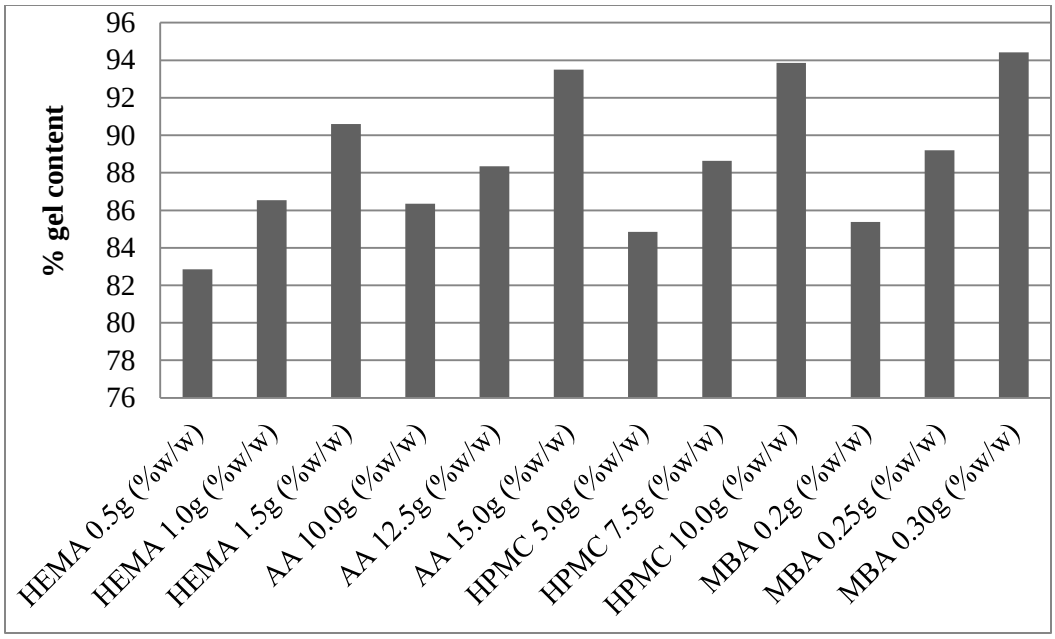

Figure 4.26. Percent gel content ($\%g_C$) of HPMC-co-AA-co-HEMA hydrogels containing different %w/w of components

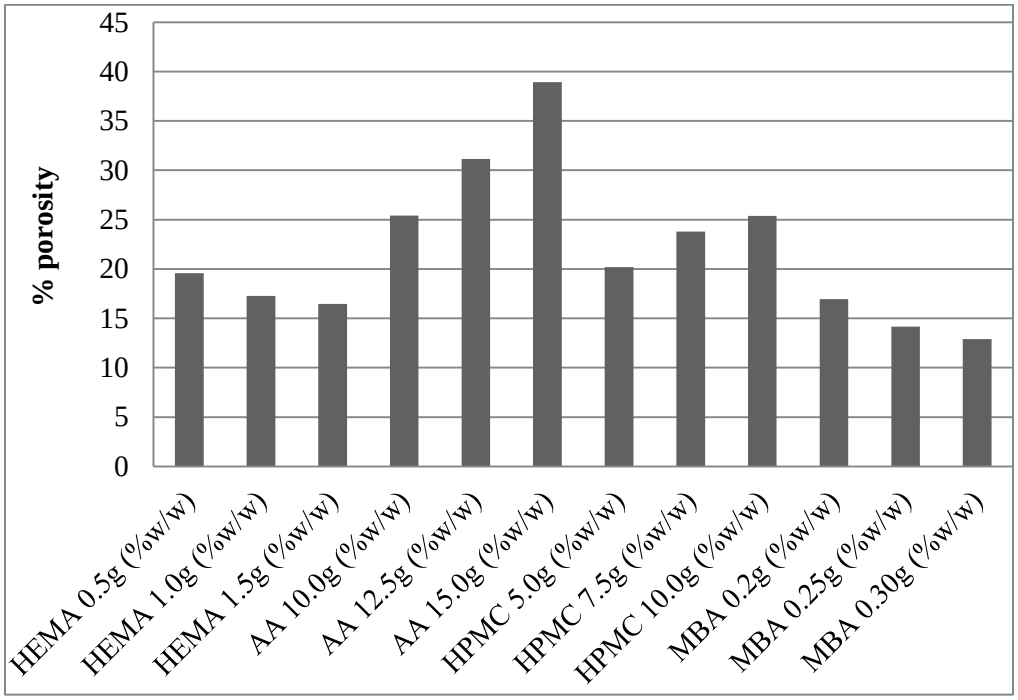

Figure 4.27. Percent porosity (% P) of HPMC-co-AA-co-HEMA hydrogels containing different %w/w of components

Effect of changing concentrations of MAA, AMPS, CMC and MBA on percent gel content (%g_c), percent porosity (%P) and drug loading was observed as in formulations F31 to F42. Formulations (F31 to F33) with increasing concentration of MAA exhibited % gel fraction ranging from 82.016% to 89.179%, % porosity from 42.278% to 36.278% and drug loading from 117.417mg to 106.371 mg indicating that with increasing concentration of HEMA percent gel content (%g_c) was increased while percent porosity (%P) and drug loading was decreased. Similarly increasing concentration of AMPS (4 g to 6 g) also has direct influence on percent gel content (%g_c), percent porosity (%P) and drug loading as these were noted to be increased from 92.804 % to 96.515%, 45.104 to 59.489% and 123.714 mg to 145.732 mg respectively as in case of formulation F34 to F36. Increasing concentration of CMC (F37 to F39) also resulted in increase in percent gel content (%g_c), percent porosity (%P) and drug loading (94.755 to 96.985, 46.291 to 53.243 and 126.634 mg to 133.153 mg respectively). Increasing concentration of MBA (F40 to F42) resulted in increased percent gel content (91.528 % to 96.703 %), decreased percent porosity (44.693 % to 35.749 %) and decrease drug loading (115.631 mg to 102.613 mg).

Table 4.25. Percent gel content (%g_C), percent porosity (%P) measurement and drug loading of CMC-co-MAA-co-AMPS hydrogels containing different %w/w of components

Formulation Code	Varying Component	%w/w Ratio (g)	% g_c	% P	Drug loading (mg/0.45g disc)
F31	MAA	6	82.016	42.278	117.417
F32		7	86.493	39.237	111.631
F33		8	89.179	36.278	106.371
F34	AMPS	4	92.804	45.104	123.714
F35		5	94.690	51.302	132.621
F36		6	96.515	59.489	145.732
F37	CMC	1	94.755	46.291	126.634
F38		1.5	96.539	49.321	130.631
F39		2	96.985	53.243	133.153
F40	MBA	0.045	91.528	44.693	115.631
F41		0.050	94.652	40.182	109.741
F42		0.055	96.703	35.749	102.613

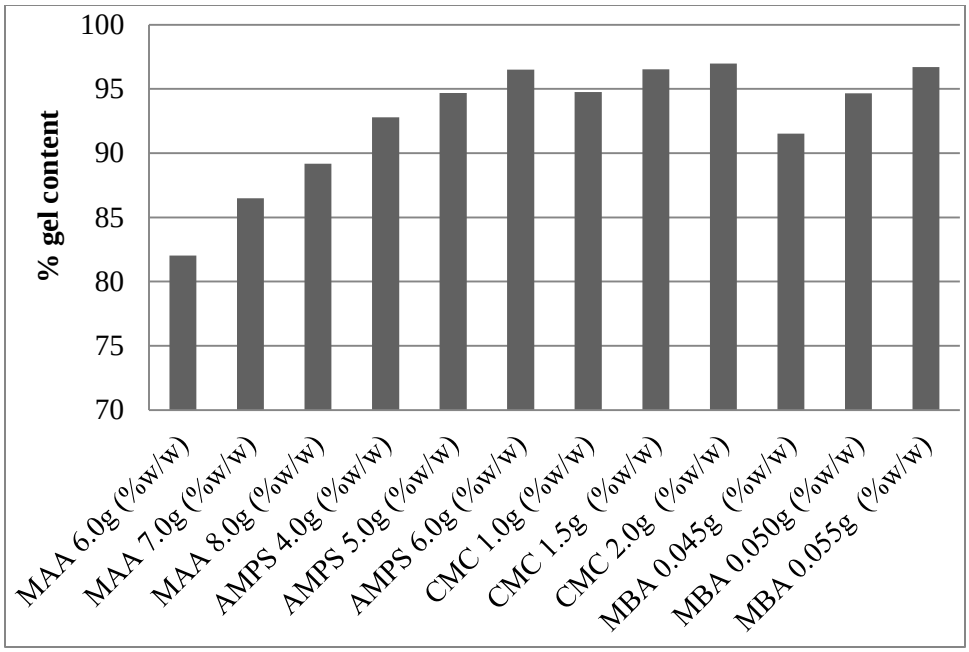

Figure 4.28. Percent gel content ($\%g_C$) of CMC-co-MAA-co-AMPS hydrogels containing different %w/w of components

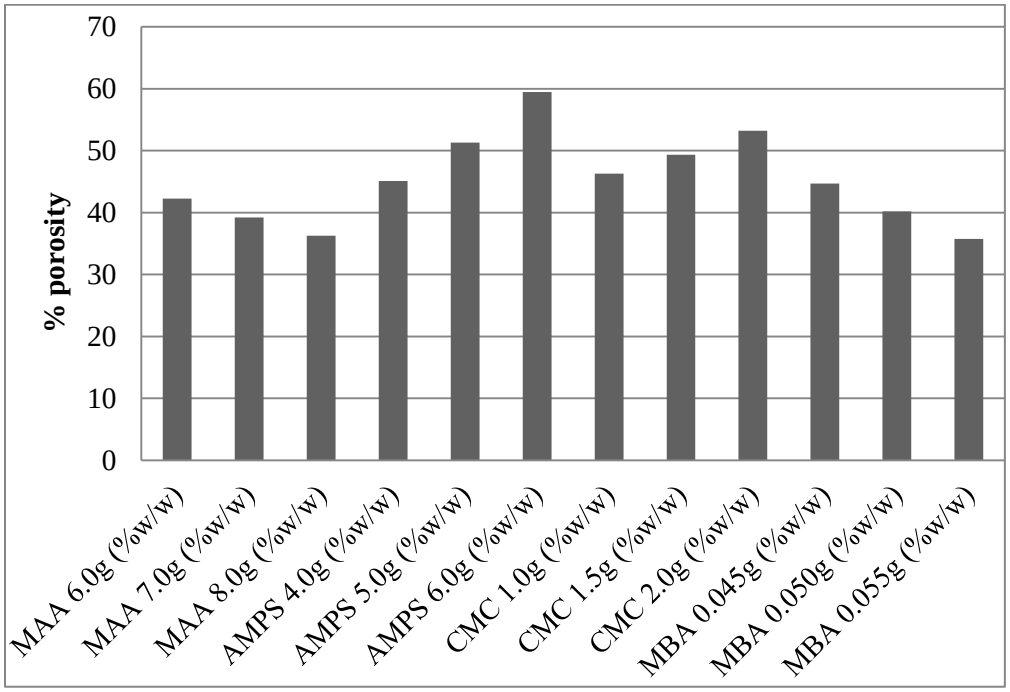

Figure 4.29. Percent porosity (% P) of CMC-co-MAA-co-AMPS hydrogels containing different %w/w of components

4.4. Characterization:

4.4.1 FTIR Analysis:

In this study, attenuated total reflectance (ATR) technology along with OPUS data collection software was employed to compute fourier transform infrared (FTIR) spectra of all samples using Bruker FTIR (Tensor 27 series, Germany) in the range of 500 cm^{-1} 4000 cm^{-1}. Characteristics band were observed 3247 cm−1 for (NH); 1675 cm−1 for (C=O, CONH) and 1362 cm−1 for (CH2). FTIR spectrum of pure components and loaded and unloaded formulations are shown in figures 4.30 to 4.33.

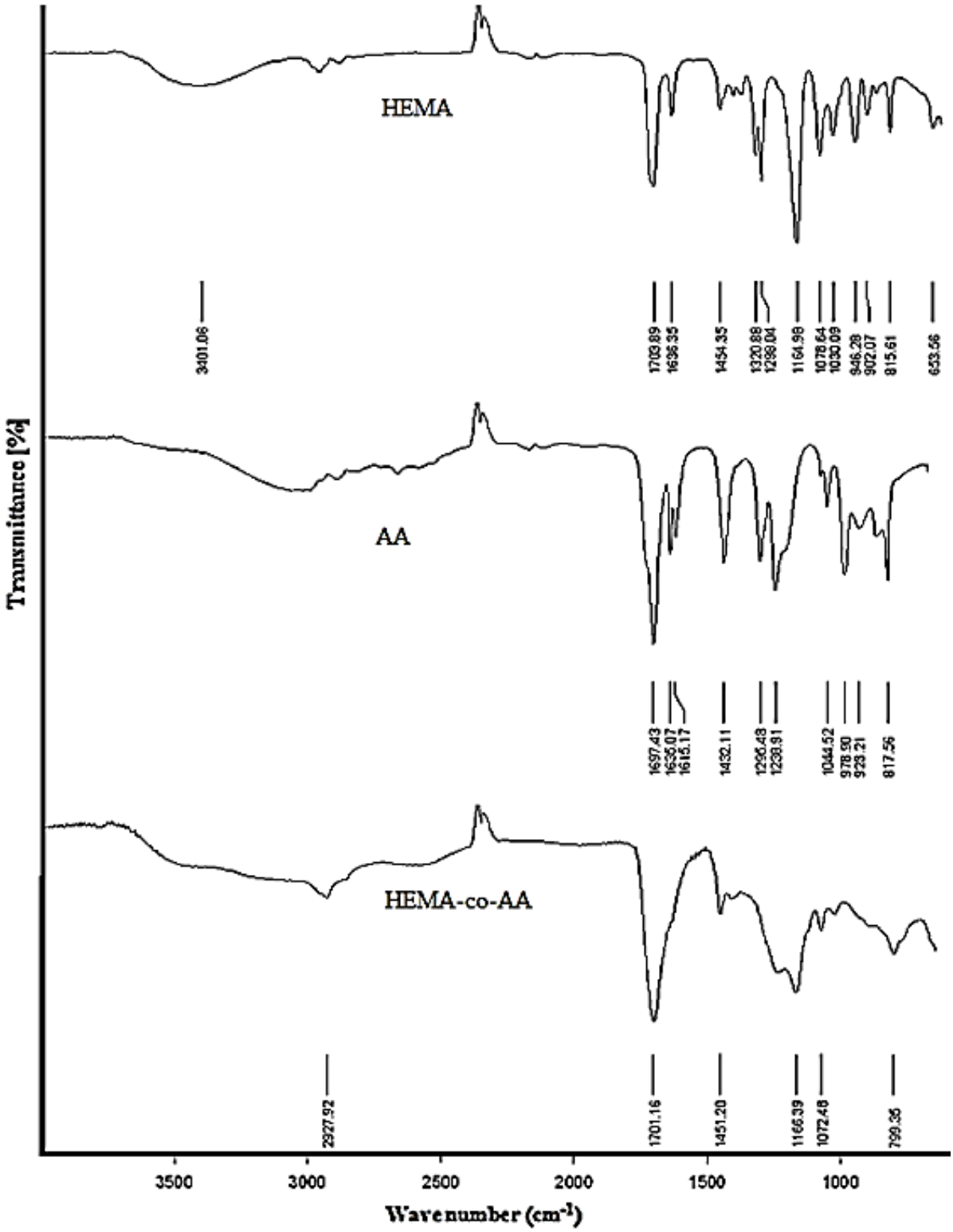

Figure 4.30. FTIR spectrum of HEMA-co-AA hydrogel

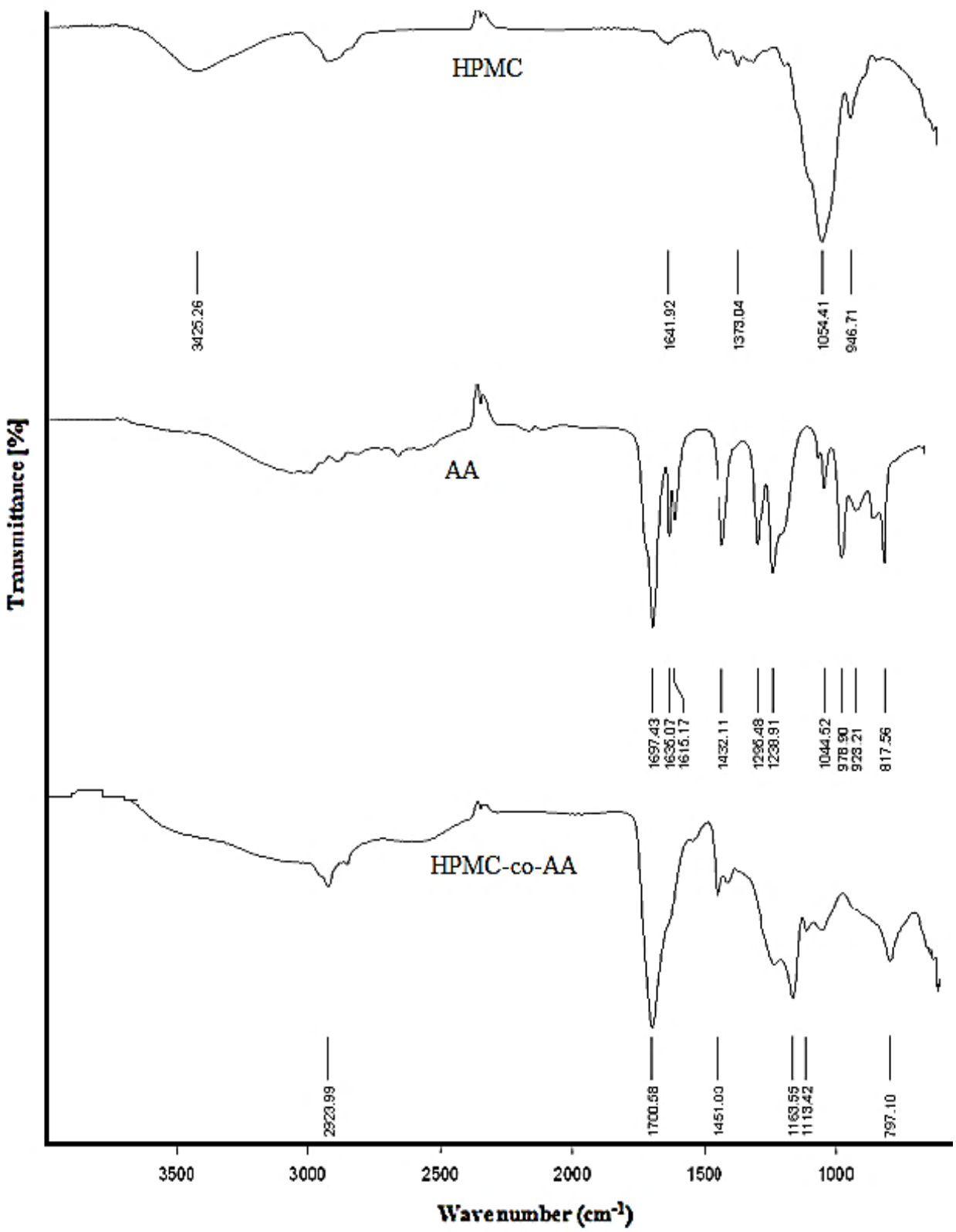

Figure 4.31. FTIR spectrum of HPMC-co-AA hydrogels

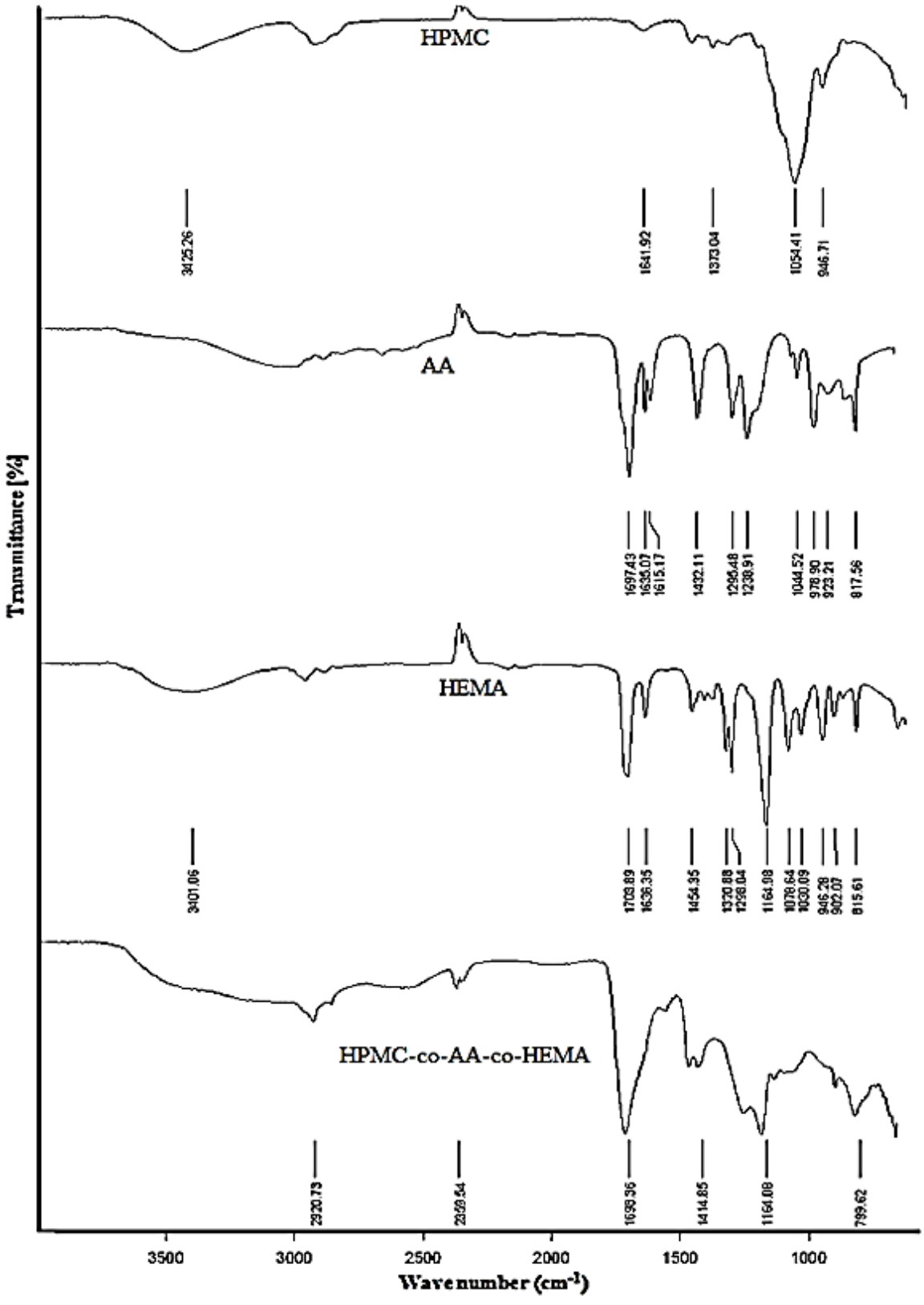

Figure 4.32. FTIR spectrum of HPMC-co-AA-co-HEMA hydrogels

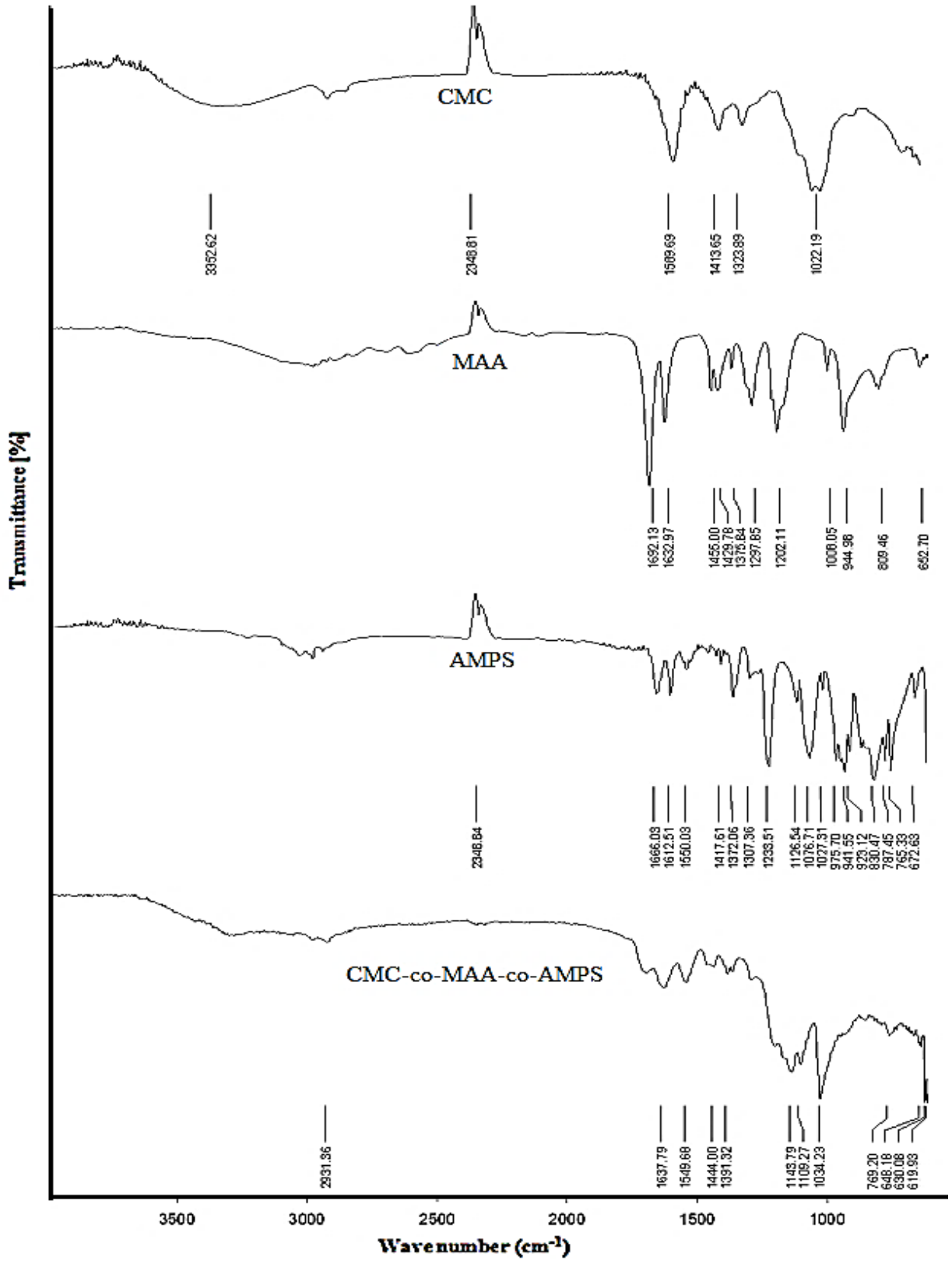

Figure 4.33. FTIR spectrum of CMC-co-MAA-co-AMPS hydrogels

4.4.2 Scanning Electron Microscopy (SEM)

For morphological studies scanning electron microscopy was carried out. Results of scanning electron microscopy (SEM) of all combinations are illustrated in figures 4.34 to 4.37.

Heterogeneous distribution of pores was observed as seen in SEM micrograph of HEMA-co-AA as shown in figure 4.34.

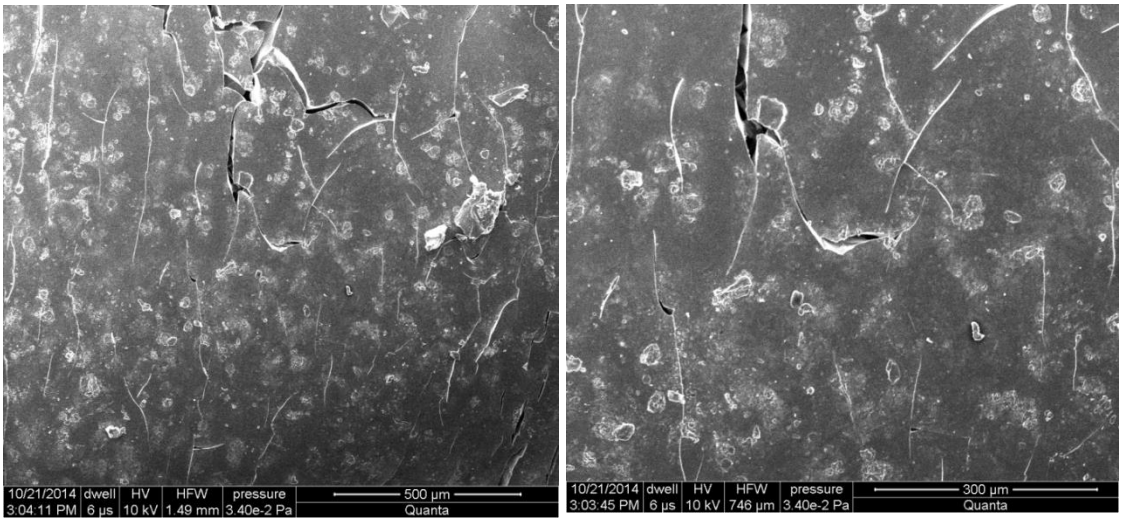

Figure 4.34. Scanning electron micrographs (SEM) of surface of HEMA-co-AA hydrogels at magnification of 100X and 200X (left to right) and 500µm scale bar and 300µm scale bar respectively

SEM micrograph of HPMC-co-AA hydrogel at magnification of 100X and 200X exhibited uneven pores in size and shape distribution as shown in figure 4.35.

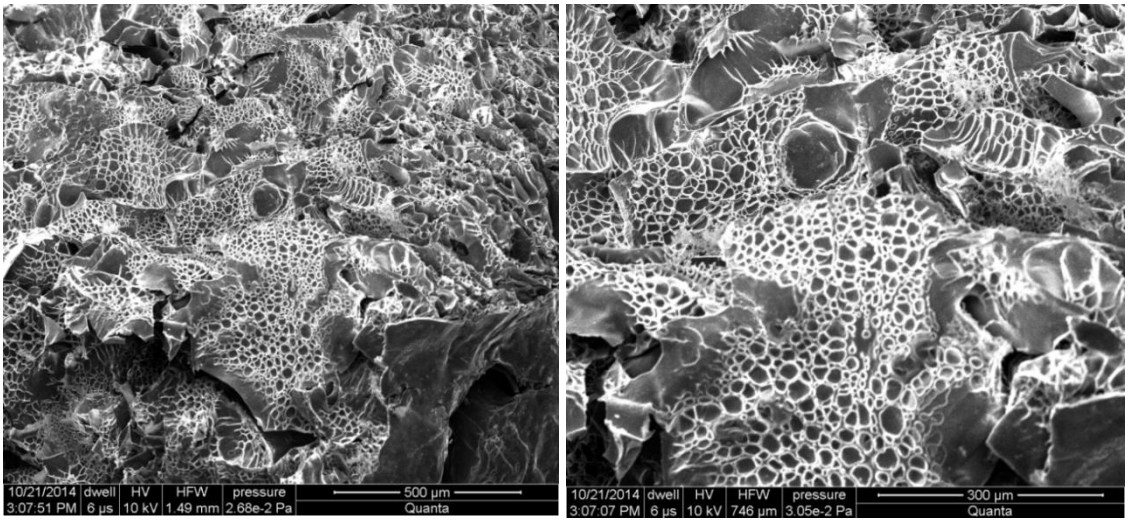

Figure 4.35. Scanning electron micrographs (SEM) of surface of HPMC-co-AA hydrogels at magnification of 100X and 200X (left to right) and 500µm scale bar and 300µm scale bar respectively

SEM images of HPMC-co-AA-co-HEMA hydrogels have given loose network structure of lamellar shape as shown in figure 4.36.

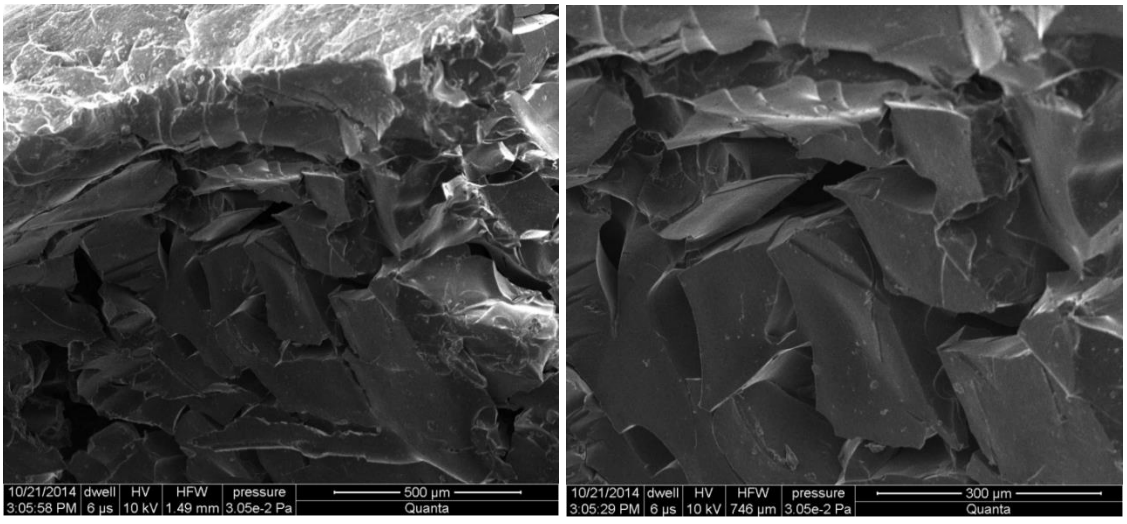

Figure 4.36. Scanning electron micrographs (SEM) of surface of HPMC-co-AA-co-HEMA hydrogels at magnification of 100X and 200X (left to right) and 500µm scale bar and 300µm scale bar respectively

Scanning electron micrograph of CMC-co-MAA-co-AMPS hydrogels showed coarse porous structure with heavy mesh networking as shown in figure 4.37.

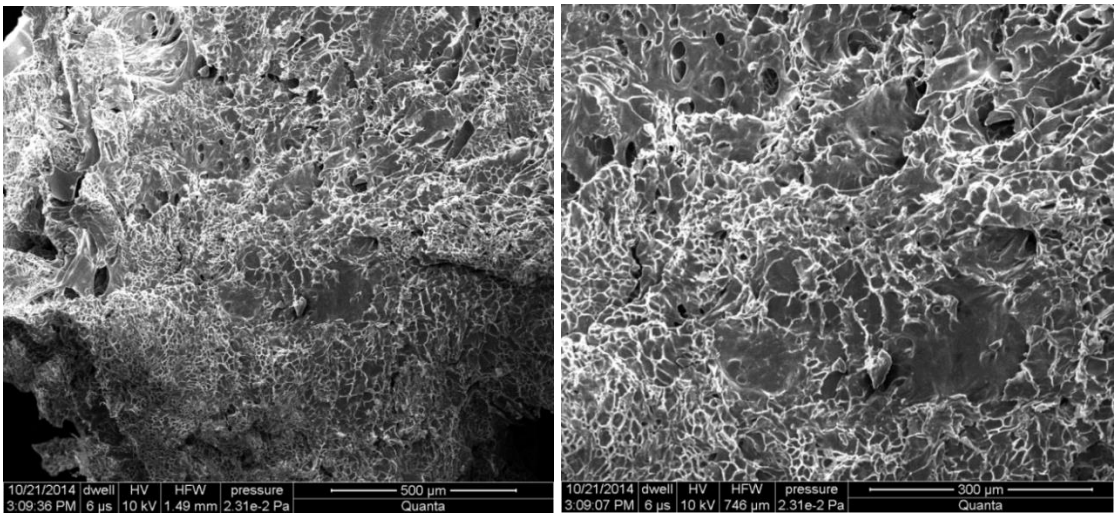

Figure 4.37. Scanning electron micrographs (SEM) of surface of CMC-co-MAA-co-AMPS hydrogels at magnification of 100X and 200X (left to right) and 500µm scale bar and 300µm scale bar respectively

4.4.3 Thermal Gravimetric Analysis and Differential Scanning Calorimetery (TGA & DSC)

Thermal transition behavior of prepared formulation was analyzed by thermal gravimetric analysis and differential scanning calorimeter (DuPont thermal analyzer with 2010 DSC194 module) in temperature range of 20 $^{\circ}$C to 900 $^{\circ}$C at heating rate of 10 $^{\circ}$C/min under nitrogen atmosphere and flow rate of 20 mL/min at temperature range of 0 $^{\circ}$C to 1000 $^{\circ}$C . Results TGA and DSC of all combinations are illustrated in figures 4.38 to 4.45 of all combinations are illustrated in figures 4.38 to 4.45.

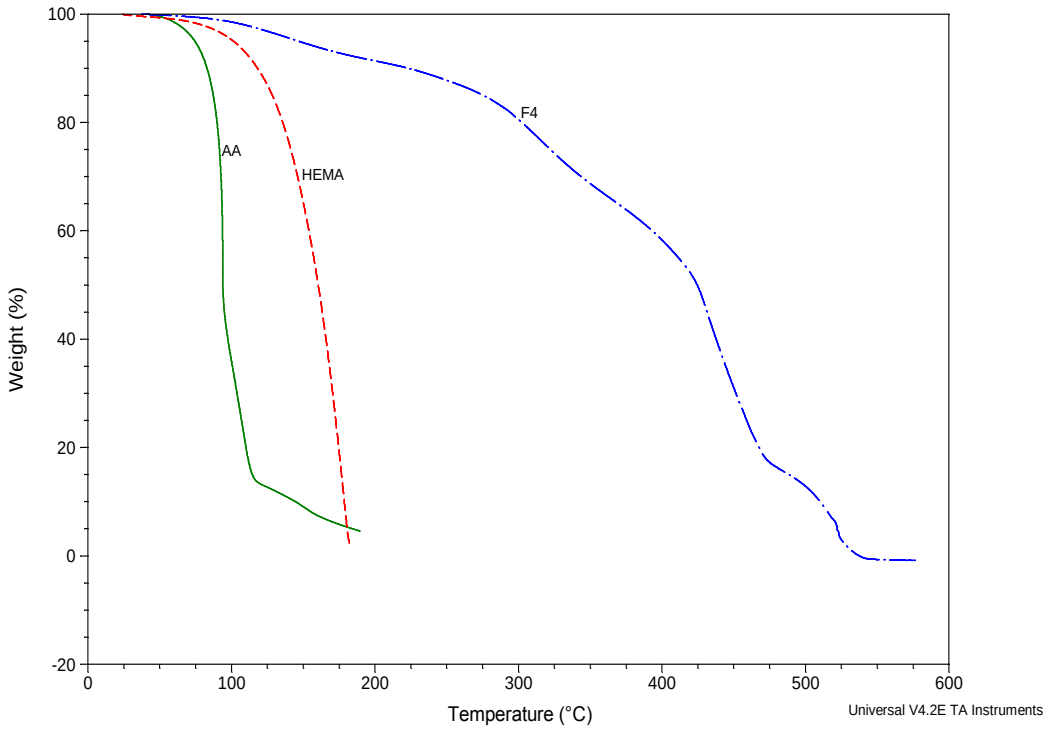

Figure 4.38. TGA thermogram for HEMA-co-AA hydrogels

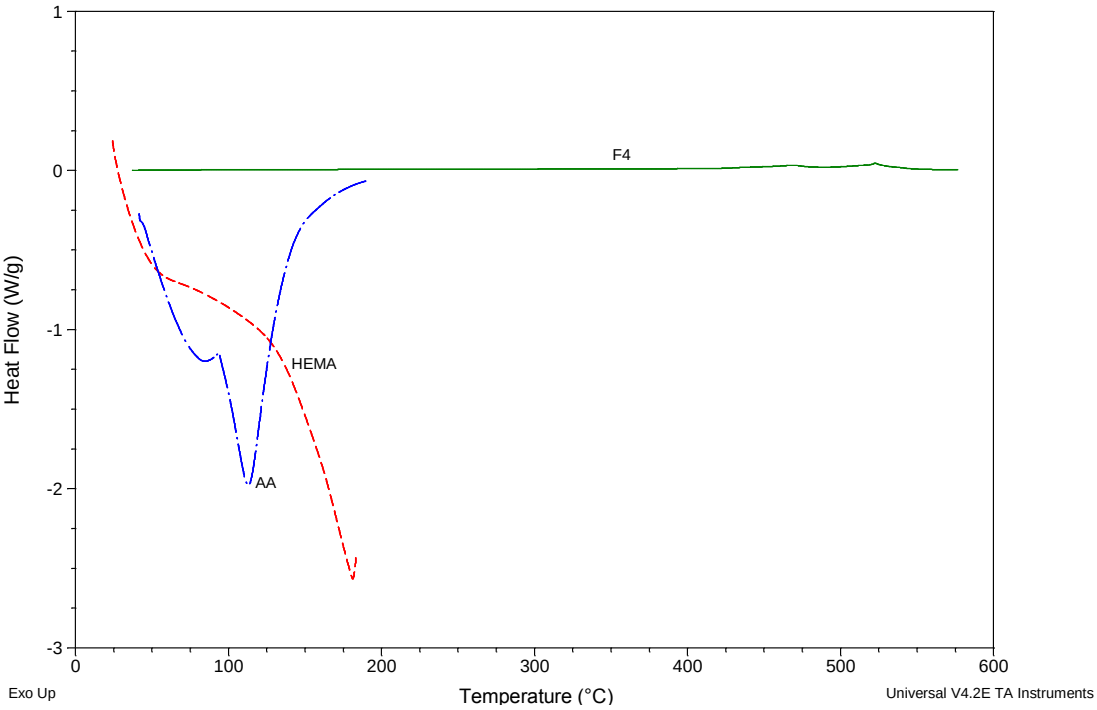

Figure 4.39. DSC thermogram for HEMA-co-AA hydrogels

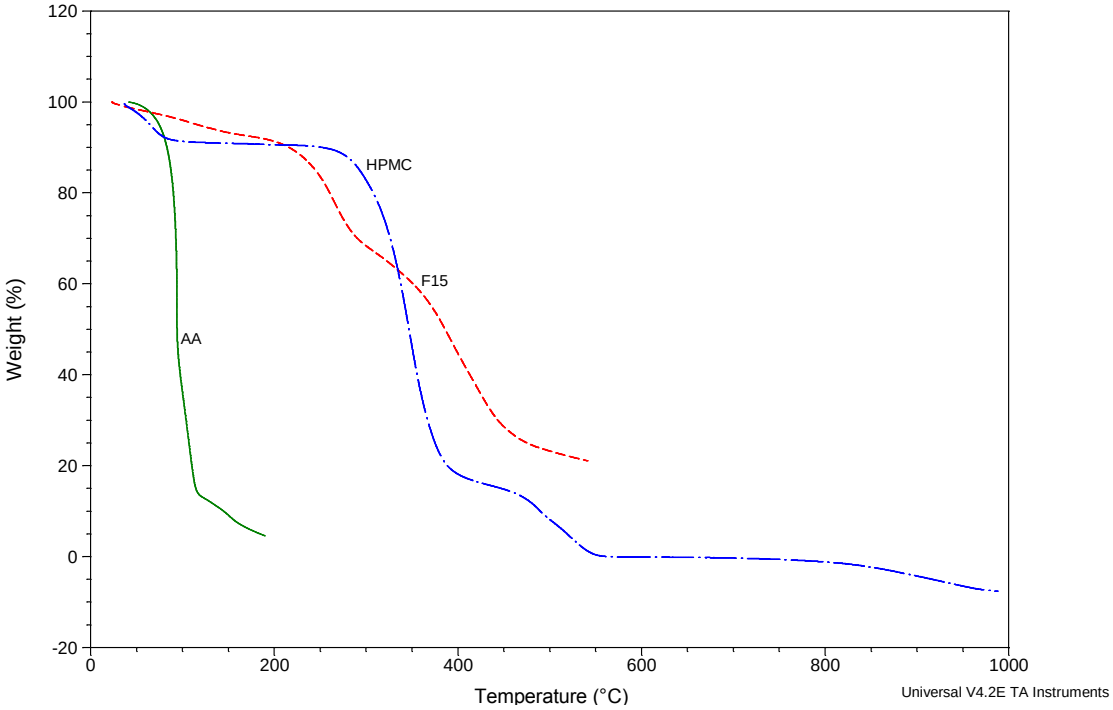

Figure 4.40. TGA thermogram for HPMC-co-AA hydrogels

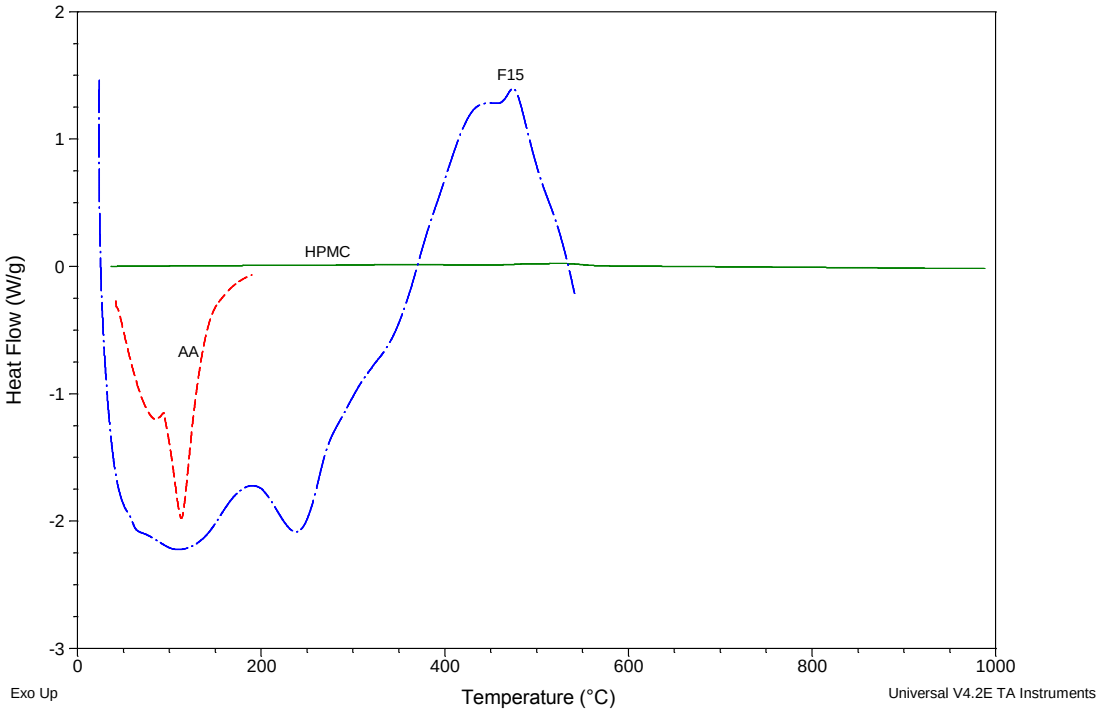

Figure 4.41. DSC thermogram for HPMC-co-AA hydrogels

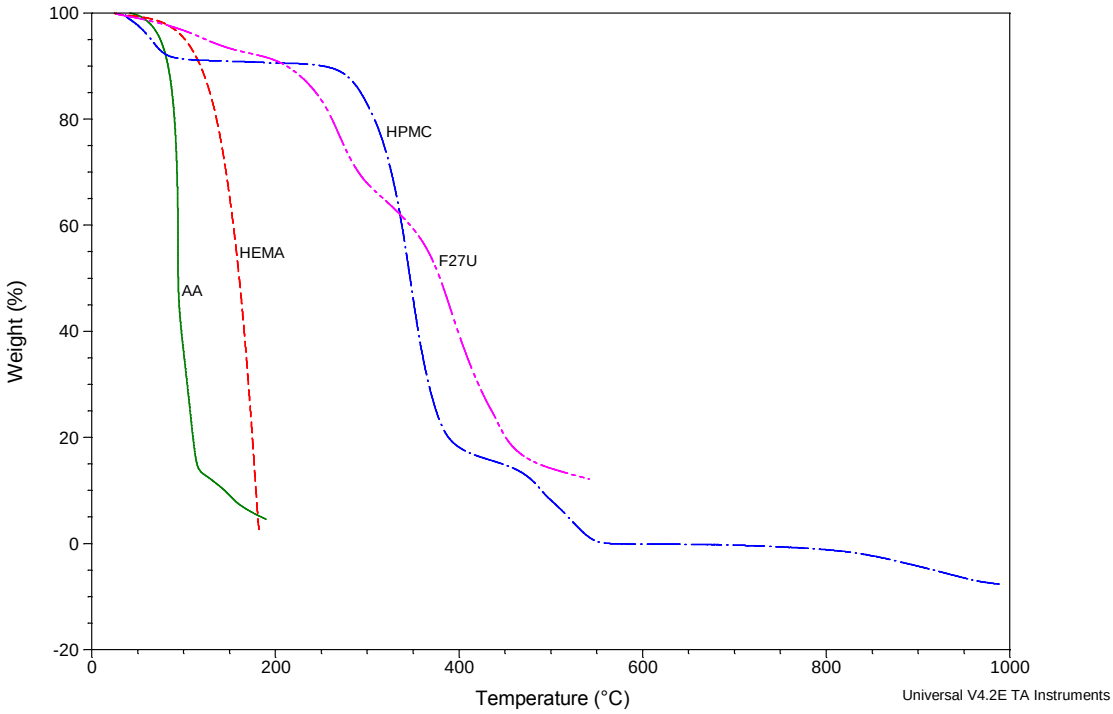

Figure 4.42. TGA thermogram for HPMC-co-AA-co-HEMA hydrogels

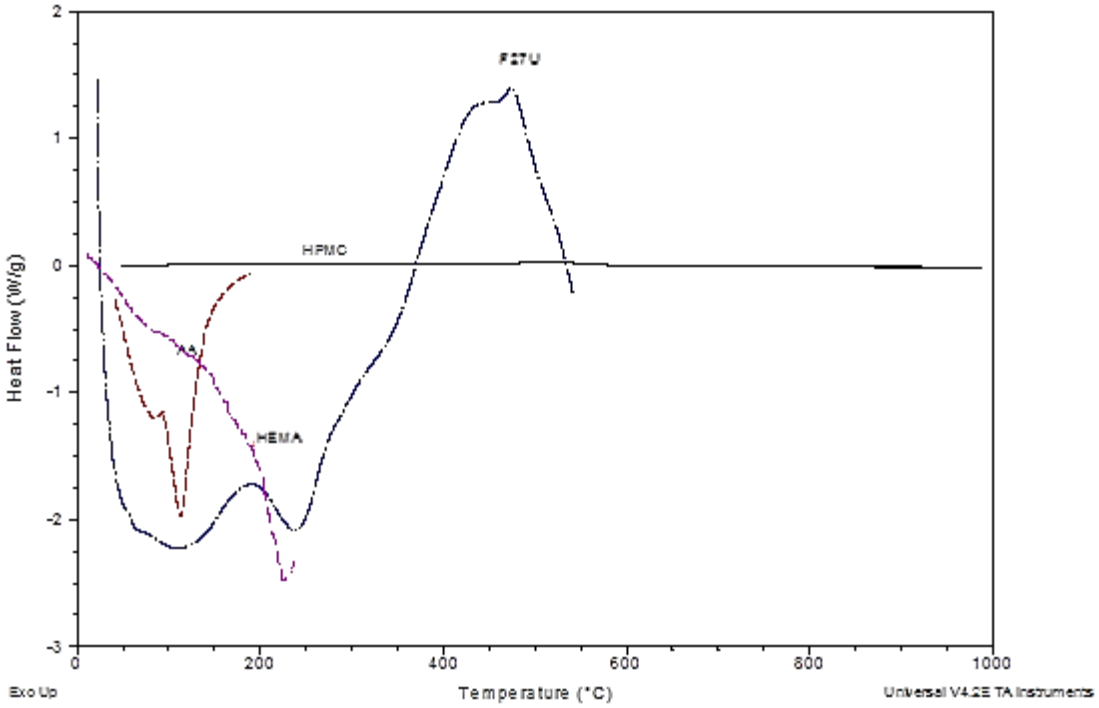

Figure 4.43. DSC thermogram for HPMC-co-AA-co-HEMA hydrogels

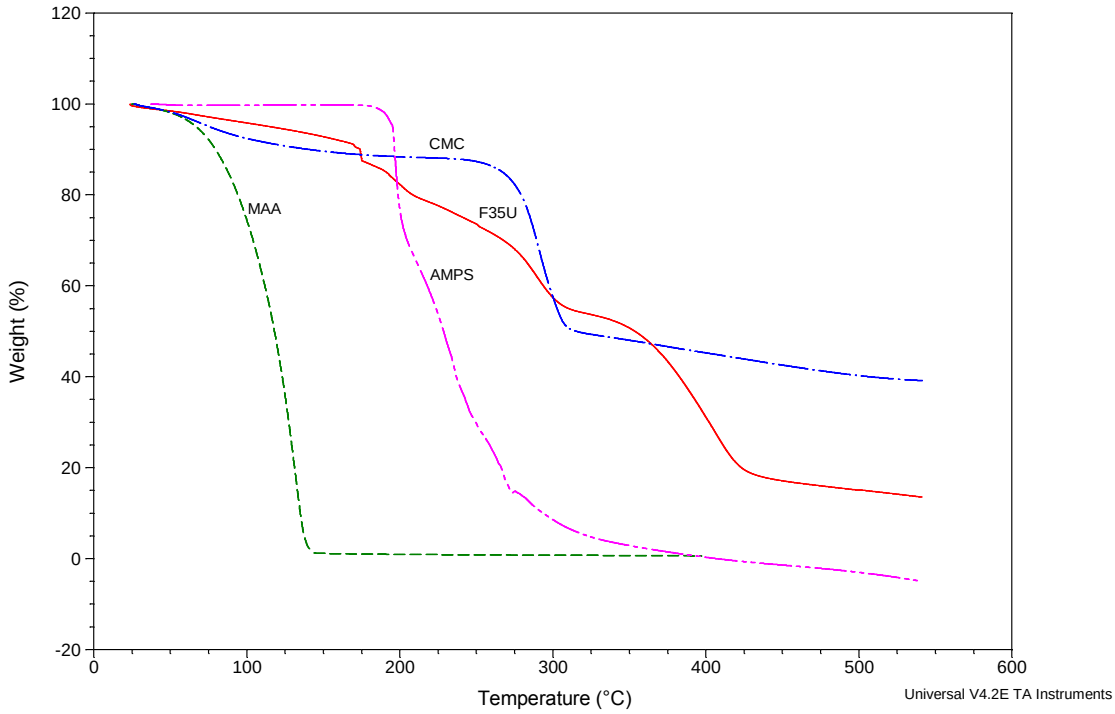

Figure 4.44. TGA thermogram for CMC-co-MAA-co-AMPS hydrogels

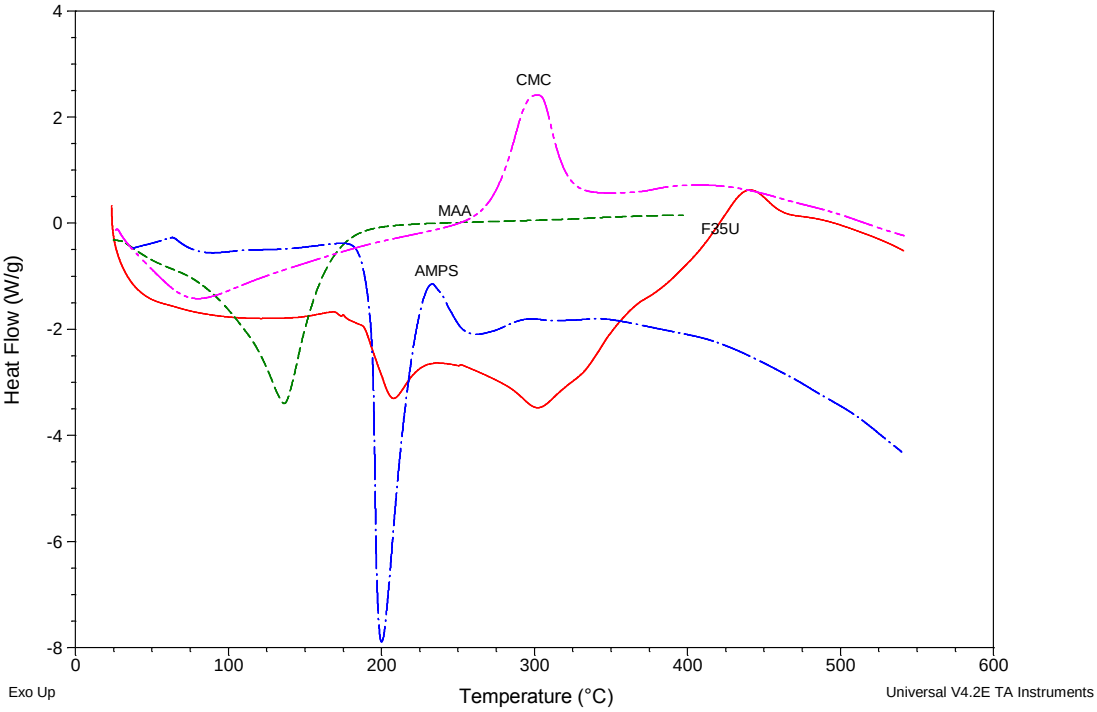

Figure 4.45. DSC thermogram for CMC-co-MAA-co-AMPS hydrogels

4.4.5 X-ray diffraction

To check crystallinity of pure drug (nicorandil), blank formulations, formulations containing drug and all formulated combinations of hydrogels were subjected to X-ray diffractometer (Bruker D8 Discover, Germany) with Ni-filtered CuK alpha radiation source having tube voltage of 35KV, current of 35 mA and scanning rate of 5° min^{-1}, over a range of 8°-60° diffraction angle (2θ) range (Osiris and Manal, 2012). Results showed amorphous nature of formulated hydrogels as given in figure 4.46.

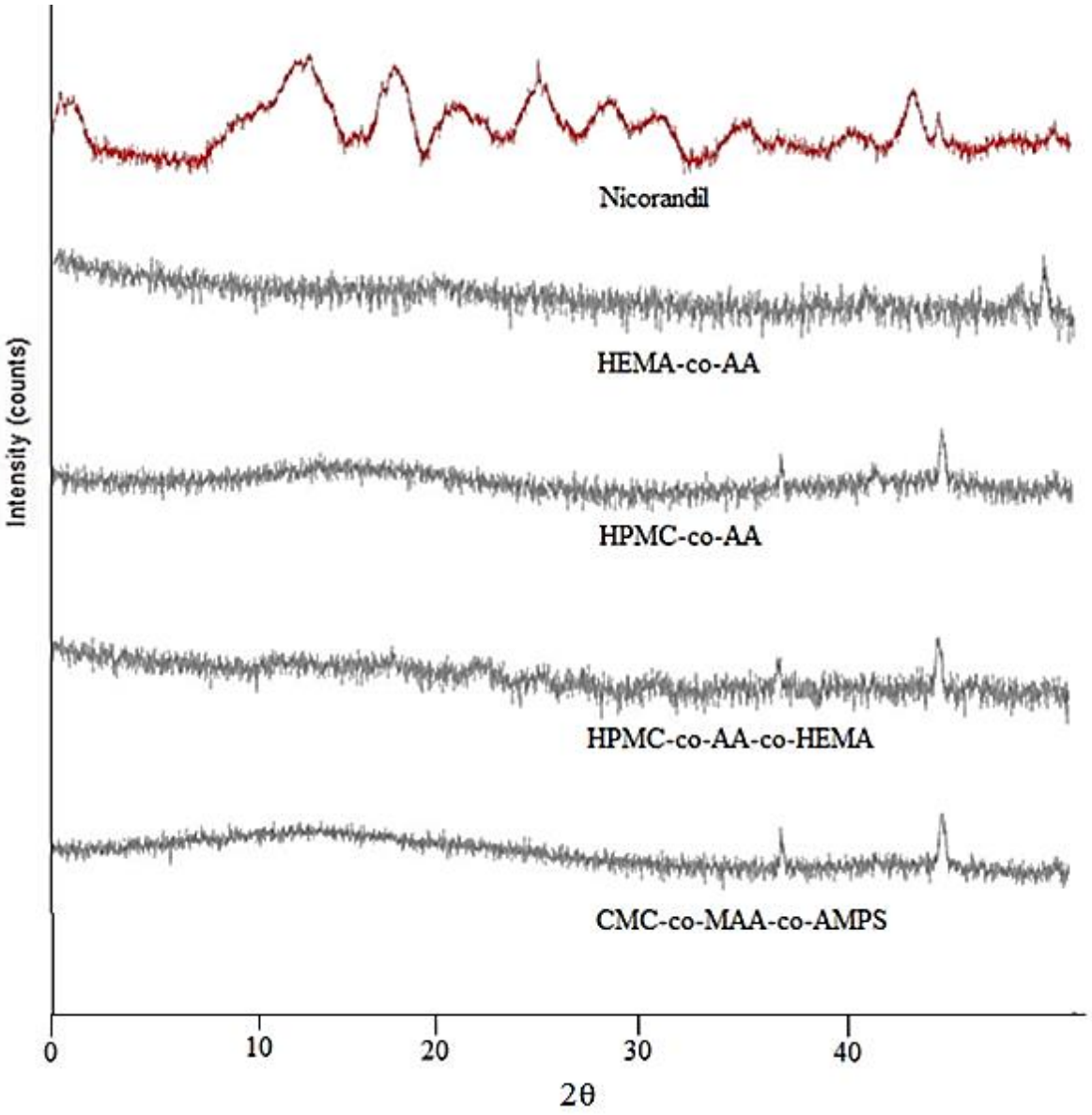

Figure 4.46: X-ray diffraction patterns of drug and formulation

4.5 *In-vitro* drug release study

4.5.1 *In vitro* drug release studies

Over all *in vitro* drug release studies were followed in ascending order with increasing pH from acidic to basic with respect to time.

Drug release was prominently affected by change in monomers concentration and as well as crosslinker concentration as elaborated in tables 4.26 to 4.40 and figures 4.47 to 4.58.

Formulations F1 to F3 having different concentrations of HEMA yielded drug release F1 (9.731 % to 17.236 %), F2 (9.716 % to 16.628 %) and F3 (9.091 % to 15.408 %) at pH 1.2. Similarly at pH 7.4 higher cumulative percent drug release was observed i.e. F1 (20.77 % to 96.09 %), F2 (14.663 b% to 92.962 %) and F3 (18.383 % to 93.702 %) as shown in table 4.26.

Table 4.26. Cumulative percent drug release of formulation F1 to F3 (n=6)

Time Hrs	F1		F2		F3	
	pH 1.2	pH 7.4	pH 1.2	pH 7.4	pH 1.2	pH 7.4
0.5	9.73±0.11	20.77±1.22	9.71±0.21	14.66±1.1	9.09±0.24	18.38±1.2
1	11.01±0.32	24.72±1.78	10.37±0.23	26.81±1.4	9.73±0.21	22.09±1.3
1.5	12.22±0.33	27.45±2.08	11.59±0.34	29.82±2.1	10.95±0.2	25.12±1.7
2	12.80±0.67	31.02±1.23	12.80±0.45	31.57±2.2	12.16±0.4	27.54±2.1
3	13.36±0.77	35.42±3.33	13.36±0.54	37.06±2.4	12.73±0.7	30.50±3.2
4	13.92±0.79	41.5±3.34	13.92±0.78	40.87±2.5	13.30±0.7	34.27±3.3
6	13.86±0.79	45.38±3.46	13.86±0.87	46.72±2.3	13.85±0.7	43.56±3.4
8	14.40±0.57	49.85±2.56	14.40±0.9	51.36±2.5	14.40±0.4	48.92±2.7
10	14.95±0.45	54.69±3.23	14.33±0.65	57.79±3.3	14.33±0.4	55.57±3
12	16.10±0.45	62.44±3.24	15.48±0.33	60.27±3.3	14.87±0.4	63.79±2.2
24	17.23±0.56	96.09±3.36	16.62±0.35	92.96±3.4	15.40±0.5	93.70±2.4

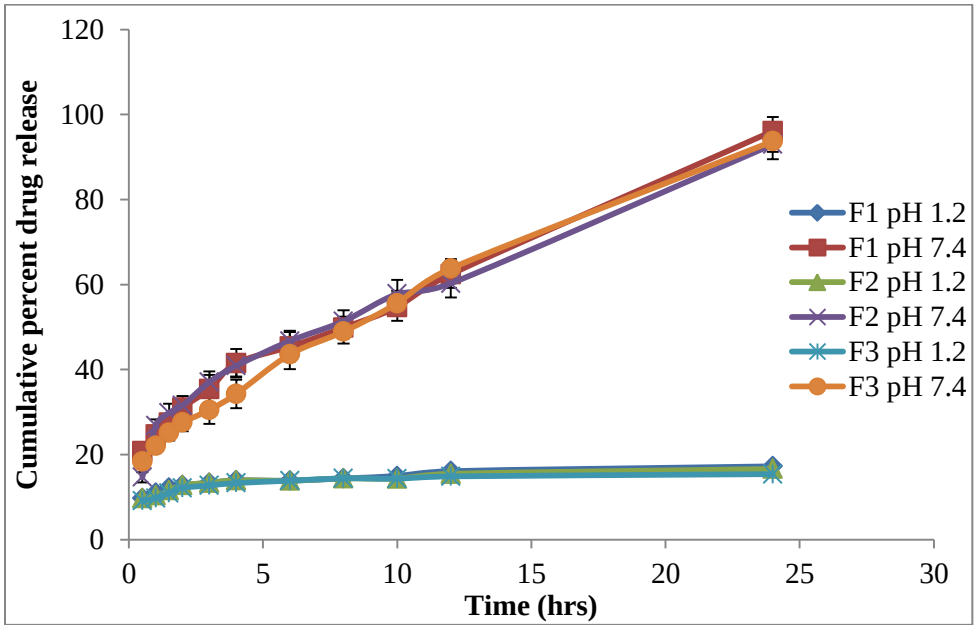

Figure 4.47. Dynamic release profile of formulations with changing concentration of HEMA

In formulations F4 to F6 cumulative percent drug release with varying concentrations of AA was observed. It was noted that cumulative percent drug release was 9.093 % to 12.962 %, 9.092 % to 13.577 % and 9.091 % to 14.794 % for F4, F5 and F6 respectively at pH 1.2. Moreover cumulative percent drug release at pH 7.4 was found to be higher than that of pH 1.2 i.e. F4 (19.777 % to 85.993 %), F5 (20.292 % to 87.726 %) and F6 (23.795 % to 89.387 %) as shown in table 4.27.

Table 4.27. Cumulative percent drug release of formulation F4 to F6 (n=6)

Time Hrs	F4		F5		F6	
	pH 1.2	pH 7.4	pH 1.2	pH 7.4	pH 1.2	pH 7.4
0.5	9.09±0.21	19.78±1.21	9.09±0.22	20.29±1.1	9.09±0.23	23.8±1.23
1	9.1±0.32	24.99±1.48	9.1±0.23	27.97±1.7	9.09±0.21	28.91±1.4
1.5	9.69±0.33	29.66±2.13	9.69±0.34	29.7±2.08	10.32±0.2	33.49±1.5
2	10.89±0.67	33.42±2.11	10.89±0.45	35.36±2.2	11.54±0.4	37.62±1.7
3	11.48±0.77	38.83±2.46	11.48±0.54	41.69±2.4	12.1±0.32	45.97±1.9
4	11.42±0.79	43.79±2.46	12.04±0.78	43.65±2.5	12.68±0.2	54.26±2.1
6	11.99±0.79	48.25±2.18	12.61±0.87	49.16±2.3	13.24±0.3	57.1±2.33
8	12.55±0.57	53.51±2.56	13.16±0.9	53.53±2.5	13.79±0.4	59.48±2.7
10	12.48±0.35	55.37±3.23	13.71±0.56	58.58±3.3	14.34±0.4	60.72±3
12	13.04±0.87	60.53±3.24	13.64±0.33	66.03±3.3	14.26±0.4	62.66±2.9
24	12.96±0.65	85.99±3.43	13.58±0.65	87.73±3.5	14.79±0.3	89.39±4.1

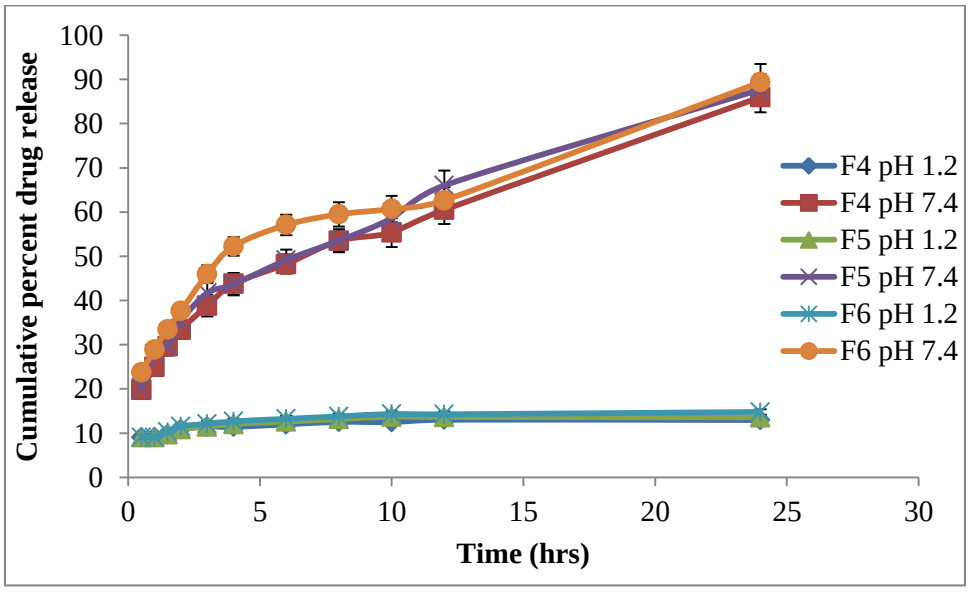

Figure 4.48. Dynamic release profile of formulations with changing concentration of AA

Cumulative percent drug release was found to be varied with changing concentration of MBA as in formulations F7 to F9. It was observed that cumulative percent drug release at pH 7.4 was higher than that of pH 1.2 as cumulative percent drug release was 8.456 % to 11.139 %, 8.459 % to 9.908 % and 8.459 % to 9.298 % at pH 1.2 for F7, F8 and F9 respectively and 17.319 % to 77.348 %, 18.066 % to 73.573 % and 15.492 % to 70.992 % at pH 7.4 for F7, F8 and F9 respectively as shown in table 4.28.

Table 4.28. Cumulative percent drug release of formulation F7 to F9 (n=6)

Time Hrs	F7		F8		F9	
	pH 1.2	pH 7.4	pH 1.2	pH 7.4	pH 1.2	pH 7.4
0.5	8.45±0.11	17.31±1.2	8.45±0.2	18.06±1.1	8.45±0.27	15.49±1.2
1	9.09±0.21	23.85±2.11	8.45±0.23	23.24±1.4	8.45±0.24	21.86±1.2
1.5	9.04±0.23	28.28±2.23	9.04±0.34	29.45±2.1	8.41±0.29	30.02±1.7
2	10.26±0.34	34.14±2.48	9.01±0.79	34.47±2.2	8.37±0.43	33.07±3.3
3	10.84±0.29	38.46±3.33	9.58±0.57	39.99±2.4	8.32±0.77	37.93±3.3
4	11.41±0.43	45.69±3.34	10.16±0.45	48.85±2.5	8.91±0.79	42.76±3.4
6	11.36±0.79	51.38±3.46	10.11±0.45	53.14±2.3	8.86±0.79	47.54±2.5
8	11.31±0.57	57.01±2.56	10.06±0.9	56.24±2.5	8.82±0.43	52.26±3.2
10	11.24±0.45	58.69±3.23	10.01±0.56	60.41±3.3	9.39±0.45	56.32±3.3
12	11.19±0.56	61.29±3.24	9.96±0.33	63.44±3.3	9.34±0.21	60.94±3.4
24	11.13±0.45	77.34±3.42	9.91±0.64	73.57±3.5	9.29±0.34	70.99±3.9

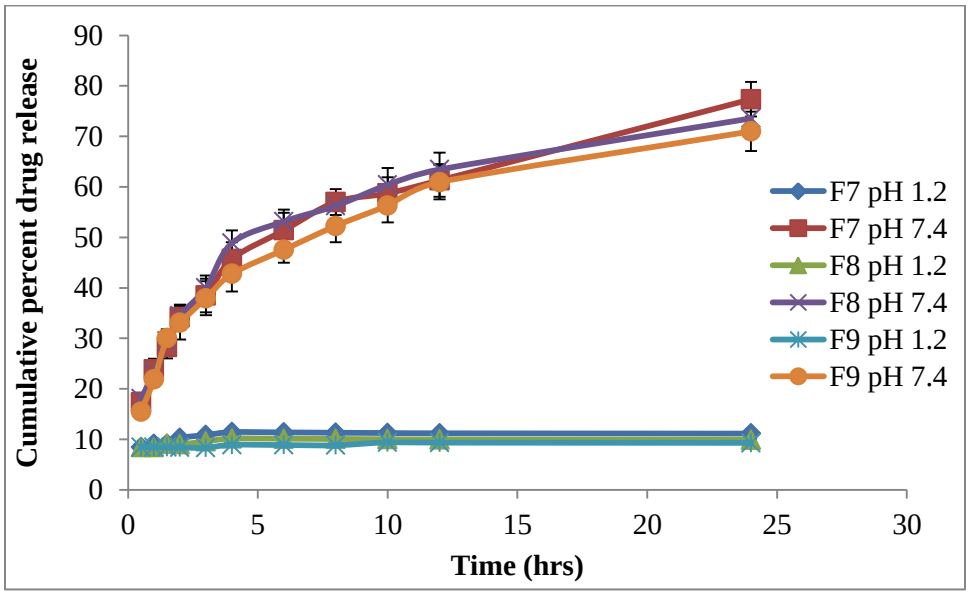

Figure 4.49. Dynamic release profile of formulations with changing concentration of MBA

Kinetics of drug release of formulation F1 to F9 was found to be varied with changing concentration of components i.e. polymer, monomer and crosslinker. Release exponent (n) was found vary in range of 0.625 to 0.214. Higuchi model was found to best fit as value of R_2 lies between 0.901 to 0.996 i.e. close to 1.

Table 4.29. Kinetics of drug release of formulation F1 to F9

Code	Zero order release model		First order release model		Higuchi model		Korsmayer-Peppas model		Release exponent
	R_2	K_0	R_2	K_1	R_2	K_2	R_2	K_3	(n)
F1	0.983	2.804	0.324	0.016	0.975	19.614	0.960	13.314	0.622
F2	0.953	2.724	0.303	0.016	0.981	18.975	0.972	12.748	0.625
F3	0.984	2.493	0.359	0.014	0.984	19.126	0.996	16.074	0.555
F4	0.933	1.808	0.277	0.010	0.992	17.906	0.974	23.835	0.410
F5	0.872	2.227	0.248	0.013	0.958	18.245	0.901	17.539	0.512
F6	0.935	2.123	0.283	0.013	0.990	17.553	0.972	17.180	0.507
F7	0.830	1.338	0.267	0.008	0.963	15.787	0.981	26.623	0.336
F8	0.767	0.844	0.252	0.005	0.929	15.017	0.960	37.301	0.214
F9	0.804	0.838	0.259	0.006	0.950	14.491	0.991	35.256	0.220

Cumulative percent drug release was found to be varied with changing concentration of HPMC as in formulations F10 to F12. It was observed that cumulative percent drug release at pH 7.4 was higher than that of pH 1.2 as cumulative percent drug release was 7.812 % to 15.408 %, 8.451 % to 16.017 % and 8.459 % to 17.239 % at pH 1.2 for F10, F11 and F12 respectively and 12.932 % to 89.817 %, 13.573 % to 91.038 % and 15.493 % to 92.878 % at pH 7.4 for F7, F8 and F9 respectively as shown in table 4.30.

Table 4.30. Cumulative percent drug release of formulation F10 to F12 (n=6)

Time Hrs	F10		F11		F12	
	pH 1.2	pH 7.4	pH 1.2	pH 7.4	pH 1.2	pH 7.4
0.5	7.81±0.11	12.93±1.22	8.45±0.2	13.57±1.1	8.46±0.23	15.49±1.2
1	8.46±0.32	22.49±1.78	8.46±0.23	23.76±1.4	9.1±0.21	26.33±1.4
1.5	9.69±0.33	28.76±2.08	10.94±0.34	30.04±2.1	12.22±0.2	31.95±1.5
2	10.89±0.67	32.44±1.23	12.16±0.79	33.71±2.2	12.18±0.4	36.24±1.7
3	12.11±0.77	36.68±3.33	12.11±0.57	37.94±2.4	12.74±0.3	40.47±1.9
4	12.67±0.79	40.27±3.34	13.3±0.45	39.65±2.5	13.3±0.22	42.77±2.1
6	13.24±0.79	44.43±3.46	13.23±0.45	42.55±2.3	13.86±0.3	46.3±2.33
8	13.79±0.57	48.54±2.56	14.4±0.9	47.91±2.5	14.4±0.43	49.16±2.7
10	13.71±0.45	52.62±3.23	14.34±0.56	53.23±3.3	14.95±0.4	53.23±3
12	14.26±0.45	56.03±3.24	14.87±0.33	55.43±3.3	15.49±0.4	59.7±2.99
24	15.41±0.56	89.82±3.36	16.02±0.64	91.04±3.5	17.24±0.3	92.88±4.1

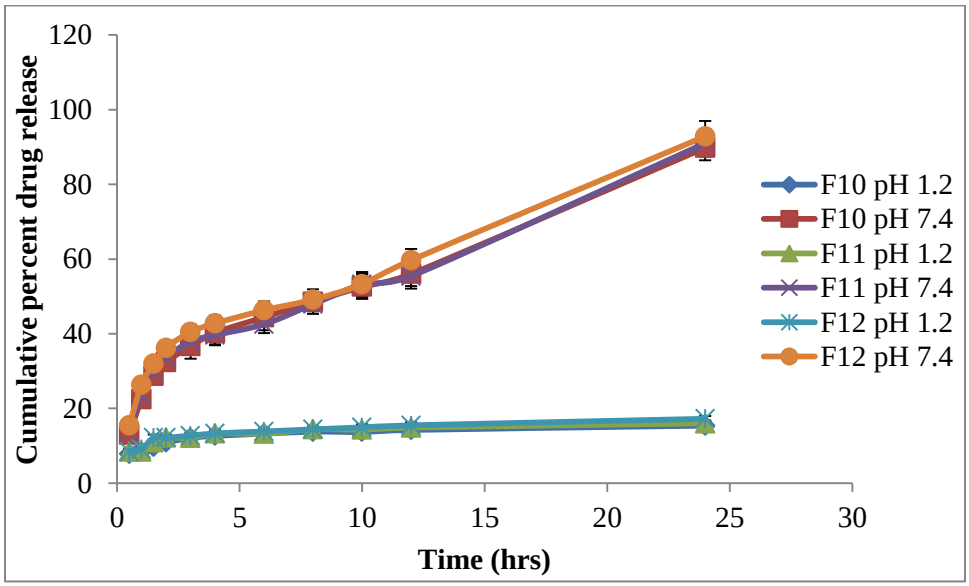

Figure 4.50. Dynamic release profile of formulations with changing concentration of HPMC

Formulations F13 to F15 having different concentrations of AA yielded drug release F13 (7.17 % to 13.57 %), F14 (7.81 % to 14.18 %) and F15 (7.81 % to 14.79 %) at pH 1.2. Similarly at pH 7.4 higher cumulative percent drug release was observed i.e. F13 (12.96 % to 75.78 %), F14 (12.93 % to 78.83 %) and F15 (12.29 % to 84.93 %) as shown in table 4.31.

Table 4.31. Cumulative percent drug release of formulation F13 to F15 (n=6)

Time Hrs	F13		F14		F15	
	pH 1.2	pH 7.4	pH 1.2	pH 7.4	pH 1.2	pH 7.4
0.5	7.17±0.11	12.96±1.24	7.81±0.2	12.93±1.17	7.81±0.27	12.29±1.23
1	7.81±0.32	16.75±2.11	7.81±0.23	17.39±1.44	8.45±0.24	19.3±1.28
1.5	7.77±0.33	19.86±2.23	8.4±0.34	21.76±2.13	9.68±0.29	24.31±1.75
2	8.36±0.67	24.19±2.48	9±0.79	24.83±2.23	9.63±0.43	27.99±3.33
3	8.95±0.77	26.6±3.33	9.58±0.57	27.86±2.48	10.84±0.77	36.03±3.34
4	9.53±0.79	30.84±3.34	10.16±0.45	33.35±2.5	10.79±0.79	38.38±3.46
6	10.11±0.79	35.68±3.46	10.73±0.45	36.93±2.38	11.98±0.79	41.92±2.56
8	10.68±0.57	37.99±2.56	11.3±0.9	41.09±2.56	11.92±0.43	44.2±3.24
10	11.24±0.45	43.34±3.23	11.86±0.56	45.2±3.33	13.09±0.45	50.74±3.36
12	12.41±0.45	48.03±3.24	13.02±0.33	48.65±3.34	13.64±0.21	52.96±3.43
24	13.57±0.56	75.78±3.42	14.18±0.64	78.83±3.57	14.79±0.34	84.93±3.9

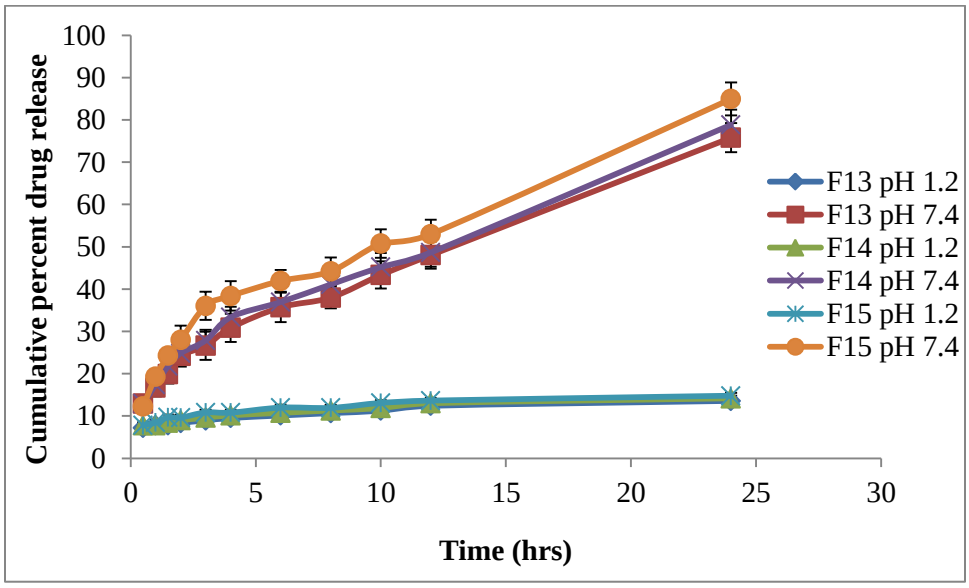

Figure 4.51. Dynamic release profile of formulations with changing concentration of AA

In formulations F16 to F18 cumulative percent drug release with varying concentrations of MBA was observed. It was noted that cumulative percent drug release was 7.15 % to 12.98 %, 7.15 % to 12.31 % and 6.53 % to 11.72 % for F16, F17 and F18 respectively at pH 1.2. Moreover cumulative percent drug release at pH 7.4 was found to be higher than that of pH 1.2 i.e. F16 (13.57 % to 66.63 %), F17 (12.29 % to 60.53 %) and F18 (12.29 % to 56.26 %) as shown in table 4.32.

Table 4.32. Cumulative percent drug release of formulation F16 to F18 (n=6)

Time Hrs	F16		F17		F18	
	pH 1.2	pH 7.4	pH 1.2	pH 7.4	pH 1.2	pH 7.4
0.5	7.15±0.21	13.57±1.22	7.15±0.21	12.29±1.18	6.53±0.24	12.29±1.26
1	7.79±0.23	17.39±1.78	7.17±0.23	16.11±1.48	7.16±0.21	15.48±1.3
1.5	7.73±0.34	19.23±2.08	7.68±0.24	17.32±2.13	7.72±0.29	16.68±1.78
2	7.76±0.45	21.66±1.23	7.72±0.21	20.39±2.23	7.78±0.21	18.5±2.08
3	8.24±0.54	25.33±2.33	8.29±0.29	24.07±2.48	7.88±0.23	22.8±3.24
4	8.29±0.23	29.59±2.34	8.18±0.23	27.71±2.5	8.26±0.24	25.83±3.36
6	8.75±0.34	31.94±2.46	8.74±0.34	30.69±2.38	8.81±0.21	30.06±3.43
8	8.79±0.45	34.88±2.56	9.38±0.45	32.4±2.56	8.85±0.29	31.17±2.77
10	10.11±0.65	37.79±2.23	10.08±0.45	35.32±2.33	9.33±0.23	34.08±3
12	11.25±0.33	41.28±2.24	11.19±0.65	38.21±2.34	10.51±0.34	36.37±2.23
24	12.98±0.35	66.63±2.36	12.31±0.33	60.53±2.46	11.72±0.45	56.26±2.48

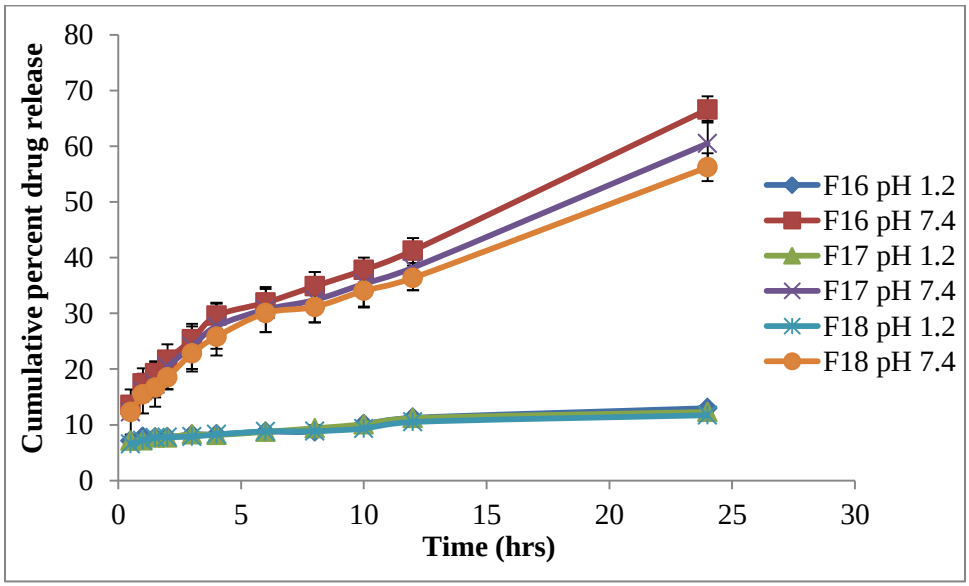

Figure 4.52. Dynamic release profile of formulations with changing concentration of MBA

Kinetics of drug release of formulation F10 to F18 was found to be varied with changing concentration of components i.e. polymer, monomer and crosslinker. Release exponent (n) was found vary in range of 0.7159 to 0.6375. Higuchi model was found to best fit as value of R_2 lies between 0.952 to 0.982 i.e. close to 1.

Table 4.33. Kinetics of drug release of formulation F10 to F18

Code	Zero order release model		First order release model		Higuchi model		Korsmayer-Peppas model		Release exponent
	R_2	K_0	R_2	K_1	R_2	K_2	R_2	K_3	(n)
F10	0.940	2.815	0.305	0.017	0.966	18.332	0.937	10.324	0.680
F11	0.944	2.967	0.299	0.018	0.953	18.581	0.913	9.355	0.715
F12	0.939	2.764	0.282	0.016	0.952	18.957	0.901	12.246	0.637
F13	0.938	2.664	0.326	0.017	0.970	17.336	0.914	9.741	0.681
F14	0.969	2.515	0.354	0.017	0.979	16.091	0.964	8.622	0.696
F15	0.975	2.312	0.364	0.016	0.979	15.468	0.969	9.365	0.657
F16	0.975	2.112	0.344	0.017	0.970	13.600	0.939	7.418	0.690
F17	0.965	1.860	0.344	0.016	0.975	12.355	0.940	7.343	0.663
F18	0.962	1.657	0.346	0.015	0.982	11.484	0.957	7.612	0.629

Cumulative percent drug release was found to be varied with changing concentration of HEMA as in formulations F19 to F21. It was observed that cumulative percent drug release at pH 7.4 was higher than that of pH 1.2 as cumulative percent drug release was 7.04 % to 13.02 %, 6.98 % to 12.95 % and 6.79 % to 11.79 % at pH 1.2 for F19, F20 and F21 respectively and 12.36 % to 67.46 %, 12.16 % to 63.62 % and 11.65 % to 59.64 % at pH 7.4 for F19, F20 and F21 respectively as shown in table 4.34.

Table 4.34. Cumulative percent drug release of formulation F19 to F21 (n=6)

Time Hrs	F19		F20		F21	
	pH 1.2	pH 7.4	pH 1.2	pH 7.4	pH 1.2	pH 7.4
0.5	7.04±0.11	12.36±1.24	6.98±0.2	12.16±1.17	6.79±0.27	11.65±1.23
1	7.62±0.21	18.72±1.17	7.42±0.23	17.96±1.44	7.17±0.24	16.68±1.28
1.5	7.64±0.23	24.34±1.44	7.52±0.34	21.8±2.13	7.2±0.29	19.25±1.17
2	8.17±0.2	26.14±2.23	7.92±0.27	24.87±2.23	7.48±0.43	21.7±1.44
3	8.64±0.23	31.37±2.48	8.32±0.24	29.49±2.48	7.69±0.34	26.33±2.48
4	9.22±0.34	35.07±2.5	8.66±0.29	32.56±2.5	8.28±0.57	30.67±2.5
6	9.8±0.57	38.65±2.38	8.92±0.2	37.39±2.38	8.61±0.45	36.14±2.38
8	10.37±0.45	42.11±2.56	9.93±0.23	39.63±2.56	9.43±0.45	37.77±2.56
10	10.93±0.45	44.43±2.23	10.62±0.34	42.58±2.23	10.07±0.45	41.34±2.16
12	11.79±0.56	50.47±2.24	10.57±0.33	48.69±2.24	10.38±0.21	47.46±2.33
24	13.02±0.45	67.46±2.42	12.95±0.45	63.62±2.47	11.79±0.34	59.64±2.49

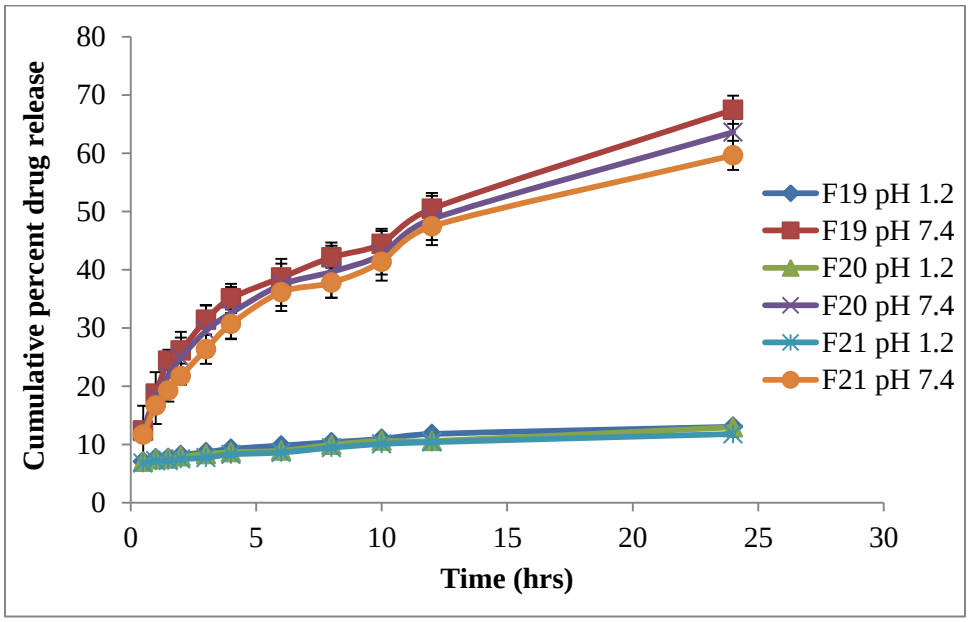

Figure 4.53. Dynamic release profile of formulations with changing concentration of HEMA

Formulations F22 to F24 having different concentrations of AA yielded drug release F22 (7.81 % to 18.44 %), F 23 (7.90 % to 19.05 %) and F24 (8.03 % to 21.49 %) at pH 1.2. Similarly at pH 7.4 higher cumulative percent drug release was observed i.e. F22 (12.93 % to 75.80 %), F23 (12.29 % to 78.25 %) and F24 (13.57 % to 82.82 %) as shown in table 4.35.

Table 4.35. Cumulative percent drug release of formulation F22 to F24 (n=6)

Time Hrs	F22		F23		F24	
	pH 1.2	pH 7.4	pH 1.2	pH 7.4	pH 1.2	pH 7.4
0.5	7.81±0.11	12.93±1.24	7.9±0.2	12.29±1.17	8.03±0.27	13.57±1.23
1	8.45±0.32	19.3±2.11	8.72±0.23	20.57±1.44	8.85±0.24	23.02±1.28
1.5	9.04±0.33	24.94±2.23	9.17±0.34	25.58±2.13	9.42±0.29	27.94±1.75
2	9.13±0.67	28±2.48	9.39±0.79	29.89±2.23	9.58±0.43	31.71±3.33
3	9.46±0.77	33.52±3.33	9.69±0.57	35.41±2.48	9.95±0.77	37.75±3.34
4	9.91±0.79	37.74±3.34	10.03±0.45	40.25±2.5	10.5±0.79	42.16±3.46
6	10.57±0.79	41.3±3.46	10.63±0.45	43.18±2.38	10.94±0.79	46.16±2.56
8	11.17±0.57	43.58±2.56	11.26±0.9	45.44±2.56	11.51±0.43	49.08±3.24
10	11.61±0.45	47.67±3.23	11.72±0.56	50.14±3.33	13.53±0.45	51.89±3.36
12	14.43±0.45	51.72±3.24	14.56±0.33	54.18±3.34	16.41±0.21	55.93±3.43
24	18.44±0.56	75.8±3.42	19.05±0.64	78.25±3.57	21.49±0.34	82.82±3.9

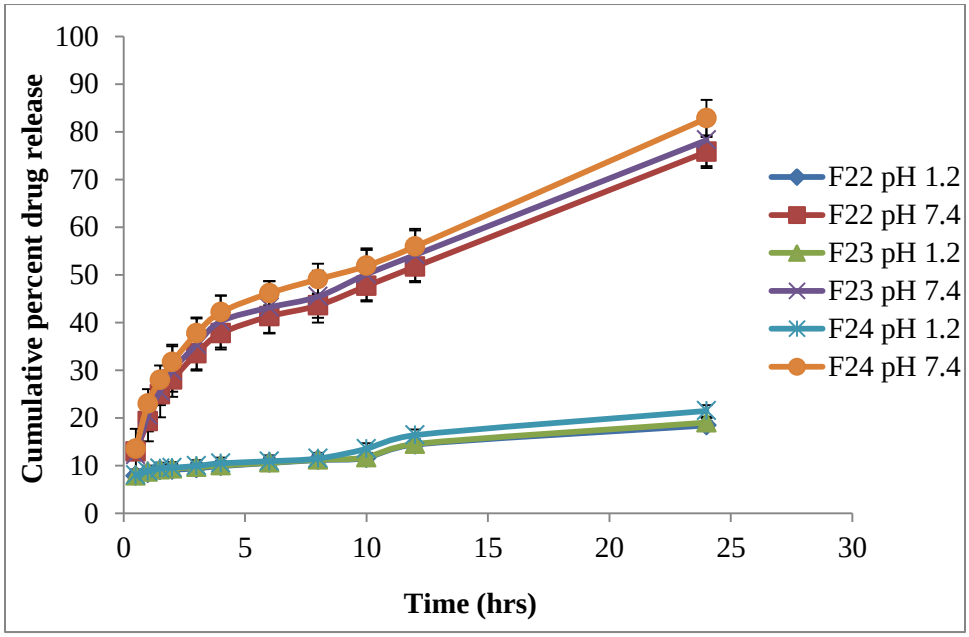

Figure 4.54. Dynamic release profile of formulations with changing concentration of AA

In formulations F25 to F27 cumulative percent drug release with varying concentrations of HPMC was observed. It was noted that cumulative percent drug release was 7.11 % to 14.24 %, 7.43 % to 16.07 % and 7.68 % to 17.77 % for F25, F26 and F27 respectively at pH 1.2. Moreover cumulative percent drug release at pH 7.4 was found to be higher than that of pH 1.2 i.e. F25 (12.61 % to 69.29 %), F26 (12.87 % to 71.73 %) and F27 (13.06 % to 73.38 %) as shown in table 4.36.

Table 4.36. Cumulative percent drug release of formulation F25 to F27 (n=6)

Time Hrs	F25		F26		F27	
	pH 1.2	pH 7.4	pH 1.2	pH 7.4	pH 1.2	pH 7.4
0.5	7.11±0.21	12.61±1.22	7.43±0.21	12.87±1.18	7.68±0.24	13.06±1.26
1	7.81±0.23	19.24±1.78	8.25±0.23	20±1.48	8.59±0.21	21.28±1.3
1.5	7.96±0.34	25.67±2.08	8.53±0.24	26.08±2.13	8.98±0.29	27.35±1.78
2	8.3±0.45	27.53±1.23	8.74±0.21	28.03±2.23	9.27±0.21	29.3±2.08
3	8.83±0.54	33.89±2.33	9.08±0.29	34.08±2.48	9.57±0.23	35.34±3.24
4	9.41±0.23	35.71±2.34	9.53±0.23	36.01±2.5	9.91±0.24	36.64±3.36
6	9.98±0.34	39.89±2.46	10.11±0.34	40.52±2.38	10.51±0.21	41.14±3.43
8	10.55±0.45	43.35±2.56	10.68±0.45	44.59±2.56	11.14±0.29	45.21±2.77
10	11.12±0.65	45.06±2.23	11.24±0.45	46.29±2.33	11.59±0.23	46.91±3
12	13.02±0.33	51.09±2.24	13.63±0.65	52.32±2.34	14.44±0.34	53.54±2.23
24	14.24±0.35	69.29±2.36	16.07±0.33	71.73±2.46	17.77±0.45	73.38±2.48

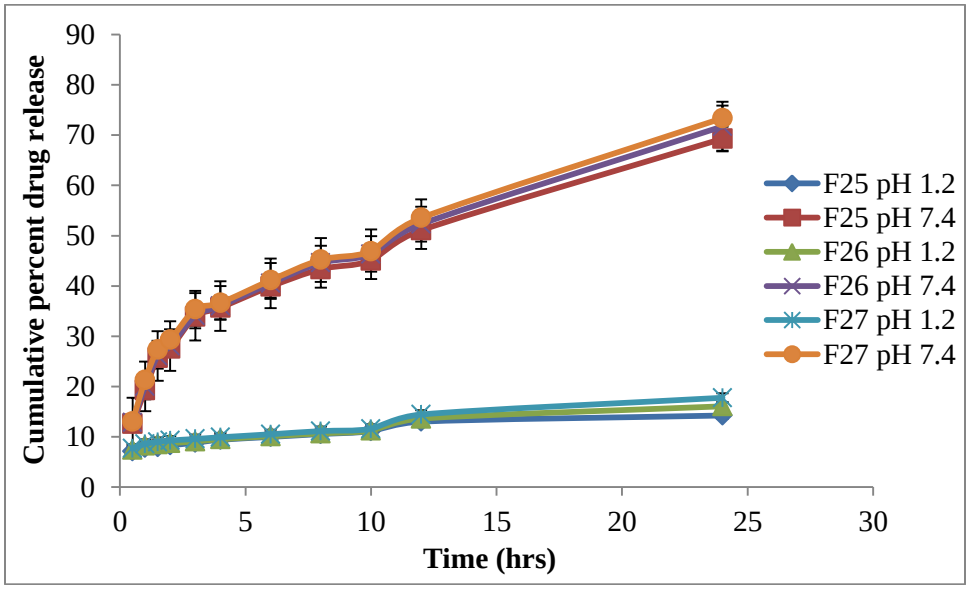

Figure 4.55. Dynamic release profile of formulations with changing concentration of HPMC

Cumulative percent drug release was found to be varied with changing concentration of MBA as in formulations F28 to F30. It was observed that cumulative percent drug release at pH 7.4 was higher than that of pH 1.2 as cumulative percent drug release was 7.23 % to 15.88 %, 7.04 % to 11.71 % and 6.85 % to 10.49 % at pH 1.2 for F28, F29 and F30 respectively and 11.01 % to 60.58 %, 10.37 % to 54.48 % and 9.73 % to 48.37 % at pH 7.4 for F28, F29 and F30 respectively as shown in table 4.37.

Table 4.37. Cumulative percent drug release of formulation F28 to F30 (n=6)

Time Hrs	F28		F29		F30	
	pH 1.2	pH 7.4	pH 1.2	pH 7.4	pH 1.2	pH 7.4
0.5	7.23±0.21	11.01±1.22	7.04±0.21	10.37±1.18	6.85±0.24	9.73±1.26
1	8.19±0.23	17.38±1.18	7.81±0.23	16.1±1.48	7.3±0.21	14.19±1.3
1.5	8.28±0.21	21.79±1.26	7.9±0.24	19.89±1.13	7.51±0.29	18.61±1.18
2	8.43±0.23	23.6±1.3	8.11±0.21	21.07±1.23	7.6±0.21	19.81±1.08
3	8.57±0.24	29.48±1.78	8.32±0.29	27.59±1.48	7.82±0.23	25.7±1.24
4	8.91±0.23	31.94±1.32	8.47±0.23	30.06±1.5	8.15±0.24	26.93±1.36
6	9.36±0.29	36.15±1.46	8.74±0.24	32.41±1.35	8.3±0.21	29.91±1.43
8	9.75±0.23	39.01±1.56	9±0.21	35.9±1.56	8.44±0.29	32.18±1.77
10	10.5±0.34	42.58±1.23	9.33±0.29	39.49±1.37	8.77±0.23	37.01±1.73
12	13.63±0.33	48.02±1.28	10.56±0.23	44.33±1.34	9.95±0.34	40.04±1.83
24	15.88±0.35	60.58±1.36	11.71±0.34	54.48±1.46	10.49±0.35	48.37±1.98

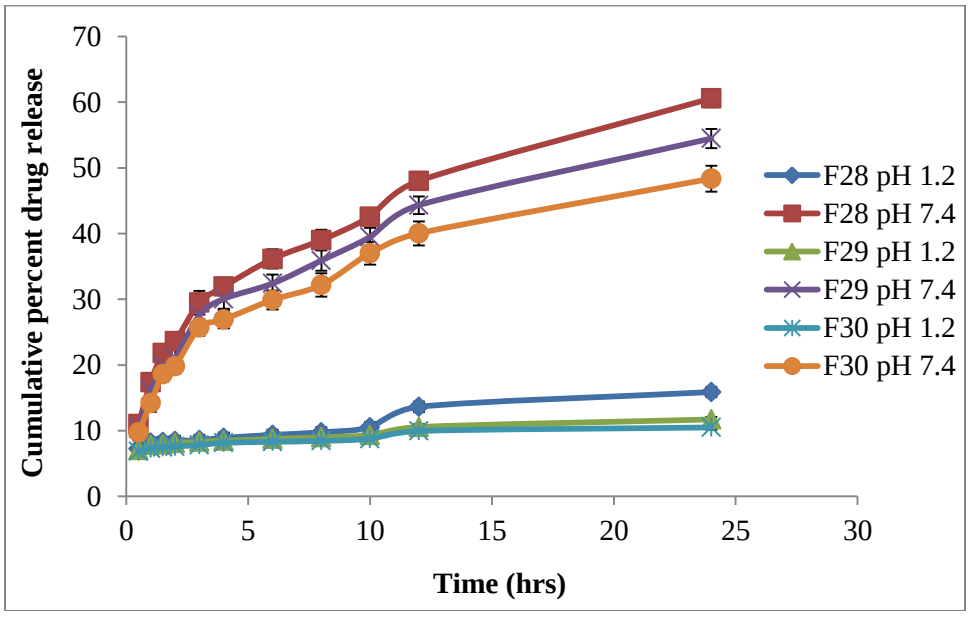

Figure 4.56. Dynamic release profile of formulations with changing concentration of MBA

Kinetics of drug release of formulation F19 to F30 was found to be varied with changing concentration of components i.e. polymer, monomer and crosslinker. Release exponent (n) was found vary in range of 0.272 to 0.566. Higuchi model was found to best fit as value of R_2 lies between 0.9673 to 0.988 i.e. close to 1.

Table 4.38. Kinetics of drug release of formulation F19 to F30

Code	Zero order release model		First order release model		Higuchi model		Korsmayer-Peppas model		Release exponent (n)
	R_2	K_0	R_2	K_1	R_2	K_2	R_2	K_3	
F19	0.901	1.415	0.298	0.010	0.983	13.770	0.977	17.835	0.418
F20	0.902	1.244	0.305	0.009	0.987	12.986	0.984	18.665	0.385
F21	0.892	1.015	0.323	0.008	0.988	12.174	0.987	20.924	0.329
F22	0.921	2.006	0.306	0.013	0.979	15.472	0.952	13.137	0.551
F23	0.905	2.005	0.298	0.013	0.974	15.972	0.949	14.505	0.530
F24	0.909	2.240	0.287	0.014	0.971	16.905	0.942	13.691	0.566
F25	0.895	1.516	0.289	0.011	0.976	14.143	0.962	17.136	0.439
F26	0.905	1.617	0.292	0.011	0.980	14.641	0.967	16.881	0.455
F27	0.906	1.653	0.284	0.011	0.976	14.978	0.957	17.294	0.454
F28	0.878	1.046	0.302	0.008	0.980	12.365	0.988	20.877	0.335
F29	0.864	0.845	0.304	0.007	0.975	11.120	0.981	21.169	0.297
F30	0.845	0.694	0.303	0.006	0.967	9.873	0.977	20.334	0.272

Cumulative percent drug release was found to be varied with changing concentration of MAA as in formulations F31 to F33. It was observed that cumulative percent drug release at pH 7.4 was higher than that of pH 1.2 as cumulative percent drug release was 25.73 % to 81.74 %, 23.81 % to 79.59 % and 23.49 % to 78.99 % at pH 1.2 for F31, F32 and F33 respectively and 26.37 % to 82.84 %, 24.45 % to 80.21 % and 23.75 % to 79.32 % at pH 7.4 for F31, F32 and F33 respectively as shown in table 4.39.

Table 4.39. Cumulative percent drug release of formulation F31 to F33 (n=6)

Time Hrs	F31		F32		F33	
	pH 1.2	pH 7.4	pH 1.2	pH 7.4	pH 1.2	pH 7.4
0.5	25.73±1.24	26.37±1.17	23.81±1.112	24.45±1.17	23.49±1.23	23.75±1.23
1	37.07±2.11	37.71±1.44	35.15±1.78	35.86±1.24	33.88±1.45	34.26±1.28
1.5	49.94±2.23	51.21±2.13	47.39±2.08	47.78±2.33	46.12±1.54	46.5±1.75
2	56.12±2.48	57.39±2.23	53.58±2.23	54.22±2.43	52.32±1.78	52.76±3.33
3	67.63±3.33	68.27±2.48	65.74±2.48	66.37±2.68	64.48±1.99	64.7±3.34
4	81.61±3.34	82.24±2.5	79.1±2.5	79.73±2.85	78.54±2.11	79.04±3.46
6	81.33±3.46	82.57±2.38	79.39±2.38	80.01±2.88	78.58±2.33	79.14±2.56
8	81.47±2.56	82.65±2.56	78.99±2.56	80.1±2.96	78.74±2.77	79.23±3.24
10	81.6±3.23	82.72±3.33	79.07±3.33	81.04±3.73	78.82±3	79.26±3.36
12	81.73±3.24	82.78±3.34	79.09±3.34	80.2±3.84	78.91±2.99	79.28±3.43
24	81.74±3.42	82.84±3.57	79.59±3.54	80.21±3.77	78.99±4.11	79.32±3.9

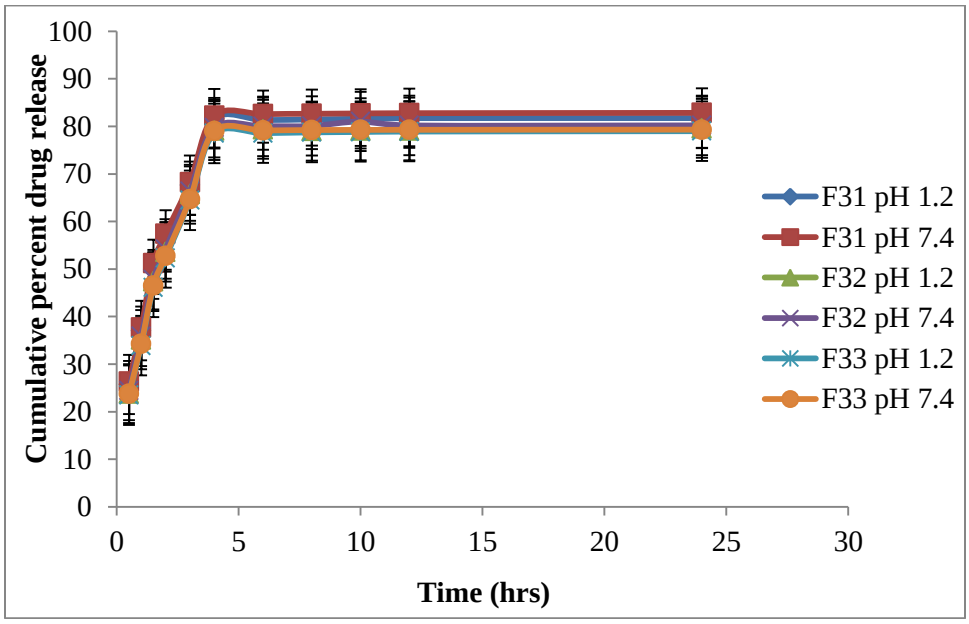

Figure 4.57. Dynamic release profile of formulations with changing concentration of MAA

Formulations F1 to F3 having different concentrations of AMPS yielded drug release F34 (26.37 % to 87.06 %), F35 (27.02 % to 88.89 %) and F36 (28.30 % to 90.66 %) at pH 1.2. Similarly at pH 7.4 higher cumulative percent drug release was observed i.e. F34 (27.02 % to 88.83 %), F35 (27.66 % to 90.48 %) and F36 (30.22 % to 94.88 %) as shown in table 4.26.

Table 4.40. Cumulative percent drug release of formulation F34 to F36 (n=6)

Time Hrs	F34		F35		F36	
	pH 1.2	pH 7.4	pH 1.2	pH 7.4	pH 1.2	pH 7.4
0.5	26.37±1.24	27.02±1.17	27.02±1.112	27.66±1.17	28.3±1.23	30.22±1.23
1	38.35±1.23	39.12±1.44	39.63±1.78	42.18±1.24	41.54±1.45	42.83±1.78
1.5	51.21±1.24	51.53±2.13	52.48±2.08	53.76±2.33	53.76±1.54	55.04±2.08
2	58.02±2.33	60.54±2.23	59.29±2.23	60.55±2.43	60.55±1.78	61.82±2.96
3	69.74±2.43	70.38±2.48	71.63±2.48	74.77±2.68	74.15±1.99	76.04±3.73
4	86.61±2.68	87.87±2.5	88.5±2.5	88.82±2.85	90.38±2.23	93.51±3.84
6	86.88±3.46	88.13±2.38	88.57±2.38	88.82±2.88	90.44±2.48	94.37±3.77
8	86.93±2.56	88.36±3.46	88.68±2.56	88.85±2.96	90.47±3.33	94.51±3.24
10	86.98±3.23	88.52±2.56	88.77±3.33	89.75±3.73	90.5±3.34	94.64±3.36
12	86.99±3.24	88.68±3.24	88.8±3.34	89.97±3.84	90.58±3.46	94.76±3.43
24	87.06±3.32	88.83±3.66	88.89±3.55	90.48±3.67	90.66±3.98	94.88±3.89

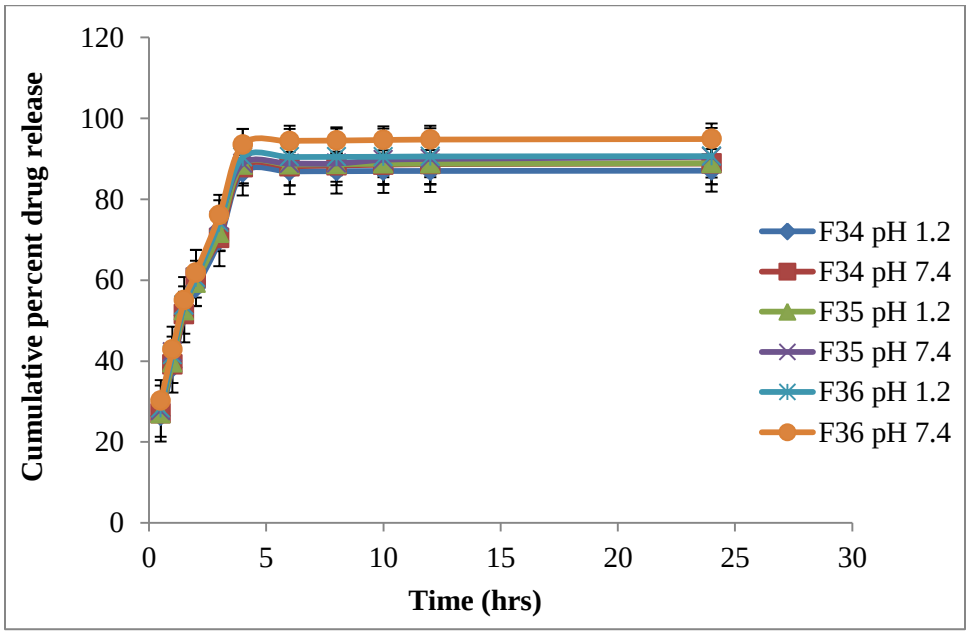

Figure 4.58. Dynamic release profile of formulations with changing concentration of AMPS

4.6 *In vivo* evaluation

4.6.1 Standard curve

The standard curve of nicorandil was constructed using known plasma concentrations within ranges of 31.25 ng/mL to 500 ng/mL and linear regression was applied to fit straight line. Mean r^2 value was also determined 0.9974. Standard curve is given in figure 4.59. Chromatograms of spiked plasma is given in figures 4.60 to 4.63.

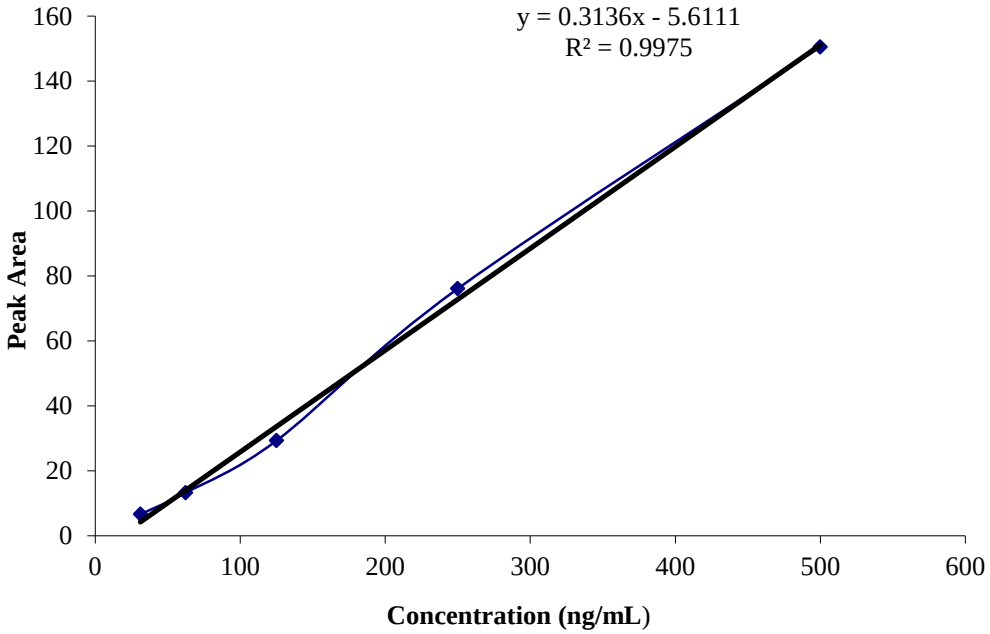

Figure 4.59. Standard curve of nicorandil

Rabbits are divided into groups G1, G2, G3 and G4 having 6 rabbits in each group. F1 (HEMA-co-AA), F12 (HPMC-co-AA), F24 (HPMC-co-AA-co-HEMA) and drug solution (1mg/mL) were administered to G1, G2, G3 and G4 respectively as a single dose equivalent to 15mg. Results are given in tables 4.37 to 4.95 and figures 4.72 to 4.100.

Retention time of drug peak (500 ng of drug spiked in plasma) was found at 4.5 min as shown in chromatogram given in figure 4.60.

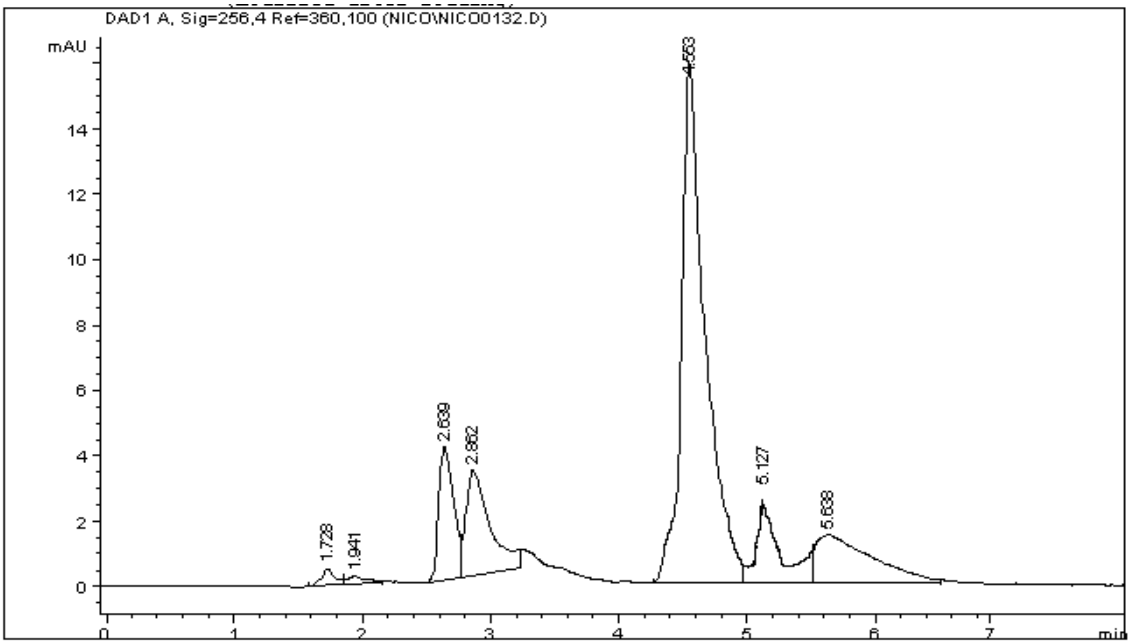

Figure 4.60. Spiked plasma with 500 ng drug

Plasma spiked with 250 ng of drug gave desired peak at 4.5 min as shown in chromatogram given in figure 4.61.

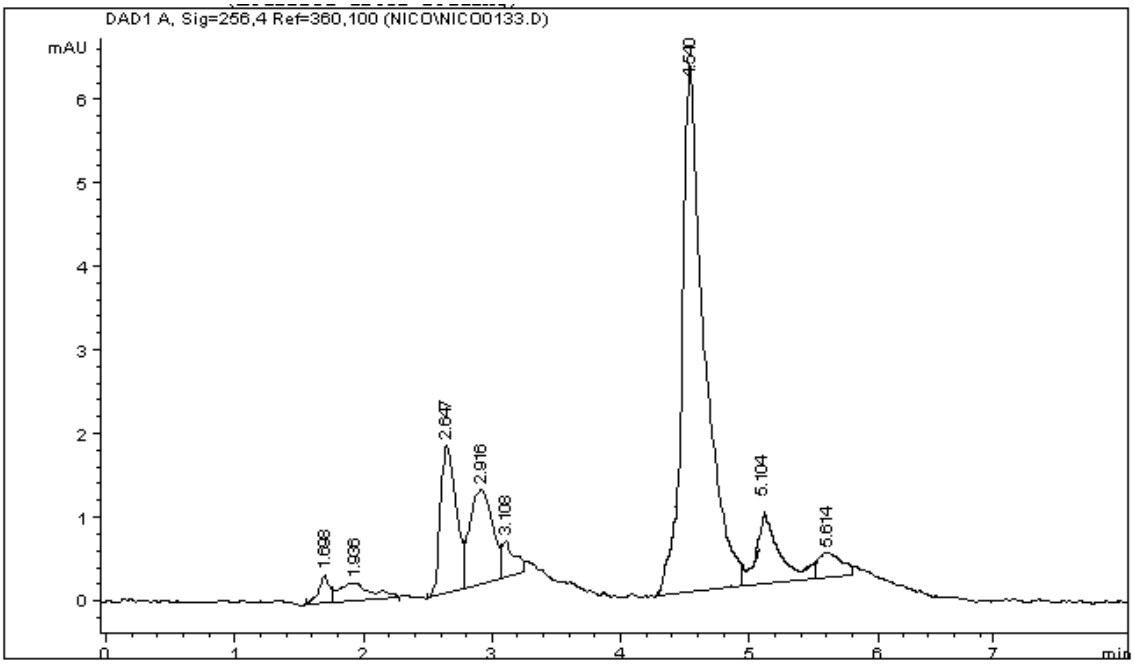

Figure 4.61. Spiked plasma with 250 ng drug

Retention time of drug peak (125 ng of drug spiked in plasma) was found at 4.5 min as shown in chromatogram given in figure 4.62.

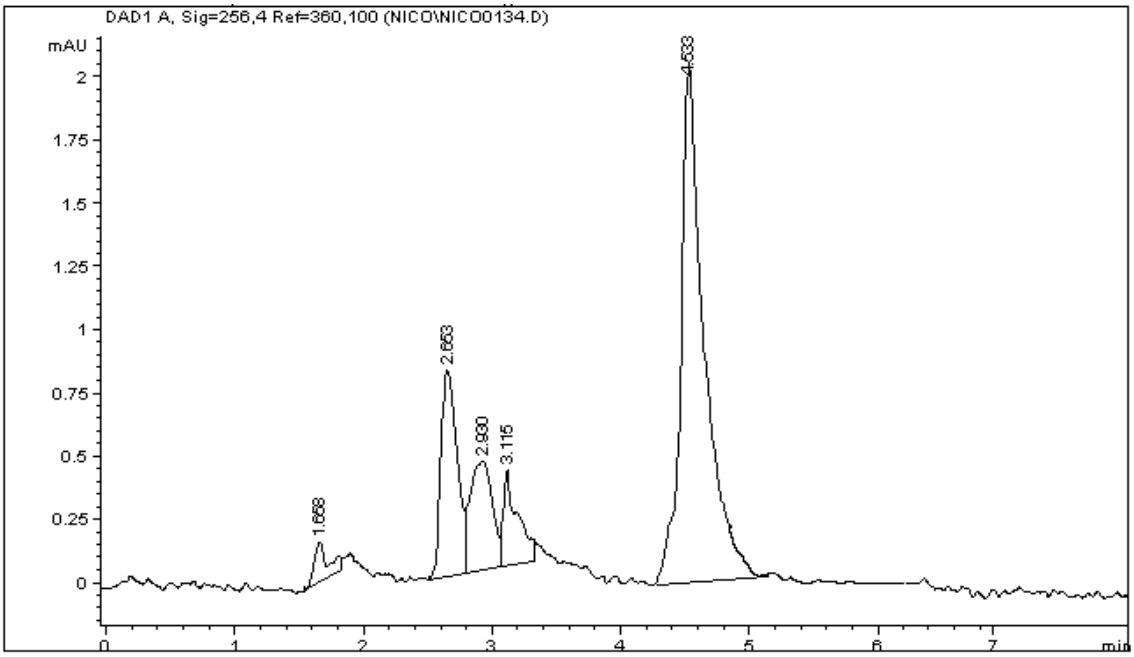

Figure 4.62. Spiked plasma with 125 ng drug

Plasma spiked with 62.5 ng of drug gave desired peak at 4.5 min as shown in chromatogram given in figure 4.63.

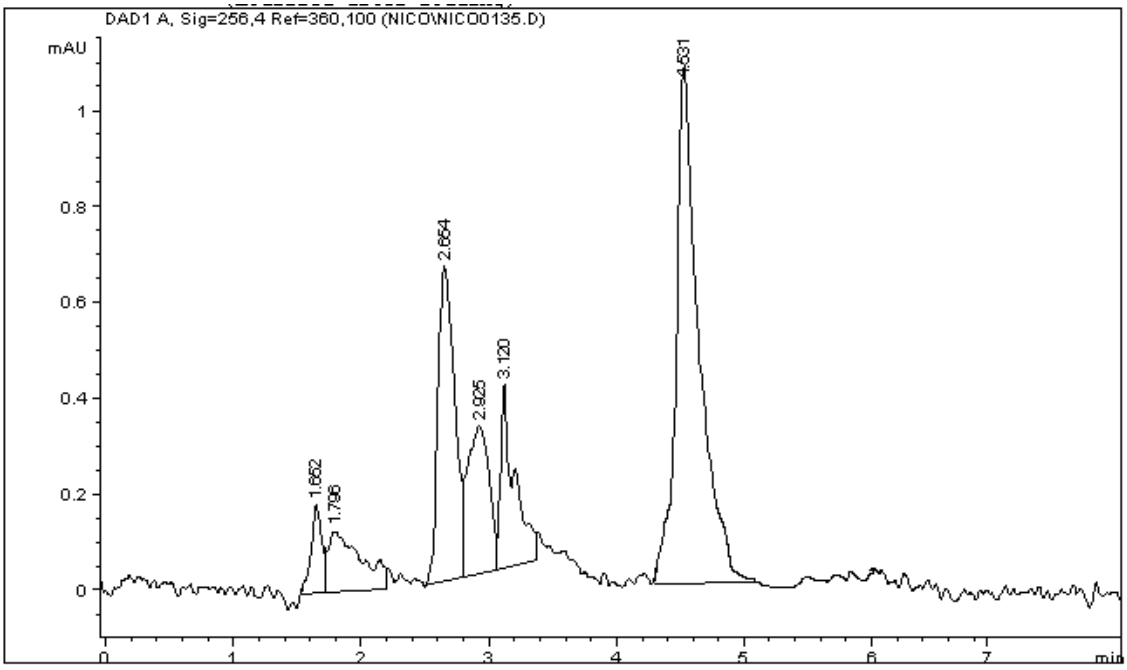

Figure 4.63. Spiked plasma with 62.5 ng drug

4.6.2. Precision and accuracy

Percent coefficient of variation (%CV) was determined to calculate intra-day and inter-day precision and accuracy of present method for nicorandil in rabbit plasma. The results are given in table 4.41. The validation run was consisted of calibration curve and three replicates of each low and high quantification concentrations. For inter-day analysis three batches of drug nicorandil was run on three different days and for intra-day analysis three batches of drug nicorandil was run on three different time points of same day.

Table 4.41. Intra-day and Inter-day precision and accuracy of nicorandil in rabbit plasma

Nicorandil		
Intra day		
Parameter	LQC (ng/mL)	HQC (ng/mL)
Nominal Conc.	18	500
Mean	16.14	497.27
S.D.	0.19	1.19
Precision CV (%)	0.6	0.2
Accuracy (%)	97.4	99.5
Inter day		
Parameter	LQC (ng/mL)	HQC (ng/mL)
Nominal Conc.	18	500
Mean	16.07	496.27
S.D.	0.25	1.02
Precision CV (%)	0.8	0.2
Accuracy (%)	95.1	99.3

4.6.3. Quantification and detection limits

Limit of detection (LOD) and limit of quantitation (LOQ) of nicorandil as mean ± SD were 10.0 ± 0.227 ng/mL and 16.0 ± 0.528 ng/mL. Lower quantitation limits give greater sensitivity of present method.

Table: 4.42. Plasma concentration (ng/mL) of nicorandil administered as an oral dose of HEMA-co-AA hydrogels equivalent to 15 mg in rabbit no. 1

Sr. No.	Time (Hrs)	Concentration (ng/mL)
1	0	0
2	0.5	20.23296
3	1	52.09269
4	2	54.59021
5	3	51.42908
6	4	46.22155
7	6	45.0774
8	8	41.48149
9	12	36.30666

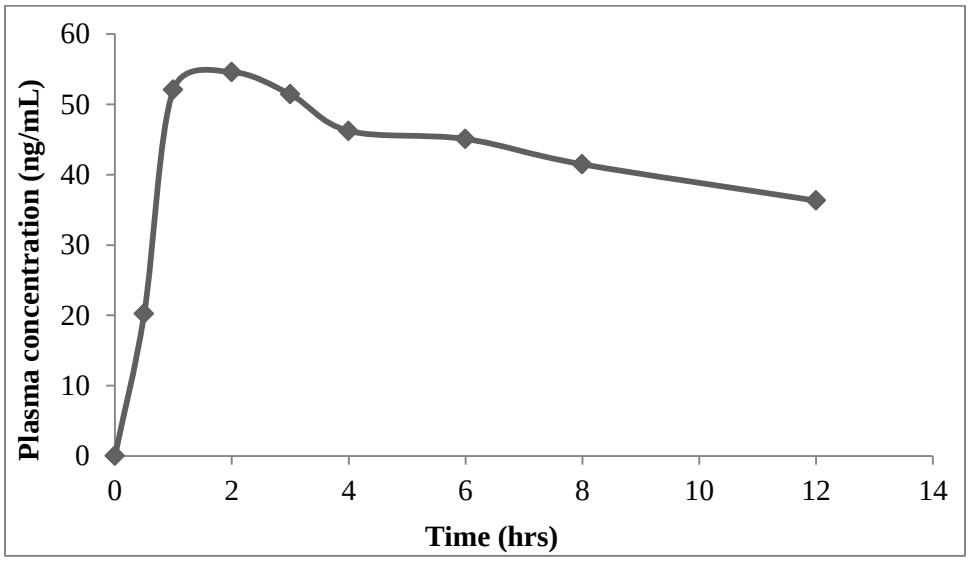

Figure 4.64. Plasma concentration vs. time profile of nicorandil administered as an oral dose of HEMA-co-AA hydrogels equivalent to 15 mg in rabbit no. 1

Table 4.43. Pharmacokinetic parameters of nicorandil administered as an oral dose of HEMA-co-AA hydrogels equivalent to 15 mg in rabbit no. 1

Prameters	Nicorandil
C_{max} (ng/mL)	54.5902
T_{max} (Hrs)	2
AUC_{tot} (ng.h/mL)	973.22
$AUMC_{tot}$ (ng.h^2/mL)	13622
MRT (Hrs)	13.9968
K_e (Hr^{-1})	0.0773602
$t_{1/2\ el}$ (Hrs)	8.96

Table 4.44. Plasma concentration (ng/mL) of nicorandil administered as an oral dose of HEMA-co-AA hydrogels equivalent to 15 mg in rabbit no. 2

Sr. No.	Time (Hrs)	Concentration (ng/mL)
1	0	0
2	0.5	22.84816
3	1	55.68859
4	2	61.45512
5	3	63.5244
6	4	56.35547
7	6	51.28851
8	8	49.65401
9	12	47.09438

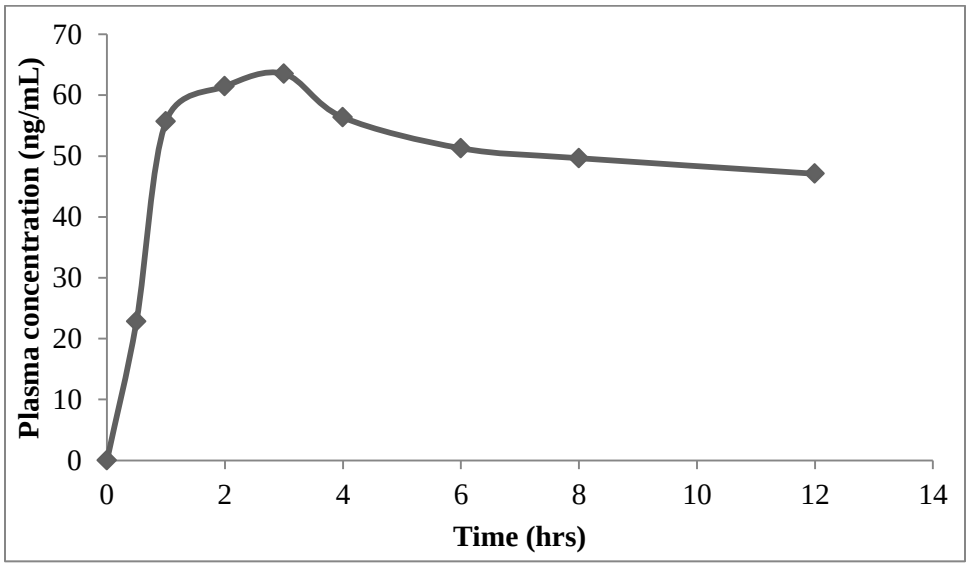

Figure 4.65. Plasma concentration vs. time profile of nicorandil administered as an oral dose of HEMA-co-AA hydrogels equivalent to 15 mg in rabbit no. 2

Table: 4.45. Pharmacokinetic parameters of nicorandil administered as an oral dose of HEMA-co-AA hydrogels equivalent to 15 mg in rabbit no. 2

Prameters	Nicorandil
C_{max} (ng/mL)	63.5244
T_{max} (Hrs)	3
AUC_{tot} (ng.h/mL)	1103.9
$AUMC_{tot}$ (ng.h^2/mL)	13634.7
MRT (Hrs)	12.3514
K_e (Hr^{-1})	0.0927887
$t_{1/2\ el}$ (Hrs)	7.47017

Table: 4.46. Plasma concentration (ng/mL) of nicorandil administered as an oral dose of HEMA-co-AA hydrogels equivalent to 15 mg in rabbit no. 3

Sr. No.	Time (Hrs)	Concentration (ng/mL)
1	0	0
2	0.5	26.77097
3	1	60.2652
4	2	66.03173
5	3	63.1975
6	4	58.64377
7	6	55.86512
8	8	53.24991
9	12	48.07508

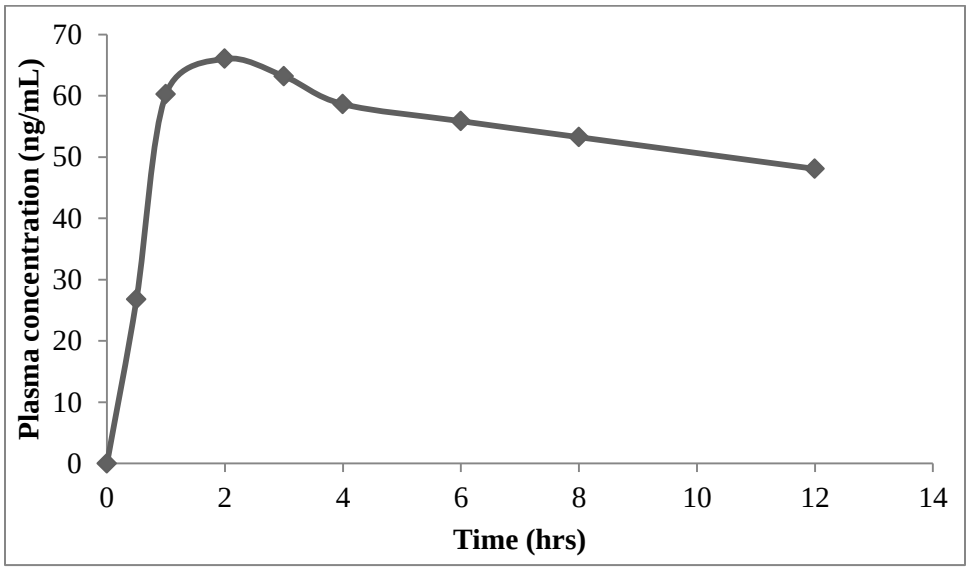

Figure 4.66. Plasma concentration vs. time profile of nicorandil administered as an oral dose of HEMA-co-AA hydrogels equivalent to 15 mg in rabbit no. 3

Table: 4.47. Pharmacokinetic parameters of nicorandil administered as an oral dose of HEMA-co-AA hydrogels equivalent to 15 mg in rabbit no. 3

Prameters	Nicorandil
C_{max} (ng/mL)	66.0317
T_{max} (Hrs)	2
AUC_{tot} (ng.h/mL)	1130.97
$AUMC_{tot}$ (ng.h^2/mL)	13360.1
MRT (Hrs)	11.813
K_e (Hr^{-1})	0.0983562
$t_{1/2\ el}$ (Hrs)	7.04732

Table: 4.48. Plasma concentration (ng/mL) of nicorandil administered as an oral dose of HEMA-co-AA hydrogels equivalent to 15 mg in rabbit no. 4

Sr. No.	Time (Hrs)	Concentration (ng/mL)
1	0	0
2	0.5	18.27155
3	1	45.55467
4	2	48.706
5	3	49.79458
6	4	50.47126
7	6	47.0388
8	8	44.7505
9	12	41.53707

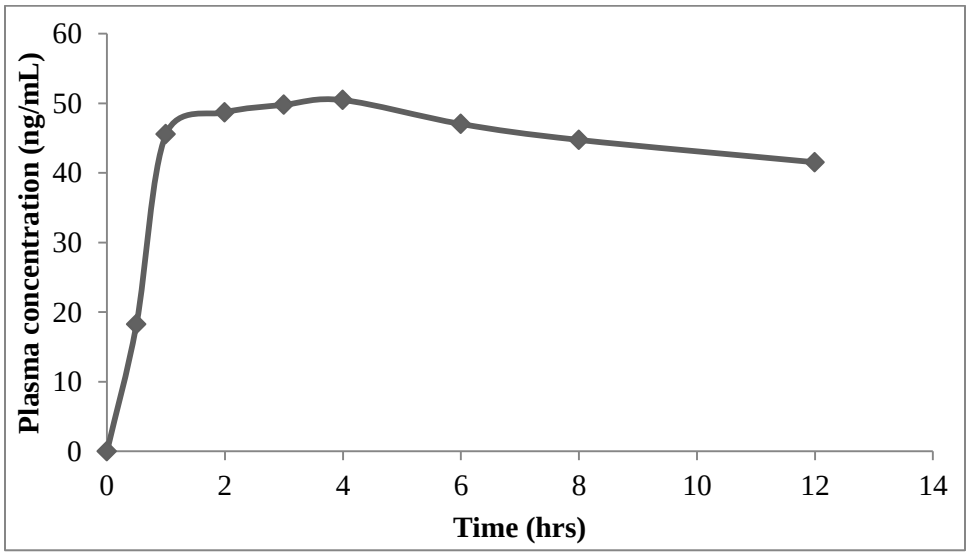

Figure 4.67. Plasma concentration vs. time profile of nicorandil administered as an oral dose of HEMA-co-AA hydrogels equivalent to 15 mg in rabbit no. 4

Table: 4.49. Pharmacokinetic parameters of nicorandil administered as an oral dose of HEMA-co-AA hydrogels equivalent to 15 mg in rabbit no. 4

Prameters	Nicorandil
C_{max} (ng/mL)	50.4713
T_{max} (Hrs)	4
AUC_{tot} (ng.h/mL)	993.097
$AUMC_{tot}$ (ng.h^2/mL)	13013.5
MRT (Hrs)	13.1039
K_e (Hr^{-1})	0.0872032
$t_{1/2\ el}$ (Hrs)	7.94865

Table: 4.50. Plasma concentration (ng/mL) of nicorandil administered za an oral dose of HEMA-co-AA hydrogels equivalent to 15 mg in rabbit no. 5

Sr. No.	Time (Hrs)	Concentration (ng/mL)
1	0	0
2	0.5	27.09787
3	1	60.2652
4	2	66.35863
5	3	68.42791
6	4	63.54728
7	6	57.17272
8	8	52.92301
9	12	51.34408

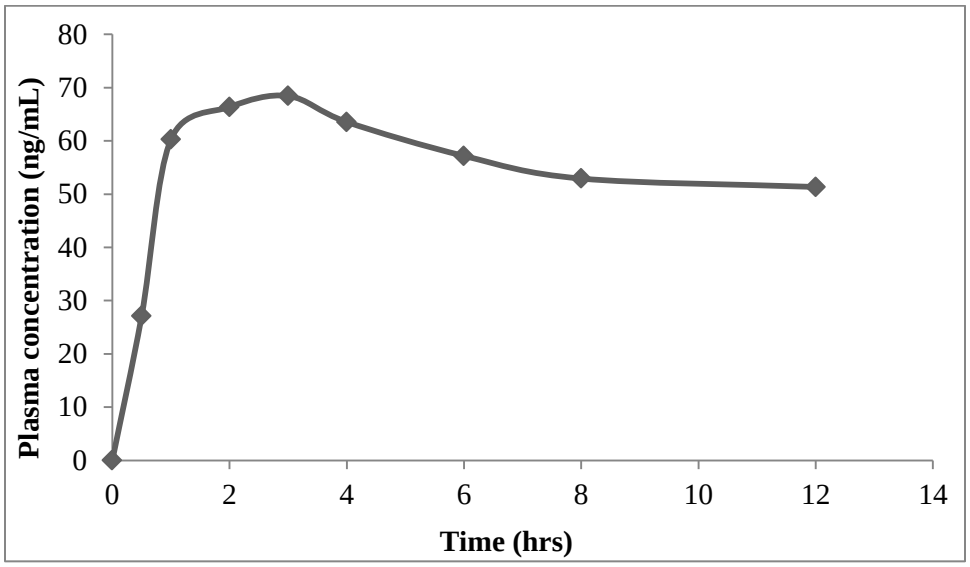

Figure 4.68. Plasma concentration vs. time profile of nicorandil administered as an oral dose of HEMA-co-AA hydrogels equivalent to 15 mg in rabbit no. 5

Table: 4.51. Pharmacokinetic parameters of nicorandil administered as an oral dose of HEMA-co-AA hydrogels equivalent to 15 mg in rabbit no. 5

Prameters	Nicorandil
C_{max} (ng/mL)	68.4279
T_{max} (Hrs)	3
AUC_{tot} (ng.h/mL)	1226.27
$AUMC_{tot}$ ($ng.h^2$/mL)	16000.1
MRT (Hrs)	13.0477
K_e (Hr^{-1})	0.0794126
$t_{1/2\ el}$ (Hrs)	8.72843

Table: 4.52. Plasma concentration (ng/mL) of nicorandil administered as an oral dose of HEMA-co-AA hydrogels equivalent to 15 mg in rabbit no. 6

Sr. No.	Time (Hrs)	Concentration (ng/mL)
1	0	0
2	0.5	30.36687
3	1	48.82368
4	2	56.55161
5	3	59.60159
6	4	60.60518
7	6	52.26921
8	8	49.65401
9	12	45.13297

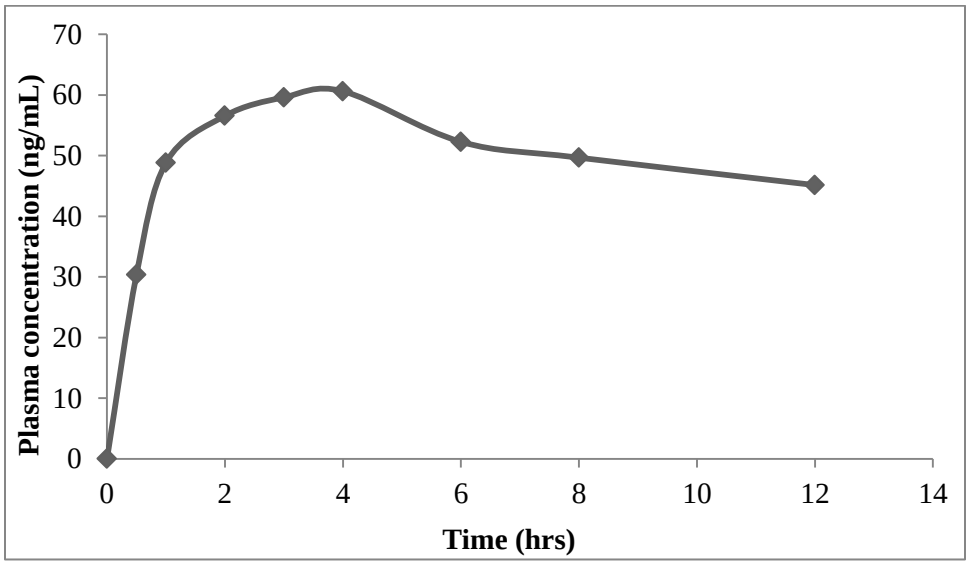

Figure 4.69. Plasma concentration vs. time profile of nicorandil administered as an oral dose of HEMA-co-AA hydrogels equivalent to 15 mg in rabbit no. 6

Table: 4.53. Pharmacokinetic parameters of nicorandil administered as an oral dose of HEMA-co-AA hydrogels equivalent to 15 mg in rabbit no. 6

Prameters	Nicorandil
C_{max} (ng/mL)	60.6052
T_{max} (Hrs)	4
AUC_{tot} (ng.h/mL)	1087.8
$AUMC_{tot}$ ($ng.h^2$/mL)	13524.8
MRT (Hrs)	12.4331
K_e (Hr^{-1})	0.091721
$t_{1/2\ el}$ (Hrs)	7.55712

Table: 4.54. Plasma concentration (ng/mL) of nicorandil administered as an oral dose of HEMA-co-AA hydrogels equivalent to 15 mg in G 1

G1									
Time (hrs)	**R1**	**R2**	**R3**	**R4**	**R5**	**R6**	**Mean**	**Std Dev**	**SEM**
0	0	0	0	0	0	0	0	0	0
0.5	20.232	22.848	26.770	18.271	27.097	30.366	24.264	4.598	1.877
1	52.092	55.688	60.265	45.554	60.265	48.823	53.781	6.046	2.469
2	54.590	61.455	66.031	48.706	66.358	56.551	58.948	6.942	2.834
3	51.429	63.524	63.197	49.794	68.427	59.601	59.329	7.331	2.993
4	46.221	56.355	58.643	50.471	63.547	60.605	55.974	6.503	2.655
6	45.077	51.288	55.865	47.038	57.172	52.269	51.451	4.754	1.941
8	41.481	49.654	53.249	44.750	52.923	49.654	48.618	4.648	1.898
12	36.306	47.094	48.075	41.537	51.344	45.132	44.915	5.322	2.173

Table: 4.55. Mean plasma concentration (ng/mL) of nicorandil administered as an oral dose of HEMA-co-AA hydrogels equivalent to 15 mg in G1

Sr. No.	Time (Hrs)	Mean concentration (ng/mL) ± SEM
1	0	0 ± 000
2	0.5	24.26473 ± 1.877
3	1	53.78167 ± 2.469
4	2	58.94888 ± 2.834
5	3	59.32918 ± 2.993
6	4	55.97409 ± 2.655
7	6	51.45196 ± 1.941
8	8	48.61882 ± 1.898
9	12	44.91504 ± 2.173

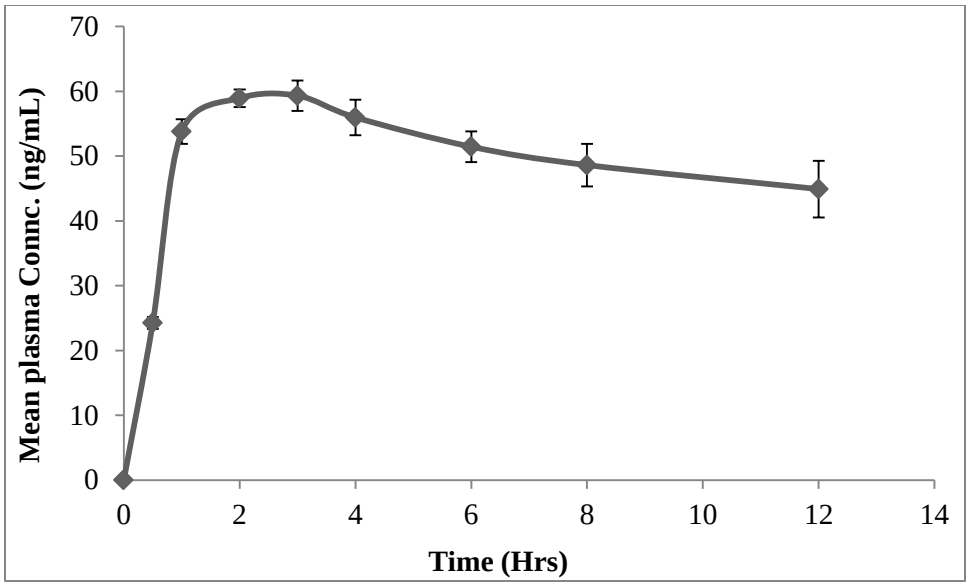

Figure 4.70. Mean plasma concentration vs. time profile of nicorandil administered as an oral dose of HEMA-co-AA hydrogels equivalent to 15 mg in G1

Table: 4.56. Pharmacokinetic parameters of nicorandil administered as an oral dose of HEMA-co-AA hydrogels equivalent to 15 mg in G1

Prameters	**Mean ± SEM**
C_{max} (ng/mL)	60.60 ± 2.81
T_{max} (Hrs)	3 ± 0.36
AUC_{tot} (ng.h/mL)	1085.87 ± 38.02
$AUMC_{tot}$ ($ng.h^2$/mL)	13859.2 ± 438.41
MRT (Hrs)	12.79 ± 0.311
K_e (Hr^{-1})	0.087807 ± 0.01
$t_{1/2\ el}$ (Hrs)	7.95 ± 0.31

Table: 4.57. Plasma concentration (ng/mL) of nicorandil administered as an oral dose of HPMC-co-AA hydrogels equivalent to 15 mg in rabbit no. 7

Sr. No.	Time (Hrs)	Concentration (ng/mL)
1	0	0
2	0.5	28.9903
3	1	62.06315
4	2	106.2405
5	3	116.2469
6	4	110.3627
7	6	107.45
8	8	104.8348
9	12	102.7067

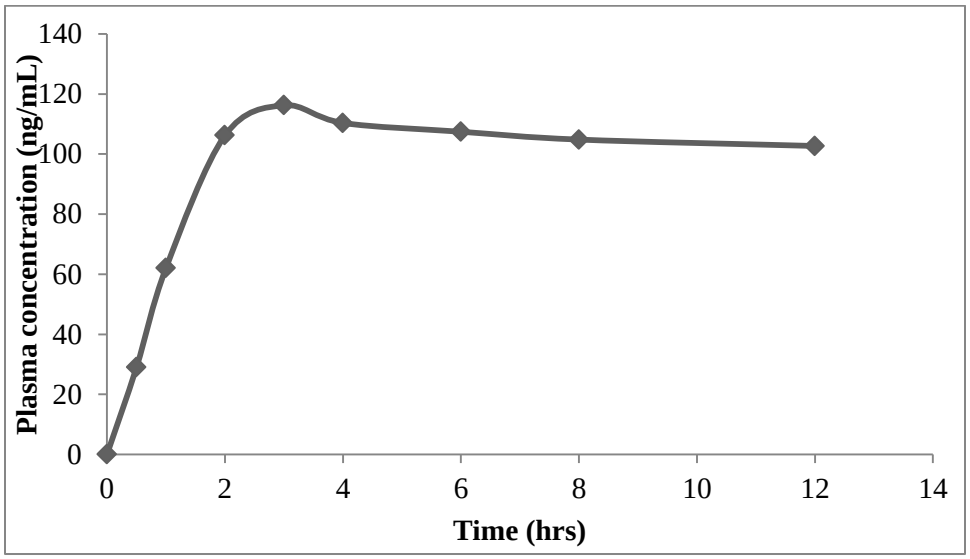

Figure 4.71. Plasma concentration vs. time profile of nicorandil administered as an oral dose of HPMC-co-AA hydrogels equivalent to 15 mg in rabbit no. 7

Table: 4.58. Pharmacokinetic parameters of nicorandil administered as an oral dose of HPMC-co-AA hydrogels equivalent to 15 mg in rabbit no. 7

Prameters	Nicorandil
C_{max} (ng/mL)	116.247
T_{max} (Hrs)	3
AUC_{tot} (ng.h/mL)	2229.96
$AUMC_{tot}$ ($ng.h^2/mL$)	28174.9
MRT (Hrs)	12.6347
K_e (Hr^{-1})	0.0954547
$t_{1/2\ el}$ (Hrs)	7.26153

Table: 4.59. Plasma concentration (ng/mL) of nicorandil administered as an oral dose of HPMC-co-AA hydrogels equivalent to 15 mg in rabbit no. 8

Sr. No.	Time (Hrs)	Concentration (ng/mL)
1	0	0
2	0.5	27.45746
3	1	57.15965
4	2	101.0101
5	3	108.0744
6	4	107.0937
7	6	104.181
8	8	101.5658
9	12	100.7453

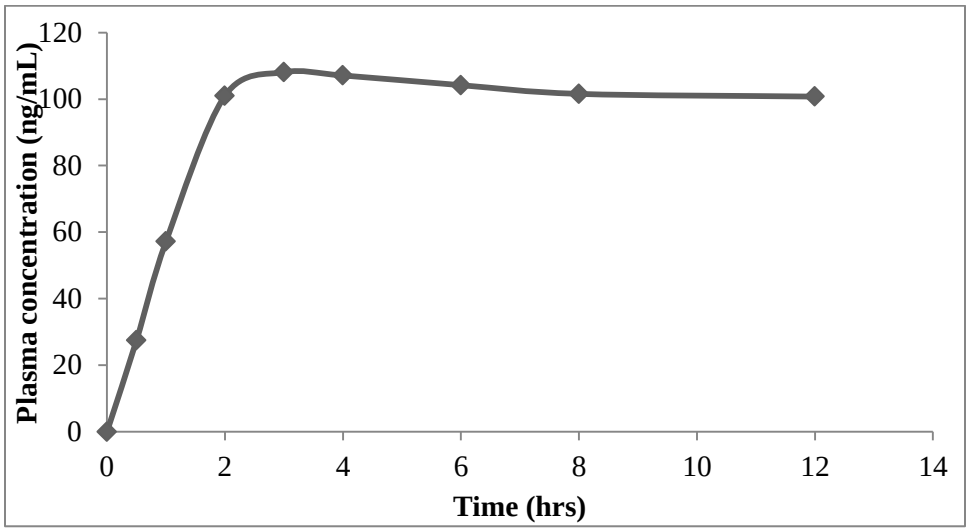

Figure 4.72. Plasma concentration vs. time profile of nicorandil administered as an oral dose of HPMC-co-AA hydrogels equivalent to 15 mg in rabbit no. 8

Table: 4.60. Pharmacokinetic parameters of nicorandil administered as an oral dose of HPMC-co-AA hydrogels equivalent to 15 mg in rabbit no. 8

Prameters	Nicorandil
C_{max} (ng/mL)	108.074
T_{max} (Hrs)	3
AUC_{tot} (ng.h/mL)	2103.33
$AUMC_{tot}$ (ng.h^2/mL)	25367.4
MRT (Hrs)	12.0606
K_e (Hr^{-1})	12.0606
$t_{1/2\ el}$ (Hrs)	6.73627

Table: 4.61. Plasma concentration (ng/mL) of nicorandil administered as an oral dose of HPMC-co-AA hydrogels equivalent to 15 mg in rabbit no. 9

Sr. No.	Time (Hrs)	Concentration (ng/mL)
1	0	0
2	0.5	26.19889
3	1	52.619
4	2	98.20528
5	3	104.9198
6	4	104.0503
7	6	103.2003
8	8	101.1245
9	12	97.22458

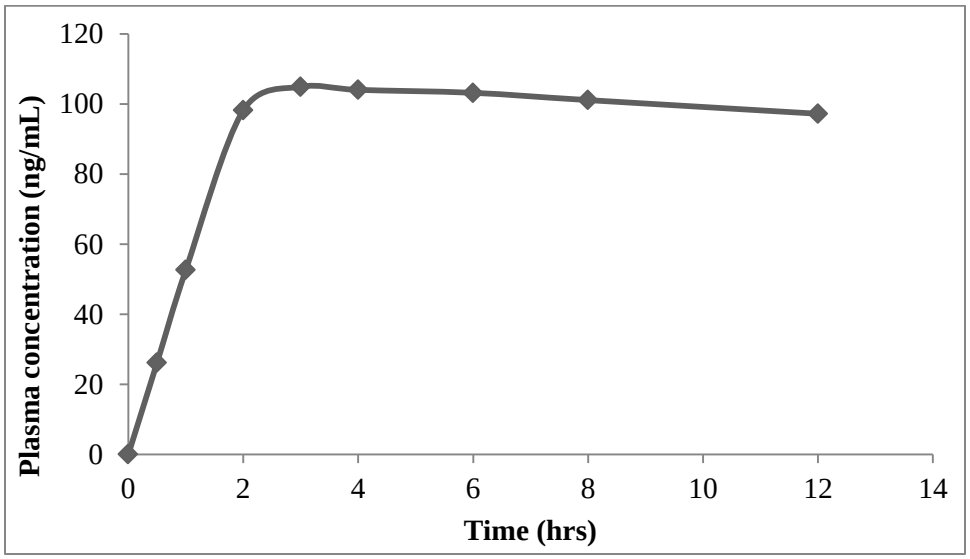

Figure 4.73. Plasma concentration vs. time profile of nicorandil administered as an oral dose of HPMC-co-AA hydrogels equivalent to 15 mg in rabbit no. 9

Table: 4.62. Pharmacokinetic parameters of nicorandil administered as an oral dose of HPMC-co-AA hydrogels equivalent to 15 mg in rabbit no. 9

Prameters	Nicorandil
C_{max} (ng/mL)	104.92
T_{max} (Hrs)	3
AUC_{tot} (ng.h/mL)	2047.09
$AUMC_{tot}$ ($ng.h^2$/mL)	24640.9
MRT (Hrs)	12.037
K_e (Hr^{-1})	0.103524
$t_{1/2\ el}$ (Hrs)	6.69554

Table: 4.63. Plasma concentration (ng/mL) of nicorandil administered as an oral dose of HPMC-co-AA hydrogels equivalent to 15 mg in rabbit no. 10

Sr. No.	Time (Hrs)	Concentration (ng/mL)
1	0	0
2	0.5	29.51039
3	1	63.10924
4	2	105.8548
5	3	111.0165
6	4	113.501
7	6	101.2389
8	8	94.83167
9	12	83.92627

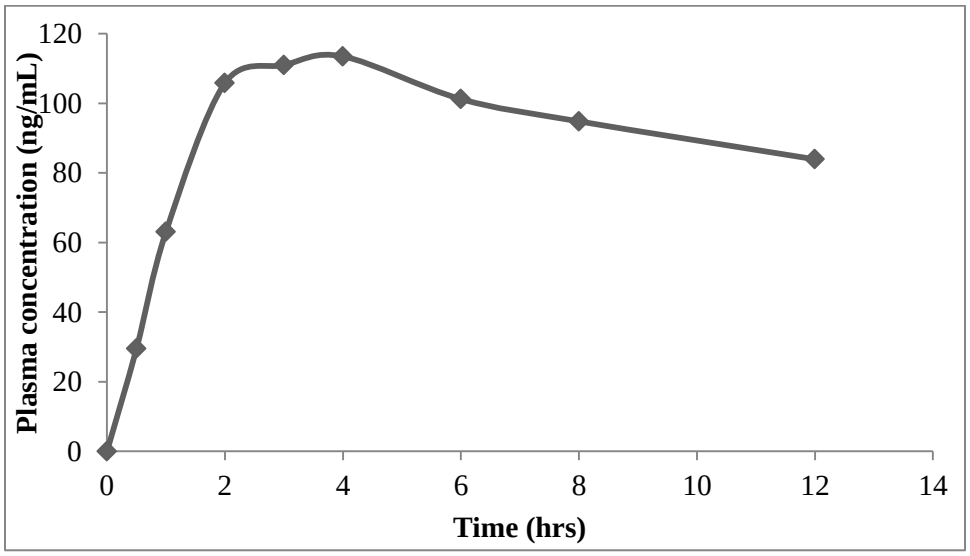

Figure 4.74. Plasma concentration vs. time profile of nicorandil administered as an oral dose of HPMC-co-AA hydrogels equivalent to 15 mg in rabbit no. 10

Table: 4.64. Pharmacokinetic parameters of nicorandil administered as an oral dose of HPMC-co-AA hydrogels equivalent to 15 mg in rabbit no. 10

Prameters	Nicorandil
C_{max} (ng/mL)	113.501
T_{max} (Hrs)	4
AUC_{tot} (ng.h/mL)	2161.43
$AUMC_{tot}$ (ng.h^2/mL)	31016.2
MRT (Hrs)	14.3499
K_e (Hr^{-1})	0.0777844
$t_{1/2\ el}$ (Hrs)	8.91113

Table: 4.65. Plasma concentration (ng/mL) of nicorandil administered as an oral dose of HPMC-co-AA hydrogels equivalent to 15 mg in rabbit no. 11

Sr. No.	Time (Hrs)	Concentration (ng/mL)
1	0	0
2	0.5	32.34462
3	1	64.48549
4	2	100.4936
5	3	99.16637
6	4	93.91635
7	6	90.7781
8	8	82.16427
9	12	74.99534

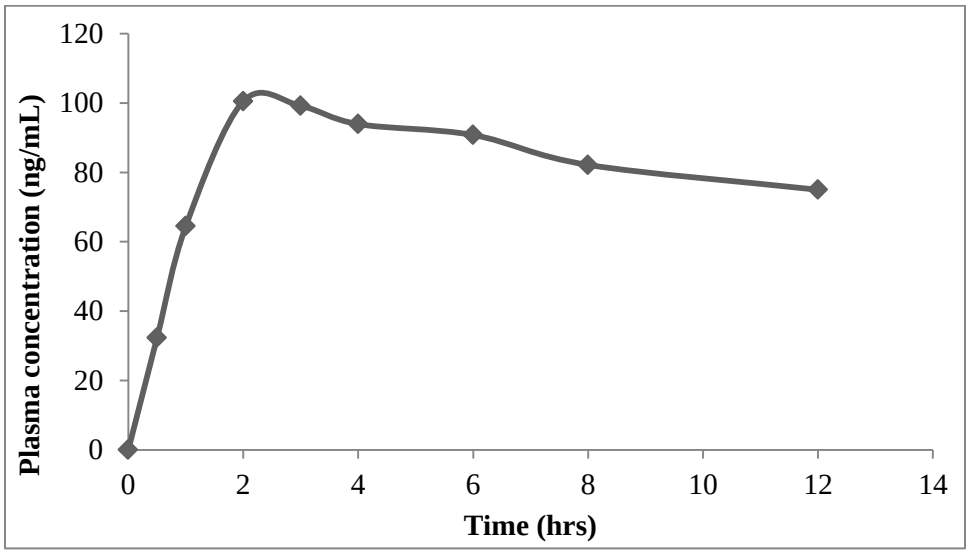

Figure 4.75. Plasma concentration vs. time profile of nicorandil administered as an oral dose of HPMC-co-AA hydrogels equivalent to 15 mg in rabbit no. 11

Table: 4.66. Pharmacokinetic parameters of nicorandil administered as an oral dose of HPMC-co-AA hydrogels equivalent to 15 mg in rabbit no. 11

Prameters	Nicorandil
C_{max} (ng/mL)	100.494
T_{max} (Hrs)	2
AUC_{tot} (ng.h/mL)	1944.85
$AUMC_{tot}$ (ng.h^2/mL)	28605.7
MRT (Hrs)	14.7084
K_e (Hr^{-1})	0.0730844
$t_{1/2\ el}$ (Hrs)	9.48421

Table: 4.67. Plasma concentration (ng/mL) of nicorandil administered as an oral dose of HPMC-co-AA hydrogels equivalent to 15 mg in rabbit no. 12

Sr. No.	Time (Hrs)	Concentration (ng/mL)
1	0	0
2	0.5	26.77097
3	1	56.01549
4	2	104.9329
5	3	107.0937
6	4	105.0637
7	6	104.2464
8	8	97.38149
9	12	91.83726

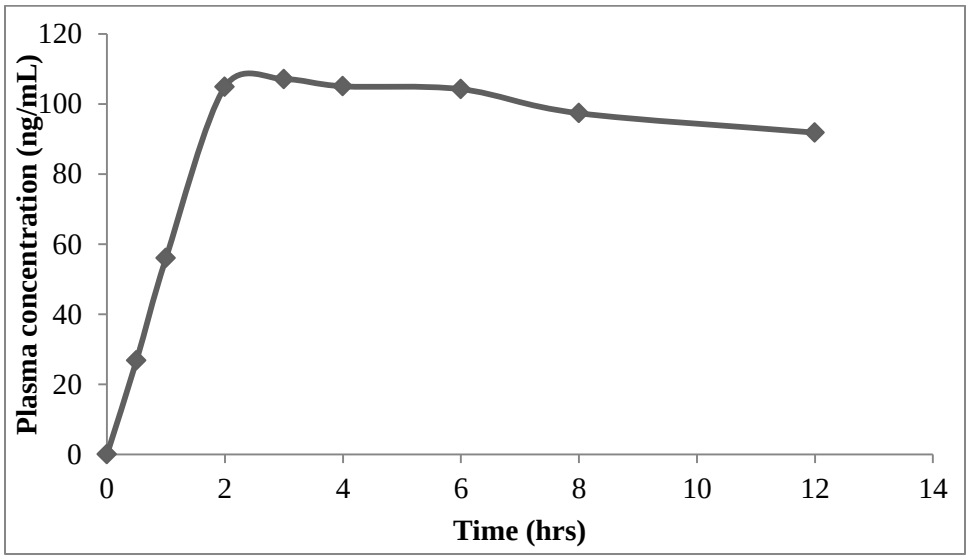

Figure 4.76. Plasma concentration vs. time profile of nicorandil administered as an oral dose of HPMC-co-AA hydrogels equivalent to 15 mg in rabbit no. 12

Table: 4.68. Pharmacokinetic parameters of nicorandil administered as an oral dose of HPMC-co-AA hydrogels equivalent to 15 mg in rabbit no. 12

Prameters	Nicorandil
C_{max} (ng/mL)	107.094
T_{max} (Hrs)	3
AUC_{tot} (ng.h/mL)	2122.4
$AUMC_{tot}$ (ng.h^2/mL)	28187.5
MRT (Hrs)	13.281
K_e (Hr^{-1})	0.0880364
$t_{1/2\ el}$ (Hrs)	7.87342

Table: 4.69. Plasma concentrations (ng/mL) of nicorandil administered as an oral dose of HPMC-co-AA hydrogels equivalent to 15 mg in G2

G2									
Time (hrs)	**R7**	**R8**	**R9**	**R10**	**R11**	**R12**	**Mean**	**Std Dev**	**SEM**
0	0	0	0	0	0	0	0	0	0
0.5	28.990	27.457	26.198	29.510	32.344	26.770	28.545	2.253	0.920
1	62.063	57.159	52.619	63.109	64.485	56.015	59.242	4.669	1.906
2	106.240	101.010	98.205	105.854	100.493	104.932	102.789	3.327	1.358
3	116.246	108.074	104.919	111.016	99.166	107.093	107.752	5.746	2.346
4	110.362	107.093	104.050	113.501	93.916	105.063	105.664	6.730	2.748
6	107.451	104.181	103.200	101.23	90.778	104.246	101.849	5.784	2.362
8	104.834	101.565	101.124	94.831	82.164	97.381	96.983	8.052	3.287
12	102.706	100.745	97.224	83.926	74.995	91.837	91.905	10.702	4.369

Table: 4.70. Mean plasma concentration (ng/mL) of nicorandil administered as an oral dose of HPMC-co-AA hydrogels equivalent to 15 mg in G2

Sr. No.	Time (Hrs)	Concentration (ng/mL) ± SEM
1	0	0
2	0.5	28.54544 ± 0.920
3	1	59.242 ± 1.906
4	2	102.7895 ± 1.358
5	3	107.7529 ± 2.346
6	4	105.6646 ± 2.748
7	6	101.8491 ± 2.362
8	8	96.98376 ± 3.287
9	12	91.90591 ± 4.369

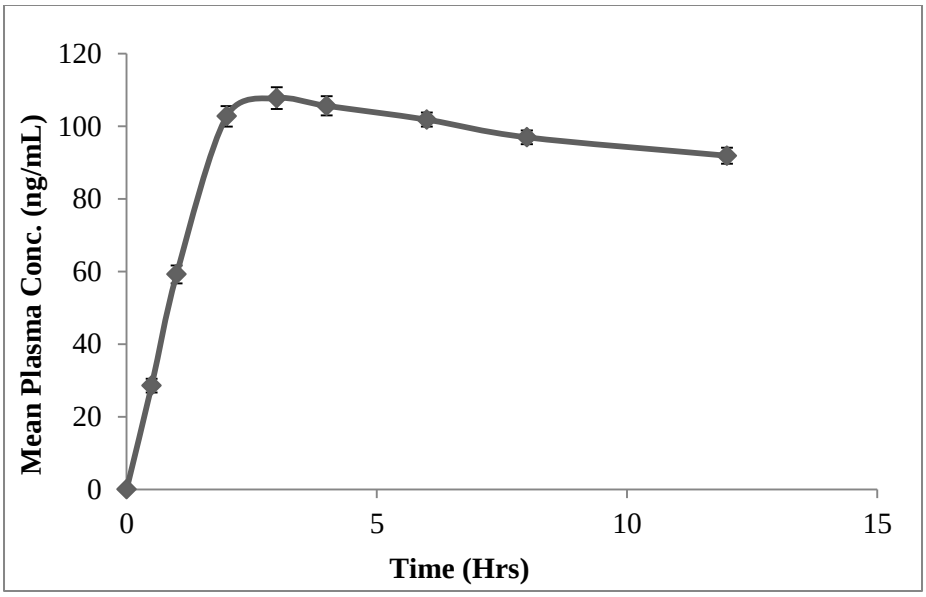

Figure 4.77. Mean plasma concentration vs. time profile of nicorandil administered as an oral dose of HPMC-co-AA hydrogels equivalent to 15 mg in G2

Table: 4.71. Pharmacokinetic parameters of nicorandil administered as an oral dose of HPMC-co-AA hydrogels equivalent to 15 mg in G2

Prameters	Mean ± SEM
C_{max} (ng/mL)	108.38 ± 2.33
T_{max} (Hrs)	3 ± 0.25
AUC_{tot} (ng.h/mL)	2101.51 ± 40.01
$AUMC_{tot}$ ($ng.h^2$/mL)	27665.43 ± 949.95
MRT (Hrs)	13.17 ± 0.46
K_e (Hr^{-1})	2.08 ± 1.99
$t_{1/2\ el}$ (Hrs)	7.82 ± 0.47

Table: 4.72. Plasma concentration (ng/mL) of nicorandil administered as an oral dose of HPMC-co-AA-co-HEMA hydrogels equivalent to 15 mg in rabbit no. 13

Sr. No.	Time (Hrs)	Concentration (ng/mL)
1	0	0
2	0.5	29.40252
3	1	52.06327
4	2	66.49593
5	3	84.78275
6	4	95.22395
7	6	90.7781
8	8	88.37538
9	12	77.61055

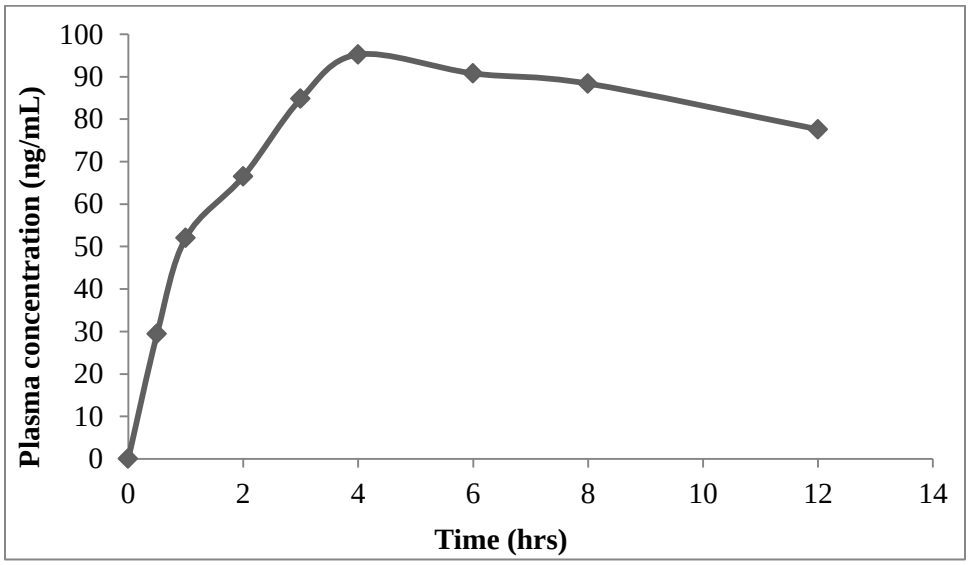

Figure 4.78. Plasma concentration vs. time profile of nicorandil administered as an oral dose of HPMC-co-AA-co-HEMA hydrogels equivalent to 15 mg in rabbit no. 13

Table: 4.73. Pharmacokinetic parameters of nicorandil administered as an oral dose of HPMC-co-AA-co-HEMA hydrogels equivalent to 15 mg in rabbit no. 13

Prameters	Nicorandil
C_{max} (ng/mL)	95.224
T_{max} (Hrs)	4
AUC_{tot} (ng.h/mL)	1794.72
$AUMC_{tot}$ ($ng.h^2$/mL)	23481.1
MRT (Hrs)	13.0834
K_e (Hr^{-1})	0.091393
$t_{1/2\ el}$ (Hrs)	7.58425

Table: 4.74. Plasma concentration (ng/mL) of nicorandil administered as an oral dose of HPMC-co-AA-co-HEMA hydrogels equivalent to 15 mg in rabbit no. 14

Sr. No.	Time (Hrs)	Concentration (ng/mL)
1	0	0
2	0.5	27.27766
3	1	56.31297
4	2	74.99534
5	3	98.51257
6	4	91.95494
7	6	88.8167
8	8	86.41398
9	12	82.84096

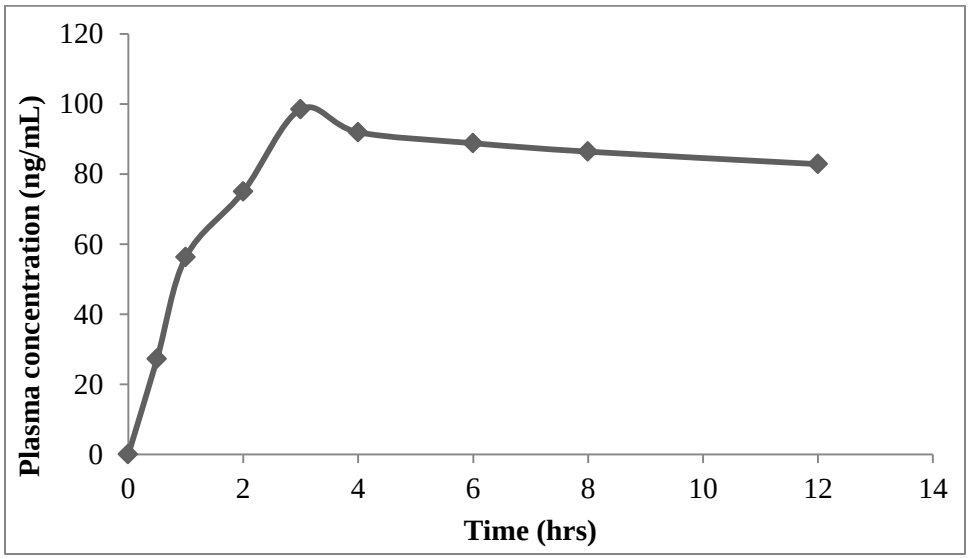

Figure 4.79. Plasma concentration vs. time profile of nicorandil administered as an oral dose of HPMC-co-AA-co-HEMA hydrogels equivalent to 15 mg in rabbit no. 14

Table: 4.75. Pharmacokinetic parameters of nicorandil administered as an oral dose of HPMC-co-AA-co-HEMA hydrogels equivalent to 15 mg in rabbit no. 14

Prameters	Nicorandil
C_{max} (ng/mL)	98.5126
T_{max} (Hrs)	3
AUC_{tot} (ng.h/mL)	1882.88
$AUMC_{tot}$ (ng.h^2/mL)	25278.1
MRT (Hrs)	13.4253
K_e (Hr^{-1})	0.0876654
$t_{1/2\ el}$ (Hrs)	7.90674

Table: 4.76. Plasma concentration (ng/mL) of nicorandil administered as an oral dose of HPMC-co-AA-co-HEMA hydrogels equivalent to 15 mg in rabbit no. 15

Sr. No.	Time (Hrs)	Concentration (ng/mL)
1	0	0
2	0.5	25.12012
3	1	66.77379
4	2	83.06652
5	3	79.87924
6	4	78.22512
7	6	75.74068
8	8	74.31866
9	12	69.76493

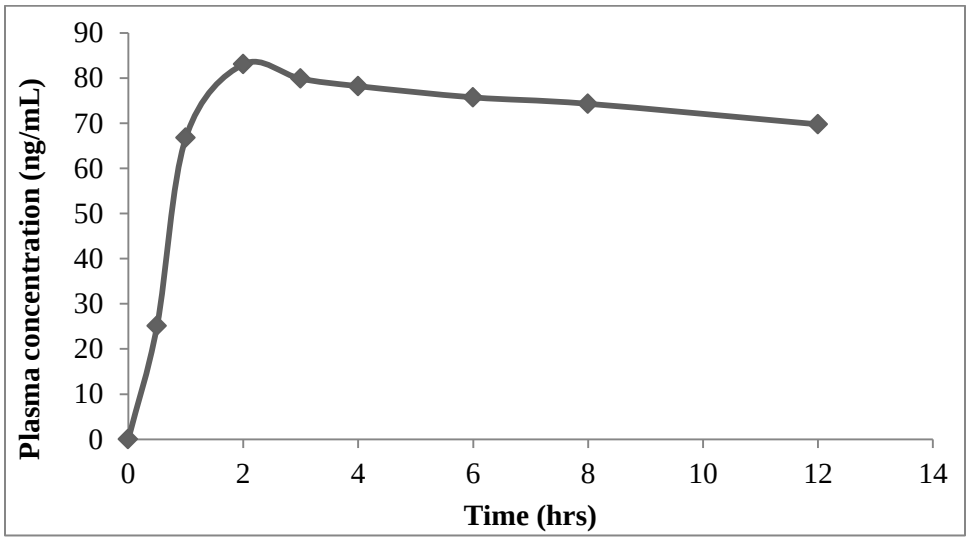

Figure 4.80. Plasma concentration vs. time profile of nicorandil administered as an oral dose of HPMC-co-AA-co-HEMA hydrogels equivalent to 15 mg in rabbit no. 15

Table: 4.77. Pharmacokinetic parameters of nicorandil administered as an oral dose of HPMC-co-AA-co-HEMA hydrogels equivalent to 15 mg in rabbit no. 15

Prameters	Nicorandil
C_{max} (ng/mL)	83.0665
T_{max} (Hrs)	2
AUC_{tot} (ng.h/mL)	1706.73
$AUMC_{tot}$ ($ng.h^2$/mL)	24415.4
MRT (Hrs)	14.3054
K_e (Hr^{-1})	0.0790355
$t_{1/2\ el}$ (Hrs)	8.77008

Table: 4.78. Plasma concentration (ng/mL) of nicorandil administered as an oral dose of HPMC-co-AA-co-HEMA hydrogels equivalent to 15 mg in rabbit no. 16

Sr. No.	Time (Hrs)	Concentration (ng/mL)
1	0	0
2	0.5	31.65813
3	1	69.0621
4	2	79.79751
5	3	77.59093
6	4	76.59062
7	6	75.83875
8	8	74.64556
9	12	71.07253

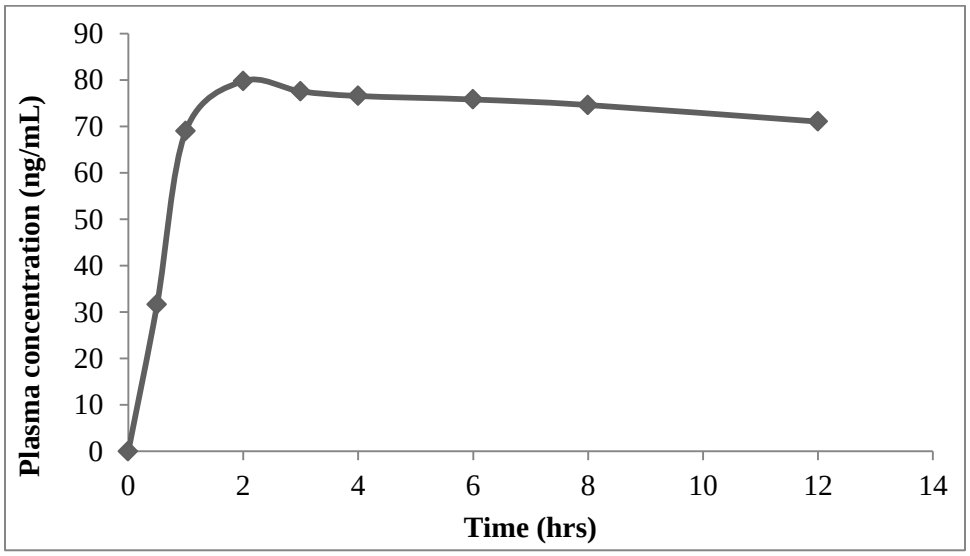

Figure 4.81. Plasma concentration vs. time profile of nicorandil administered as an oral dose of HPMC-co-AA-co-HEMA hydrogels equivalent to 15 mg in rabbit no. 16

Table: 4.79. Pharmacokinetic parameters of nicorandil administered as an oral dose of HPMC-co-AA-co-HEMA hydrogels equivalent to 15 mg in rabbit no. 16

Prameters	Nicorandil
C_{max} (ng/mL)	79.7975
T_{max} (Hrs)	2
AUC_{tot} (ng.h/mL)	1713.92
$AUMC_{tot}$ (ng.h^2/mL)	24451.5
MRT (Hrs)	14.2664
K_e (Hr^{-1})	0.0796036
$t_{1/2\ el}$ (Hrs)	8.70749

Table: 4.80. Plasma concentration (ng/mL) of nicorandil administered as an oral dose of HPMC-co-AA-co-HEMA hydrogels equivalent to 15 mg in rabbit no. 17

Sr. No.	Time (Hrs)	Concentration (ng/mL)
1	0	0
2	0.5	32.50807
3	1	62.85099
4	2	81.53335
5	3	102.7623
6	4	98.81986
7	6	92.41261
8	8	89.35608
9	12	78.26435

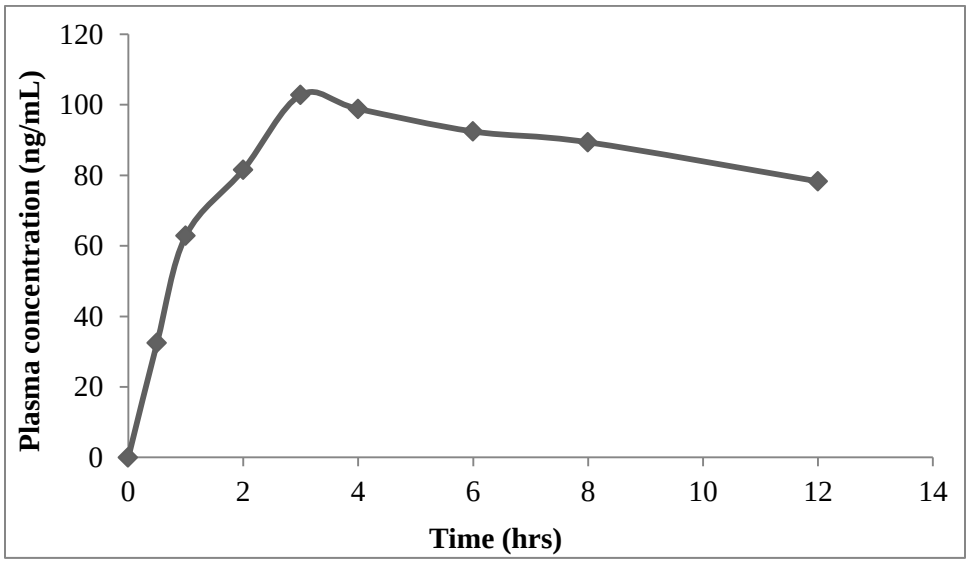

Figure 4.82. Plasma concentration vs. time profile of nicorandil administered as an oral dose of HPMC-co-AA-co-HEMA hydrogels equivalent to 15 mg in rabbit no. 17

Table: 4.81. Pharmacokinetic parameters of nicorandil administered as an oral dose of HPMC-co-AA-co-HEMA hydrogels equivalent to 15 mg in rabbit no. 17

Prameters	Nicorandil
C_{max} (ng/mL)	102.762
T_{max} (Hrs)	3
AUC_{tot} (ng.h/mL)	1860.58
$AUMC_{tot}$ (ng.h^2/mL)	23911.6
MRT (Hrs)	12.8517
K_e (Hr^{-1})	0.0910878
$t_{1/2\ el}$ (Hrs)	7.60966

Table: 4.82. Plasma concentration (ng/mL) of nicorandil administered as an oral dose of HPMC-co-AA-co-HEMA hydrogels equivalent to 15 mg in rabbit no. 18

Sr. No.	Time (Hrs)	Concentration (ng/mL)
1	0	0
2	0.5	32.31193
3	1	63.83169
4	2	75.5478
5	3	92.95526
6	4	94.57015
7	6	89.1436
8	8	80.85667
9	12	73.03394

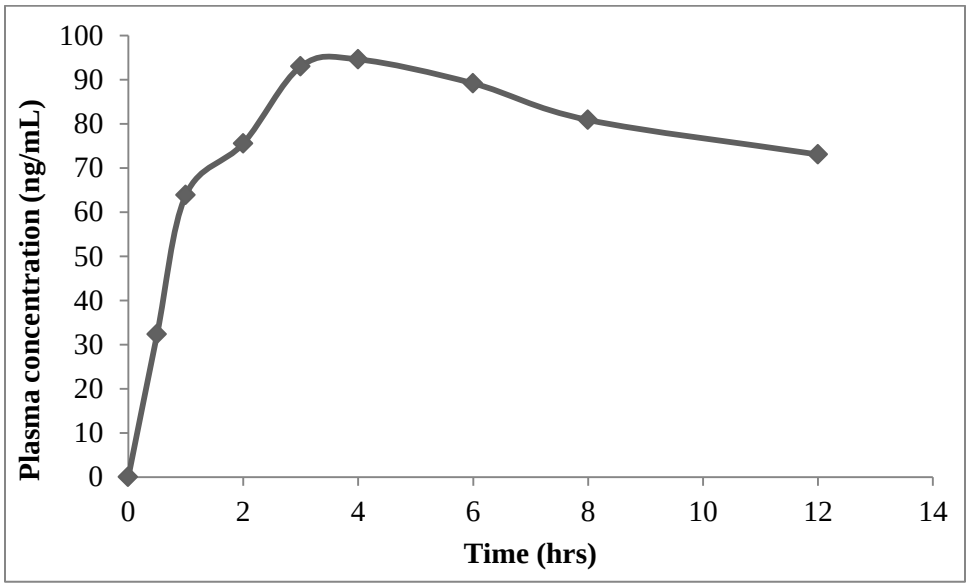

Figure 4.83. Plasma concentration vs. time profile of nicorandil administered as an oral dose of HPMC-co-AA-co-HEMA hydrogels equivalent to 15 mg in rabbit no. 18

Table: 4.83. Pharmacokinetic parameters of nicorandil administered as an oral dose of HPMC-co-AA-co-HEMA hydrogels equivalent to 15 mg in rabbit no. 18

Prameters	Nicorandil
C_{max} (ng/mL)	94.5701
T_{max} (Hrs)	4
AUC_{tot} (ng.h/mL)	1792.91
$AUMC_{tot}$ (ng.h^2/mL)	24507.4
MRT (Hrs)	13.6691
K_e (Hr^{-1})	0.0808116
$t_{1/2\ el}$ (Hrs)	8.57733

Table: 4.84. Plasma concentrations (ng/mL) of nicorandil administered as an oral dose of HPMC-co-AA-co-HEMA hydrogels equivalent to 15 mg in G3

G3									
Time (hrs)	**R13**	**R14**	**R15**	**R16**	**R17**	**R18**	**Mean**	**Std Dev**	**SEM**
0	0	0	0	0	0	0	0	0	0
0.5	29.403	27.278	25.120	31.658	32.508	32.312	29.713	3.016	1.231
1	52.063	56.313	66.774	69.062	62.851	63.832	61.816	6.444	2.631
2	66.496	74.995	83.067	79.798	81.533	75.548	76.906	6.026	2.460
3	84.783	98.513	79.879	77.591	102.762	92.955	89.414	10.253	4.186
4	95.224	91.955	78.225	76.591	98.820	94.570	89.231	9.431	3.850
6	90.778	88.817	75.741	75.839	92.413	89.144	85.455	7.596	3.101
8	88.375	86.414	74.319	74.646	89.356	80.857	82.328	6.753	2.757
12	77.611	82.841	69.765	71.073	78.264	73.034	75.431	4.991	2.037

Table: 4.85. Mean plasma concentration (ng/mL) of nicorandil administered as an oral dose of HPMC-co-AA-co-HEMA hydrogels equivalent to 15 mg in G3

Sr. No.	Time (Hrs)	Concentration (ng/mL) ± SEM
1	0	0
2	0.5	29.71307 ± 1.231
3	1	61.8158 ± 2.631
4	2	76.90608 ± 2.460
5	3	89.41384 ± 4.186
6	4	89.23077 ± 3.850
7	6	85.45507 ± 3.101
8	8	82.32772 ± 2.757
9	12	75.43121 ± 2.037

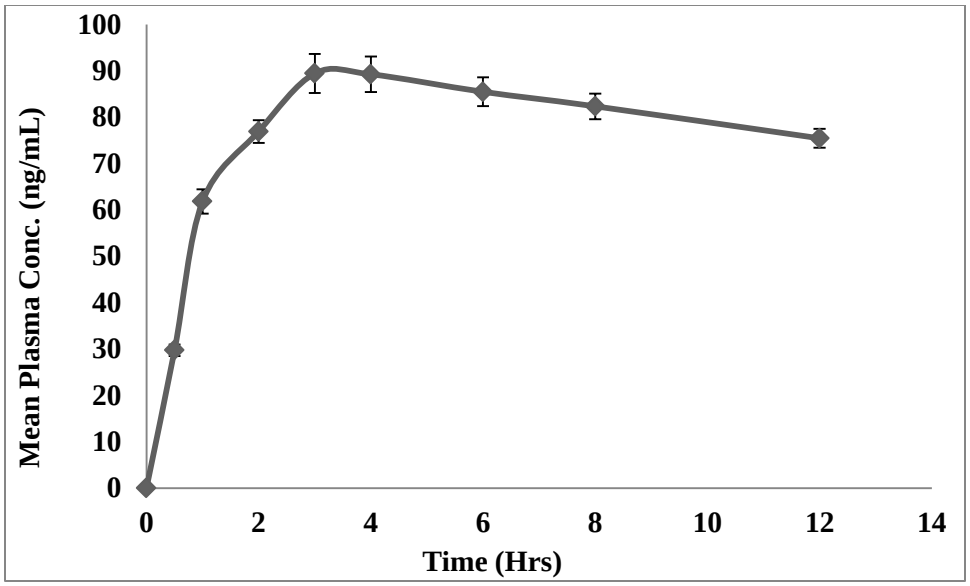

Figure 4.84. Mean plasma concentration vs. time profile of nicorandil administered as an oral dose of HPMC-co-AA-co-HEMA hydrogels equivalent to 15 mg in G3

Table: 4.86. Pharmacokinetic parameters of nicorandil administered as an oral dose of HPMC-co-AA-co-HEMA hydrogels equivalent to 15 mg in G3

Prameters	Mean ± SEM
C_{max} (ng/mL)	92.32 ± 3.66
T_{max} (Hrs)	3 ± 0.36
AUC_{tot} (ng.h/mL)	1791.95 ± 29.63
$AUMC_{tot}$ (ng.h^2/mL)	24340.85 ± 248.15
MRT (Hrs)	13.60 ± 0.24
K_e (Hr^{-1})	0.08 ± 0.01
$t_{1/2\ el}$ (Hrs)	8.19± 0.22

Table: 4.87. Plasma concentration (ng/mL) of nicorandil administered as an oral solution equivalent to 15 mg in rabbit no. 19

Sr. No.	Time (Hrs)	Concentration (ng/mL)
1	0	0
2	0.5	87.88503
3	1	112.8668
4	2	52.66476
5	3	30.84415
6	4	12.1912
7	6	11.66489

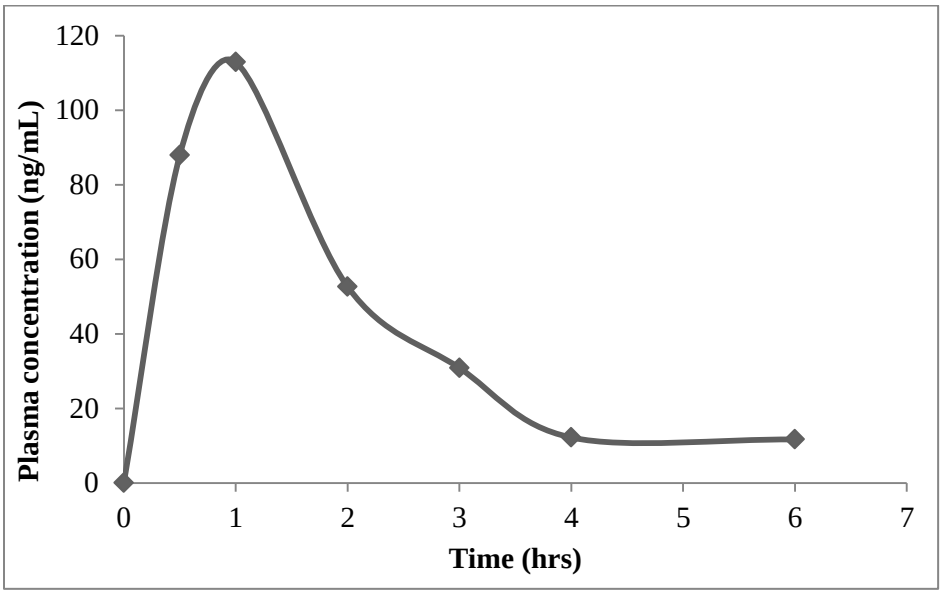

Figure 4.85. Plasma concentration vs. time profile of nicorandil administered as an oral solution equivalent to 15 mg in rabbit no. 19

Table: 4.88. Pharmacokinetic parameters of nicorandil administered as an oral solution equivalent to 15 mg in rabbit no. 19

Prameters	Nicorandil
C_{max} (ng/mL)	112.867
T_{max} (Hrs)	1
AUC_{tot} (ng.h/mL)	259.386
$AUMC_{tot}$ (ng.h^2/mL)	588.464
MRT (Hrs)	2.26869
K_e (Hr^{-1})	0.47035
$t_{1/2\ el}$ (Hrs)	1.47368

Table: 4.89. Plasma concentration (ng/mL) of nicorandil administered as an oral solution equivalent to 15 mg in rabbit no. 20

Sr. No.	Time (Hrs)	Concentration (ng/mL)
1	0	0
2	0.5	81.34702
3	1	109.5978
4	2	49.39576
5	3	27.90204
6	4	12.06044
7	6	11.66489

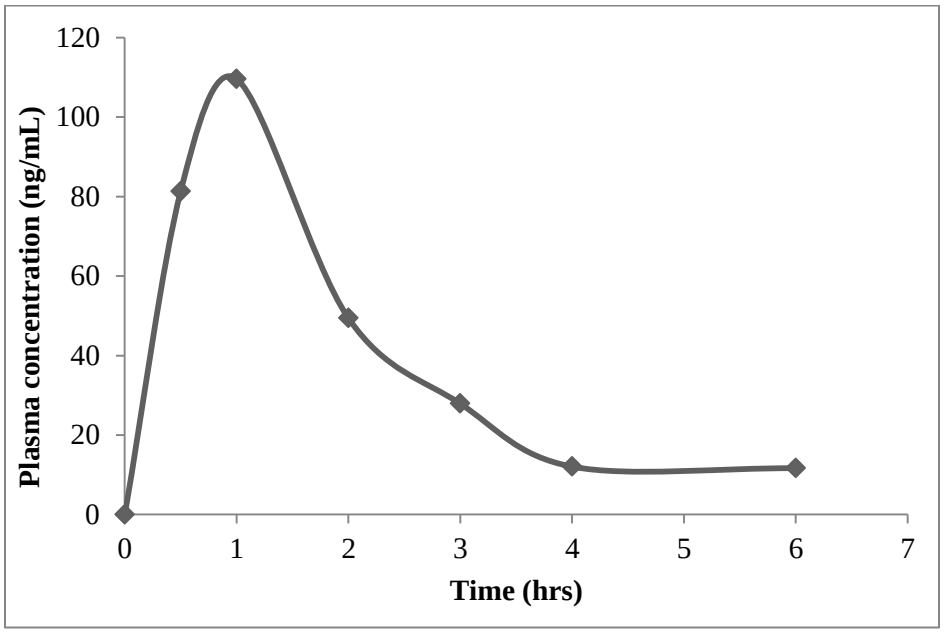

Figure 4.86. Plasma concentration vs. time profile of nicorandil administered as an oral solution equivalent to 15 mg in rabbit no. 20

Table: 4.90. Pharmacokinetic parameters of nicorandil administered as an oral solution equivalent to 15 mg in rabbit no. 20

Prameters	Nicorandil
C_{max} (ng/mL)	109.598
T_{max} (Hrs)	1
AUC_{tot} (ng.h/mL)	247.436
$AUMC_{tot}$ ($ng.h^2$/mL)	570.519
MRT (Hrs)	2.30572
K_e (Hr^{-1})	0.460013
$t_{1/2\ el}$ (Hrs)	1.5068

Table: 4.91. Plasma concentration (ng/mL) of nicorandil administered as an oral solution equivalent to 15 mg in rabbit no. 21

Sr. No.	Time (Hrs)	Concentration (ng/mL)
1	0	0
2	0.5	91.15404
3	1	118.4241
4	2	63.12558
5	3	32.80555
6	4	12.06044
7	6	11.70085

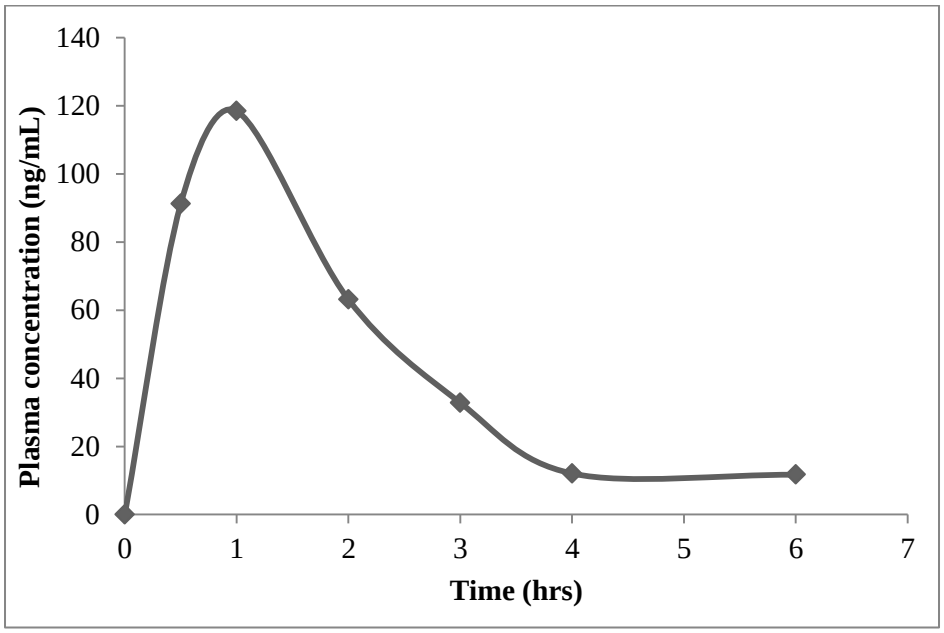

Figure 4.87. Plasma concentration vs. time profile of nicorandil administered as an oral solution equivalent to 15 mg in rabbit no. 21

Table: 4.92. Pharmacokinetic parameters of nicorandil administered as an oral solution equivalent to 15 mg in rabbit no. 21

Prameters	Nicorandil
C_{max} (ng/mL)	118.424
T_{max} (Hrs)	1
AUC_{tot} (ng.h/mL)	276.541
$AUMC_{tot}$ ($ng.h^2$/mL)	610.69
MRT (Hrs)	2.20832
K_e (Hr^{-1})	0.493018
$t_{1/2\ el}$ (Hrs)	1.40593

Table: 4.93. Plasma concentration (ng/mL) of nicorandil administered as an oral solution equivalent to 15 mg in rabbit no. 22

Sr. No.	Time (Hrs)	Concentration (ng/mL)
1	0	0
2	0.5	92.46164
3	1	124.9621
4	2	66.06769
5	3	36.9889
6	4	12.11601
7	6	11.71066

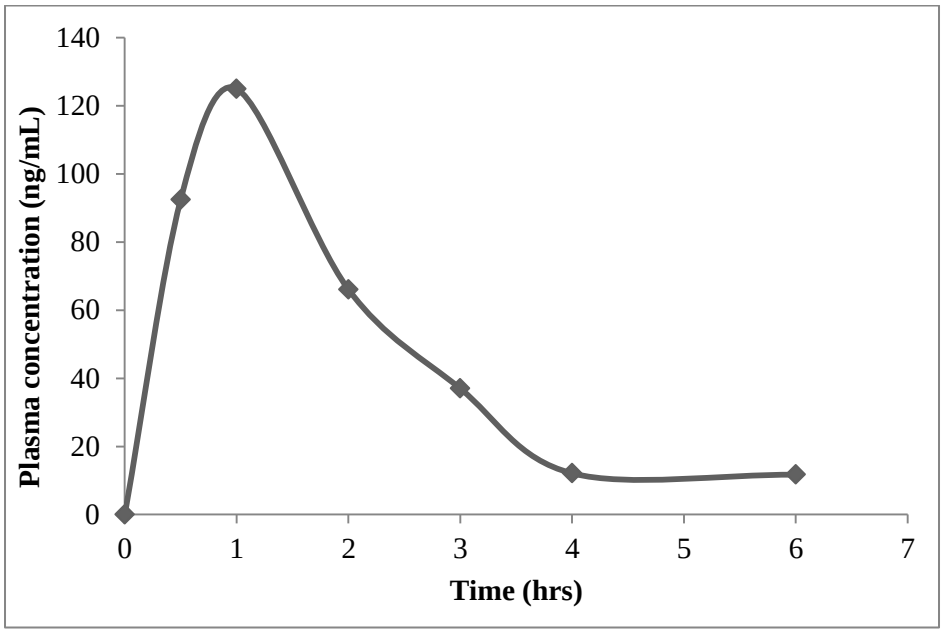

Figure 4.88. Plasma concentration vs. time profile of nicorandil administered as an oral solution equivalent to 15 mg in rabbit no. 22

Table: 4.94. Pharmacokinetic parameters of nicorandil administered as an oral solution equivalent to 15 mg in rabbit no. 22

Prameters	Nicorandil
C_{max} (ng/mL)	124.962
T_{max} (Hrs)	1
AUC_{tot} (ng.h/mL)	289.04
$AUMC_{tot}$ (ng.h^2/mL)	631.692
MRT (Hrs)	2.18548
K_e (Hr^{-1})	0.505915
$t_{1/2\ el}$ (Hrs)	1.37009

Table: 4.95. Plasma concentration (ng/mL) of nicorandil administered as an oral solution equivalent to 15 mg in rabbit no. 23

Sr. No.	Time (Hrs)	Concentration (ng/mL)
1	0	0
2	0.5	85.92363
3	1	128.2311
4	2	69.99049
5	3	40.58481
6	4	12.1487
7	6	11.70085

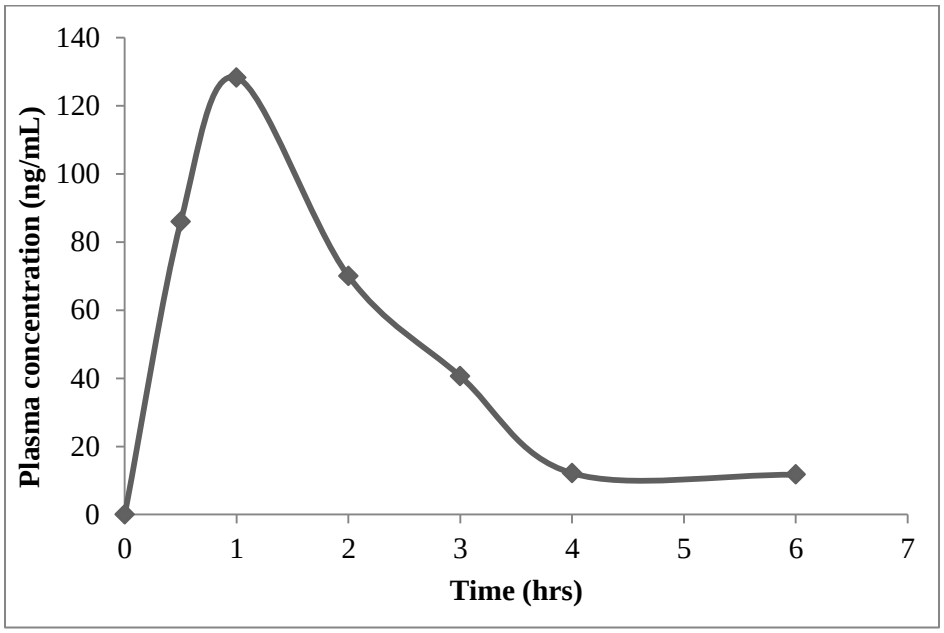

Figure 4.89. Plasma concentration vs. time profile of nicorandil administered as an oral solution equivalent to 15 mg in rabbit no. 23

Table: 4.96. Pharmacokinetic parameters of nicorandil administered as an oral solution equivalent to 15 mg in rabbit no. 23

Prameters	Nicorandil
C_{max} (ng/mL)	128.231
T_{max} (Hrs)	1
AUC_{tot} (ng.h/mL)	295.605
$AUMC_{tot}$ ($ng.h^2$/mL)	649.283
MRT (Hrs)	2.19645
K_e (Hr^{-1})	0.515697
$t_{1/2\ el}$ (Hrs)	1.3441

Table: 4.97. Plasma concentration (ng/mL) of nicorandil administered as an oral solution equivalent to 15 mg in rabbit no. 24

Sr. No.	Time (Hrs)	Concentration (ng/mL)
1	0	0
2	0.5	76.11661
3	1	111.8861
4	2	60.18348
5	3	34.04679
6	4	12.08332
7	6	11.69758

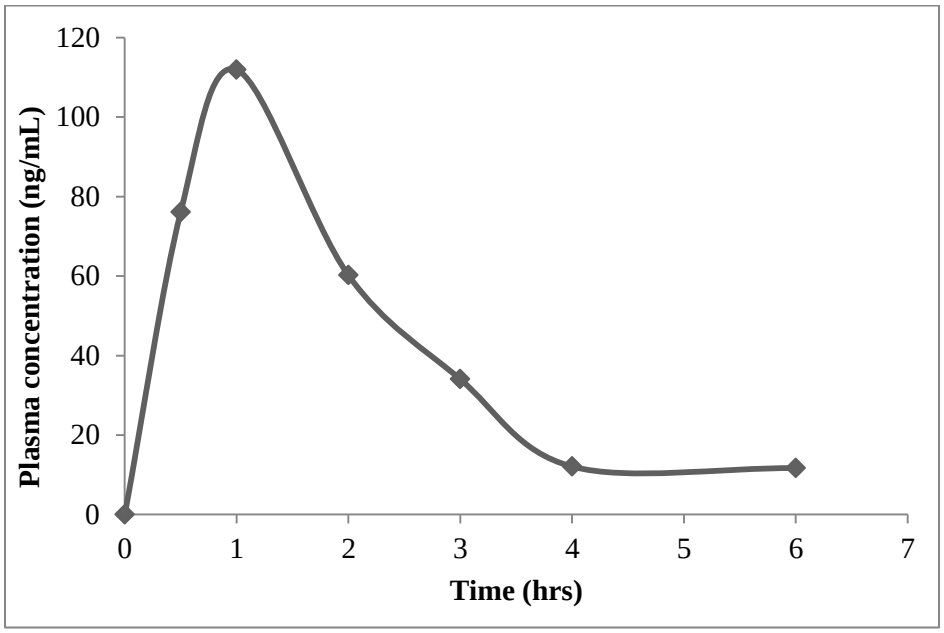

Figure 4.90. Plasma concentration vs. time profile of nicorandil administered as an oral solution equivalent to 15 mg in rabbit no. 24

Table: 4.98. Pharmacokinetic parameters of nicorandil administered as an oral solution equivalent to 15 mg in rabbit no. 24

Prameters	Nicorandil
C_{max} (ng/mL)	111.886
T_{max} (Hrs)	1
AUC_{tot} (ng.h/mL)	263.194
$AUMC_{tot}$ ($ng.h^2$/mL)	606.829
MRT (Hrs)	2.30563
K_e (Hr^{-1})	0.481159
$t_{1/2\ el}$ (Hrs)	1.44058

Table: 4.99. Mean plasma concentration (ng/mL) of nicorandil administered as an oral solution equivalent to 15 mg in G4

G4									
Time (hrs)	**R19**	**R20**	**R21**	**R22**	**R23**	**R24**	**Mean**	**Std Dev**	**SEM**
0	0	0	0	0	0	0	0	0	0
0.5	87.885	81.347	91.154	92.462	85.924	76.117	85.815	6.181	2.523
1	112.86	109.598	118.424	124.962	128.231	111.886	117.661	7.576	3.093
2	52.665	49.396	63.126	66.068	69.990	60.183	60.238	7.904	3.227
3	30.844	27.902	32.806	36.989	40.585	34.047	33.862	4.489	1.833
4	12.191	12.060	12.060	12.116	12.149	12.083	12.110	0.052	0.021
6	11.665	11.665	11.701	11.711	11.701	11.698	11.690	0.020	0.008

Table: 4.100. Mean plasma concentration (ng/mL) of nicorandil administered as an oral solution equivalent to 15 mg in G4

Sr. No.	Time (Hrs)	Concentration (ng/mL) ± SEM
1	0	0
2	0.5	85.81466 ± 2.523
3	1	117.6613 ± 3.093
4	2	60.23796 ± 3.227
5	3	33.86204 ± 1.833
6	4	12.11002 ± 0.021
7	6	11.68995 ± 0.008

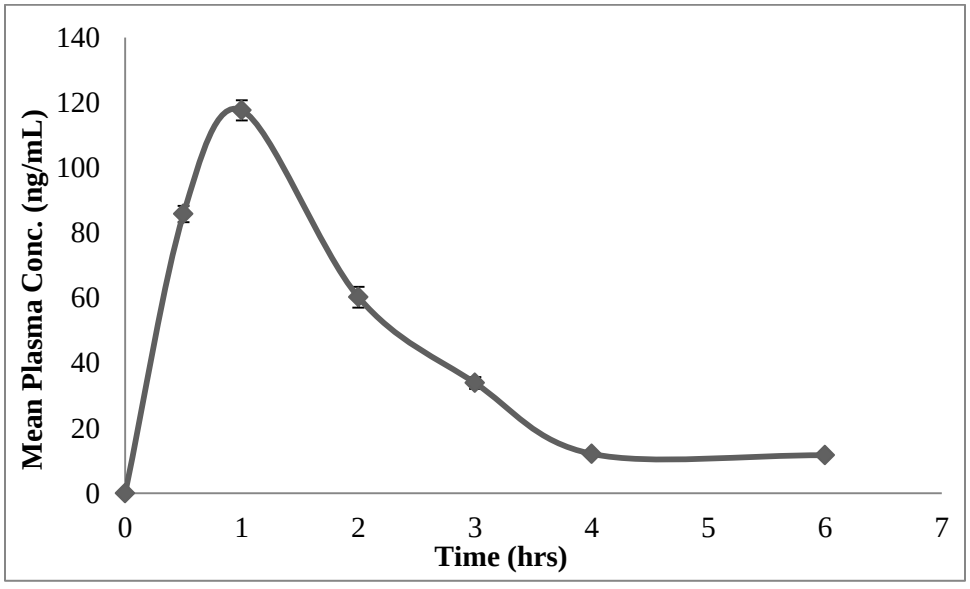

Figure 4.91. Mean plasma concentration vs. time profile of nicorandil administered as an oral solution equivalent to 15 mg in G4

Table: 4.101. Pharmacokinetic parameters of nicorandil administered as an oral solution equivalent to 15 mg in G4

Prameters	Mean ± SEM
C_{max} (ng/mL)	117.66 ± 3.09
T_{max} (Hrs)	1 ± 0.01
AUC_{tot} (ng.h/mL)	271.86 ± 7.54
$AUMC_{tot}$ (ng.h^2/mL)	609.57 ± 11.61
MRT (Hrs)	2.24 ± 0.02
K_e (Hr^{-1})	0.48 ± 0.01
$t_{1/2\ el}$ (Hrs)	1.42 ± 0.02

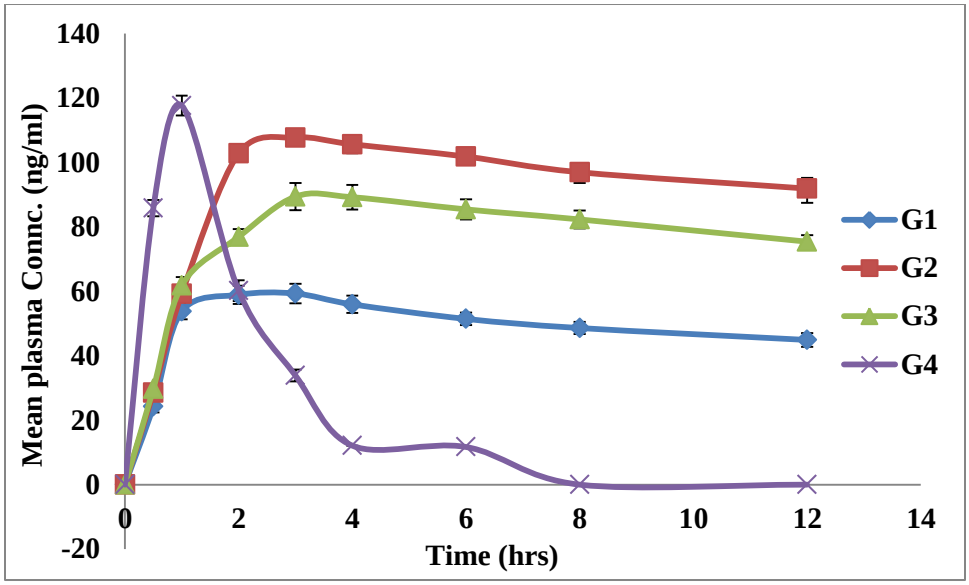

Figure 4.92. Mean plasma concentration vs. time profile of nicorandil administered as an oral dose equivalent to15 mg

4.7 Statistical analysis

One way ANOVA was applied to determined level of significance between pharmacokinetic parameters of different formulation groups. Results are given table no 4.96.

Table 4.102. Statistical analysis

Pharmacokinetic parameter	df	SS	MS	F	P-value	Statistical result
C_{max}	3	11294.881	3764.960	68.9344	0.0004 (< 0.05)	Highly significant
T_{max}	3	17.701	5.900	11.7910	0.0001 (< 0.05)	Highly significant
AUC	3	11920143.071	3973381.024	665.2715	1.0000 (> 0.05)	Highly insignificant

df = Degree of freedom
SS = Sum of squares
MS = Mean of squares

5.0 Discussion

5.1 Swelling behavior

5.1.1 HEMA-co-AA hydrogel

Various factors control swelling behavior of hydrogel in different media or at different pH like equilibrium water content, pKa value, chemical architecture of molecular chains. As far as ionization concerned, it depends on external pH of media. At lower pH carboxylic groups were protonated leading to a few ionized groups in existing network resulting in contracted state of polymer network. Ultimately less swelling ratio were observed at lower pH. At higher pH swelling capacities were enhanced justified by opening out of originally coiled molecules due to electrostatic repulsion forces (Nazar *et al.,* 2014).

In present study swelling ratios of formulations F4 to F6 were increased from 15.013 to 16.420 by increasing monomer concentration (AA) ranging from 10.5 to 14.5 w/w at pH 7.4 because of higher hydrophilic content in polymer chain as shown in table 4.2 and figure 4.2. Whereas swelling ratio of formulations F7 to F9 were decreased from 10.104 to 8.775 by increasing cross linker concentration ranging from 0.020 to 0.030 (%w/w) at pH 7.4 due to the establishment of close-fitted network structure shown in table 4.3 and figure 4.3. Swelling ratio of formulations F1 to F3 were decreased from 16.358 to 13.696 by increasing HEMA concentration ranging from 0.84 to 3.36 (%w/w) at pH 7.4 due to formation of compact network structure shown in table 4.1 and figure 4.1. This swelling behaviour can be attributed to acidic content from acrylic acid. As acidic component increases electrostatic repulsive force also increases resulting in overall increases in hydration. As a result swelling increases with increase in acrylic acid content. While upon increasing acrylate component electrostatic repulsive forces decrease resulting in decreased swelling capacity (Patankar and Bhitre, 2013).

Same pattern studies were conducted by Das in 2014 where swelling ratio was increased by increasing monomer concentration due to increased hydration content and decreased by increasing cross linker concentration because of more compact network formation and as result less hydration or water penetration (Das *et al.*, 2014).

5.1.2 Swelling kinetics HPMC-co-AA hydrogel

Dynamic swelling of formulations F10 to F18 was determined till swelling equilibrium reached in buffer solution of different pH i.e. 1.2, 5.8 and 7.4 keeping in view different pH environment through gastrointestinal track. Percent gel content and percent porosity was also found. Over all swelling ratio is higher in basic medium as compared to acidic medium because of higher pK_a value of basic medium. Depending upon varying components swelling ratio was also affected in different pH. Results showed that swelling ratios of formulations F10 to F12 were increased by increasing HPMC concentration from as shown in table 4.4 and figure 4.4. It was also noted that swelling ratio was increased by increasing AA content and vice versa. Dynamic swelling ratio of formulations F13 to F15 was increased by increasing acrylic acid content as shown in table 4.5 and figure 4.5. While increase in cross linker (MBA) concentration resulted in overall decreased swelling ratio.

By addition of pendant acidic or basic functional groups to a polymer chain, pH sensitivity can be imparted to polymer backbone. This addition of acidic or basic functional groups enable network to either release or accept protons in different pH medium. As a result electrostatic repulsion is produced which ultimately controls porosity of network. Ionic hydrogels having carboxylic or acid groups exhibit changes in swelling behaviour in different pH medium. Polymer networks having more pendant acidic groups show more electrostatic repulsions resulting in greater porosity and swelling at high pH (pH 7.4) while networks with basic pendant groups exhibit electrostatic repulsion at low pH values (pH 1.2). In present study HPMC-co-AA hydrogel has more acidic pendant groups from acrylic acid, that's why these hydrogels showed greater swelling at pH 7.4 (basic pH) as compared to acidic pH

1.2 e.g F13 showed swelling ratio 6.719 and 47.380 at pH1.2 and 7.4 (Robert and Nicholas, 2003; Zhang *et al.,* 2005).

Same pattern of study was conducted by Patankar and Bhitre in 2003 where they prepared poly (acrylamide-co-acrylic acid) hydrogel and studied their swelling behavior at different pH. Their results showed that greater swelling was there at basic pH as compared to acidic pH. More over swelling ratio was increased with increase in acidic content that was acrylic acid. This factor was in good support with results of present study (Patankar and Bhitre, 2013).

5.1.3 Swelling kinetics of HPMC-co-AA-co-HEMA hydrogel

Dynamic swelling as function of concentration for HPMC-co-AA-co-HEMA hydrogels was determined at various pH buffer solution i.e. pH 1.2, pH 5.8 and pH 7.4. Percent porosity and percent gel content was also determined for various weight ratios of components. Swelling ratio, percent porosity and percent gel content of hydrogel formulation was found to be greatly affected by varying weight ratios of component.

Dynamic equilibrium swelling of HPMC-co-AA-co-HEMA hydrogels was increased with increased monomer concentration i.e. acrylic acid as acrylic acid hydrogel are anionic in nature (Esmaiel and Samyra, 2000). It can be justified as percent swelling of an ionic network greatly depends on concentration of ionizable groups in network (Tasdelen *et al.,* 2004). Dynamic equilibrium swelling ratio for formulations F22 to F23 was increased from 5.000 to 5.784 in pH 1.2 and 47.436 to 62.270 in pH 7.4 by increasing AA concentration from 10 to 15 (%w/w) shown in table and figure 4.8. HPMC-co-AA-co-HEMA hydrogel contains anionic acrylic acid and non-ionic acrylate unit which give adequate polarity, charge and hydrogen bonding responsible for better hydration. Swelling ratio was also increased from 4.127 to 4.500 and 42.618 to 49.011in buffer solution of pH 1.2 and 7.4 respectively by increasing concentration of HPMC from 5 to 10 (%w/w) as depicted by formulations F25 to F28 shown in table and figure 4.9. The basic reason for this type of swelling of hydrogels was free carboxylic acid groups. These carboxylic acid groups have ability

to release proton and have a tendency to dissociate at basic pH resulting in greater hydration and swelling. While at acidic pH great quantities of hydrogen bonds were present due to acrylic acid and acrylate chain. As pH was raised break down of hydrogen bonds occured, moreover carboxylic acid groups started to ionize resulting in greater inside osmotic pressure and electrostatic repulsion. Overall result was greater expansion of hydrogel at basic pH i.e. 7.4. Present data had depicted that formulated hydrogels have greater sensitivity towards pH so it can be used for sustained drug delivery through gestro intestinal tract on behalf of different pH environments throughout tract (Nihar and Patel, 2014).

Similar type of study was conducted by Nihar and Patel in 2014. They formulated pH sensitive poly acrylamide-co-acrylic acid hydrogel for controlled and sustained drug delivery. They studied swelling behaviour of the hydrogels in solutions having different pH values and found that swelling of formulated hydrogels were increased with increased monomer concentration as also depicted by present study (Nihar and Patel, 2014). Carboxylic acid groups present in hydrogel structure were thought to be responsible for pH sensitive swelling behaviour. At lower or acidic pH values large quantities of hydrogen bonds formed were found and carboxylic acid remains in form of COOH. While at basic pH (7.4) carboxylic acid groups were present in free state able to lose proton and dissociate. As a result inner osmotic pressure of hydrogels was increased and electrostatic repulsion promoted network expansion (Patankar and Bhitre, 2013).

5.1.4 Dynamic swelling studies of CMC-co-MAA-co-AMPS hydrogel

Swelling behaviour of CMC-co-MAA-co-AMPS hydrogels was investigated at different pH i.e. pH 1.2, pH 5.8 and pH 7.4. Swelling ratio was noted to be increased from 66.638 to 76.489 at pH 7.4 and 65.965 to 75.043 at pH 1.2 with increasing AMPS content from 4 to 6 (%w/w) in formulations from F34 to F36 as given in table and figure 4.11. Repulsion among sulfonate groups were thought to be responsible for increased swelling with increasing AMPS concentration as it improved

hydrophilicity formulation resulting ultimately increase in swelling ratio (Yizhe *et al.*, 2013).

Present study was in good justification with study conducted by Yizhe *et al.,* in 2013. Yizhe prepared CMC-g -poly(AA-co-AMPS) hydrogel. They have reported that swelling ratio was increased with increasing content of AMPS (Yizhe *et al.*, 2013).

Another study conducted by Amr in 2011 declares that increasing AMPS content would result in increased hydrophilicity which ultimately leads to enhanced swelling ability. Moreover increasing AMPS content leads to more perfect crosslinking structure which has capability to absorb and retain water (Amr, 2012). CMC-co-MAA-co-AMPS hydrogel exhibited abrupt change in swelling at lower pH even at pH 2. AMPS possess pKa value 2. At pH less than the pKa value sulfonic groups collapsed and show comparatively less swelling.

Swelling ratio was noted to be decreased from 69.662 to 64.683 at pH 7.4 and 59.898 to 57.441 at pH 1.2 with increasing MAA content from 6 to 8 (%w/w) in formulations from F31 to F33 as given in table and figure 4.10. As MAA concentration increased more compact network was formed with less porosity and less hydration. As a result over swelling ratio was decreased. This fact could be justified by presence of reactive vinyl groups present in polymeric network.

5.1.5 Percent gel content (%g_c) and %porosity (%P) measurement

Percent porosity depends on the volume of the pores present scaffolds of hydrogels and percent gel content depends upon cross linking density.

Porosity decreased with increasing concentration of monomer i.e. HEMA and cross linker i.e. MBA while percent gel contentment increased due to enhanced cross linking density and greater physical entanglement resulting in compact structure with less pore density. Ultimately swelling ratio or water retention capacity was decreased leading to decreased drug release. While higher concentration of monomer AA led to lesser cross linking density and lesser physical entanglement, as a result more pore volume or greater pore density was observed. Same pattern study was conducted by

Shivani in 2013 where he confirmed that percent gel content increased with increase cross linking density and percent porosity was decreased and vice versa (Shivani *et al.,* 2013).

Percent gel content was noted to increase with increasing content of HEMA, HPMC and AMPS from 83.758% to 93.269% (F1 to F3), 85.614% to 93.990% (F10 to F12) and 92.804% to 96.515% (F34 to F36) respectively at pH 7.4. In hydrogel preparation free radicals are generated on polymer/monomer leading to formation of cross linked macromolecules. As concentration of polymer/monomer increased macromolecules come closer to each other resulting in more facilitated cross linking which ultimately leads to increase in gel content (Dafader *et al.,* 2011). Similar kind of results was reported by Dafader *et al.,* in 2011. Percent gel content was found increasing with increasing feed of monomer HEMA. Percent gel content was found to increase with increasing ratio of AA from 80.577% to 85.536% (F4 to F6). This can be attributed to increase in cross liking ratio with increase in monomer concentration. Results of present study were in good agreement with the studies conducted by Dafader *et al.,* in 2012. He reported that gel content was increased with increase in AA content (Dafader *et al.,* 2012). Similar type of results were reported by Kamal *et al.,* in 2014 where he reported that % gel content was found to increase with increasing concentration of AA. He reported that cross liking density increases with increasing monomer concentration resulting in enhanced gel content (Kamal *et al.,* 2014). In present study percent gel content was increased with increase in cross linker concentration from 81.382% to 87.988% (F7 to F9), 82.180% to 88.268% (F16 to F18) and 85.372% to 94.413% (F28 to F30) at pH 7.4. Results are in good agreement with studies conducted by Samiullah and Nazar in 2014 where they have reported that percent gel content increases with increase in cross linker concentration because of increase in cross linking density (Samiullah and Nazar, 2014). Nazar and Umbreen also reported same kind of results (Nazar and Umbreen, 2014).

Percent porosity was noted to decrease with increase in monomer concentration i.e. HEMA and MAA while it was noted to increase with increasing concentration of AA, HPMC and AMPS. Percent porosity was noted to decrease with increasing cross

linker concentration. Increase in percent porosity can be justified by fact that viscosity of solution increases in such cases which prevent bubbles from escape and form more interconnected channels. These interconnected channels result in more porous network. While on other hands in cases where porosity is decreased more cross linking occurred resulting in formation of more entanglement structures as in case of increasing cross linking concentration.

Same kind of results was reported by Samiullah and Nazar in 2014. They reported that percent porosity decreased with increasing concentration of cross linker while it increased with increasing polymer/monomer concentration (Samiullah and Nazar, 2014). Same pattern of results were reported by Nazar and Umbreen (Nazar and Umbreen, 2014).

5.2 Characterization

5.2.1 FTIR Analysis

5.2.1.1 HEMA-co-AA hydrogel

FTIR results revealed drug excipients compatibility. In FTIR spectra of pure drug and excipients many prominent peaks are observed depicting presence of functional groups. Characteristics band were observed 3247 cm^{-1} for (NH); 1675 cm^{-1} for (C=O, CONH) and 1362 cm^{-1} for (CH2) (Sunitha *et al.*, 2014).

FTIR spectra of excipients and formulation were shown in figure 4.30 depicting characteristic bands of functional groups like 3243.17 cm^{-1} for (NH); 1627.97 cm^{-1} for (C=O, CONH) and 1361.55 cm^{-1} for (CH2). A scientist named Abdul worked with FTIR spectra of nicorandil with different excipients in 2014. His work found to be in good support with present study (Abdul and Lila, 2014). Sindhu also conducted same pattern of study and results of his study supports well the results of present study (Sindhu *et al.*, 2015).

5.2.1.2 HPMC-co-AA hydrogel

FTIR spectra of HPMC-co-AA hydrogel were shown in figure 4.31. Absorption bands that appears near 3419 cm^{-1} refer to OH group stretching while absorption bands at 1617 cm^{-1} correspond to CH=CH stretching. In FTIR spectra of pure HPMC peak at 2922.90 cm^{-1} is representative of methyl and hydroxypropyl group responsible for –CH stretching of these groups. More over peak at 1641.92 cm^{-1} is representative of C-O stretching (Patitapabana and Subash, 2012). In FTIR spectra of HPMC-co-AA hydrogel peak at 1697.92 cm^{-1} could be representative of C=O stretching of carboxylic group. Peak at 1450.52 cm^{-1} in formulated hydrogel refers to C-H deformation of alkane. Peak at 1163.16 cm^{-1} in hydrogel could be representative of C-O stretching in C-O-C group. These functional groups clarify presence of representative functional groups of HPMC and acrylic acid after synthesis of HPMC-co-AA hydrogels.

Patitapabana and Subash also worked with HPMC and AA hydrogels. They describe FTIR spectra of HPMC-g-AA hydrogels. They also found peak around 1637cm^{-1} representing C=O stretching of COOH and at 1116 cm^{-1} representing C-O stretching in C-O-C group. Their results are in very good agreement with present study (Patitapabana and Subash, 2012).

5.2.1.3 HPMC-co-AA-co-HEMA hydrogel

FTIR is an important identification tool for new formulations. FTIR spectra of HPMC-co-AA-co-HEMA hydrogel and of individual components were obtained as shown in figure 4.32. In pure HPMC spectra a broad peak at 3425.26 cm^{-1} was due to –OH stretching vibrations of the hydroxyl groups and peak at 1641.92 cm^{-1} could be representative of N-H group (Patitapabana and Subash, 2012). In prepared hydrogel a peak obtained at 2920.73 cm^{-1} was representing –CH stretching of methyl and hydroxypropyl groups and peak at 1698.36 cm^{-1} showed N-H deformation bending of hydroxypropyl methy cellulose. Prepared hydrogel consist of hydroxypropyl methyl cellulose back bone having carboxylate and ester functional

groups as side chains which are identified by sharp peak at 1698.36 cm^{-1}. Peak at 1414.85 cm^{-1} could be representative of C=O stretching.

Muhammad in 2010 also conducted same pattern of study with chitosan, acrylic acid and HEMA hydrogel. He has reported peaks of monomer AA and HEMA as found in FTIR spectra of present study like peak at 1414.85 cm^{-1} representative of C=O stretching and peak around 1637cm^{-1} representing C=O stretching of COOH and at 1116 cm^{-1}. So it can be concluded that results of his study were in good agreement with present study. (Muhammad, 2010).

5.2.1.4 CMC-co-MAA-co-AMPS hydrogel

FTIR spectra of CMC-co-MAA-co-AMPS hydrogels confirmed grafting of MAA and AMPS with CMC as shown in figure 4.33. Characteristic sharp absorption peak of pure CMC at 1022.19 cm^{-1} (-OH groups) was shifted after reaction depicting that CMC has taken part in graft copolymerization via -OH groups. Appearance of peak at 1637.97 cm^{-1} was characteristic of COO asymmetrical stretching vibration of -COO – groups while peak at 1444.00 cm^{-1} was characteristic representative of COO symmetrical stretching vibration of -COO – groups. Appearance of peak at 1143.79 cm^{-1} in CMC-co-MAA-co-AMPS hydrogels showed stretching vibration of $-SO_3$-H groups which is characteristic peak of AMPS existence in grafted system. On behalf of these results it can be clearly stated that that AMS and MAA were positively grafted onto CMC backbones.

Yizhe also studied FTIR spectra of similar type of grafted system where he grafted AMPS and AA on CMC backbones. Characteristic bands of CMC and AMPS he mentioned were also found in FTIR spectra of present study. So we can sate that his results are in good support with present study (Yizhe *et al.,* 2013).

5.2.2. Scanning Electron Microscopy (SEM)

5.2.2.1 HEMA-co-AA hydrogels

Surface SEM microgram of HEMA-co-AA hydrogels showed porous structure responsible for swelling of hydrogels and ultimately drug release (shown in figure 4.34), as these pores act as water channels and serve as transporter for guest molecules. Shevani *et al.,* in 2013 also reported SEM image of hydrogel having porous structure (Shivani *et al.,* 2013).

Heterogeneous distribution of pores was observed as seen in SEM micrograph that led to formation of medical devices with a desired morphology for successful sustained drug delivery. Simonida *et al.,* in 2010 also worked with HEMA hydrogels and he also found porous morphology of gel responsible for its functionality (Simonida *et al.,* 2010).

5.2.2.2 HPMC-co-AA hydrogels

SEM micrograph of HPMC-co-AA hydrogel at magnification of 100X and 200X exhibited uneven pores in size and shape distribution as shown in figure 4.35. This porous network was thought to be responsible for entrapment of aqueous media. This porous network is formed by grafting of monomer acrylic acid on polymer HPMC. Patitapabana also worked on hydroxyl propyl methyl cellulose and acrylic acid hydrogels. He reported that SEM image of hydrogel have porous structure with smooth surface. His results were in good agreement with present study (Patitapabana and Subash, 2012).

Another scientist name Pitta worked with acrylic acid and HPMC hydrogels in various formulations. He also reported that these formulations have porous morphology which is responsible for their water retention capacities. These results are also in good agreement with results of present study (Pitta *et al.,* 2014).

5.2.2.3 HPMC-co-AA-co-HEMA hydrogels

Via SEM images of freeze dried HPMC-co-AA-co-HEMA hydrogels morphology of the hydrogels was shown in figure 4.36. Loose network structure of lamellar shape was thought to be responsible for water holding or absorbing capacity. This network structure was considered to be formed as a result of cross linking of polymer/monomer.

Guo *at al.,* also in 2014 worked on various HPMC and AA formulations. He also reported network structure of lamellar shape which is considered to be responsible for functionality of hydrogels (Guo *et al.,* 2014). A scientist named Mohammad Sadegh said that microstructure morphology must be considered among the most important properties of hydrogel. His work was based on same pattern as that of present study. He also reported micro-porous morphology of hydrogels. He declared that these pores act as regions of water permeation and provides interaction sites of external stimuli (Mohammad, 2010). A scientist also studied scanning electron micrograph of HPMC and AA hydrogel in various formulation and they reported that these hydrogels possess porous structure and have good water absorbing and retention capacities (Mohammad and Mojgan, 2011).

5.2.2.4 CMC-co-MAA-co-AMPS hydrogels

Scanning electron microgram of CMC-co-MAA-co-AMPS hydrogels showed coarse porous structure with heavy mesh networking which clearly justifies its greater water absorbing and retention capacities as shown in figure 4.37. Mechanism behind can be better told by fact that sulfonate groups exert greater electrostatic repulsive forces as compared to carboxylate groups, so as AMPS ratio increased porosity was increased resulting in more water absorption and retention capacities. More over alkyl group of AMPS form hydrophobic regions which have capability to decrease hydrogen bonding among hydrophilic groups of polymer chain which will lead to increased pore size and expansion of polymeric network (Aiqin *et al.,* 2010).

Yizhe also performed same pattern of study in 2013 where he confirmed highly porous network of CMC-AMPS hydrogels, which is in good agreement with results of present study (Yizhe *et al.,* 2013).

5.2.3. Thermal Gravimetric Analysis and Differential Scanning Calorimetery (TGA & DSC)

5.2.3.1. HEMA-co-AA hydrogels

TGA had depicted thermal stability of HEMA-co-AA hydrogel (F4) as shown in figures 4.38. Decomposition of formulation was observed in four steps. The first step of degradation attributed by dehydration was observed up to 275 $^{\circ}$C with 21.17 % weight loss. Next step of degradation was observed from 275 to 400 $^{\circ}$C with 35.28 % weight loss and third step from 400 $^{\circ}$C to 475 $^{\circ}$C with 30.72 % weight loss attributed by decomposition of functional groups of hydrogel. Final degradation of hydrogel was noticed at 550 $^{\circ}$C with 20.71 % weight loss.

Same pattern of study was conducted by Das in 2014 where he observed thermal behavior of hydrogels in TGA and found that hydrogels were thermo stable and showed thermal decomposition in four distinct steps (Das *et al.,* 2014).

Simonida have also observed thermal stability of HEMA hydrogels by TGA. He reported that copolymer samples exhibited much improved thermal stability than monomer. This can be justified probably by higher effective cross-link density (Simonida *et al.,* 2010). Generally speaking we can say that formulated copolymeric hydrogel network has batter thermal stability as compared to reactants i.e. HEMA and AA. As these formulations were prepared to work at 37 °C, these showed the best thermal stability at this range.

DSC thermogram of HEMA-co-AA hydrogels also declared that formulation was more stable as compare to individual components. Melting point range of acrylic acid was found in range of 60°C to 175 °C with an endothermic peak at 125 °C while melting range of hydroxy ethylmethacrylate was found in temperature range of 75 °C

to almost 200 °C with an endothermic peak at 178.4 °C. Formulation showed greater stability even at high temperature range up to 600 °C. Sindhu *et al.*, (2015) conducted same kind of study. Results of his study were same as that of present study (Sindhu *et al.*, 2015). Mary and Nikolaos also worked on HEMA and acrylic acid hydrogels. He mentioned that DSC thermogram cleared that thermal stability of hydrogel was increased after cross linking so hid results supported results of present study (Mary and Nikolaos, 1969).

5.2.3.2. HPMC-co-AA hydrogels

For determination of effect of chemical cross linking on the thermal stability of final formulation TGA and DSC was performed as given in figures 4.40 and 4.41 respectively. Thermograms were drawn by scheming percentage residual weight against temperature. End of first straight line portion of curve was used to find out initial decomposition temperature. HPMC and AA showed less thermal stability as compared to grafted copolymer as depicted in figure 4.36. HPMC showed for phase of decomposition. First decomposition was noted at 301°C with 10.2% weight loss. Second phase was of great decomposition phase as almost 70% weigh loss was observed at narrow temperature range of 301 $^{\circ}$C to 350 $^{\circ}$C. For acrylic acid almost 90% weight loss was observed at temperature range of 90 $^{\circ}$C to 100 $^{\circ}$C. While thermogram of HPMC-co-AA hydrogel showed greater stability as compared to basic components. Only 10% weight loss was observed in first phase at 204 $^{\circ}$C. Further 20% weight loss was observed in temperature range of 205 $^{\circ}$C to 280 $^{\circ}$C. 25% weigh was found to be remaining even at 500 $^{\circ}$C in case of HPMC-co-AA hydrogel. On behalf of these results we can state formulate hydrogel was more thermostable as compared to basic ingredients.

DSC thermogram of HPMC-co AA hydrogel depicted that formulation showed a broad exothermic peak transition at temperature range of 225 °C to 550 °C. Acrylic acid was thermo degradable as it showed a sharp endothermic peak at 75 °C having peak spectrum at temperature range of 35 °C to 100 °C. HPMC was found to be

more stable even over temperature of 800 °C. Above data clearly describes that formulation is more thermo-degradable than individual ingredient HPMC.

DSC data of present study was in good agreement with DSC studies conducted somewhere else by Patitapabana and Subash in 2012 where they studied thermal stability of HPMC-co-AA hydrogel by TGA and DSC. They reported that HPMC and AA hydrogel are more thermostable as compared to individual component. Grafting g is noted to improve thermal stability of formulation. These results are in support with results of present study (Patitapabana and Subash, 2012). Osiris and Manal also reported increase thermal stability of HPMC after hydrogel preparation which was also in good support with present study (Osiris and Manal, 2012).

5.2.3.3. HPMC-co-AA-co-HEMA hydrogels

TGA graphs of HPMC-co-AA-co-HEMA hydrogels described its thermal stability as shown in figure 4.42. Cross linked HPMC-co-AA-co-HEMA hydrogels exhibited three step degradation starting at 200°C. Only 20% weight loss was observed in temperature range of 200°C to 300 °C which showed grafted copolymer was more thermostable as compared to individual components i.e. hydroxypropyl methyl cellulose, acrylic acid and HEMA. Significant weight loss i.e. 35% was observed at temperature range of 350 °C to 450 °C. In comparison AA and HEMA exhibited slight two-step decomposition at temperature range of 75 °C to 100 °C and 100 °C to 175 °C respectively with almost 80% weight loss. This fact clearly showed that grafting has greatly improved thermal stability.

In DSC thermogram of HPMC-co-AA-HEMA hydrogel cleared that formulation exhibited a broad exothermic peak transition peak at temperature range of 223 °C to 545 °C as shown in figure 4.43. Thermal degradability of acrylic acid was showed by a sharp endothermic peak at 70 °C. HPMC behaved more stable over temperature of 900 °C. Melting range of HEMA lied in temperature range of 100 °C to almost 225 °C with an endothermic peak at 202 °C. Above data exhibited that formulation was more thermo-degradable than individual ingredient HPMC and more thermostable as compared to AA.

Podko also worked with TGA and DSC of various HEMA hydrogels. His work is in good support with present study (Podko *et al.,* 2012). Results of study conducted by Monica *et al.* (2014) were also in good agreement with results of present study.

5.2.3.4. CMC-co-MAA-co-AMPS hydrogels

CMC-co-MAA-co-AMPS hydrogels were characterized by thermal analysis to find out percentage of weight loss of CMC-co-MAA-co-AMPS hydrogel as well as pure components. Pure hydrogel has four decomposition curves below 500°C as given in figure 4.44. While pure components MAA and AMPS have two distinct degradation steps below 15 °C and 375 °C respectively with almost 100% weight loss. This fact clearly depicts that thermal stability of hydrogel was increased by grafting as compared to pure ingredients.

Chandra *et al.,* in 2013 conducted same pattern of study in 2013 and reported that stability of hydrogel was increased as compared to individual ingredient. His results were in support with present study.

In DSC thermogram AMPS showed a clear sharp endothermic peak at 200°C while melting range of hydroxyethylmethacrylate lies in temperature range of 75°C to almost 175°C with an endothermic peak at 125.4°C as given in figure 4.45. DSC thermogram of CMC displayed a broad exothermic peak transition peak over temperature range of 275°C to 335°C. DSC thermogram of formulated hydrogel had small endothermic peaks at 200°C and 300°C which was good indicative of cross linking as newer peaks justify formation of new bonds. Wang studied same pattern of study. Results of his studies of DSC were in good agreement with results of present work (Wang *et al.,* 2011).

5.2.4. XRD Analysis

All formulations and drug were investigated for amorphous or crystalline nature by X-ray diffraction as shown in figure 4.46. In general at low intensities diffraction decreased and peaks become broader when angle was increased depicting partial crystallinity of substance. Diffractogram of XRD of formulations proved that graft

copolymerization enlarges amorphous regions resulting in decreased value of percentage crystallinity. Grafting was thought to be basic reason behind amorphous nature of hydrogels as grafting of monomer side chain on basic polymer back bone imparts amorphous regions to copolymer. Chandra also reported that hydrogel formulations did not have any peak on x-ray difractogram giving justification on its highly amorphous nature (Chandra *et al.,* 2013).

Diffractogram of drug Nicorandil showed diffraction at 2θ value about 20°, 22.5°, 25°, 37.5°, 43.5° and 44.5°. As peak intensity represents crystallinity so values of these peaks showed that drug is moderately amorphous as no intense peak was found.

Results of X-ray diffraction studies of Yonghyun were also in good support with results of present study. He studied X-ray diffraction patterns copolymeric hydrogel and copolymeric-silver nanocomposite. He reported that sharp and intense peaks representative of highly crystalline of any substance. According to his study pure copolymeric hydrogels did not have any peak because of amorphous nature of hydrogel (Yonghyun *et al.,* 2011). Results of present study were well supported by a study conducted somewhere else by a researcher named Ray. Results of his x-ray studies clearly stated that only crystalline substances show intense peaks at x-ray diffractogram while amorphous substance show not any single peak at all (Ray *et al.,* 2010).

5.2.5. In vitro drug release studies

5.2.5.1. HEMA-co-AA hydrogels

Results showed that release of nicorandil from F1 was increased up to 96.09 % by highest monomer AA concentration at pH 7.4 because of polymer chain relaxation or expansion of polymer network and thus increased water penetration and increased water holding capacity shown in table 4.26 and figure 4.47, while drug release profile was found to be minimal at acidic pH. Cross linker concentration also affected drug release profile. Moreover, increased cross linker concentration in

formulation F7 to F9 resulted in decreased drug release ranging from 77.34 % to 70.99 % at pH 7.4 as shown in table 4.29 and figure 4.48. Mechanism behind this kind release can be batter explained by swelling of polymer ionic network. At low pH polymer ionizes resulting in formation of anionic centers which ultimately leads to domination of compact polymer interaction leading to compact network. This over all mechanism offered hindrance to water penetration resulting in decrease water holding capacity and thus ultimately lessen drug release. At lower pH 1.2, approximately no noticeable difference in release profile was observed.

As cross linker concentration was increased ionization of carboxylic group and deprotonation of take place leading to creation of new cross linked sections by hydrogen bonding. These electrostatic interaction forces between functional groups caused compact arrangement and thus allow less chain relaxation leading to low swelling and release profile (Suseem *et al.,* 2013). Sindhu *et al.* (2015) also conducted *in vitro* release studies of HEMA-co-AA and results of his studies were in good agreement with present study.

5.2.5.2. HPMC-co-AA hydrogels

Drug release basically depends upon to swelling mechanism of hydrogels which ultimately depends upon chemical architecture of hydrogels. All formulations of HPMC-co-AA hydrogels (F10-F18) were subjected to *in vitro* release study in both acidic and basic media at pH 1.2 and pH 7.4 to simulate conditions of gastric fluid (SGF) and intestinal fluid (SIF), respectively. Percentage drug release in acidic media at pH 1.2 was found to be less i.e. in range of 8.742 % to 17.239 % for varying polymer, monomer or cross linker concentrations. Reason for less drug release in acidic media can be better explained by less hydrogel swelling in acidic media as anionic regions form more compact arrangement result in low polymer chain relaxation or less water holding capacity thus ultimately leading to less drug release. Drug release at basic media was increased as function of time for different polymer, monomer or cross linker concentration ranging from 30.061 % to 92.878 % due to polymer chain relaxation increased leading to more water penetration and release. Drug release was noticed to increase with increasing concentration of acrylic

acid and hydroxypropyl methyl cellulose from 75.78 % to 84.93% and 89.817 % to 92.878 % as shown in table 4.31 and 4.30 respectively as depicted by formulations F1 to F15. In formulations F16 to F18 drug release was also decreased with increasing cross linker concentration from 66.63 % to 56.26 % as shown in table 4.32. Reason for less drug release by increasing cross linker concentration was increased crosslink density in polymeric structure. Same pattern of study was conducted by Sindhu *et al.* (2015) where he reported that drug release was greater in basic media s compare to acidic media, moreover drug release was decreased with increasing cross linker concentration while it was increased with increasing acrylic acid concentration. So his results supported well the results of present study.

Kinetic evaluation of all formulations was also performed by applying various kinetic models. Selection of the best fit method depends upon value of regression coefficient (r). The model that best fits release data was evaluated by value of regression coefficient (r). As value of regression coefficient (r) approaches more close to 1 model is considered best fit for drug release mechanism for that formulation. Values of regression coefficient (r) for varying concentration of components range from 0.939 to 0.9756 for zero order and from 0.9522 to 0.9826 for Higuchi model. Values of regression co-efficient (r) were higher for zero order and Higuchi model than Corsmayer-Peppas model or first order release model. These values of regression coefficient (r) in Higuchi model designated that drug release followed diffusion mechanism as graph of drug released versus square root of time is linear suggesting diffusion controlled drug release. The value of release exponent ‘n’ for different polymer/monomer concentrations were also calculated which fall between 0.5 and 1.0 suggesting non-Fickian or anomalous diffusion mechanism. Same pattern of studies were conducted by Nazar and Umbreen. Results of their studies are in very well agrrement with results of present study. They also found that drug release from HPMC-co-AA hydrogels followed non-fickian diffusion controlled mechanism (Nazar and Umbreen, 2014). Sindhu another researcher also studied drug release mechanism of hydrogels of AA and he reported that release followed non-fickian diffusion controlled mechanism, a supportive reference to results of present study (Sindhu *et al.*, 2015).

5.2.5.3. HPMC-co-AA-co-HEMA hydrogels

In vitro drug release studies were conducted to find out percentage drug release and drug release mechanism. Analysis of in vitro release data was done by employing various kinetic models like Zero order release model, first order release model, Higuchi model and Korsmayer-Peppas model for better understanding of release mechanism. Value of regression coefficient (r) was used to decide upon best fit model for drug release.

Drug release studies were carried out at acidic pH (i.e. pH 1.2) and basic pH (i.e. pH7.4). Drug release was found to be less at acidic pH as compared to basic pH following same mechanism as that of percent swelling. Percent drug release was found to be varied with varying concentrations of polymer or monomer. Percent drug release was decreased from 67.46 % to 59.64 % in formulations F19 to F21 by increasing concentration of HEMA from 0.5 to 1.5 (%w/w) as a result of more compact structure formation with less porosity as shown in table 4.34 and figure 4.53. Percent release was increased from 69.29 % to 73.38 % and 75.80 % to 82.82 % in formulations F22 to F27 with increasing concentration of HPMC and AA from 5 to10 and 10 to 15 (%w/w) respectively as more polymer chain relaxation occur leading to more water absorbing and retention capacities as shown in tables 4.36 and 4.35 and figures 4.55 and 4.54.

These formulations were also subjected to kinetic evaluation by applying various kinetic models. Best fit method was decided upon value of regression coefficient (r) keeping in view the fact that as value of regression coefficient (r) approaches more close to 1 model is thought to be the best fit for drug release mechanism for that formulation. Values of regression coefficient (r) lie in range of 0.9673 to 0.988 for Higuchi model and from 0.949 to 0.9885 for Korsmayer-Peppas model and plot of drug released versus square root of time was linear justifying at diffusion controlled drug release. Value of release exponent “n” for increasing concentration of HEMA and crosslinker MBA lie in range of 0.3296 to 0.4186 and 0.2727 to 0.3352 respectively indicating that drug release followed fickian diffusion mechanism as given in table 4.34. Value of release exponent “n” for acrylic acid was greater than

0.5 indicating that that drug release followed non-Fickian or anomalous mechanism. Sindhu *et al.,* conducted same pattern of studies. Results of his studies were in good support to results of present studies as he stated that percent drug relase was increased by increasing concentration of acrylic acid and also release of acrylic acid hydrogels followed non-fickian diffusion controlled mechanism (Sindhu *et al.,* 2015). *In vitro* drug release profile HPMC and acrylic acid hydrogels was studied by Nazar and Umbreen with supportive results to present studies (Nazar and Umbreen, 2014).

5.2.5.4. CMC-co-MAA-co-AMPS hydrogels

In vitro release profile of CMC-co-MAA-co-AMPS hydrogels with varying amount of MAA and AMPS in buffer solutions of pH 1.2 and pH 7.4 were studied as function of time. All formulations of CMC-co-MAA-co-AMPS hydrogels (F31-F42) were subjected to *in vitro* release study in both acidic and basic media at pH 1.2 and pH 7.4 to simulate conditions of gastric fluid (SGF) and intestinal fluid (SIF) respectively. Over all drug release was found greater at pH 7.4 as compared to pH 1.2. Drug release basically follows same mechanism as that of swelling of hydrogels. Percentage drug release in acidic media at pH 1.2 was found to be less for varying polymer, monomer or cross linker concentrations. Reason for less drug release in acidic media can be better understand by less hydrogel swelling in acidic media as anionic regions form more compact arrangement leading to low polymer chain relaxation or less water holding capacity thus ultimately resulting in less drug release. Drug release at basic media was increased as function of time due to increased polymer chain relaxation leading to more water penetration and more drug release.

It was found that cumulative % drug release gradually increased with increasing concentration of AMPS from 88.68 % to 94.76 % as given in table 4.40. Introduction of increasing concentration of monomer methacrylic acid increased cross linking density and increased porosity resulted in more water absorption leading to more drug release. More over increased concentration of AMPS causes repulsion among sulfonate groups resulting in improved hydrophilicity leading to increase in swelling

ratio and ultimate increased percent drug release (Yizhe *et al.*, 2013). Cumulative % drug release was noted to decrease gradually with increasing MAA concentration from 57.441 % to 64.683 % given in table 4.39, as hydrophobic methyl group in methacrylic acid results in decreased water penetration. Moreover creation of compact network structure at higher content of MAA led to decreased swelling and ultimately decreased cumulative % drug release. Same kind of study was conducted by Das and Nirada with results that were supportive to results of in vitro release of present study (Das and Nirada, 2015).

5.2.6. Pharmacokinetic Evaluation

Desired drug delivery system with controlled release profile was achieved by formulating hydrogels of various components that delivered therapeutic agent at a desired rate for a specified period of time. Nicorandil was used as model drug to evaluate prepared hydrogels systems. For conventional immediate release dosage forms reported C_{max} of nicorandil was 300 ng/mL approximately in humans for a dose of 20 mg b.i.d. Cmax is attained rapidly within 30 min after administration for immediate release dosage forms. Nicorandil show extensive metabolism and kidney is major route of elimination (Frydman, 1992).

Various pharmacokinetic parameters like C_{max} (ng/mL), T_{max} (Hrs), AUC_{tot} (ng.h/mL), $AUMC_{tot}$ (ng.h^2/mL), MRT (Hrs), K_e (Hr^{-1}) and $t_{1/2\ el}$ (Hrs) of model drug nicorandil were determined for HPMC-co-AA, HEMA-co-AA, HPMC-co-AA-co-HEMA hydrogels and oral solution after administering 15 mg.

From pharmacokinetic data obtained it was found that mean plasma concentrations were 60.60845 ± 2.816851 ng/mL, 108.3883 ± 2.338 ng/mL, 92.32212 ± 3.667 ng/mL and 117.6613 ± 3.093 ng/mL for HEMA-co-AA (F1), HPMC-co-AA (F12), HPMC-co-AA-co-HEMA(F24) hydrogels and oral solution respectively. By comparison of plasma concentrations of these formulations it was noticed that difference between C_{max} of these was highly significant as p value is less than 0.05. C_{max} of HPMC-co-AA hydrogel was observed as 108.3883 ± 2.338 ng/mL which was found greater than other two combinations. Moreover, this value was found to

be closer to C_{max} of pure solution even with desired controlled release profile. The reason behind this improved pharmacokinetic profile of HPMC-co-AA hydrogel was that have more cross linking density with greater porosity. It also had greater water retention and controlled release capacities (Sindhu *et al.*, 2015).

From pharmacokinetic data it was observed that the time taken to reach peak plasma concentration *T*max were 3 ± 0.365148 hrs, 3 ± 0.258 hrs, 3 ± 0.365 hrs and 1 ± 0.017 hrs for HEMA-co-AA, HPMC-co-AA, HPMC-co-AA-co-HEMA hydrogels and oral solution respectively. Similarly mean elimination half-life $t_{1/2}$ for HEMA-co-AA, HPMC-co-AA, HPMC-co-AA-co-HEMA hydrogels and oral solution were 0.087807 ± 0.003324 hr^{-1}, 2.083081 ± 1.996 hr^{-1}, 0.084933 ± 0.002 hr^{-1} and 0.487692 ± 0.009 hr^{-1}, respectively. The mean AUC_{tot} values were 1085.876 ± 38.02274 (ng.h/mL), 2101.51 ± 40.014 (ng.h/mL), 1791.957 ± 29.630 (ng.h/mL) and 271.867 ± 7.546 (ng.h/mL) for HEMA-co-AA, HPMC-co-AA, HPMC-co-AA-co-HEMA hydrogels and oral solution, respectively.

So on behalf of these stated results HPMC-co-AA hydrogels considered the best than other two formulations i.e. HEMA-co-AA and HPMC-co-AA-co-HEMA as it provided a prolonged and controlled *in vivo* delivery of model drug.

Same pattern of *in vivo* studies were conducted by researchers named Hemant and Shivakumar on controlled release hydrogel formulations. He also made comparison of two different hydrogel formulations and found that one gave more sustained release profile so gave better results (Hemant and Shivakumar, 2012).

6.0 Conclusion

The study was designed to develop an oral controlled release system to deliver drug at predetermined and reproducible rate over a prolong period of time. In this regard different crossed linked polymeric networks were designed and their capability of delivering drug at predefined rate over a period sufficient for once daily dose was evaluated.

From this study following main conclusions were drawn:

Free radical solution polymerization technique was used to prepare pH sensitive crosslink polymeric networks using different polymer, monomer and cross linker concentrations. Their responsiveness to buffer solutions of different pH i.e. pH 1.2, pH 5.8 and pH 7.4 was evaluated. Cross linking structure of all formulations were confirmed by FTIR, XRD and SEM. *In-vitro* drug release and *in-vivo* evaluation of the best formulations were also performed.

a) HEMA-co-AA hydrogels were prepared by using MBA as cross linker. HEMA-co-AA hydrogels showed good pH responsiveness as they showed maximum swelling at alkaline pH i.e pH 7.4 as compared to acidic pH i.e. pH 1.2. This property was used as a key factor to design sustained release drug delivery system that deliver drug in gastrointestinal tract in response of different pH environment. Among combination HEMA-co-AA hydrogels F1 was found to be the best as it showed maximum cumulative drug release i.e. 92.878% at pH 7.4. Desired release profile was noticed to be greatly affected by varying concentrations of polymer, monomer or cross linker.
b) HPMC-co-AA hydrogels had good pH sensitivity as these showed better and maximum swelling at pH 7.4 and minimum swelling at pH 1.2. Among this combination F1 depicted better desired properties regarding pH sensitivity, greater swelling ratio and desired sustained drug release profile etc. Swelling ratio, gel fraction and cumulative percent drug release was decreased with increasing cross linker concentration i.e. MBA while these parameters were noted to be increased

with increasing AA and HPMC concentration. Desired sustained release profile could be attained by adjusting polymer, monomer and cross linker ratio.

c) HPMC-co-AA-co-HEMA hydrogels were developed by free radical polymerization technique using MBA as cross linker. Formulations were subjected to swelling (at pH 1.2, pH 5.8 and pH 7.4) and in-vitro drug release studies (at pH 1.2 and pH 7.4). Swelling and percent drug release was noted to be decreased with increasing MBA and HEMA concentration while it was noted to be increased with increasing AA and HPMC concentration. More over swelling ratio and percent drug release was also increased gradually with increasing pH from acidic to alkaline i.e. pH 1.2 to pH 7.4. All formulations were noted to be stable and intact during swelling and in-vitro drug release studies. Among this combination F24 was found to be the best as it gave best results for swelling and cumulative percent drug release i.e. 82.820%. It also showed better pharmacokinetic profile as well.
d) Developed CMC-co-MAA-co-AMPS showed less pH sensitivity as compared to all other three combinations as difference in swelling ratio and cumulative percent drug release at acidic and alkaline pH was negligible. Formulations were noted to be unstable and broken during swelling and *in-vitro* drug release studies.

HEMA-co-AA (F1), HPMC-co-AA (F12) and HPMC-co-AA-co-HEMA (F24) hydrogels were subjected to *in vivo* evaluation using animal model rabbits as all these formulation give sustained release profile in *in vitro* studies. After oral administration of these formulations C_{max} was noted to be 60.608 ± 2.816 ng/mL, 108.388 ± 2.338 ng/mL and 92.322 ± 3.667 ng/mL respectively. MRT was noted to be 12.790 ± 0.310 hrs, 13.1786 ± 0.468 hrs and 13.600 ± 0.245 hrs for HEMA-co-AA (F1), HPMC-co-AA (F12) and HPMC-co-AA-co-HEMA (F24) hydrogels. On behalf of these *in-vivo* findings it can be concluded that these cross linked polymeric networks can be used as good sustain release drug delivery system.

Overall it could be concluded that among formulated four different cross linked polymeric networks, HPMC-co-AA (F12) hydrogel could be regarded as superior or the best one as it gave better *in-vitro in-vivo* release profile and thus proven suitable for desired sustained release effect at predetermined rate over prolong period of time. However, these findings are preliminary and studies can proceed to further investigations.

7.0 Future Suggestions/Recommendations

1. In this dissertation FTIR studies were performed on individual ingredients and on prepared formulations to check chemical interaction. In future these studies can further be extended for evaluation of drug and drug loaded formulations to check drug and excipients compatibility.

2. In this work for surface morphological studies Scanning Electron Microscopy (SEM) was used. In future more advanced technique for study of structural morphology "Transition Electron Microscopy" (TEM) can also be included for clear structural elucidations.

3. Drug loading was checked by gravimetric analysis after loading through absorption method. It could also be verified by extraction method or by percent content analysis.

8.0 Reference

1. Aaron C Foss and Nicholas A Peppas (2004). Investigation of the cytotoxicity and insulin transport of acrylic-based copolymer protein delivery systems in contact with caco-2 cultures. European Journal of Pharmaceutics and Biopharmaceutics, 57: 447-455.

2. Abdul BA and Lila KN (2014). Drug excipients compatibility studies of nicorandil in controlled release floating tablet. International Journal of Pharmacy and Pharmaceutical Sciences, 6: 468-475.

3. Achilleos EC, Prudhomme RK, Christodoulou KN, Gee KR and Kevrekidis IG (2000). Dynamic deformation visualization in swelling of polymer gels. Chem Eng Sci, 55:3335-3340.

4. Ades PA, Waldmann ML, Poehlman ET, Gray P, Horton ED, Horton ES and Lewinter MM (1993). Exercise conditioning in older coronary patients. Submaximal lactate response and endurance capacity. Circulation, 88 (2): 572-577.

5. Ahmet Gultek, Turgay Seckin, Yunus Onal and Galip Icduygu M (2002). Poly(methacrylic) acid and γ-methacryloxypropyltrimethoxy silane/clay nanocomposites prepared by in-situ polymerization. Turkish Journal of Chemistry, 26: 925-937.

6. Ajji Z, Mirjalili G, Alkhatab A and Dada H (2008). Use of electron beam for the production of hydrogel dressings. Radiat Phys Chem, 77 (2):200-202.

7. Amir Mellati, Sheng Dai, Jingxiu Bi, Bo Jin and Hu Zhang (2014). A biodegradable thermosensitive hydrogel with tuneable properties for mimicking three-dimensional microenvironments of stem cells. RSC Advances. 4: 63951-63961.

8. Amr El-Hag Ali (2012). Removal of heavy metals from model wastewater by using carboxymehyl cellulose/2-acrylamido-2-methyl propane sulfonic acid hydrogels. Journal of Applied Polymer Science, 123: 763-769.

9. Amulya Saxena K (2010). Synthetic biodegradable hydrogel (Pleura Seal) sealant for sealing of lung tissue after thoracoscopic resection. The Journal of Thoracic and Cardiovascular Surgery, 139 (2): 496-497.

10. Andrew Gelman, Ginger L Chew and Michael Shnaidman (2004). Bayesian Analysis of Serial Dilution Assays. Biometrics, 60: 407–417.

11. Arifin DY, Lee LY and Wang CH (2006). Mathematical modeling and simulation of drug release from microspheres: Implications to drug delivery systems. Adv Drug Deliv Rev, 58: 1247-1325.

12. Ashish Chauhan and Balbir Kaith (2012). Using the advanced analytical techniques to investigating the versatile cellulosic graft copolymers. Analytical & Bioanalytical Techniques, 3(5): 2-8.

13. Bajpai AK, Sandeep Shukla K, Smitha Bhanu and Sanjana Kankane (2008). Responsive polymers in controlled drug delivery. Progr. Polym. Sci, 33: 1088-1118.

14. Barnett H, Burrill P and Iheanacho I (2010). Don't use aspirin for primary prevention of cardiovascular disease. Archive of British Medical Journal, 340: 1805-1809.

15. Bellas Vasilios and Rehahn Matthias (2007). Universal Methodology for Block Copolymer Synthesis. Macromolecular Rapid Communications, 28(13):1415-1421.

16. Berger J (2004). Structure and interactions in covalently and ionically crosslinked chitosan hydrogels for biomedical applications. Eur. J. Pharm. Biopharm, 57: 19-34.

17. Brannon Peppas L and Harland RS (1991). Absorbent polymer technology. Journal of Controlled Release, 17 (3):297-298.

18. Carretti E, Dei L and Weiss RG (2005). Soft matter and art conservation. Rheoreversible gels and beyond. Soft Matter 1: 17-22.

19. Chandel Priya and Rajkumari Kapoor Ankita (20013). Polymer; a boon to controlled drug delivery system. Internation Research Journal of Pharmacy, 4(4): 28-34.

20. Chandra Babu A, Prabhakar M N, Suresh Babu A, Mallikarjuna, Subha M C S and Chowdoji Rao K (2013). Development and characterization of semi-IPN silver nanocomposite hydrogels for antibacterial applications. International Journal of Carbohydrate Chemistry, 13: 1-8.

21. Chen J and Zhao Y (2000). Relation between water absorbency and reaction conditions in aqueous solution polymerization of polyacrylate superabsorbent polymers. J Appl Polym Sci, 75: 808-814.

22. Chen X, Martin BD, Neubauer TK, Linhardt RJ, Dordick JS and Rethwisch DG (1995). Enzymatic and chemoenzymatic approaches to synthesis of sugar based polymer and hydrogels. Carbohydrate Polymers, 28: 15-21.

23. Chobanian, AV, Bakris GL, Black HR, Cushman WC, Green LA, Izzo JL, Jones DW, Materson, BJ, Oparil, S, Wright J.T and Roccella, EJ (2003). Seventh report of the joint national committee on prevention, detection, evaluation, and treatment of high blood pressure. Hypertension, 42 (6): 1206-1252.

24. Croweley MN, Zhang F, Koleng JJ and McGinity JW (2002). Stability of polyethylene oxide in matrix tablets prepared by hot melt extrusion. Biomaterials, 23: 4241-4248.

25. Dafader N C, Adnan M N, Haque M E, Huq D and Akhtar F (2011). Study on the properties of copolymer hydrogel obtained from acrylamide/2-hydroxyethyl

methacrylate by the application of gamma radiation. African Journal of Pure and Applied Chemistry, 5(5): 111-118.

26. Dafader N C, Tahmina Akter, Haque M E, Swapna S P, Sadia Islam and Huq D (2012). Effect of acrylic acid on the properties of polyvinylpyrrolidone hydrogel prepared by the application of gamma radiation. African Journal of Biotechnology, 11(66): 13049-13057.

27. Daly LE, Graham IM, Hickey N and Mulcahy R (1985). Does stopping smoking delay onset of angina after infarction?. Archive of British Medical Journal, 291 (6500): 935-937.

28. Das M, Devi N and Sarma J (2014). Preparation, characterization, and water sorption study of 2-acrylamido-2- methylpropane sulfonic acid (AMPS) based hydrogel. Journal of Chemical and Pharmaceutical Research, 6: 800-806.

29. Das Manali and Nirada Devi (2015). Preparation, characterization, water sorption and drug release study of 2-acrylamido-2-methylpropane sulfonic acid (amps) based hydrogel. International Journal of Research in Chemistry and Environment, 5(1): 69-75.

30. Debashish Roy, Jennifer Cambre N and Brent Sumerlin S (2010). Future perspectives and recent advances in stimuli-responsive materials. Progress in Polymer Science, 35 (12): 278–301.

31. Deguchi Shigeru, Tsujii Kaoru and Horikoshi, Koki (2006). Cooking cellulose in hot and compressed water. Chemical Communications, 4(31): 3293-3295.

32. Dieter Klemm, Brigitte Heublein, Hans-Peter Fink and Andreas Bohn (2005) Cellulose: fascinating biopolymer and sustainable raw material. Angewandte Chemie International Edition, 44: 3358-3393.

33. Dimitrios Stamatialis F, Bernke Papenburg J, Miriam Girones, Saiful Saiful, Srivatsa Bettahalli NM, Stephanie Schmitmeier and Matthias Wessling (2008). Medical applications of membranes: drug delivery, artificial organs and tissue engineering. Journal of Membrane Science, 308 (1–2): 1–34.

34. Dimitrov M, Lambov N, Shenkov S and Dosseva V (2003). Hydrogels based on the chemically crosslinked polyacrylic acid. Biopharmaceutical characterization. Acta Pharm, 53: 25-31.

35. Enas Ahmed M, Fatma Aggor S, Ahmed Awad M and Ahmed El-Aref T (2013). An innovative method for preparation of nanometal hydroxide superabsorbent hydrogel. Carbohydrate Polymer, 91:693–698.

36. Esmaiel Jabbari and Samyra Nozari (2000). Swelling behavior of acrylic acid hydrogels prepared by γ-radiation crosslinking of polyacrylic acid in aqueous solution. European Polymer Journal**,** 36(12): 2685-2692.

37. Fariba Ganji, Samira Vasheghani Farahani and Ebrahim Vasheghani Farahani (2010). Theoretical description of hydrogel swelling: a review. Iranian Polymer Journal, 19 (5): 375-398.

38. Fatemeh A., Rudabeh V. and Rassoul D. (2004). Preparation of ethylcellulose coated gelatin microspheres as a multiparticulate colonic delivery system for 5-aminosalicilic acid. Iranian J. Pharmaceu. Res., 2: 81-86.

39. Feng Wang, Zhenqing Li, Mahmood Khan, Kenichi Tamama, Periannan Kuppusamy, et al., (2010). Injectable, rapid gelling and highly flexible hydrogel composites as growth factor and cell carriers. Acta Biomaterialia, 6 (6):1978–1991.

40. Fournier F, Passirani C, Montero-Menci CN and Benoit JP (2003). Biocompatibility of implantable synthetic polymeric drug carriers: focus on brain compatibility. Biomaterials, 24: 3311–31.

41. Frydman A (1992). Pharmacokinetic profile of nicorandil in humans: an overview. Journal of Cardiovascular Pharmacology, 20(3): 34-44.

42. Gemma Vilar, Judit Tulla-Puche and Fernando Albericio (2012). Polymers and Drug Delivery Systems. Current Drug Delivery, 9: 1-28.

43. Gilberto Siqueira, Julien Bras and Alain Dufresne (2010). Cellulosic Bionanocomposites: A Review of Preparation, Properties and Applications. Polymer, 2: 728-765.

44. Gulati M, Shaw LJ and Bairey Merz C Noel (2012). Myocardial ischemia in women: lessons from the NHLBI WISE study. Clinical Cardiology, 35: 141-148.

45. Guo Feng Wang, Hui Juan Chu, Hong Liang Wei, Xiao Qian Liu, Zi Xuan Zhao and Jing Zhu (2014). Click synthesis by Diels–Alder reaction and characterization of hydroxypropyl methylcellulose-based hydrogels. Chemical Papers, 68(10): 1390-1399.

46. Hamid Naghash J and Oguz Okay (1996). Formation and structure of polyacrylamide gels. Journal of Applied Polymer Science, 60(7): 971-979.

47. Hassan Jalalizadeh, Effat Souri, Hassan Farsam and Mehdi Ansari (2003). A high-performance liquid chromatographic assay for the determination of losartan in plasma. Iranian Journal of Pharmacology & Therapeutics, 2:18-21.

48. Heinze T and Liebert T (2001). Unconventional methods in cellulose functionalization. Progress in Polymer Science, 26: 1689-1762.

49. Hemant Kumar Singh Yadav and Shivakumar H G (2012). In vitro and in vivo evaluation of pH-sensitive hydrogels of carboxymethyl chitosan for intestinal delivery of theophylline. International Scholarly Research Notices, 12: 1-9.

50. Hickey AS and Peppas NA (1997). Solute diffusion in poly(vinyl alcohol)/poly(acrylic acid) composite membranes prepared by freezing/thawing techniques. Polymer, 38:5931-5936.

51. Hombach V, Höher M, Kochs M, Eggeling T, Schmidt A, Hopp H W and Hilger HH (1988). Pathophysiology of unstable angina pectoris correlations with coronary angioscopic imaging. European Heart Journal, 9: 40-45.

52. Huang Y, Yu H and Xiao C (2007). pH-sensitive cationic guargum/poly (acrylic acid) polyelectrolyte hydrogels; swelling and in vitro drug release. Carbohydrate Polymer, 69: 774–83.

53. Jenkins A D, Kratochvíl P, Stepto R F T and Suter U W (1996). Glossary of basic terms in polymer science. Pure and Applied Chemistry, 68: 2287–2311.

54. Jinsub Shin, Paul Braun V and Wonmok Lee(2010). Fast response photonic crystal pH sensor based on templated photo-polymerized hydrogel inverse opal. Sensors and Actuators B: Chemical, 150 (1): 183-190.

55. Jun Li, Xiping Ni and Kam W Leong (2003). Injectable drug-delivery systems based on supramolecular hydrogels formed by poly(ethylene oxide)s and α-cyclodextrin. Journal of Biomedical Materials Research Part A, 65A: (2) 196-202.

56. Kajal Ghosal, Subrata Chakrabarty and Arunabha Nanda (2011). Hydroxypropyl methylcellulose in drug delivery. Der Pharmacia Sinica, 2 (2): 152-168.

57. Kamal K, EL-Sayed A Hegazy, Hayat M Sharada, Sawsan A Abd elhalim, Lotfy S and Randa D Mohamed (2014). Immobilization of glucose isomerase onto radiation synthesized P(AA-co-AMPS) hydrogel and its application. Journal of Radiation Research and Applied Sciences 7(2): 154-162.

58. Kamel S, Ali N, Jahangir K, Shah S M and El-Gendy A A (2008). Pharmaceutical significance of cellulose: A review. Express Polymer Lette, 2(11): 758–778.

59. Kandabashi T, Shimokawa H, Miyata K, Kunihiro I, Kawano Y, Fukata Y, Higo T, Egashira K, Takahashi S, Kaibuchi K and Takeshita A (2000). Inhibition of myosin phosphatase by upregulated rho-kinase plays a key role for coronary artery spasm in a porcine model with interleukin-1beta. Circulation, 101 (11): 1319-1323.

60. Karadao E, Saraydin D and Guven O (2001). Radiation induced superabsorbent hydrogels. acrylamide/itaconic acid copolymers. Macromol Mater Eng, 286: 34-42.

61. Kashyap N, Kumar N and Kumar M(2005). Hydrogels for pharmaceutical and biomedical applications. Critical Reviews in Therapeutic Drug Carrier Systems. 22:107-149.

62. Kiatkamjornwong Suda (2007). Superabsorbent polymers and superabsorbent polymer composites. Science Asia, 33:39-43.

63. Kifayat Ullah Shah and Gul Majid Khan (2012). Regulating drug release behavior and kinetics frommatrix tablets based on fine particle-sized ethyl cellulose ether derivatives: an in vitro and in vivo evaluation. The ScientificWorld Journal, 2: 1-8.

64. Klemm Dieter, Heublein Brigitte, Fink Hans-Peter and Bohn Andreas (2005). Cellulose, Fascinating Biopolymer and Sustainable Raw Material. Polymer Science. 44 (22): 3358 – 3393.

65. Knight C, Purcell H and Fox K (1995). Potassium channel openers: clinical applications in ischemic heart disease; overview of clinical efficacy of nicorandil. Cardiovascular Drugs and Therapy, 1995 2:229-236.

66. Kobayashi Shiro, Kashiwa Keita, Shimada Junji, Kawasaki Tatsuya, Shoda Shin-ichiro (1992). Enzymatic polymerization, The first in vitro synthesis of cellulose via nonbiosynthetic path catalyzed by cellulase. Macromolecular Symposia. 54(1): 509–518.

67. Koichi Ito, Hiroyuki Tsuchida, Akio Hayashi and Toshiaki Kitano (1985). Reactivity of poly(ethylene oxide) macromonomers in radical copolymerization. Polymer Journal, 17 (7): 827–839.

68. Kukovetz W and Holzmann S (1987). Cyclic GMP in nicorandil-induced vasodilation and tolerance development. Journal of Cardiovascular Pharmacology, 10(8): 25-30.

69. Kumar R and Katare OP (2005). Lecithin organogels as a potential phospholipid-structured system for topical drug delivery: A review. AAPS PharmSciTech, 6(2):298-310.

70. Linden Wolfgang, Stossel Carmen and Maurice Jeffrey (1996). Psychosocial Interventions for Patients with Coronary Artery Disease: A Meta-analysis. Archives of Internal Medicine, 156 (7): 745-52.

71. Ling Zhang, Kuifeng Li, Wenqian Xiao, Li Zheng, Yumei Xiao, Hongsong Fan et al. (2011). Preparation of collagen chondroitin sulfate hyaluronic acid hybrid hydrogel scaffolds and cell compatibility in vitro. Carbohydrate Polymers, 84 (1):118–125.

72. Liu Y, Sato T, O'Rourke B and Marban E (1998). Mitochondrial ATP dependent potassium channels: novel effectors of cardioprotection. Circulation, 97 (24): 2463-2469.

73. Liu Z L, Hu H and Zhuo R X (2004). Konjac glucomannan graft acrylic acid hydrogels containing azo crosslinker for colon specific delivery. Journal of Polymer Science Part A, Polymer Chemistry, 42: 4370-4380.

74. Maolin M, Jun L, Min Y and Hongfei H (2000). The swelling behaviour of radiation prepared semi-interpenetrating polymer networks composed of polyNIPAAm and hydrophilic polymers. Radiation Physics and Chemistry, 58:397-400.

75. Markham A, Plosker G and Goa K (2000). Nicorandil: an updated review of its use in ischemia heart disease with emphasis on its cardioprotective effects. Drugs, 60(4): 955-974.

76. Mary Tanya Am Ende and Nikolaos Peppas A (1969). Transport of ionizable drugs and proteins in crosslinked poly(acrylic acid) and poly(acry1ic acid-co-2-hydroxyethyl methacrylate) hydrogels. 1. polymer characterization. Journal of Applied Polymer Science, 59: 673-685.

77. McNaught A D and Wilkinson A (1996). Glossary of basic terms in polymer science (IUPAC Recommendations 1996. Pure and Applied Chemistry, 68: 2287–2311.

78. Mehrdad Hamidi, Amir Azadi and Pedram Rafiei (2009). Hydrogel nanoparticles in drug delivery. Advanced Drug Delivery Reviews, 60 (15):1638–-649.

79. Mohammad Sadegh (2010). Synthesis and Swelling Behaviors of graft copolymer based on chitosan-g-poly(AA-co-HEMA). International Journal of Chemical Engineering and Applications, 1(4): 354-358.

80. Mohammad Sadeghi and Mojgan Yarahmadi (2011). Synthesis of a novel pH- and salt-responsive super absorbent hydrogel based on collagen-g-poly(AA-co-IA). Oriental Journal of Chemistry, 27(2): 453-460.

81. Mohammad Zohuriaan Mehr J and Kourosh Kabiri (2008). Superabsorbent Polymer Materials: A Review. Iranian Polymer Journal, 17 (6):451-477.

82. Monica Beatriz Thurmer, Carlos Eduardo Diehl, Fabio Jose, Bento Brum and Luis Alberto dos Santos (2014). Preparation and characterization of hydrogels with potential for use as biomaterials. Materials Research, 17: 109-113.

83. Moyer Virginia A (2012). Behavioral counseling interventions to promote a healthful diet and physical activity for cardiovascular disease prevention in adults: US preventive services task force recommendation statement. Annals of Internal Medicine, 157 (5): 367-372.

84. Muhammad Akhlaq, Gul Majid Khan, Syed Umer Jan, Abdul Wahab, Abid Hussain, Asif Nawaz and Hamdy Abdelkader (2014). A simple and rapid approach to evaluate the in vitro in vivo role of release controlling agent ethyl cellulose ether derivative polymer. Pakistan Journal of Pharmaceutical Sciences, 27(6): 1789-1798.

85. Nakae I, Matsumoto T, Horie H, Yokohama H, Omura T, Minai K, Matsui T, Nozawa M, Takahashi M, Sugimoto Y, Ito M, Izumi M, Nakamura Y, Mitsunami K and Kinoshita M (2000). Effects of intravenous nicorandil on coronary circulation in humans: plasma concentration and action mechanism. Journal of cardiovascular pharmacology, 35 (6): 919-25.

86. Nazar M R, Asadullah M, Abdullah A B, Nuzhat T, Saeed A and Hassan A (2014). Preparation and characterization of isosorbide mononitrate hydrogels obtained by free-

radical polymerization for site-specific delivery. Tropical Journal of Pharmaceutical Research, 13: 1979-1985.

87. Nazar Muhammad Ranjha and Umbreen Fatima Qureshi (2014). Preparation and characterization of crosslinked acrylic acid/hydroxypropyl methyl cellulose hydrogels for drug delivery. International Journal of Pharmacy and Pharmaceutical Sciences, 6 (4): 400-410.

88. Nihar Shah and Dr. Patel K R (2014). Formulation and development of hydrogel for poly acrylamide-co-acrylic acid. Journal of Pharmaceutical Science and Bioscientific Research, 4(1): 114-120.

89. Osiris W Guirguis and Manal T H Moselhey (2012). Thermal and structural studies of poly(vinyl alcohol) and hydroxypropyl cellulose blends. Natural Science, 4: 57-67.

90. Panprung Sikareepaisan, Uracha Ruktanoncha and Pitt Supaphol (2011). Preparation and characterization of asiaticoside loaded alginate films and their potential for use as effectual wound dressings. Carbohydrate Polymers, 83 (4): 1457–1469.

91. Patankar P and Bhitre M J (2013). Synthesis and characterization of poly (acrylamide-co-acrylic acid) hydrogel for drug delivery. International Journal for Pharmaceutical Research Scholars, 2: 183-191.

92. Patitapabana Parida and Subash Chandra Mishra (2012). Synthesis, crosslinking and evaluation of graft polymer for biomedical use. Research & Reviews: Journal of Pharmaceutical Science, 3(1): 37-45.

93. Payen A (1838). Mémoire sur la composition du tissu propre des plantes et du ligneux (Memoir on the composition of the tissue of plants and of woody material). Comptes Rendus, 7(2): 1052–1056.

94. Peng BL, Dhar N, Liu HL and Tam KC. (2011). Chemistry and applications of nanocrystalline cellulose and its derivatives: A nanotechnology perspective. The Canadian Journal of Chemical Engineering, 89 (5): 1191–1206.

95. Peppas N A and Barr-Howel B D (1987). Charectarization of cross linked structure of hydrogels, hydrogels in medicine and pharmacy fundamentals. Boca Raton, 1: 22-56.

96. Peppas NA and Khare AR (1993). Preparation, structure and diffusional behavior of hydrogels in controlled release. Advance Drug Delivery Review, 11:1-35.

97. Pernetti M, Van Malssen KF, Floter E and Bot A (2007). Structuring of edible oils by alternatives to crystalline fat. Current Opinion in Colloid & Interface Science 12 (4–5): 221-231.

98. Peter Krsko, Thomas McCann E, Thu-Trang Thach, Tracy Laabs L, Herbert Geller M and Matthew Libera R (2009). Length-scale mediated adhesion and directed growth of

neural cells by surface-patterned poly(ethylene glycol) hydrogels. Biomaterials, 30 (5):721–729.

99. Pitta Lavanya, Raja Rajeswari K and Ramesh B (2014). Formulation and evaluation of modified release oral hydrogel beads of antidiabetic drug. World Journal of Pharmacy and Pharmaceutical Sciences, 3(3): 2134-2142.

100. Podko Cielna B, Bartnicki A and Gawdzik B (2012). New crosslinked hydrogels derivatives of 2-hydroxyethyl methacrylate: Synthesis, modifications and properties. Express Polymer Letters, 6(9): 759-771.

101. Podkoecielna B, Bartnicki A and Gawdzik B (2012). New crosslinked hydrogels derivatives of 2-hydroxyethyl methacrylate: Synthesis, modifications and properties. Express Polymer Letters, 6 (9):759-771.

102. Raju KM and Raju MP (2001). Synthesis of novel superabsorbing copolymers for agricultural and horticultural applications. Polym Int, 50:946–951.

103. Ranjha M N, Mudassir J Sheikj Z Z (2011). Synthesis and charectarization of pH sensitive pectin/acrylic acid hydrogels for verapamil release study. Iranian Polymer Journal, 20: 147-159.

104. Ray D, Sahoo PK and Mohanta GP (2008). Designing of superporous crosslinked hydrogels containing acrylic- based polymer network. Asian Journal of Pharmaceutics, 123: 123-127.

105. Ray M, Pal K, Anis A and Banthia A K (2010). Development and characterization of chitosan based polymeric hydrogel membranes. Designed Monomers and Polymers, 13(3): 193-206.

106. Richard A Gemeinhart, Haesun Park and Kinam Park (2000). Pore structure of superporous hydrogels. Polymers for Advanced Technologies, 11: 617-625.

107. Robert Langer and Nicholas Peppas A (2003). Advances in biomaterials, drug delivery and bionanotechnology. Alche Journal, 49 (12): 2990-3006.

108. Roorda WE, Bodde HE, De Boer AG and Junginger HE(1986). Synthetic hydrogels as drug delivery systems. Pharmaceutisch weekblad. Scientific edition, 8: 165-189.

109. Sabyasachi M, Somdipta R and Biswanath S (2010). Polysaccharide-based graft copolymers in controlled drug delivery. International Journal of PharmTech Research, 2(2): 1350-1358.

110. Sachiko Kaihara, Shuichi Matsumura and John P(2008). Fisher Synthesis and characterization of cyclic acetal based degradable hydrogels. European Journal of Pharmaceutics and Biopharmaceutics, 68 (1): 67-73.

111. Samiullah Khan and Nazar Mohammad Ranjha (2014). Effect of degree of cross-linking on swelling and on drug release of low viscous chitosan/ poly(vinyl alcohol) hydrogels. Polymer Bulletin, 71: 2133-2158.

112. Sauzeau V, Le Jeune H, Cario Toumaniantz C, Smolenski A, Lohmann SM, Bertoglio J, Chardin P, Pacaud P and Loirand G (2000). Cyclic GMP-dependent protein kinase signaling pathway inhibits RhoA induced Ca2+ sensitization of contraction in vascular smooth muscle. The Journal of Biological Chemistry, 275 (28): 21722-21729.

113. Shantha KL and Harding DRK (2002). Synthesis and evaluation of sucrose-containing polymeric hydrogels for oral drug delivery J Appl Polym Sci, 84 (2002), p. 2597.

114. Sherif Keshk (2014). Bacterial cellulose production and its industrial applications. Journal of Bioprocessing Biotechniq , 4(2): 1-10.

115. Shinozaki Norihiko, Yuasa Toyoshi, Takata Shigeo (2008). Cigarette smoking augments sympathetic nerve activity in patients with coronary heart disease. International Heart Journal, 49 (3): 261-272.

116. Shivani N, Nikhil S, Reddy BVK and Tanmay MS (2013). Preparation and characterization of poly(vinyl alcohol) chondroitin sulphate hydrogel as scaffolds for articular cartilage regeneration. Indian Journal of Materials Science, 2: 1-8.

117. Siepmann J and Gopferich A (2001). Mathematical modeling of biodegradable polymeric drug delivery systems. Adv. Drug Del. Rev, 48: 229-247.

118. Siepmann J and Siepmann F (2008). Mathematical modeling of drug delivery. International Journal of Pharmaceutics, 364: 328-343.

119. Simonida Lj Tomic, Maja M Micic, Sava N Dobic, Jovanka M Filipovic and Edin H Suljovrujic (2010).Smart poly(2-hydroxyethyl methacrylate/itaconic acid) hydrogels for biomedical application. Radiation Physics and Chemistry, 79: 643-649.

120. Sina Burkert, Thomas Schmidt, Uwe Gohs, Helmut Dorschner and Karl-Friedrich Arndt (2007). Cross-linking of poly(N-vinyl pyrrolidone) films by electron beam irradiation. Radiation Physics and Chemistry, 76 (8–9) :1324–1328.

121. Sindhu S K, Siddaramaiah, Vishakante Gowda D, Vishnu Datta M and Atul Srivastava (2015). Formulation and evaluation of pH sensitive poly(acrylic acid-co-hydroxy ethylmethacrylate) hydrogels for specific site drug delivery. Der Pharma Chemica, 7(1): 35-45.

122. Sing K S W (1985). Reporting physisorption data for gas/solid systems with Special Reference to the Determination of Surface Area and Porosity. Pure and Applied Chemistry, 57(4): 603–619.

123. Singh Anisha, Sharma Pramod Kumar, Garg Vipin Kumar and Garg Garima (2010). Hydrogels: a review. International Journal of Pharmaceutical Sciences, 4(2): 97-98.

124. Sonia T and Sharma P (2011). Chitosan and its derivatives for drug delivery perspective. Advances in Polymer Science, 243: 23-54.

125. Sudhair Abbas, Bashir Ahmad, Zafar Iqbal, Shumaila Bashir and Javid Ali (2013). Study and evaluation of poly (n-vinyl-2-pyrrolidone) hydrogel swelling, theophylline loading and release. World Applied Sciences Journal, 27:236-249.

126. Sulfi S and Timmis AD (2006). Ivabradine - the first selective sinus node if channel inhibitor in the treatment of stable angina. International Journal of Clinical Practice 60(2): 222-228.

127. Sun Hongtao, Mohri Masahiro, Shimokawa Hiroaki, Usui Makoto, Urakami Lemmy, Takeshita, Akira (2002). Coronary microvascular spasm causes myocardial ischemia in patients with vasospastic angina. Journal of the American College of Cardiology, 39 (5): 847-851.

128. Sun X, Zhang G, Shi Q, Tang B and Wu ZJ (2002). Preparation and characterization of water-swellable natural rubbers. Journal of Applied Polymer Science, 86:3212-3717.

129. Sunil C. Joshi (2011). Sol-Gel Behavior of Hydroxypropyl Methylcellulose (HPMC) in Ionic Media Including Drug Release. Materials, 4: 1861-1905.

130. Sunitha S, Thirupathi A and Vijaya K (2014). Preparation and evaluation of liposome entrapped hydrogel complex system of itraconazole for enhanced transdermal permeation. Journal of Pharmaceutical & Scientific Innovation, 3: 25-29.

131. Suseem SR, Ojha Khyati, Shenoy Vranda and Gupta Saumya (2013). Formulation and evaluation of hydrogel with ascorbic acid using aloe vera gel powder as a drug carrier. Innovare Journal of Sciences, 1: 18-20.

132. Susheel Kalia, Anil Kumar and Kaith B S (2011). Sunn hemp cellulose graft copolymers polyhydroxybutyrate composites:morphological and mechanical studies. Advanced Materials Letters, 2(1): 17-25.

133. Tabata Y (2009). Biomaterial technology for tissue engineering applications. Journal of The Royal Society Interface, 6:311-324.

134. Takashi L, Hatsumi T, Makoto M, Takashi I, Takehiko G and Shuji S (2007). Synthesis of porous poly(N-isopropylacrylamide) gel beads by sedimentation polymerization and their morphology. Journal of Applied Polymer Science, 104 (2): 842-850.

135. Takeda H and Taniguchi Y (1985). Production process for highly water absorbable polymer. US Patent, 4:525-527.

136. Takemoto M, Sun J, Hiroki J, Shimokawa H and Liao JK (2002). Rho-kinase mediates hypoxia-induced downregulation of endothelial nitric oxide synthase. Circulation, 106 (1): 57-62.

137. Talaat HA, Sorour MH, Aboulnour AG, Shaalan HF, Enas Ahmed M, Awadn AM and Ahmed MA (2008). Development of a multi-component fertilizing hydrogel with relevant techno-economic indicators. Am-Euras J Agric Environ Sci, 3 (5):764-770.

138. Tasdelen B, Kayaman Apohan, Guven O and Baysa MB (2004). Investigation of drug release from thermo and pH-sensitive poly(N-isopropylacrylamide/itaconic acid) copolymeric hydrogels. POLYMERS FOR ADVANCED TECHNOLOGIES, 15: 528-532.

139. Tobin Kenneth J. (2010). Stable angina pectoris: what does the current clinical evidence tell us? The Journal of the American Osteopathic Association, 110 (7): 364-70.

140. Tomonari Ogata, Kana Nagayoshi, Tadashi Nagasako, Seiji Kurihara and Takamasa Nonaka (2006). Synthesis of hydrogel beads having phosphinic acid groups and its adsorption ability for lanthanide ions. React Funct Polym, 66 (6) :625-633.

141. Tong Qunyi and Zhang Ganwei Rapid synthesis of a superabsorbent from a saponified starch and acrylonitrile/AMPS graft copolymers Carbohydr Polym, 62 (2005), pp. 74-79.

142. Updegraff D and Semimicro M (1969). Determination of cellulose in biological materials. Analytical Biochemistry, 32 (3):420-424.

143. Van der Linden HJ, Herber S, Olthuis W and Bergveld P (2003). Patterned dual pH responsive core shell hydrogels with controllable swelling kinetics and volume. Analyst, 128: 325–331.

144. Veeran Gowda Kadajji and Guru V Betageri (2011). Water Soluble Polymers for Pharmaceutical Applications. Polymers, 3: 1972-2009.

145. Vervoort S, Patlazhan S, Weyts J and Budtova T (2005). Solvent release from highly swollen gels under compression. Polymer, 46, 121-127.

146. Vrolix M, Raeymaeker, L, Wuytack F, Hofmann F and Casteels R (1988). Cyclic GMP-dependent protein kinase stimulates the plasmalemmal Ca2+ pump of smooth muscle via phosphorylation of phosphatidylinositol. The Biochemical journal, 255 (3): 855-863.

147. Wang W B, Xu J X and Wang A Q (2011). A pH-, salt- and solvent-responsive carboxymethylcellulose-g-poly(sodium acrylate)/medical stone superabsorbent composite with enhanced swelling and responsive properties. Express Polymer Letters, 5(5): 385-400.

148. Wenbo Wang, Yuru Kang and Aiqin Wang (2010). Synthesis, characterization and swelling properties of guar gum-*g*-poly(sodium acrylate-*co*-styrene)/muscovite superabsorbent composites. Science and Technology of Advanced Materials, 11(2): 1-10.

149. Wichterle O and Lim D (1960). Hydrophilic gels for biological use. Nature, 185:117-118.

150. William Boden E, Robert O'Rourke A and Koon K (2014). Optimal medical therapy with or without PCI for stable coronary disease. The New England Journal of Medicine, 356: 1503-1516.

151. Yang L, Chu J S and Fix JA (2002). Colon-specific drug delivery: new approaches and in vitro/in vivo evaluation. International Journal of Pharmaceutics, 235:1–15.

152. Yizhe Wang, Xiaoning Shi, Wenbo Wang and Aiqin Wang (2013). Synthesis, characterization, and swelling behaviors of a pH-responsive CMC-g -poly(AA-co-AMPS) superabsorbent hydrogel. Turkish Journal of Chemistry, 37: 149-159.

153. Yizhe Wang, Xiaoning Shi, Wenbo Wang, Aiqin Wang (2012). Synthesis, characterization, and swelling behaviors of a pH-responsive CMC-g -poly(AA-co-AMPS) superabsorbent hydrogel. Turkish Journal of Chemistry, 37: 149-159.

154. Yonghyun Kim, Ramesh Babu V, Daniel Thangadurai T, krishna Rao K S V, Hyeongrae Cha, Changdae Kim, Woohong Joo and Yong Lee (2011). Synthesis, characterization, and antibacterial applications of novel copolymeric silver nanocomposite hydrogels. Bulletin of the Korean Chemical Society, 32(2): 553-558.

155. Yuhui Li, Guoyou Huang, Xiaohui Zhang, Baoqiang Li, Yongmei Chen, Tingli Lu, Tian Jian Lu and Feng Xu (2013). Magnetic hydrogels and their potential biomedical applications. Advanced Functional Materials, 23 (6): 660–672.

156. Zhang R, Tang M, Bowyer A, Eisenthal R and Hubble J (2005). A novel pH and ionic strengthsensitive carboxymethyl dextran hydrogel. Biomaterials, 26: 4677–4683.

157. Zhao Wen, Jin Xing, Cong Yang, Liu Yuying and Fu Jun (2013). Degradable natural polymer hydrogels for articular cartilage tissue engineering. Journal of Chemical Technology and Biotechnology, 88 (3): 327-339.

PHARMACY RESEARCH ETHICS COMMITTEE
The Islamia University of Bahawalpur

Ref. No. 105-2014/PREC
Date: 12-02-2014

APPROVAL CERTIFICATE

The research project entitled "Preparation of Cellulose Based Graft Copolymer; Characterization and Evaluation" submitted by the applicant Ms. Ayesha Rashid through application no. 109 dated November 28, 2013. Pharmacy Research Ethics Committee (PREC), in its meeting held on January 21, 2014, has recruited the research project and reviewed all aspects of ethical issues with reference to its policy. After the agreement of all members, the committee has approved above mentioned research study. Moreover the principal investigator has directed to assure the strict adherence to protocols recommended by the PREC during the conduct of study.

Prof. Dr. Mahmood Ahmad
Chairman,
Pharmacy Research Ethics Committee (PREC)

For any query please contact:
Department of Pharmacy, Khawaja Fareed Campus, Railway Road
The Islamia University of Bahawalpur, Bahawalpur-Punjab, Pakistan
Tel. +92629255565; Fax. +92629255565; E-mail. ma786_786@yahoo.com